TRIBOLOGICAL ANALYSIS OF DIAMOND-LIKE CARBON COATINGS IN COMBINATION WITH BIO-LUBRICANTS FOR ENGINE CAM-TAPPET INTERACTION

REHAN ZAHID

FACULTY OF ENGINEERING
UNIVERSITY OF MALAYA
KUALA LUMPUR

2017

TRIBOLOGICAL ANALYSIS OF DIAMOND-LIKE CARBON COATINGS IN COMBINATION WITH BIO-LUBRICANTS FOR ENGINE CAM-TAPPET INTERACTION

REHAN ZAHID

THESIS SUBMITTED IN FULFILMENT OF THE REQUIREMENTS FOR THE DEGREE OF DOCTOR OF PHILOSOPHY

FACULTY OF ENGINEERING
UNIVERSITY OF MALAYA
KUALA LUMPUR

2017

UNIVERSITY OF MALAYA

ORIGINAL LITERARY WORK DECLARATION

Name of Candidate: **Rehan Zahid**

Registration/Matric No: **KHA 130091**

Name of Degree: **Doctor of Philosophy**

Title of Project Paper/Research Report/Dissertation/Thesis ("this Work"):

Tribological analysis of diamond-like carbon coatings in combination with bio-lubricants for engine cam-tappet interaction

Field of Study: **Energy**

I do solemnly and sincerely declare that:

(1) I am the sole author/writer of this Work;
(2) This Work is original;
(3) Any use of any work in which copyright exists was done by way of fair dealing and for permitted purposes and any excerpt or extract from, or reference to or reproduction of any copyright work has been disclosed expressly and sufficiently and the title of the Work and its authorship have been acknowledged in this Work;
(4) I do not have any actual knowledge nor do I ought reasonably to know that the making of this work constitutes an infringement of any copyright work;
(5) I hereby assign all and every rights in the copyright to this Work to the University of Malaya ("UM"), who henceforth shall be owner of the copyright in this Work and that any reproduction or use in any form or by any means whatsoever is prohibited without the written consent of UM having been first had and obtained;
(6) I am fully aware that if in the course of making this Work I have infringed any copyright whether intentionally or otherwise, I may be subject to legal action or any other action as may be determined by UM.

Candidate's Signature Date:

Subscribed and solemnly declared before,

Witness's Signature Date:

Name:

Designation:

ABSTRACT

In an internal combustion engine, a considerable improvement in tribological performance of components operating under boundary lubrication regime, like cam-tappet interface of valve train assembly, can be achieved by depositing diamond-like carbon (DLC) coatings. These coatings possess a unique combination of properties with the help of which they can help in minimizing friction induced energy and material losses. The lubricity of DLC coatings can be further enhanced by using lubricants having polar components and an unsaturated structure such as vegetable oils. Fossil fuel reserves are depleting at a rapid pace and there are many environmental/health issues associated with conventional lubricants. Therefore, there is a need to shift to environmentally sustainable and biodegradable ones. Bio-based lubricants especially chemically modified vegetable oils such as trimethylolpropane ester of palm oil (TMP) have certain characteristics which make them potential candidate for substituting conventional base oils. Since, lubricant additives are manufactured to interact synergistically with conventional base oils and metallic surfaces, therefore, the main focus of the research presented in this thesis is to analyze tribological compatibility of TMP with most widely used lubricant additives [Glycerol Mono-Oleate (GMO), Molybdenum Dithiocarbamate (MoDTC), Zinc Dialkyldithiophosphate (ZDDP)] in combination with various types of DLC coatings [hydrogen-free tetrahedral DLC coating (ta-C), hydrogenated amorphous DLC coating (a-C:H) and tungsten-doped DLC coating (a-C:H:W)]. Three formulated versions of TMP were prepared by mixing 1 wt.% of GMO, MoDTC and ZDDP separately in 99 wt.% of base oil whereas fourth sample was synthesized by mixing 1 wt.% of each additive in 97 wt.% of base oil. For reference, PAO was used as conventional base oil, with and without additives. Extreme pressure characteristics of lubricant samples on steel/steel contact were evaluated using four-ball wear tester whereas tribological performance of steel/steel, DLC/steel and DLC/DLC contacts had been evaluated using a universal wear testing

machine. Moreover, cylinder head tests were also performed using a direct acting valve train test rig and valve train performance parameters of a DLC-coated cam/tappet interface were compared with those of uncoated ones. Mechanisms responsible for a particular tribological behavior were investigated using various material characterization techniques. Formulated and additive-free versions of TMP showed superior extreme pressure characteristics and resulted in higher weld load values compared to PAO-based lubricants due to their polar structure and better lubricity. During the tribotesting phase, up to 73% and 97% reduction in friction and wear coefficient values were observed respectively when DLC-coated surfaces were used instead of uncoated ones. Symmetrical a-C:H contact proved to be tribologically most efficient among all the considered contacts. In single additive-containing lubricants, TMP+GMO facilitated the sliding between uncoated and DLC-coated surfaces whereas TMP+ZDDP resulted in maximum surface protection. When multi-additive containing lubricants were used, PAO+GMO+MoDTC+ZDDP demonstrated lowest friction coefficient values whereas TMP+GMO+MoDTC+ZDDP was proved to be most effective in mitigating the wear of contact surfaces. During cylinder head testing, significant improvement in wear resistance of valve train components was observed when a-C:H-coated tappets were used against a-C:H-coated camlobes in the presence of TMP+GMO+MoDTC+ZDDP.

ABSTRAK

Di dalam enjin pembakaran dalam, peningkatan yang besar dalam prestasi tribologi oleh komponen-komponen yang beroperasi di bawah rejim pelinciran sempadan sepertimana antara sesondol-tapet pada pemasangan deretan injap, boleh dicapai dengan pengendapan salutan-salutan keras seperti salutan karbon seperti-berlian (DLC). Salutan-salutan ini memiliki kombinasi ciri-ciri unik yang membantu mengurangkan geseran. Geseran boleh menyebabkan kehilangan tenaga dan bahan. Kelinciran salutan DLC boleh dipertingkatkan lagi dengan menggunakan pelincir yang mempunyai komponen polar dan struktur tidak tepu seperti minyak-minyak sayuran. Pada masa yang sama, simpanan bahan api fosil menyusut pada kadar yang pantas dan terdapat banyak isu-isu alam semulajadi/kesihatan yang berkaitan dengan pelincir-pelincir konvensional. Oleh itu, terdapat keperluan untuk bertukar kepada pelincir yang mesra alam dan boleh biorosot. Pelincir berasaskan bio terutamanya minyak sayuran yang diubahsuai secara kimia seperti ester trimethylolpropane (TMP) dari minyak sawit; mempunyai beberapa ciri-ciri yang membuatkan mereka calon yang berpotensi untuk menggantikan pelincir konvensional. Bahan tambah pelincir konvensional pula dihasilkan untuk bertindakbalas secara sinergi dengan minyak asas konvensional dan dioptimumkan untuk prestasi tribologi permukaan. Oleh itu, fokus utama kajian dibentangkan dalam tesis ini adalah untuk menganalisis keserasian tribologi TMP dengan bahan tambah pelincir yang digunakan secara meluas [gliserol mono-oleate (GMO), molybdenum dithiocarbamate (MoDTC), zink dialkyldithiophosphate (ZDDP)] digabungkan dengan pelbagai jenis salutan DLC [karbon tetrahedron bebas-hidrogen (ta-C), karbon amorfus terhidrogen (a-C:H) dan karbon didopkan tungsten (a-C:H:W)]. Tiga sampel ester TMP dengan bahan tambah disediakan dengan menggunakan 99 %berat minyak asas dan 1 %berat GMO, MoDTC dan ZDDP secara berasingan dimana sampel keempat telah disintesis dengan mencampurkan 1 %berat setiap bahan tambah di dalam 97 %berat minyak asas. Sebagai

rujukan, PAO telah digunakan sebagai minyak asas konvensional, dengan dan tanpa bahan tambah. Ciri-ciri tekanan lampau bagi sampel-sampel pelincir pada sentuhan keluli/keluli dinilai dengan menggunakan penguji hausan empat-bola. Sementara itu, prestasi tribologi pertemuan keluli/keluli, DLC/keluli dan DLC/DLC telah dinilai dengan menggunakan mesin penguji hausan universal. Tambahan pula, kajian pada kepala silinder enjin juga telah dilakukan dengan menggunakan pelantar ujian deretan injap enjin tindakan langsung dan parameter prestasi deretan injap bagi sesondol/tapet yang disalut DLC telah dibandingkan dengan yang tidak disalut. Mekanisme yang bertanggungjawab untuk kelakuan tribologi yang tertentu telah disiasat dengan pelbagai teknik pencirian bahan. TMP tanpa bahan - tambah dan dengan bahan tambah menunjukkan ciri-ciri tekanan lampau yang lebih baik jika dibandingkan dengan PAO. TMP menunjukkan nilai beban kimpalan yang lebih tinggi oleh kerana struktur polar dan pelinciran yang lebih baik. Semasa fasa pengujian tribo, pengurangan nilai pekali geseran dan haus masing-masing sehingga 73% dan 97% telah diperhatikan pada permukaan salutan DLC jika dibandingkan dengan permukaan tanpa salutan. Sentuhan a-C:H simetri dibuktikan sebagai sentuhan paling cekap secara tribologi di antara semua sentuhan yang dipertimbangkan. Di dalam pilincir-pilincir yang mengandungi bahan tambah tunggal, TMP+GMO memudahkan gelangsar antara permukaan-permukaan tanpa dan dengan salutan DLC. Sementara itu, TMP+ZDDP menghasilkan perlindungan permukaan maksima. Apabila pilincir-pilincir yang mengandungi berbilang bahan tambah digunakan, PAO+GMO+MoDTC+ZDDP menunjukkan nilai pekali geseran terendah. Sementara itu, TMP+GMO+MoDTC+ZDDP dibuktikan sebagai paling efektif dalam mengurangkan penghausan permukaan sentuh. Semasa ujian kepala silinder enjin, peningkatan yang nyata dalam haus rintangan pada komponen-komponen deretan injap diperhatikan apabila tapet disalut a-C:H digunakan bersama dengan cuping sesondol disalut a-C:H semasa adanya TMP+GMO+MoDTC+ZDDP.

ACKNOWLEDGEMENTS / DEDICATIONS

First of all, I would like to thank ALMIGHTY ALLAH, who gave me courage and strength to complete this research work to the best of my abilities.

I would also like to thank my supervisors Prof. Dr. Masjuki Bin Haji Hassan, Dr. Mahendra Varman and Assoc. Prof. Dr. Md. Abul Kalam, who guided me right throughout the course of the project and enlighten me with their valuable suggestions and useful recommendations. I would also like to extend my gratitude towards my colleagues and faculty members especially Prof. Dr. Riaz Ahmed Mufti and Dr. Nurin Wahidah Binti Mohd Zulkifli for their support and guidance.

I am grateful to lab technicians of Department of Mechanical Engineering and Department of Physics of University of Malaya, Malaysia and National University of Sciences and Technology, Pakistan for allowing me to use their research labs and guiding me in carrying out the experimental work.

I would also like to express my gratitude towards University of Malaya and Malaysia Ministry of Higher Education (MOHE) for funding this research through High Impact Research Chancellory grant project titled ‘‘Clean Diesel Technology for Military and Civilian Transport Vehicles,’’ Grant Number: UM.C/HIR/ MOHE/ENG/07

In the end, I would like to thank my loved ones, especially my parents and wife, who gave me confidence, encouragement and unconditional support to make this possible.

TABLE OF CONTENTS

LIST OF FIGURES

LIST OF TABLES

LIST OF SYMBOLS AND ABBREVIATIONS

a-C	Hydrogen-free Amorphous DLC Coating
a-C:H - a-C:H	a-C:H-coated cam/a-C:H-coated tappet Interface
a-C:H	Hydrogenated Amorphous DLC Coating
a-C:H:Cr	Chromium-doped DLC coating
a-C:H:Si	Silicon-doped DLC coating
a-C:H:Ti	Titanium-doped DLC coating
a-C:H:W - a-C:H:W	a-C:H:W-coated cam/a-C:H:W-coated tappet Interface
a-C:H:W	Tungsten-doped DLC Coating
a-C:H:WC	Tungsten Carbide-doped DLC Coating
A-I	American Petroleum Institute Group I Lubricants
A-II	American Petroleum Institute Group II Lubricants
A-II	American Petroleum Institute Group III Lubricants
AISI	American Iron and Steel Institute
Al_2O_3	Aluminum Oxide
AP	Amine Phosphate
API	American Petroleum Institute
A-IV	American Petroleum Institute Group IV Lubricants
A-V	American Petroleum Institute Group V Lubricants
Ar	Argon
ASTM	American Society for Testing and Materials
b-TPPT	Butyl-Triphenylphosphorothionate
BTU	British Thermal Unit
C	Carbon
C_2H_2	Ethyne
CO_2	Carbon Dioxide

COF	Coefficient of friction
-COOR-	Ester Group
Cr	Chromium
CrC	Chromium Carbide
CrN	Chromium Nitride
CuO	Copper(II) Oxide
DAQ	Data Acquisition
DC	Direct Current
DLC	Diamond-Like Carbon
EDS	Energy Dispersive X-ray Spectroscopy
EHL	Elastohydrodynamic
F	Fluorine
FCVA	Filtered Cathodic Vacuum Arc
Fe	Iron
Fe_2O_3	Ferric Oxide
Fe_3O_4	Magnetite
FeO	Ferrous Oxide
FeS	Ferrous Sulfide
FESEM	Field Emission Scanning Electron Microscope
FTIR	Fourier Transform Infrared Spectroscopy
GMO	Glycerol Mono-Oleate
GMR	Giant Magnetoresistance
I_D/I_G	Ratio between the D and G peaks
ISL	Initial Seizure Load
JBWL	Just Before Weld Load
LabVIEW	Laboratory Virtual Instrument Engineering Workbench

LNSL	Last Non-Seizure Load
LVDT	Linear Variable Differential Transformer
M	Paraffinic Mineral Oil
ML-DLC	Multilayered-DLC coating
Mo	Molybdenum
MoDTC	Molybdenum Dithiocarbamate
MoO_3	Molybdenum Trioxide
MoS_2	Molybdenum Disulfide
N	Nitrogen
NCG	Nano-Crystalline Graphite
NI	National Instruments
Ni	Nickel
O	Oxygen
-OH-	Hydroxyl Group
P	Phosphorus
P/S ratio	Phosphorus/Sulfur ratio
PACVD	Plasma-Assisted Chemical Vapor Deposition
PAO	Polyalphaolefin
P+G+M+Z	PAO+GMO+MoDTC+ZDDP
PID	Proportional–Integral–Derivative Controller
PVD	Physical Vapor Deposition
Ra	Average Surface Roughness
RO	Rapeseed Oil
RPM	Revolutions Per Minute
S	Sulfur
SAE	Society of Automotive Engineers

SEM	Scanning Electron Microscopy
Si	Silicon
Si_3N_4	Silicon Nitride
SiO_2	Silicon Dioxide
SO	Sunflower Oil
ta-C	Hydrogen-free Tetrahedral DLC Coating
ta-C:H	Hydrogenated Tetrahedral DLC Coating
TAN	Total acid number
TBN	Total base number
T+G+M+Z	TMP+GMO+MoDTC+ZDDP
Ti	Titanium
TiB_2	Titanium Diboride
TiCN	Titanium Carbo-Nitride
TiN	Titanium Nitride
TiO_2	Titanium Dioxide
TMP	Trimethylolpropane ester of palm oil
ToF-SIMS	Time-of-Flight Secondary Ion Mass Spectrometry
U - U	Uncoated Cam/Uncoated Tappet Interface
VI	Viscosity Index
W	Tungsten
WL	Weld Load
WS_2	Tungsten Disulfide
WSD	Wear Scar Diameter
XPS	X-ray Photoelectron Spectroscopy
ZDDP	Zinc Dialkyldithiophosphate
Zn	Zinc

$Zn_3(PO_4)_2$	Zinc Phosphate
ZnO	Zinc Oxide
ZnS	Zinc Sulfide
ZrO_2	Zirconium Dioxide

CHAPTER 1: INTRODUCTION

1.1 Overview

In order to meet the energy needs of the modern world, natural resources such as petroleum, coal and gas are depleting at ever increasing rate due to which they are at the verge of scarcity (del Castillo-Mussot, Ugalde-Véle, Montemayor-Aldrete, de la Lama-García, & Cruz, 2016). According to International Energy Outlook 2016, total world energy consumption will rise to 814.95 x 10^{15} British Thermal Unit (BTU) by the year 2040 (*International Energy Outlook*, 2016)(**Figure 1.1**). If this trend continues, our future generations will be hardly left with any energy sources and it will become extremely difficult to fulfill the requirements of commercial and domestic users. Not only this, excessive usage of hydrocarbons is increasing the concentration of carbon dioxide (CO_2) and other toxic gases in the atmosphere causing drastic climatic changes and posing a potential threat to the environment (Tan, 2014). By 2040, world energy-related CO_2 emissions will increase to 43.20 x 10^9 metric tons which is presently at 33.96 x 10^9 metric tons (*International Energy Outlook*, 2016)(**Figure 1.1**). Due to the poorly implemented principles of tribology in industry, a significant amount of input energy is wasted in the form of friction and heat losses without doing any useful work (Spencer & Tysoe, 2015). These challenges can be met either directly or indirectly by conservation and efficient use of energy resources (Bilgili, Ozbek, Sahin, & Kahraman, 2015). There is also a need to look for renewable energy sources such as wind, solar, biomass to decrease our dependency on fossil fuels (Mathiesen et al., 2015).

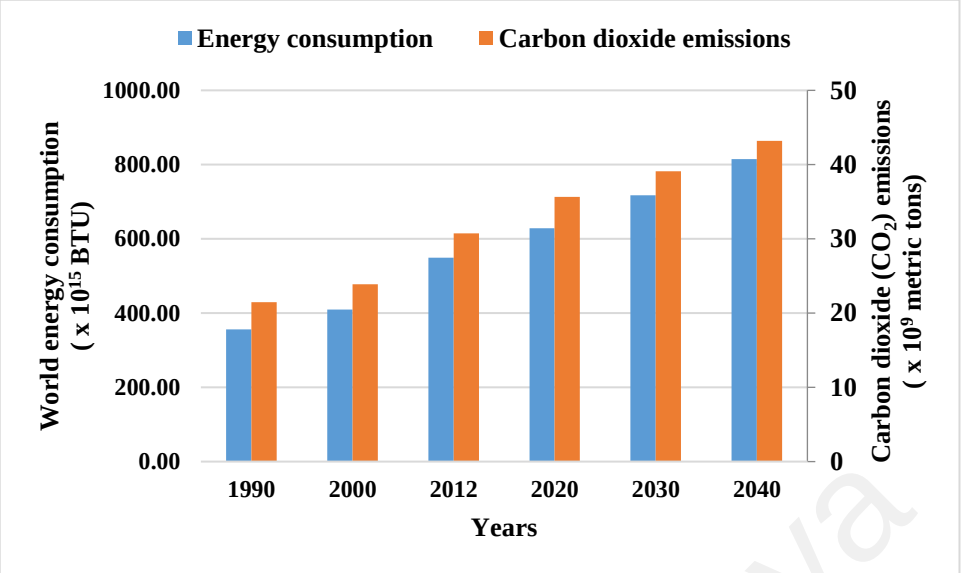

Figure 1.1: History and forecast of total world energy consumption and energy-related CO_2 emissions
(*International Energy Outlook*, 2016)

The transportation sector, comprised of passenger cars, trucks, buses, aircrafts, rails and ships, not only consumes a major portion of non-renewable energy produced worldwide but also contributes air pollutants to the environment more than any other energy consuming sector (Ong, Mahlia, & Masjuki, 2012)(**Figure 1.2**). Therefore, environmental legislators and government authorities are putting immense pressure on the automotive Original Equipment Manufacturers (OEMs) to produce vehicles with increased fuel efficiency, less harmful emissions, improved service intervals and reliable components (Enomoto & Yamamoto, 1998; Riaz Ahmad Mufti, Zahid, Qureshi, Aslam, et al., 2015). In addition to that, revolutionary ideas such as mass transit projects, magnetic levitation trains and hybrid cars are coming from different parts of the world to help this sector in decreasing hazardous emissions and dependency on fossil fuels (Annema, Van den Brink, & Walta, 2013; Senge, 2014).

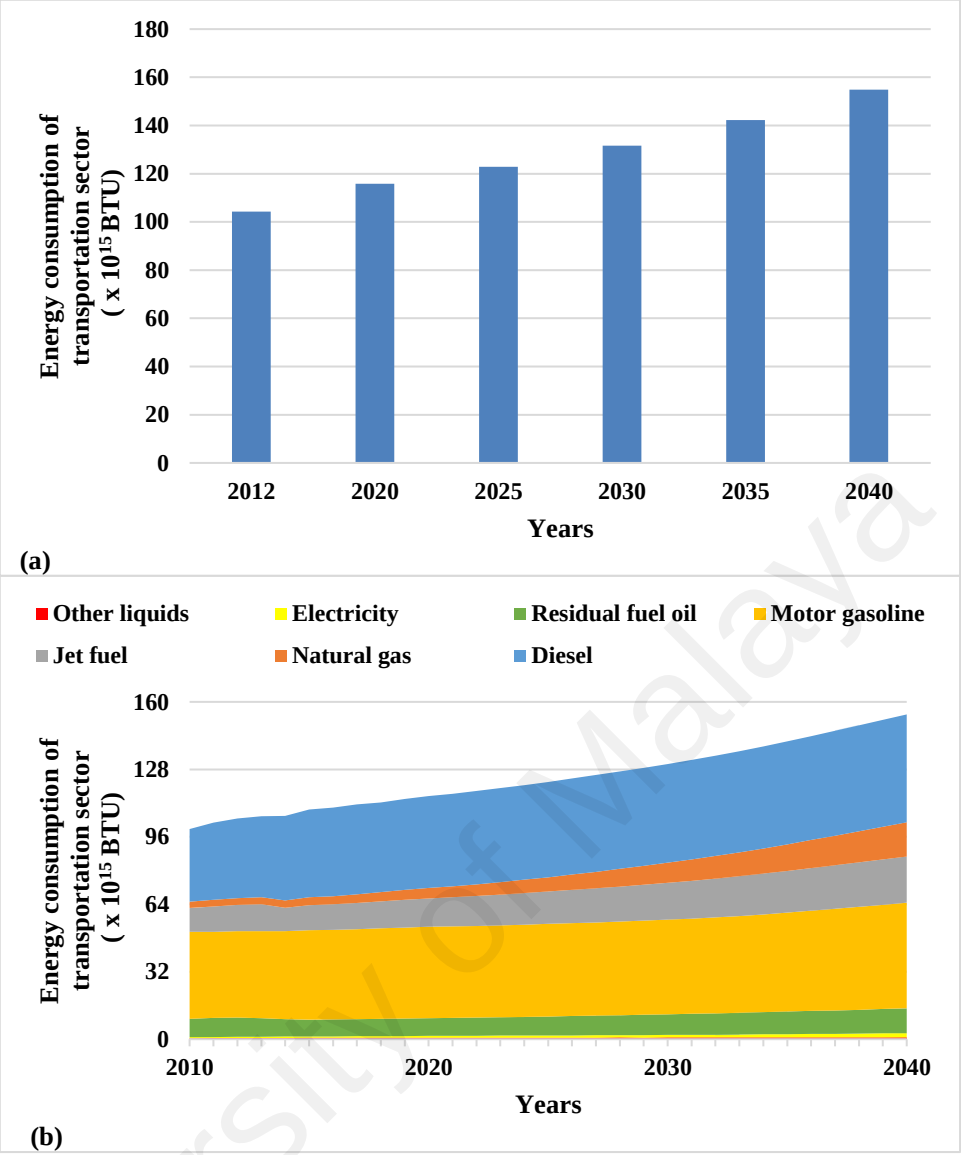

Figure 1.2: History and forecast of (a) total energy consumption of transportation and (b) its breakdown by energy source sector (*International Energy Outlook*, 2016)

A considerable amount of energy produced by combustion of fuel inside the automotive engine is wasted due to thermal and mechanical inefficiencies (Roberts, Brooks, & Shipway, 2014). Although, mechanical losses are small as compared to thermal ones but still tremendous amount of useful energy can be conserved by reducing friction between the moving parts. In order to do so, automotive manufacturers are working closely with their lubricant partners to formulate lubricants that can work synergistically with the tribopairs involved in the functioning of internal combustion

engines. There is a continuous drive among the lubricant formulators to develop less viscous lubricants, without compromising on their primary role of lubrication, so that they offer less shear friction between the interacting surfaces (Khurram et al., 2014). Since, petroleum-based lubricants pose potential threat to the environment due to their toxicity, unsustainability, non-renewability and poor biodegradability, therefore, lubricant companies are referring back to bio-based lubricants such as vegetable oils (McNutt & He, 2016). In an automotive engine, major frictional losses occur in piston assembly, bearings and valve train (Rosenberg, 1982)(**Figure 1.3**). Due to higher values of applied load and extreme temperatures, viscosity of lubricant decreases and it slips out from the interacting surfaces. Hence, chances of metal-to-metal contact increases exponentially which not only amplifies the friction, but also adversely affects the reliability and service life of the components due to elevated wear rates. This catastrophic effect of lubricant starvation can be avoided to an appreciable extent by protecting the contact surfaces with hard coatings having self-lubrication capability (Kalin, Velkavrh, Vižintin, & Ožbolt, 2008). These high quality surface protective coatings include nitrides [titanium nitride (TiN), titanium carbo-nitride (TiCN), and chromium nitride (CrN)], carbides (metallic carbides) and diamond-like carbon (DLC) films (Schamel, Grischke, & Bethke, 1997). These coatings not only facilitate sliding but also increase the wear resistance of the moving parts. Among these coatings, DLCs come forth as most dependable and reliable surface coatings for wide range of industrial applications due to their unique blend of mechanical, chemical, optical, electrical and tribological properties, (Bewilogua & Hofmann, 2014; Deng, Kousaka, Tokoroyama, & Umehara, 2014; Oksanen et al., 2014; Tasdemir, Wakayama, et al., 2014) (Erdemir & Donnet, 2006).

Since, lubricant additives are manufactured to interact synergistically with conventional base oils and optimized to enhance tribological performance of metallic surfaces, therefore, a lot of experimental studies were carried out by researchers to

investigate tribological compatibility of vegetable oils with conventional lubricant additives in combination with various types of DLC coatings. Kalin and Vižintin (2006a) studied tribological characteristics of hydrogenated amorphous DLC coating (a-C:H) and tungsten-doped DLC coating (a-C:H:W) using sunflower oil (SO) and paraffinic mineral oil (M) formulated with Zinc Dialkyldithiophosphate (ZDDP) and amine phosphate (AP) additives. They reported enhanced tribological performance of above-mentioned DLC coatings with sunflower-based lubricants due to their unsaturated and polar nature. They also observed significant improvement in wear resistance of DLC coatings when conventional additives were used as a result of tribochemical interactions. In a similar study, Kalin, Vižintin, Vercammen, Barriga, and Arnšek (2006) observed 30 - 50% reduction in wear of a-C:H/a-C:H contacts when AP and dialkyl dithiophosphate ester were used as additives in SO. They also reported improved tribological performance of symmetrical a-C:H contacts when formulated versions of SO were used instead of mineral oils irrespective of their formulation. Symmetrical contacts are those in which both interacting surfaces are of the same material e.g. steel/steel contacts, DLC/DLC contacts whereas in case of asymmetrical contacts, sliding surfaces are of different materials e.g. DLC/steel contacts, steel/cast iron contacts, DLC/cast iron contact. In another experimental study, Kržan, Novotny-Farkas, and Vižintin (2009) reported enhanced wear resistance of a-C:H:W-coated interacting surfaces with rapeseed oil (RO) compared to PAO. They also observed that a-C:H:W/a-C:H:W contact resulted in lower values of friction coefficient compared to steel/steel contact but this enhanced friction performance is not because of the additive but actually due to the inherent lubricity of a-C:H:W coating. In most of those studies, RO and SO, formulated with conventional additives, were used as bio-lubricants. Although, few of the researchers also considered palm oil in combination with DLC coatings but without conventional additives. Al Mahmud, Kalam, Masjuki, and Abdollah (2015) studied tribological characteristics of additive-free

sunflower, palm and coconut oils in combination with hydrogen-free tetrahedral DLC coating (ta-C)/steel contacts and found that lowest values of friction and wear coefficients can be achieved with SO as a result of graphitization and carbon transfer layer.

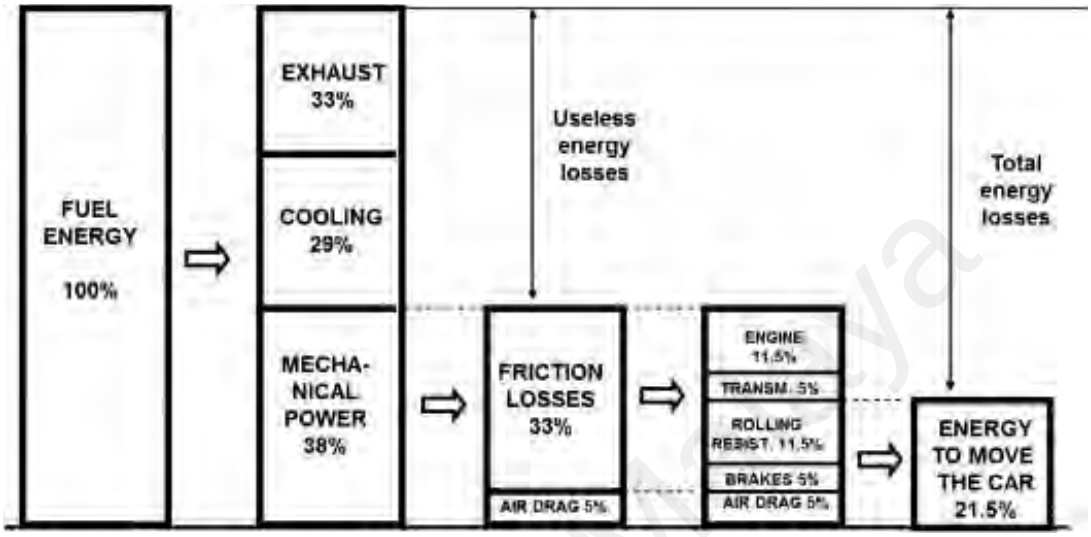

Figure 1.3: Breakdown of passenger car energy consumption (Holmberg, Andersson, & Erdemir, 2012)

1.2 Problem Statement

In an automobile engine, the valve train is one of the most challenging assemblies to lubricate efficiently due to extreme operating conditions such as varying applied loads, elevated temperatures, asymmetrical cam profiles, changing entrainment velocities etc. (Khurram et al., 2014). Although engine valve train operates under multiple lubricant regimes, but mostly boundary lubrication regime prevails. In boundary lubrication regime, there is a huge possibility of metal-to-metal contact due to negligible lubricant film present between the camlobes and tappets. Lubricant starvation conditions not only amplify the friction but also adversely affects the reliability and service life of the components due to elevated wear rates. These catastrophic effects can be avoided to an appreciable extent by using lubricant additives and protecting the contact surfaces with hard coatings having self-lubrication capability such as DLC coatings (Kalin et al., 2008)

(Bewilogua & Hofmann, 2014; Deng et al., 2014; Erdemir & Donnet, 2006; Oksanen et al., 2014; Tasdemir, Wakayama, et al., 2014).

Conventional lubricant additives which include friction modifiers, antiwear additives and extreme pressure additives, can play an important role in applications operating under boundary lubricant regime. Most of the lubricant additives are optimized to formulate with synthetic and petroleum-based oils. Moreover, lubricant manufacturers engineered their products by keeping in mind that they will only interact with conventional materials such as iron, aluminum, copper etc. Therefore, there is a need to see the effectiveness of these additives when they are formulated with lubricant base oils and used in combination with various types of DLC coatings. In the last few decades, many researchers have conducted experimental investigations to understand the behavior of DLC coatings in combination with additive-free and formulated versions of synthetic and petroleum-based oils. However, there are few studies in which bio base oils such as SO, RO, and palm oil were used. Still, there is a lack of understanding about how various DLC coatings interact with conventional lubricant additives and whether they are compatible with each other or not. Some researchers reported tribologically beneficial interactions between the DLC coatings and formulated lubricants while others observed no such behavior.

In order to select the optimum DLC coating and see the suitability of bio lubricants especially those containing trimethylolpropane ester of palm oil (TMP), which is not frequently evaluated in the literature, for cam/tappet interface of direct acting valve train assembly of passenger car engine, there is a need to further investigate their compatibility with conventional lubricant additives in the original environment of the engine using realistic test conditions. Although, few studies were carried out by researchers in this regard, but none of the researchers used TMP in combination with DLC-coated camlobes and tappets coated in their investigations.

1.3 Aims and Objectives of the research

The overall aim of this research work is to see the tribological compatibility of conventional lubricant additives such as GMO, MoDTC and ZDDP with TMP and various types of non-doped (ta-C and a-C:H) and doped (a-C:H:W) DLC coatings. The primary focus of this thesis is to select tribologically most suitable DLC coating and see the potential of TMP to be used as lubricant base oil for direct valve train application. The main objectives of this study are as follows:

- To inspect the compatibility of conventional lubricant additives with TMP (bio base oil) by analyzing and comparing load-carrying capacity and extreme pressure characteristics with PAO-based lubricants (synthetic base oil) using four-ball wear tester
- To investigate the tribological compatibility of each conventional lubricant additive with TMP and various types of DLC coatings using universal wear testing machine
- To analyze the suitability of bio-lubricant and various types of DLC coatings for cam/tappet interface by simulating the contact using universal wear testing machine
- To explore the suitability of TMP-based lubricants and various types of DLC coatings for cam/tappet interface of direct acting valve train by comparing their tribological performance parameters using Mercedes Benz OM646LA cylinder head-based valve train test rig

In objective 2, tribochemical compatibility of conventional lubricant additives with TMP and various types of DLC coatings were analyzed. Single-additive additives were used in objective 2 so that tribology of each additive can be investigated in isolation without the interference of other additives. Since, AISI 52100 chrome steel interacting

surfaces were used in most of the tribotesting studies in the literature therefore, AISI 52100 chrome steel balls were used as counterbody. As point contacts can be most effectively analyzed using material characterization techniques compared to line contact due to smaller contact area that's why ball-on-plate geometric configuration was selected to Objective 2.

Objective 3 was designed to simulate cam/tappet interface of direct acting valve train assembly of automotive engine. As most of the automotive engine camshafts are made up of cast iron and tappets are made up of steel that's why steel/cast iron contact was used in objective 3. Since, fully-formulated lubricants are used in automotive engine containing all the additives, therefore, multi-additive containing lubricants were used in objective number 3. When camlobe and tappet come into contact with each other, line contact establishes between them. Due to this reason pin-on-plate geometric configuration was considered in objective 3.

1.4 Scope of research

In the first phase of this research work, compatibility of conventional lubricant additives [Glycerol Mono-Oleate (GMO), MoDTC and ZDDP) with TMP has been analyzed by conducting tribotests using four-ball wear tester with ball-on-ball geometric configuration according to the procedure described in American Society for Testing and Materials (ASTM) D-2783 standard. Load carrying capacity and extreme pressure characteristics of TMP-based single and multi-additive containing lubricants are compared with those of PAO-based lubricants by correlating wear scar diameters, last non-seizure loads (LNSL), initial seizure loads (ISL) and weld loads (WL).

In the second phase, tribological characteristics of various types of DLC coatings (ta-C, a-C:H and a-C:H:W) selected on the basis of literature review and availability, is evaluated in combination with additive-free and additive-containing TMP using universal

wear testing machine with ball-on-plate and pin-on-plate geometric configurations. Tribotests with ball-on-plate geometric configuration are carried out with single-additive containing lubricants to see the compatibility of each additive with TMP and DLC coatings in isolation. Since, fully formulated lubricants are used in passenger car engine, therefore, multi-additive containing lubricants are used for tribotests with pin-on-plate geometric configuration to analyze synergistic/antagonistic correlations. Tribotests conditions which include lubricant temperature, applied load, sliding speed are selected in such a way that they replicate cam/tappet interface of direct acting valve train of a passenger car engine. Friction and wear coefficients obtained with formulated TMP is compared those of PAO-based lubricants to evaluate the compatibility of TMP with conventional lubricant additives and DLC coatings. In order to investigate the role of the steel counterbody in tribological interactions of DLC coatings with additives, tribological performance of steel/steel and DLC/steel contact are also evaluated and results are compared with those of DLC/DLC contacts. Moreover, mechanisms responsible for a particular tribological behavior of DLC-lubricant pair, material characterization techniques which include SEM, EDS, Raman spectroscopy, surface profiler are deployed.

In the third phase, DLC coatings selected on the basis of tribotesting are carried forward to test in the original environment of the engine under realistic test conditions using direct acting valve train test rig. The influence of DLC-coated components and formulated TMP on tribological performance of cam/tappet interface of direct acting valve train is investigated by comparing important tribological performance parameters (friction torque, wear, rotational speed of tappet) with uncoated tappet/camlobes contact and PAO-based lubricants. Due to the space constraints, tappets and camlobes are not analyzed using Raman spectroscopy, however, SEM, EDS and surface profiler are used on tappets to understand the boundary lubricant mechanisms. Based on the experimental

results, optimum DLC coatings for cam/tappet interface of direct acting valve train application is selected and potential of TMP as lubricant base oil has been explored.

1.5 Structure of the Thesis

This thesis is comprised of 5 chapters. The overall structure of this PhD thesis is as follows:

Chapter 1 begins with a brief overview of the problems which automotive manufacturers are facing nowadays and their potential solutions. Some basic theories related to the research area are discussed in ample detail. In the end, details of the research work such as objectives, problem statement and scope are given.

Chapter 2 contains a thorough literature review about DLC coatings which encompasses their tribological interaction with lubricant additives and present state of the research. After that, influence of intrinsic and extrinsic conditions on the tribological performance of DLC coating, in combination with formulated lubricants, has been discussed in detail. Moreover, experimental studies, carried out with uncoated and DLC-coated tappets and camshafts in the past, are also reviewed.

Chapter 3 describes the materials and experimental techniques used in the research work. It also discusses the methodology including apparatuses, test conditions, specifications and procedures used for performing tribotests, cylinder head testing and material characterization to achieve the intended objectives of this study

Chapter 4 is the core of this thesis and contains all the results as well as important findings of this research work. This includes tribotesting and cylinder head testing of various types of DLC coatings in combination with PAO-based and TMP-based lubricants. In addition to that, analysis and discussion based on the results of material characterization techniques is also presented.

Chapter 5 concludes this thesis by summarizing the important findings of the experimental studies based on the results and discussions. It also contains suggestions for future research in the field of DLC coatings.

CHAPTER 2: LITERATURE REVIEW

2.1 Introduction

In this chapter, effects of lubricant formulations on tribological performance parameters of non-doped and doped-DLC coatings are presented. A special emphasis is laid upon the investigation of the mechanisms responsible for a particular tribological behavior. Average values of friction and wear coefficients are calculated from the already published data and compared for each DLC–lubricant combination. The experimental studies that are considered to calculate tribological parameters of a particular DLC type have been mentioned in the captions of friction and wear graphs. In addition to that, influence of intrinsic and extrinsic conditions on the tribological characteristics of various DLC coatings under lubricated condition is also discussed in details. Moreover, findings of the studies, in which suitability of various types of DLC coatings for cam/tappet interface of direct acting valve train assembly of passenger car engine were evaluated using original valve train components, are also deliberated.

2.2 Background theories

A tribological system or tribosystem comprised of interacting surfaces, contact area or interface, medium at the interface and operating conditions (Mang, Bobzin, & Bartels, 2011). Interacting surfaces or bodies can be in the shape of plates, spheres or cylinders, sliding or rolling on each other to transmit input energy to subsequent assembly. The relative motion of these bodies can be reciprocatory, rotary or combination of both. Contact area or interface can be point, line or area depending upon the geometric configuration of interacting bodies. If spherical body slides over plate, contact area will be categorized as “point” whereas it will either “line” or “area” in case of cylindrical body depending upon its orientation. Some of the most commonly used geometric configurations used in industrial applications are shown in **Figure 2.1**.

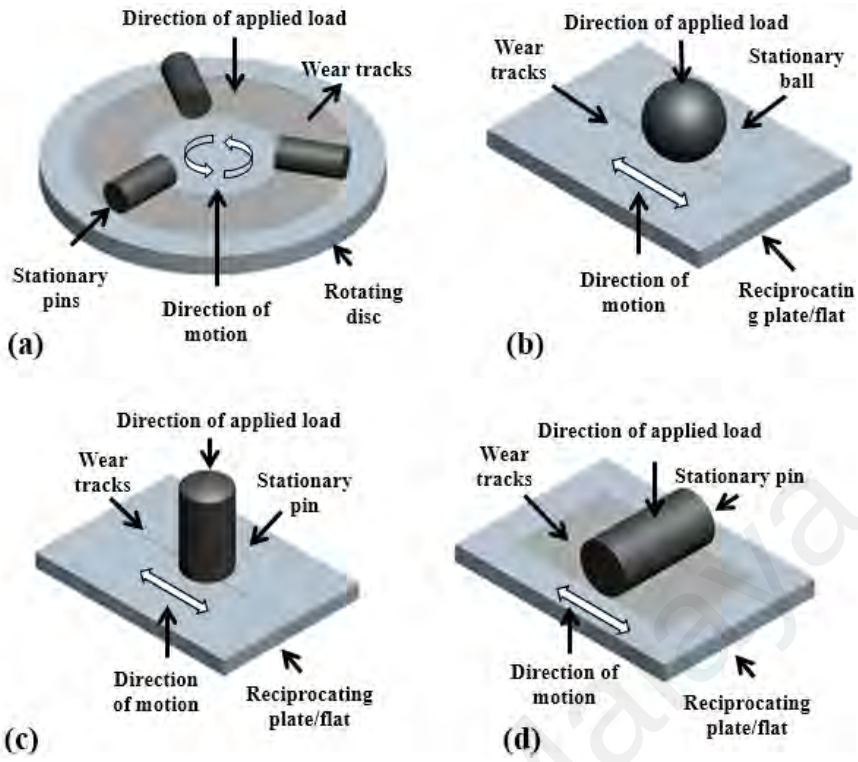

Figure 2.1: Most widely used geometry configurations: (a) pin-on-disc (b) ball-on-plate (c) pin-on-plate (vertical) (d) pin-on-plate (horizontal)

An interface medium is used to facilitate sliding by keeping the friction and wear of interacting bodies at minimum level. It can either be solid, liquid or gas. Most commonly used interface medium in industrial applications is petroleum-based lubricants formulated with multi-functional additives. Hard coatings such as DLC are also considered to enhance the tribological characteristics of contact due to their ultra-low friction and extreme wear resistance. Operating conditions also play an important role in defining the efficiency of a tribosystem. Some of the most influential conditions include temperature, applied load or hertzian contact pressure, humidity and sliding speed.

2.2.1 Tribological performance parameters

Performance enhancement of a tribosystem can be related to tribochemical interaction between lubricant and interacting bodies which include physical adsorbtion/desorption, chemical reaction or combination of both. Usually these interactions result in improved

tribological performance, but sometimes negative implications can also be observed. In order to compare the efficiency of various tribosystem, friction and wear coefficients are two most important performance parameters which are usually deliberated and compared.

2.2.1.1 Coefficient of Friction

Friction can be defined as a force which resists the motion of surfaces in contact. Although, friction is usually considered as an unacceptable phenomenon but its existence is very necessary for perform even very simple daily life activities such as walking, car braking etc. However, high levels of friction are undesirable in industrial applications because a lot of input energy is wasted in overcoming it. Moreover, friction accelerates the wearing out of interacting bodies which not only affects their reliability and overall functionality of the assembly, but also results in shortened maintenance intervals. In the field of tribology, friction is often presented as coefficient of friction (μ) which is actually a ratio of friction force to normal load. Mathematically, it can be represented as:

$$\boldsymbol{\mu = \frac{F}{N}} \qquad \textbf{2.1}$$

where, μ is coefficient of friction, F is frictional force and N is normal load.

2.2.1.2 Coefficient of Wear

Wear can be defined as gradual damage, deterioration and/or reduction in volume of a substance due to its continuous sliding, attrition, friction, exposure to atmospheric or other naturally destructive species. Although, friction is one of the most influential factor which determines the rate of wear, but tribochemical reactions can also play a significant role. Tribochemical interactions of sliding surfaces with environmental specifies (moisture, oxygen etc.) and lubricant additives are more relevant while discussing wear performance of DLC coatings due to their inherent non-reactive nature compared to conventional materials such as iron, aluminum, copper etc. Moreover, extrinsic conditions such as

sliding speed, sliding distance, applied load, temperature can also alter wear characteristics of a contact. In order to quantify the performance of tribosystems, coefficient of wear is generally used which can be mathematically expressed as:

$$\boldsymbol{k = \frac{V}{F\,s}} \qquad \textbf{2.2}$$

where, k is coefficient of wear, V is the wear volume, F is the applied load and s is the sliding distance.

2.2.2 Lubrication regimes

In modern industrial applications, lubrication of tribopairs, involved in the functioning of a machine, is mandatory to withstand extreme operating conditions and perform the intended role in the most efficient way possible without any failures. Lubricants not only reduce the friction of a contact and improve the reliability of interacting surfaces by improving their wear resistance but also help in dissipating heat, inhibiting corrosion, removing wear debris and helping in carrying load. Depending upon the physical state, lubricants can be categorized into two types i.e. solid lubricants and fluid lubricants. Solid lubricants have inherent self-lubricating capability due to their layered structure. They reside between the interacting surfaces and facilities sliding because of their low-shear strength (Zahid et al., 2015). Some of the most commonly used solid lubricants include molybdenum disulfide and graphite. As the name suggests, fluid lubricants can either be in the form of liquids or gases. All of the conventional automotive lubricants (engine oil, gear oil, transmission oil) fall in this category.

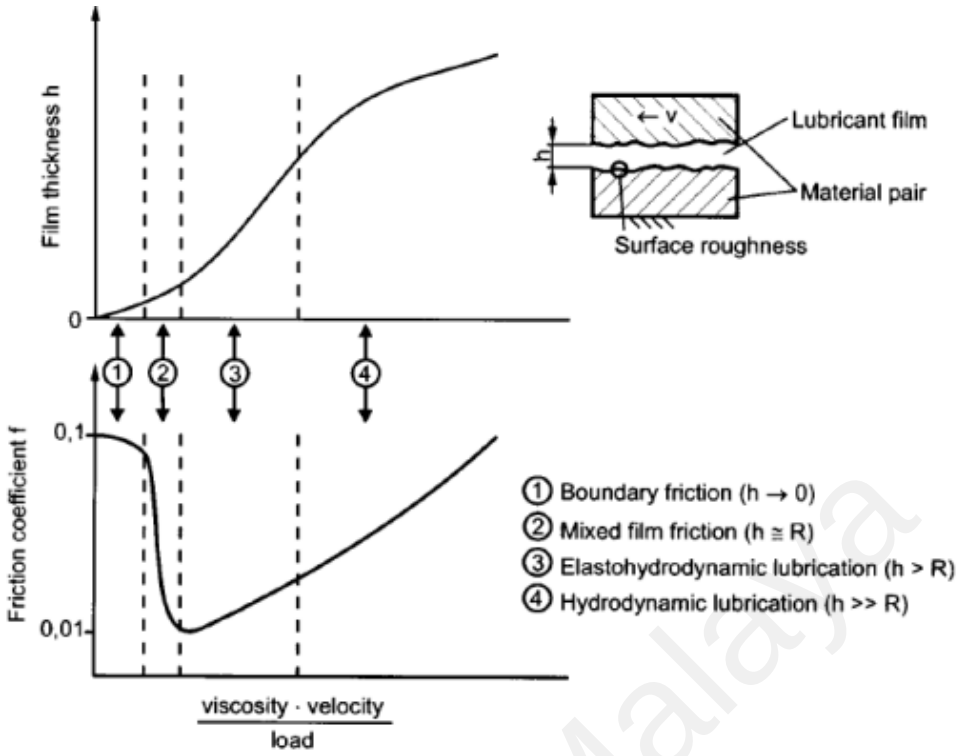

Figure 2.2: Stribeck curve which relates coefficient of friction of a tribosystem to its operating conditions (Czichos & Habig, 1992)

Lubrication modes or regimes are graphically illustrated by Stribeck curve which relates coefficient of friction to Sommerfeld number, a dimensionless parameter which represents operating conditions of a contact (Figure 2.2). Sommerfeld number is a ratio of product of lubricant viscosity and contact velocity to applied load. In another variant of Stribeck curve, coefficient of friction is related to a dimensionless film parameter, which is a ratio of minimum film thickness to roughness of interacting surfaces. In this stribeck curve, dimensionless film parameter is shown on x-axis whereas film thickness is shown on y-axis. Stribeck curve is divided into 4 sections and each section represent different lubrication regimes which are boundary, mixed, elastohydrodynamic and hydrodynamic.

2.2.2.1 Boundary lubrication

In this lubrication mode, interacting surfaces are directly in contact with negligible film thickness residing between them (Neale, 1995). It happens when lubricant slips out of the contact during sliding due to unfavorable operating conditions (low lubricant viscosity, heavier applied loads and slow relative speeds) and/or mechanical design constraints. Since, there is no lubricant cushion between the surface asperities, therefore, high level of friction and wear are experienced in this mode of lubrication compared to other. Lubricant additives can play an important role in this scenario by tribochemically interacting with the contact surfaces and forming lubricant derived tribofilms. These films not only keep the frictional forces to a minimum level and facilitate sliding but also prevent the interacting surfaces from deterioration. Some of the most commonly used boundary lubrication additives include friction modifiers, antiwear additives and extreme pressure additives (Podgornik et al., 2006). Surface modification techniques such as deposition of hard coatings having self-lubrication ability and surface texturing can also prove to be helpful in such conditions.

2.2.2.2 Mixed lubrication

Mixed lubrication regime is actually a transition from boundary lubrication to fluid-film lubrication regimes i.e. elastohydrodynamic and hydrodynamic lubrication. In mixed lubrication regime, lubrication film is largely present between the interacting surfaces but some asperities remains in contact with each other (Bhushan, 2013). If there are frequent asperity contacts at the interfere, mixed lubrication can also result in high values of friction and wear coefficients like boundary lubrication regime. This lubrication regime is mostly experienced at the start and stop of machines having hydrodynamic lubrication regime. There is an increased likelihood of slippage of lubricant from the contact at high operating temperatures due to decrease in viscosity of lubricant due to which hydrodynamic lubrication can changed into mixed lubrication.

2.2.2.3 Elastohydrodynamic lubrication

Although, elastohydrodynamic lubrication is a separate lubrication regime but sometimes it is considered as a subset of hydrodynamic lubrication. In elastohydrodynamic regime, although a thin film (0.5 – 5 mm thickness) of lubricant exists between the interacting surfaces but heavier localized applied load increases the lubricant viscosity and elastically deform the contact area. If the load is further increased, lubricant slips out of the contact area and asperities of interacting surface come directly in contact with each other and regime changes to boundary lubrication.

2.2.2.4 Hydrodynamic lubrication

Hydrodynamic lubrication is considered as ideal lubrication regime. It occurs when a thick lubrication film completely separates the interacting surfaces. Lubrication film not only prevent direct asperity contacts but also supports the applied load without slipping out of the contact. Contrary to elastohydrodynamic regime, lubricant properties such as viscosity and density remains constant and determines the tribological characteristics of a contact. Since, interacting surface are physically separated from each other therefore, hydrodynamic lubrication results in ultra-low friction and high wear resistance of a contact.

2.2.3 DLC coatings

Due to heavier applied loads and higher temperatures, viscosity of the lubricants decreases during operation and it slips out of the contact causing intensified friction and severe damage to the components. These catastrophic failures can be avoided by using surface protective coatings possessing high hardness and self-lubrication capability such as DLCs. In the last few decades, DLC coatings have attracted much attention of various industries and research groups from all over the world (**Figure 2.3**)**.** This increase in demand can be attributed to the outstanding physical and chemical properties of DLC

coatings which make them suitable for a lot of industrial applications especially those involving boundary lubricant regime. Low coefficient of friction, high resistance against wear, increased hardness and stability against environmental species are some of the distinguish characteristics of DLC coatings (Love, Cook, Harvey, Dearnley, & Wood, 2013). Another benefit of DLC coatings is that they can be deposited on literally any engineering material ranging from metals and non-metals to ceramics and metalloids. The lubricity of DLC coatings can be further enhanced by using lubricants which can physically adsorb on the interacting surfaces due to their polar components and unsaturated structure such as vegetable oils (Barriga et al., 2006; Kalin & Vižintin, 2006a).

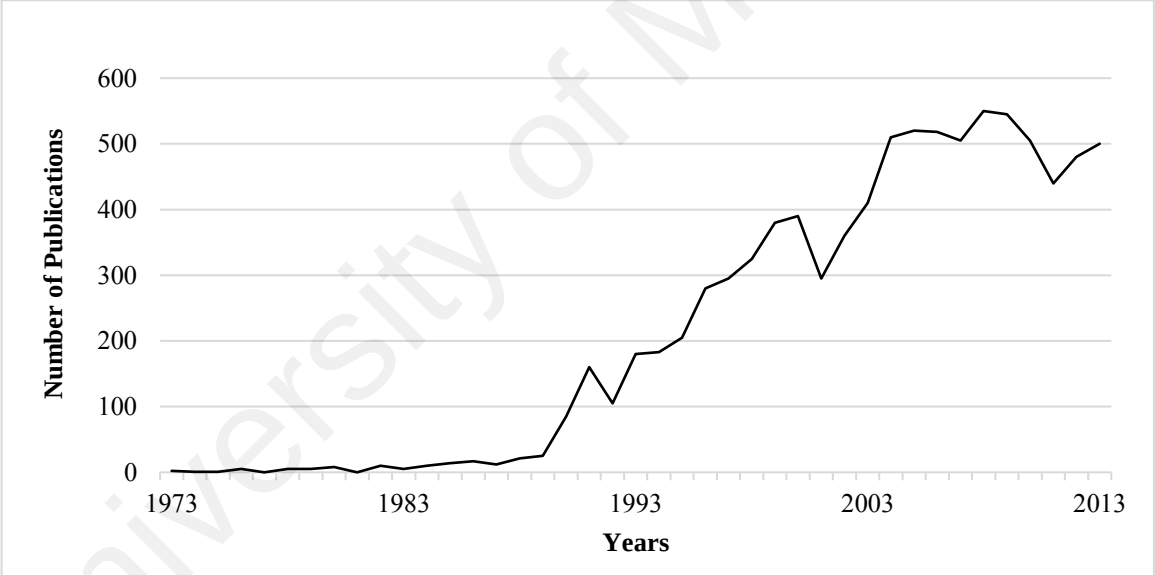

Figure 2.3: Annual number of publications on DLC coatings from 1970 to 2013 (Bewilogua & Hofmann, 2014)

2.2.3.1 Classification of DLC coatings

Nowadays, many variants of DLC coatings are available commercially as a result of various deposition techniques developed in the last few decades, In addition to that, researchers also succeeded in achieving application specific DLC coatings by tweaking the deposition parameters and using various hydrocarbons as carbon precursors

(Andersson, Berg, Norström, Olaison, & Towta, 1979). Although, DLC coatings can be classified in many ways, but the most appropriate and most widely accepted arrangement is based upon the presence or absence of foreign elements other than carbon and hydrogen in their structure. Those DLC coatings which have either metals or non-metals in their structure are known as doped-DLC coatings whereas those consists of only carbon and hydrogen atoms bonded with each other are called non-doped-DLC coatings. There is another type of DLC coatings named multilayered-DLC coating (ML-DLC) that is recently developed to combine the benefits of both doped and non-doped-DLC coatings in a single material. ML-DLC coatings generally have a top layer of doped-DLC coatings (a-C:H:W or a-C:H:WC) followed by non-doped-DLC coatings such as a-C:H or hydrogen-free amorphous (a-C) DLC coatings and then stacking of this coating pair several times. In some of the studies, ML-DLCs with a top layer of non-doped-DLC coating are also tribologically investigated to compare them with other types (Kim & Kim, 2013). ML-DLC coatings have the ability of distributing the applied load uniformly on the contact area and have superior load-carrying capacity as compared to doped and non-doped DLC coatings.

Hydrogen concentration is another important criterion by which DLC coatings can be further classified, especially non-doped DLCs. Extraordinary tribological and mechanical characteristics which distinguish DLC coatings from other materials such as high hardness and ultra-low friction are heavily dependent on concentration of hydrogen atoms within the DLC structure (Erdemir, Eryilmaz, & Kim, 2014). Non-doped DLC coatings which have hydrogen content of less than 1.0 at.% are called hydrogen-free DLC coatings whereas those with higher concentration of hydrogen atoms in their structure are known as hydrogenated DLCs (Erdemir, 2001). Since, doped-DLC coatings are generally rich in hydrogen content, therefore, they cannot be classified on this basis. The only way to further subdivide non-doped DLC coatings into different types is by the chemical nature

of dopant elements. Doped-DLC coatings which are manufactured by doping with metals [chromium (Cr), titanium (Ti), tungsten (W)] are known as metal-doped DLC coatings whereas those in which non-metals [fluorine (F), nitrogen (N), silicon (Si)] are used as dopants are denoted as non-metal-doped DLC coatings. Doping of DLC coatings with metals increased their chemical reactivity with the lubricant constituents and counterbodies making them suitable for various industrial applications in which tribochemical interaction between lubricant and contact is mandatory for optimum tribological performance. Non-metals such as silicon and fluorine improve the service life of DLC coatings by reducing the internal stresses entrapped during synthesis (Grill, 1999b; Robertson, 2002). Moreover, non-metal doping can also prove to be effective in altering the sp^3/sp^2 content of DLC coatings. By doing so, tribological properties of DLC coatings can be controlled and inclined towards either diamond or graphite (Park et al., 2012). The above-mentioned classification of DLC coatings is graphically presented in **Figure 2.4**.

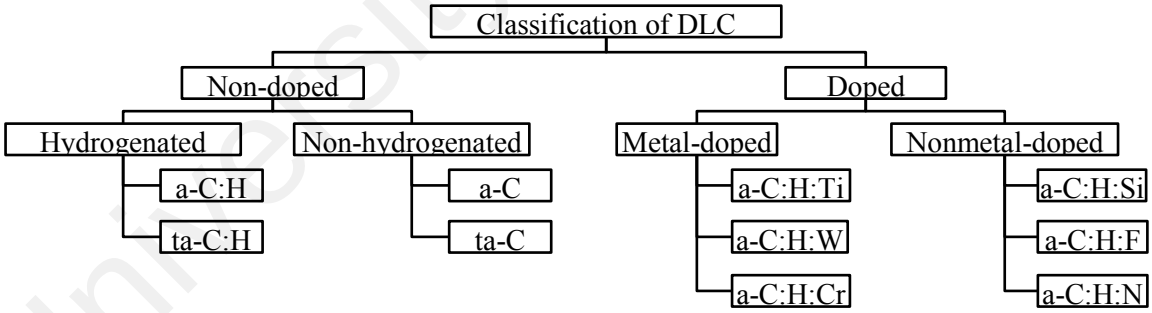

Figure 2.4: Classification of DLC coatings
(Kalin et al., 2008)

2.2.3.2 Industrial Applications of DLC coatings

Due to cut-throat competition among the rivals, industrial sectors are striving hard to run their businesses in the most efficient way possible. In order to gain the competitive edge over their competitors, manufacturers are trying hard to fabricate such products

which not only fulfill the customer requirements but also go beyond their expectations. In order to do this, there is a need to replace the conventional engineering materials with the most advanced ones which can withstand severe operating conditions such as elevated temperatures, high pressures, immense applied loads, hazardous environments and starved lubrication. Because of extensive research carried out on their development in the last few decades and due to their extraordinary mechanical, tribological and optical properties, DLC coatings are emerged as one such material. Nowadays, applications of DLC coatings can be found in almost every industry ranging from microelectromechanical systems, electronics, mechanical equipment to optics, manufacturing, biomedical systems (Erdemir & Donnet, 2006; Kalin et al., 2008; Ouyang, Sasaki, Murakami, Zhou, & Zhang, 2009). In 1973, DLC coatings found their first application on eyeglasses and paper cutting blades. Later on, these coatings become integral part of razor blades to protect them from corrosion and increase their service life (Erdemir & Donnet, 2006; Hauert, 2004). A decrease in friction coefficient was observed with the use of DLC-coated blades as compared to the uncoated ones (Aisenberg & Chabot, 1973). In the field of optics, DLC coatings are employed in the production of antireflective and scratch-resistance glasses (Grill, 1999a). Moreover, DLC coatings are also used to improve the resistance of contact lenses against abrasive wear (Kimock & Knapp, 1993). DLC coatings also proved to be very helpful for a number of automotive applications **(Figure 2.5)**. Some of the engine parts and assemblies which showed improved tribological performance after depositing DLC coatings include fuel injection system (Erdemir & Donnet, 2006; Lawes, Fitzpatrick, & Hainsworth, 2007; Vengudusamy, Grafl, & Preinfalk, 2014b), piston assembly (Cho, Lee, & Lee, 2009; Etsion, Halperin, & Becker, 2006; Tung & Gao, 2003), bearings (Franklin & Baranowska, 2007; Vanhulsel et al., 2007), valve train assembly (Gangopadhyay et al., 2012; Gangopadhyay et al., 2011; Kano, 2006; Lawes, Hainsworth, & Fitzpatrick, 2010;

Mabuchi, Hamada, Izumi, & Yasuda, 2007; Schamel et al., 1997; Yasuada, 2003) and gears (Kalin & Vižintin, 2005; Snidle & Evans, 2009). Because of their biocompatibility and outstanding material properties such as high hardness, low friction, corrosion resistance and moderate wear of counterbodies, DLC coatings found number of applications in the field of biomedical engineering (Dearnaley & Arps, 2005). An extensive research is going on to optimize DLC coatings for various biomedical applications such as orthopedic, cardiovascular and dental implants. In the field of manufacturing, DLC coatings found numerous applications ranging from machine tools and mechanical components to injection molding machines (Vandevelde, Vandierendonck, Van Stappen, Du Mong, & Perremans, 1999). DLC-coated parts are frequently used in the manufacturing of medicines, textiles, and edible items in which conventional lubricants cannot be used.

Figure 2.5: Automotive applications of DLC coatings: (a) tappet, (b) camshaft, (c) finger roller follower, (d) camshaft sprocket, (e) piston ring, and (f) piston

2.2.4 Lubricants

Lubricants industry is expected to realize a growth of 2.0 % each year and worldwide consumption of lubricant will reach approximately 45.4 million metric tons by the year

2019 ("World lubricant," 2015). The main constituents of commercially available lubricants are base oils and additives packages (friction modifiers, antiwear /extreme pressure additives, viscosity modifiers etc.). About 85% of the lubricants consumed worldwide are derived from non-renewable and non-biodegradable sources such as petroleum [American Petroleum Institute (API) Group I (A-I), API Group II (A-II), API Group III (A-III)] whereas rest of them are either synthetic [API Group IV (A-IV)] or bio-based [API Group V (A-V)] (Feng & Xia, 2012; Pop, Puşcaş, Bandur, Vlase, & Nuţiu, 2007). In order to meet the energy needs of rapidly developing world, fossil fuel reserves are depleting at a rapid pace and are at the verge of scarcity (Mobarak, Niza Mohamad, et al., 2014). Moreover, there are many environmental and health issues associated with the excessive usage of petroleum-based fuels and lubricants which include air pollution, soil contamination and difficult waste management (Mobarak, Masjuki, et al., 2014). Therefore, there is a need to reduce reliance on conventional lubricants and shift to environmentally sustainable, renewable and biodegradable ones (McNutt & He, 2016).

Although, vegetable oils have tribological characteristics [lubricity, flash point, viscosity index (VI) and evaporative losses] comparable to conventional base oils but they also have some deficiencies (Erhan, Sharma, & Perez, 2006; Liu et al., 2015; Mobarak, Niza Mohamad, et al., 2014; Sharma, Adhvaryu, & Erhan, 2009). Some of the undesirable properties of vegetable oils include oxidation instability, inferior low-temperature characteristics and thermal instability. These shortcomings arise due to the presence of carbon-carbon double bonds in their structure which react with atmospheric oxygen and cause degradation (Wagner, Luther, & Mang, 2001). In order to decrease the inherent unsaturation and improve the low temperature properties of vegetable oils, several chemical modification techniques were used by researchers which include esterification/transesterification (Hamid, Yunus, Rashid, Choong, & Ala'a, 2012; Salimon, Salih, & Yousif, 2011; Uosukainen, Linko, Lämsä, Tervakangas, & Linko,

1998; Yunus, Fakhru'l-Razi, Ooi, Iyuke, & Perez, 2004), estolide formation (García-Zapateiro et al., 2010; García-Zapateiro et al., 2013; Soni & Agarwal, 2014), epoxidation (Doll, Sharma, & Erhan, 2008; Gorla, Kour, Padmaja, Karuna, & Prasad, 2013; Saurabh, Patnaik, Bhagt, & Renge, 2011; Somidi, Sharma, & Dalai, 2014) and partial hydrogenation of carbon double bond (Balakos & Hernandez, 1997; McArdle, Curtin, & Leahy, 2010).

2.3 Bio-lubricants

Bio-based oils are those which are derived from renewable sources such as vegetables, animal fats and waste materials. Vegetable oils were widely used as lubricant till the introduction of petroleum-based oils at the start of 19th century (Choi, Ahn, Kwon, & Chun, 1997). Because of their lower cost, higher thermal stability, improved low temperature characteristics and more resistance to oxidation, petroleum-based oils replaced vegetable oils.

Generally, vegetable oils are used as bio-lubricants. Vegetable oils are mainly composed of triacylglycerides (98%), diglycerides (0.5%), free fatty acids (0.1%), sterols (0.3%), and tocopherols (0.1%) (Rudnick, 2006). In the structure of vegetable oils, various fatty acids are attached to a single triglyceride structure.

If fatty acid is fully saturated, its carbon chain is almost linear. In the absence of adjacent hydrogen atoms, carbon makes double bond with each other. If a carbon-carbon double bond exists in the structure of fatty acid, it is known unsaturated fatty acid and if there are more than one carbon-carbon double bond then its called polyunsaturated fatty acid. Low temperature characteristics and oxidation stability of vegetable oils are dependent upon number of carbon-carbon double bonds in its structure. Fully saturated fatty acids result in inferior low temperature characteristics whereas polyunsaturated fatty acids have poor oxidation stability (Erhan et al., 2006; Hwang & Erhan, 2001)

2.3.1 Sources of bio-lubricants

Vegetable oils can be classified into two categories i.e. edible and inedible. Soybean, sunflower, rapeseed and palm are some of the edible vegetable oils where jatropha, callophyllum inophyllum, neem and karanja can be categorized as inedible vegetable oils. Different regions of the world are using different vegetable oils as environment-friendly lubricants. Sunflower oil and rapeseed oil are very popular in Europe whereas soybean oil is most widely used in USA.

2.3.2 Properties of bio-lubricants

2.3.2.1 Advantages of bio-lubricants

Bio-lubricants have certain characteristics which make them one of the potential candidates for partially or completely substituting conventional base oils. Some of the tribologically favorable properties of vegetable oils include high viscosity, low volatility, high flash point, polar structure, high viscosity index, high detergency, low compressibility and high dispersibility (Nagendramma & Kaul, 2012; Zulkifli, Kalam, Masjuki, Al Mahmud, & Yunus, 2014). Moreover, they are biodegradable, renewable and non-toxic, due to which they can be termed as environmental friendly bio-lubricants (Campanella, Rustoy, Baldessari, & Baltanas, 2010).

2.3.2.2 Disadvantages of bio-lubricants

Despite of excellent tribological characteristics, there are some deficiencies associated with vegetable oils.

One of the major shortcomings of vegetable oils are their inferior pour point properties. Pour point can be defined as the lowest temperature at which a lubricant can flow without solidification. It is mentioned in the literature that some of the vegetable oil loses their flow characteristics at –10ºC if they are exposed to cold temperature for long (Quinchia, Delgado, Franco, Spikes, & Gallegos, 2012). In an experimental investigation, N. Jayadas

and Nair (2006) found that vegetable oils with high percentages of unsaturated fatty acids have low pour points. Low temperature characteristics of vegetable oils can be enhanced by introducing branched or aromatic hydrocarbon molecules of high molecular weight in their structure.

Another factor which refrains vegetable oils from using them as lubricants is their inferior oxidation stability. Due to the presence of carbon double bonds in their structure, fatty acids react with the atmospheric oxygen resulting into the polymerization, degradation and formation of radicals. Viscosity of vegetable oils increases with the increase in extent of polymerization due to which their lubricity decreases (Suda, Yokota, Inasaki, & Wakabayashi, 2002). Degradation leads to breakdown products that are volatile and corrosive, and weakens lubricant structure and properties.

2.3.3 Chemical modification of vegetable oil

In order to decrease the inherent unsaturation and improve the low temperature properties of vegetable oils, several chemical modification techniques were used by researchers which include esterification/transesterification (Hamid et al., 2012; Salimon et al., 2011; Uosukainen et al., 1998; Yunus et al., 2004), estolide formation (García-Zapateiro et al., 2010; García-Zapateiro et al., 2013; Soni & Agarwal, 2014), epoxidation (Doll et al., 2008; Gorla et al., 2013; Saurabh et al., 2011; Somidi et al., 2014) and partial hydrogenation of carbon double bond (Balakos & Hernandez, 1997; McArdle et al., 2010). Out of these techniques, transesterification using TMP is one of the most effective method of improving inherent characteristics of bio-lubricants

2.3.3.1 Transesterification

In order to improve the thermo-oxidative stability and low temperature characteristics of bio-lubricants, they are chemically modified by transesterification process. During the transesterification process, vegetable oils is first converted into its methyl ester and then

reacted with polyol. Due to its low melting point, TMP [2-ethyl-2-hydroxymethyl-1,3-propanediol] is often considered as the best option During the transesterification process, ester (-COOR-) group from the vegetable oil is replaced by hydroxyl (-OH-) group. Since, TMP has three -OH groups in its structure, therefore, monoesters, diesters and triesters were formed as a result of transesterification process with majority of triesters fatty acids. In order to minimize the saponification of ester, catalyst such as sodium methoxide are also used during the transesterification process.

2.4 Tribological interaction between doped-DLC coatings and conventional lubricant additives

2.4.1 a-C:H:Ti/a-C:H:Ti contact

Figure 2.6 shows average values of friction coefficient for self-mated Titanium-doped DLC coating (a-C:H:Ti) coatings with different formulated lubricants, calculated from already published data (de Barros'Bouchet, Martin, Le-Mogne, & Vacher, 2005; Kalin, Roman, Ožbolt, & Vižintin, 2010; Kalin et al., 2004). In **Figure 2.6a**, friction values of additive-free base oils are shown, whereas the effectiveness of additives in reducing friction is illustrated in **Figure 2.6b**. In additive-free base oil, PAO gives significantly lower values of friction than M. One possible reason for such behavior can be a tribologically beneficial interaction between PAO and self-mated a-C:H:Ti contact. Tribotest parameters, such as applied load, Hertzian contact pressure, sliding velocity, and temperature, can directly influence the tribological performance of a contact (Erdemir & Donnet, 2006). Given that test conditions used in de Barros'Bouchet et al. (2005), Kalin et al. (2004) and Kalin et al. (2010) are almost identical, one can safely state that lower friction values obtained with PAO are due to its better lubricity compared with M.

Formulation with MoDTC and ZDDP further improved the friction performance of PAO, resulting in the lowest values for symmetrical a-C:H:Ti contacts. This improvement

in friction performance can be attributed to the formation of molybdenum disulfide (MoS_2). According to the literature, decomposition of MoDTC results in the formation of MoS_2 and molybdenum trioxide (MoO_3) (de Barros'Bouchet et al., 2005; Haque, Morina, Neville, Kapadia, & Arrowsmith, 2007; Kosarieh, Morina, Lainé, Flemming, & Neville, 2013a; Vengudusamy, Green, Lamb, & Spikes, 2012). Given its low shear strength, MoS_2 facilitates the sliding of interacting surfaces, resulting in low values of friction (Kalin, Kogovšek, Kovač, & Remškar, 2014), whereas MoO_3 has no such characteristics because of its sharp edge crystalline structure (Haque et al., 2007). MoDTC can only be effective in reducing friction if its decomposition results in a higher ratio of MoS_2 compared with MoO_3 (Haque et al., 2007). Presence of ZDDP in PAO along with MoDTC further improves the friction performance of self-mated a-C:H:Ti contacts by providing sulfur for complete decomposition of MoDTC and promoting the formation of MoS_2 (de Barros'Bouchet et al., 2005). A positive effect on running-in behavior was also observed with PAO+MoDTC, and steady-state friction values were achieved after a few meters of sliding (de Barros'Bouchet et al., 2005). By contrast, formulation with AP had an adverse effect on the friction performance of M, resulting in a slight increase. This behavior can be associated with detrimental interactions of Ti-doped DLC with AP because of the availability of titanium in oxidation state, which results in deterioration of the interacting surfaces (Kalin et al., 2010; Kalin et al., 2004). Although doping of DLC with titanium increased the polarity and surface activity, no beneficial tribofilm possessing low shear strength was detected (Kalin et al., 2004).

Although, certain tribochemical interaction between titanium-doped DLC and M+ZDDP resulting in increase in phosphorus/sulfur (P/S) ratio of ZDDP from 0.5 to 12.8 after the tribotest was observed by Kalin et al. (2010) but no effect of this interaction was seen on the friction coefficient.

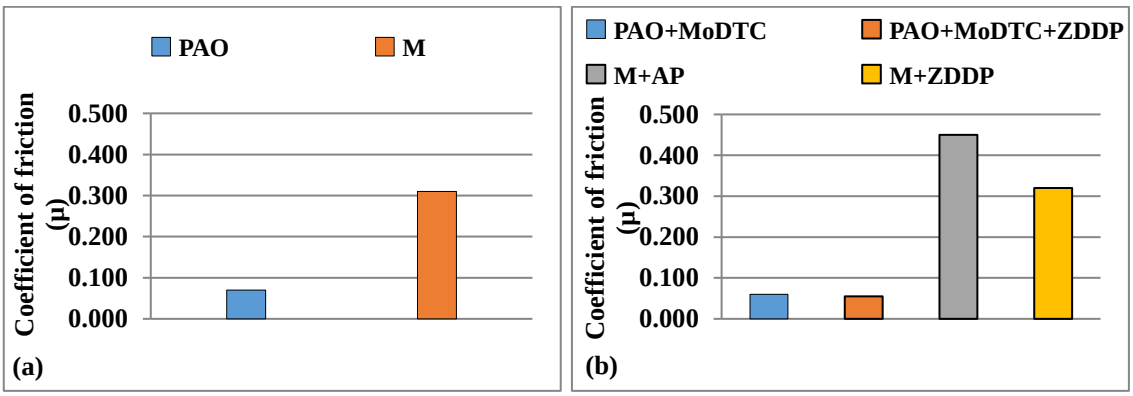

Figure 2.6: Average values of coefficient of friction for a-C:H:Ti/a-C:H:Ti contact with (a) base oils and (b) formulated lubricants (de Barros'Bouchet et al., 2005; Kalin et al., 2010; Kalin et al., 2004)

Average wear coefficients of a-C:H:Ti/a-C:H:Ti contacts in combination with different lubricants are shown in **Figure 2.7**, which shows substantial differences in the wear performance of PAO and M. The average wear coefficient obtained with PAO was almost twenty-five times less than that of M (**Figure 2.7a**). This finding can be attributed to less adsorption and slippage of lubricant from the contact because of the non-polar nature of M (Kalin et al., 2008). Unavailability of the lubricant in the contact and high affinity of similar a-C:H:Ti-coated surfaces toward each other result in increased adhesive wear (Kalin et al., 2010). Another factor that can be related to the high wear coefficients of M is delamination of a-C:H:Ti because of coating spallation (Kalin et al., 2004). Similar to friction, positive effects of PAO+MoDTC and PAO+MoDTC+ZDDP lubricants were also noted on the wear performance of symmetrical a-C:H:Ti contact (**Figure 2.7b**). Mixing of additives also proved to be helpful in improving the wear behavior of M by preventing coating spallation and delamination (Kalin et al., 2004). ZDDP proved to be more efficient on self-mated a-C:H:Ti contacts in reducing the wear compared with AP, when mixed with M.

Based on the aforementioned observations, it can be concluded that PAO is tribologically more beneficial for a-C:H:Ti/a-C:H:Ti contacts compared with M in both

additive-free and formulated forms. Among the additives, MoDTC showed better performance in further enhancing the friction and wear characteristics of self-mated a-C:H:Ti coatings.

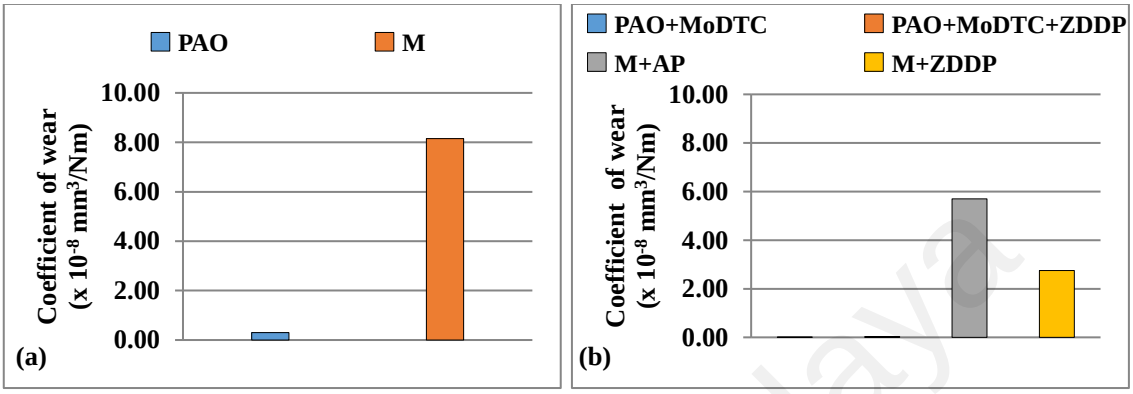

Figure 2.7: Average values of coefficient of wear for a-C:H:Ti/a-C:H:Ti contact with (a) base oils and (b) formulated lubricants
(de Barros'Bouchet et al., 2005; Kalin et al., 2010; Kalin et al., 2004)

2.4.2 a-C:H:W/a-C:H:W contact

It is one of the most widely investigated types of DLC coatings. Average friction coefficients of self-mated a-C:H:W with different base oils and their formulated versions are shown in **Figure 2.8** (Kalin et al., 2010; Kalin et al., 2004; Kržan et al., 2009; Vengudusamy, Green, Lamb, & Spikes, 2011; Vengudusamy et al., 2012; Vengudusamy, Green, Lamb, & Spikes, 2013a, 2013b; Vengudusamy, Mufti, Lamb, Green, & Spikes, 2011). Among the base oils, the highest friction was observed with M, whereas A-III and RO gave the lowest values. Friction values obtained for PAO and A-II were between those of M and RO. Friction values of PAO, A-II, and RO are taken from the experimental study carried out by Kržan et al. (2009) using identical test conditions and equipment; therefore, they can be directly compared. The mechanisms behind the high friction values of M can be explained by the same reasoning provided for symmetrical a-C:H:Ti contacts. Effects of tungsten concentration and sliding velocity on the friction properties of symmetrical a-C:H:W contacts were investigated by Vengudusamy, Mufti, et al. (2011)

and Vengudusamy et al. (2013b). They found that the lowest value of friction can be obtained when a-C:H:W coating is doped with 18 at.% of tungsten irrespective of sliding velocity. An inverse relation between sliding velocity and coefficient of friction was also observed.

Friction values either increase or change negligibly with formulated lubricants (**Figure 2.8b**). The only exception to this conclusion is A-III+MoDTC, which gave the lowest value by reducing the friction coefficient from 0.077 to 0.045. This value is almost 40% less compared with that calculated for A-III by taking the average of friction coefficients at different sliding velocities and concentrations of tungsten. This remarkable reduction in friction is assumed to be due to the formation of tungsten disulfide (WS_2), which promotes the production of MoS_2 layer as a result of MoDTC decomposition (Vengudusamy et al., 2012). Differences in friction performances were observed when base oils were formulated with ZDDP. Mixing of ZDDP with PAO and M resulted in a minute decrease in friction, whereas degradation in friction performance was noted with A-III+ZDDP and RO+ZDDP. When A-III+ZDDP lubricant was used, a tribochemical interaction between a-C:H:W and additive was confirmed by EDS and SEM. This interaction resulted in the formation of pad-like tribofilm rich in phosphorus, sulfur, and zinc, but no significant effect of this tribochemical interaction was observed on the coefficient of friction (Vengudusamy, Green, et al., 2011). A study was carried out by Vengudusamy et al. (2013a), in which durability of ZDDP-derived tribofilm on DLC surfaces was analyzed using Stribeck curves. Initially, experiments were performed using A-III, with and without ZDDP, to obtain the reference friction curves. Subsequently, DLC surfaces, which had ZDDP-derived tribofilms, were tested again with A-III for 2 hours. Symmetrical a-C:H:W contact was able to maintain the friction values obtained using ZDDP containing lubricant, which shows strong adherence of ZDDP-derived tribochemical products on a-C:H:W. When Raman spectroscopy was carried out, no

evidence of surface graphitization was detected and no positive effect on friction was observed. A negative effect on friction performance was also observed when AP was used in combination with M, resulting in an increase of around 12.5%. This result can be attributed to the synthesis of tribochemical product possessing high shear strength because of the tribochemical interaction between tungsten and lubricant additive, resulting in increased friction (Kalin et al., 2004). These observations demonstrated that a synergistic relation should exist between base oils, additives, and interacting surfaces to construct a tribologically efficient system (Kržan et al., 2009).

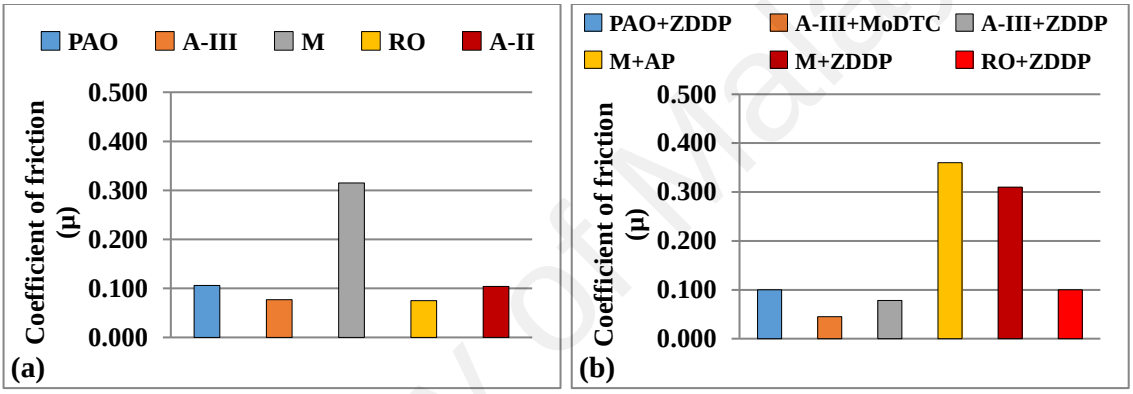

Figure 2.8: Average values of coefficient of friction for a-C:H:W/a-C:H:W contact with (a) base oils and (b) formulated lubricants
(Kalin et al., 2010; Kalin et al., 2004; Kržan et al., 2009; Vengudusamy, Green, et al., 2011; Vengudusamy et al., 2012, 2013a, 2013b; Vengudusamy, Mufti, et al., 2011)

In **Figure 2.9**, wear coefficients of a-C:H:W/a-C:H:W contacts with different lubricants are shown. In base oils, lowest wear coefficient values were observed with RO and A-III, whereas M offered the highest friction because of extreme wearing of sliding surfaces (**Figure 2.9a**). PAO and A-II were also unable to effectively control the wearing of interacting a-C:H:W-coated surfaces. Effectiveness of RO in reducing wear can be attributed to its unsaturated structure and polar nature, which results in its adsorption on a-C:H:W-coated surfaces and prevents metal-to-metal contact (Kržan et al., 2009). Inversely, no interaction was observed between lubricant and surfaces in contact because

of the non-polar nature of PAO. Although complete delamination of DLC coatings did not occur, high wear rates were observed because of abrasive wear (Kržan et al., 2009). Similarly, excessive wearing observed with M can be attributed to the wearing through of coated surfaces and coating spallation (Kalin et al., 2004). In case of A-III, graphitization of a-C:H:W-coated surfaces was observed (Kalin et al., 2010; Vengudusamy, Green, et al., 2011; Vengudusamy et al., 2012). Surface graphitization usually results in low coefficient of friction (Wang, Bai, Lu, Zhang, & Wu, 2013) and comparatively higher wear, but lower values of wear coefficients were attained with A-III compared with those of PAO, A-II, and M.

No meaningful effect on wear was observed when PAO was formulated with ZDDP (**Figure 2.9b**). Contrary to that, ZDDP reduced the wear of a-C:H:W/a-C:H:W contact to almost one-sixth when mixed with M, compared with its additive-free version. This improvement in wear performance can be related to the eradication of plastic deformation and adhesive wear caused by the presence of ZDDP-derived tribochemical products on interacting surfaces (Kalin et al., 2010). Similarly, formulation of M with AP also improved the wear resistance of self-mated a-C:H:W coatings, which then prevent coating spallation, but it was not as effective as ZDDP in countering wear. Given that mixing of additives in M resulted in the prevention of coating spallation, coating spallation is more related to wear resistance than adhesion strength between DLC coating and substrate (Kalin et al., 2004). Reduction in wear coefficient was also observed when A-III+ZDDP was used as a lubricant because of tribochemical interactions between a-C:H:W-coated surfaces and ZDDP, which resulted in the formation of pad-like additive-derived tribofilm possessing low shear strength (Vengudusamy, Green, et al., 2011). Hindrance in the occurrence of surface graphitization phenomenon caused by the presence of ZDDP can also be one of the reasons responsible for the improvement in wear behavior (Kalin, Roman, & Vižintin, 2007; Kosarieh, Morina, Lainé, Flemming, & Neville, 2013b;

Vengudusamy, Grafl, & Preinfalk, 2014a). MoDTC improved the wear performance of symmetrical a-C:H:Ti contacts when mixed with PAO **(Figure 2.7b**); however, no such behavior was observed when it was used in combination with A-III. A trivial increase in wear coefficient was observed compared with its additive-free version. Based on the literature, formulation of MoDTC in base oil can drastically increase the wear rates of a-C:H:W/steel contacts (Shinyoshi, Fuwa, & Ozaki, 2007), and presence of ZDDP can alleviate this effect (Haque, Morina, Neville, Kapadia, & Arrowsmith, 2009). A possible reason for this effect can be tribochemical interactions between MoO_3 and active sites of a-C:H:W surface (Shinyoshi et al., 2007), but this negative impact of MoDTC was not observed in symmetrical a-C:H:W contacts. Therefore, MoDTC has neither positive nor negative effect on the wear performance of symmetrical a-C:H:W contacts when mixed with A-III. Mixing of ZDDP with RO resulted in increased wear compared with its additive-free version, but RO+ZDDP offered the lowest wear coefficient among formulated lubricants with a-C:H:W/a-C:H:W contacts.

In view of the above discussion, it can be summarized that the lowest values of friction and wear coefficients can be achieved with RO among the base oils. The only drawback associated with highly unsaturated biodegradable bio-based lubricants, such as RO, is that they have low oxidation stability, which limits their applications. With most base oils, ZDDP not only plays a key role by improving wear performance but also proves to be helpful in reducing friction.

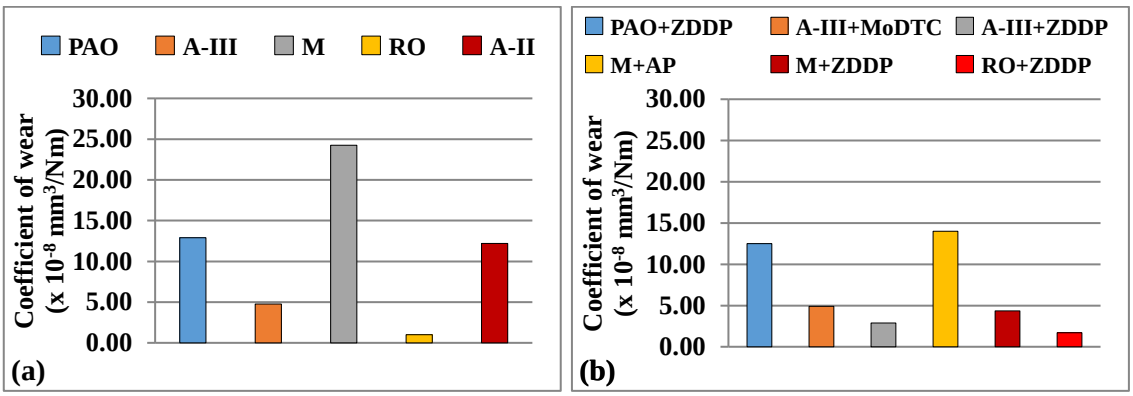

Figure 2.9: Average values of coefficient of wear for a-C:H:W/a-C:H:W contact with (a) base oils and (b) formulated lubricants
(Kalin et al., 2010; Kalin et al., 2004; Kržan et al., 2009; Vengudusamy, Green, et al., 2011; Vengudusamy et al., 2012, 2013a, 2013b; Vengudusamy, Mufti, et al., 2011)

2.4.3 a-C:H:Si /a-C:H:Si contact

Tribological performance of self-mated Silicon-doped DLC coating (a-C:H:Si) evaluated by different researchers using A-III, M, and PAO, with and without additives (**Figure 2.10** and **Figure 2.11**) (Kalin et al., 2004; Tasdemir, Tokoroyama, Kousaka, Umehara, & Mabuchi, 2013, 2014; Vengudusamy, Green, et al., 2011; Vengudusamy et al., 2012, 2013a; Vengudusamy, Mufti, et al., 2011). Similar to metal-doped DLC coatings, a-C:H:Si also resulted in very high values of friction with additive-free M, whereas A-III offered the lowest average value of friction followed by PAO (**Figure 2.10a**). A possible reason for such low friction coefficients attained with A-III can be smoothening of interacting a-C:H:Si-coated surfaces caused by sliding (Vengudusamy, Green, et al., 2011; Vengudusamy et al., 2012; Vengudusamy, Mufti, et al., 2011). This effect can also be related to the tribochemical interaction between base oil and coated surfaces, which result in the formation of low shear-strength tribofilm. Moreover, generation of oxygen-rich layers on the sliding surfaces due to the chemical reaction with environmental species, such as oxygen, can also be one of the causes behind such low friction coefficients (Kalin et al., 2010; Kalin et al., 2007; Vengudusamy, Green, et al., 2011). Given the strong dependence of tribological performance on intrinsic and extrinsic

factors, this difference in the friction performance of base oils against a-C:H:Si/a-C:H:Si contacts can also be related to the various test parameters, equipment, and procedures engaged by different researchers.

Overall, negative effects of additives were experienced on the friction performance of self-mated a-C:H:Si coating (**Figure 2.10b**). In formulated lubricants, the lowest value of friction was achieved with A-III+MoDTC, whereas M+AP gave the highest value. Adverse effects on the friction performance of symmetrical a-C:H:Si contact were observed with ZDDP containing lubricants. An increase of about 33% was recorded when M+ZDDP lubricant was used. The possible reason for this behavior can be the formation of tribofilms with high shear strength, which makes the sliding of the coated surface more difficult (Kalin et al., 2010). Similar behavior was observed when M was formulated with AP, resulting in an increase of almost 40% in friction coefficient. When A-III+ZDDP lubricant was used, ZDDP-derived tribofilm, composed of phosphorus and sulfur-containing compounds, was formed as a result of a tribochemical reaction between interacting surfaces and additive, but no effect of this interaction was observed on the friction performance of a-C:H:Si/a-C:H:Si contacts (Vengudusamy, Green, et al., 2011; Vengudusamy et al., 2013a). A similar type of tribofilm with a pad-like structure was also detected with PAO+ZDDP lubricant, which adversely affected the friction performance of symmetrical a-C:H:Si contacts, and an increase of around 17% in friction coefficient was witnessed as compared with additive-free PAO (Tasdemir, Tokoroyama, et al., 2014). Only MoDTC showed a reduction in the coefficient of friction with symmetrical a-C:H:Si contacts when mixed with A-III. It is widely accepted that MoDTC forms oxides and sulfides when it tribochemically interacts with doped DLC coatings because of its decomposition (Haque et al., 2007). Whether the tribochemical reaction between MoDTC and DLC-coated surfaces will result in a reduction in friction depends on the ratio of MoS_2 against MoO_3 formed. As stated before, higher ratios of MoS_2/MoO_3 generally

result in reduced friction (Haque et al., 2007). The enhancement in friction performance of a-C:H:Si/a-C:H:Si contact achieved with A-III+MoDTC can be linked with the formation of MoDTC products with higher percentages of MoS_2, which has characteristics similar to that of solid lubricant (Vengudusamy et al., 2012).

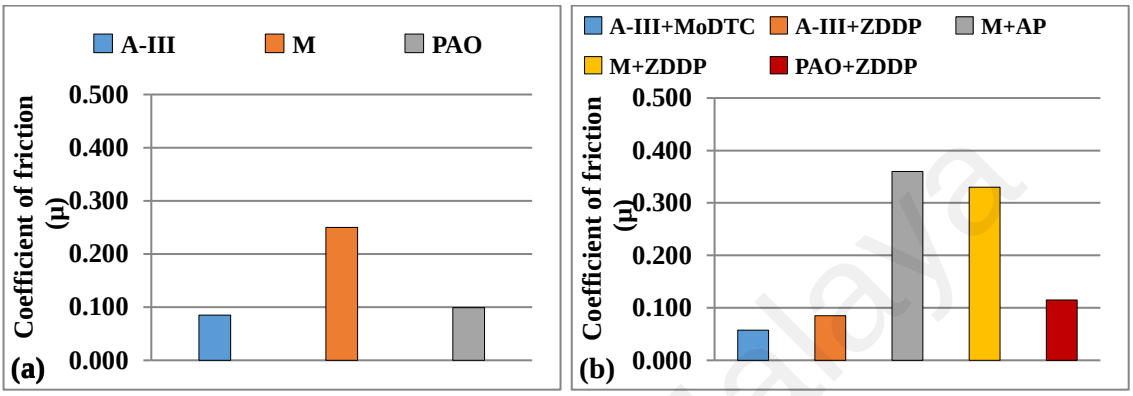

Figure 2.10: Average values of coefficient of friction for a-C:H:Si/a-C:H:Si contact with (a) base oils and (b) formulated lubricants
(Kalin et al., 2004; Tasdemir, Tokoroyama, et al., 2013, 2014; Vengudusamy, Green, et al., 2011; Vengudusamy et al., 2012, 2013a)

If we compare the wear behavior of a-C:H:Si/a-C:H:Si contacts, a significant variance is observed in the performance of the tested lubricants used by different researchers (**Figure 2.11**). Similar to the friction results, very high rates of wear were observed with M, whereas A-III and PAO proved to be more efficient in reducing wear (**Figure 2.11a**). A possible reason could be delamination and wearing through of a-C:H:Si coating from the interacting surfaces when M was used in additive-free form, whereas no such behavior was detected with A-III (Vengudusamy, Green, et al., 2011; Vengudusamy et al., 2012; Vengudusamy, Mufti, et al., 2011) and PAO.

In **Figure 2.11b**, wear coefficients of a-C:H:Si/a-C:H:Si contacts with different formulated lubricants are shown. Formulation of A-III with MoDTC and ZDDP separately did not result in any further decrease in already very low wear coefficients achieved with additive-free A-III. However, when ZDDP was used with M, a significant

reduction in wear coefficient from 23×10^{-8} to 3.4×10^{-8} mm^3/Nm was observed. Although M+AP lubricant was also able to reduce the wear coefficient, it was not as effective as M+ZDDP. Based on these observations, ZDDP is more efficient in reducing wear than AP when used as an additive in M against a-C:H:Si/a-C:H:Si contact. Similar behavior was also observed with metal-doped DLC-coated surfaces sliding under symmetrical conditions. This significant improvement in wear resistance can be attributed to the replacement of adhesive wear by polishing wear (Kalin et al., 2004). Among different versions of M, the lowest wear coefficient was achieved with M+ZDDP but it was still higher than the value observed with additive-free A-III. To investigate the causes of differences in wear performance observed with formulated and additive-free A-III and M lubricants, further tribological investigation needs to be conducted on self-mated a-C:H:Si contat. PAO formulated with ZDDP also improved the wear resistance of a-C:H:Si/a-C:H:Si contact and reduced the wear coefficient to almost one-fourth. This improvement in wear resistance can be attributed to the formation of a ZDDP-derived pad-like layer as a result of tribochemical interactions between additive and interacting surfaces. According to the values published in the literature, one cannot be certain whether the differences in tribological characteristics of a specific DLC-lubricant combination are due to the effectiveness of lubricants or if such results are the outcome of different test equipment and conditions used during tribotesting.

In summary, A-III base oil gave the lowest values of friction and wear coefficients with self-mated a-C:H:Si contacts. ZDDP proved to be effective in reducing the wear coefficients of a-C:H:Si/a-C:H:Si contacts when used in combination with most of the base oils, and only MoDTC was able to further reduce the friction values achieved with base oils.

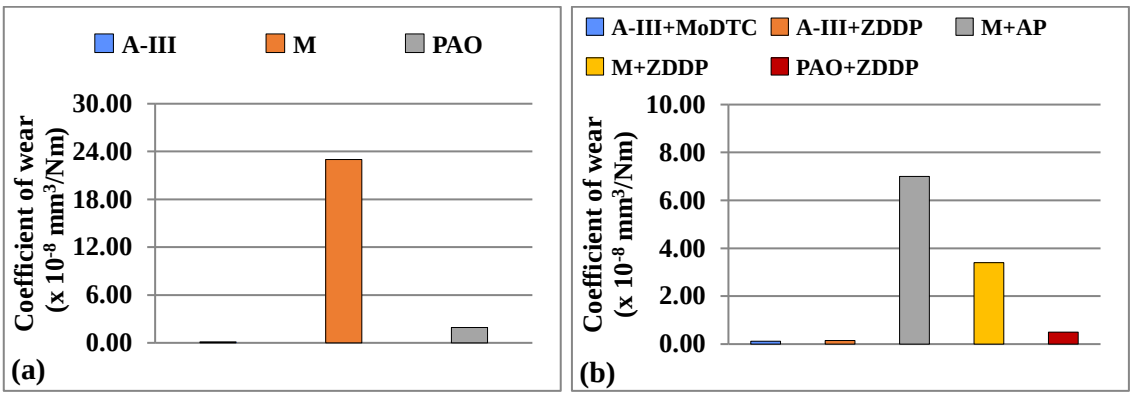

Figure 2.11: Average values of coefficient of wear for a-C:H:Si/a-C:H:Si contact with (a) base oils and (b) formulated lubricants (Kalin et al., 2004; Tasdemir, Tokoroyama, et al., 2013, 2014; Vengudusamy, Green, et al., 2011; Vengudusamy et al., 2012, 2013a; Vengudusamy, Mufti, et al., 2011)

2.4.4 a-C:H:WC/a-C:H:WC contact

a-C:H:WC is a doped DLC coating that is not widely investigated. Only a few studies have been conducted on tribological performance of symmetrical a-C:H:WC contacts using formulated and additive-free A-III (Vengudusamy, Green, et al., 2011; Vengudusamy et al., 2012, 2013a). Since, tribological data of a-C:H:WC/a-C:H:WC contact are not available for other lubricants; therefore, friction values obtained using different variants of A-III are shown in **Figure 2.12**. Additive-free A-III offered higher friction than its formulated versions. Although both MoDTC and ZDDP improved the friction performance of a-C:H:WC/a-C:H:WC contact, the former proved to be more efficient in reducing friction (from 0.094 to 0.043). This tribological improvement can be attributed to the formation of MoS_2 because of the presence of tungsten-rich regions (Vengudusamy et al., 2012). Considering the low shear strength and inherent characteristics of solid lubricant, MoS_2 made the sliding of a-C:H:WC-coated surfaces more convenient by preventing asperity contacts.

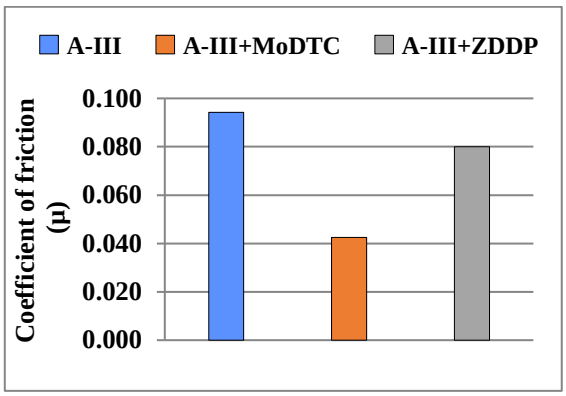

Figure 2.12: Average values of coefficient of friction for a-C:H:WC/a-C:H:WC contact with A-III (with and without additives) (Vengudusamy, Green, et al., 2011; Vengudusamy et al., 2012, 2013a)

Contrary to the friction results, wear of a-C:H:WC/a-C:H:WC contact was aggravated when A-III formulated with MoDTC was used as a lubricant (**Figure 2.13**). MoS_2 formation proved to be helpful in reducing friction, but it had adverse effects on wear characteristics of a-C:H:WC/a-C:H:WC. Similar behavior was also noted in a-C:H:W/a-C:H:W contacts with A-III+MoDTC. By contrast, MoDTC improved the wear resistance of a-C:H:Ti/a-C:H:Ti and self-mated ML-DLC coatings, when used in combination with PAO. ZDDP-containing oil, which was less effective in reducing friction than MoDTC, proved to be helpful in increasing wear resistance of a-C:H:WC-coated surfaces. Thus, the effectiveness of an additive in improving the tribological performance of a contact is a very complex function of base oil, type of DLC, and tribotest conditions.

ZDDP improved the overall tribological performance of self-mated tungsten carbide-doped DLC coatings by not only increasing the wear resistance but also reducing its friction. Therefore, to select any additive, detailed friction and wear analysis should be performed to determine whether it has a synergistic relationship with all the related components of a tribo-system or not.

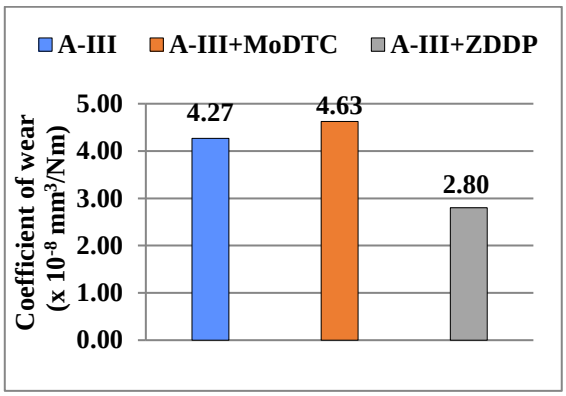

Figure 2.13: Average values of coefficient of wear for a-C:H:WC/a-C:H:WC contact with A-III (with and without additives)
(Vengudusamy, Green, et al., 2011; Vengudusamy et al., 2012, 2013a)

2.4.5 a-C:H:Cr/a-C:H:Cr contact

Chromium-doped DLC coating (a-C:H:Cr)/a-C:H:Cr contact was tribologically analyzed by different researchers using formulated and additive-free versions of A-II and PAO (Figure 2.14) (Tasdemir, Tokoroyama, et al., 2013, 2014; Topolovec-Miklozic, Lockwood, & Spikes, 2008). Regarding friction performance using additive-free lubricants, PAO demonstrated lower values than A-II (**Figure 2.14a**). In formulated lubricants, the lowest value of friction was observed when A-II was formulated with MoDTC, whereas PAO+ZDDP gave the highest value of friction (**Figure 2.14b**). The presence of chromium in the structure of DLC coating increased its chemical reactivity, and ZDDP-derived pad-like tribofilm was observed on DLC-coated pins because of tribochemical reactions; however, no positive outcome on friction performance of a-C:H:Cr/a-C:H:Cr contacts was observed when ZDDP additive was used with PAO and A-II separately. Instead of improving the friction properties, PAO+ZDDP lubricant adversely affected the inherent low friction behavior of self-mated chromium-doped DLC contacts and eloquent increase of about 50% in friction coefficient was recorded. Therefore, a synergistic correlation should exist between base oil, additives, sliding surfaces, and environmental conditions to construct a tribologically efficient system. A

substantial drop of about 25% in the friction coefficient was achieved with A-II formulated with MoDTC. This drop can be attributed to the formation of MoS_2, as a result of MoDTC decomposition (Topolovec-Miklozic et al., 2008), which acts as a solid lubricant with low shear strength. GMO reduced the friction coefficient of a-C:H:Cr/a-C:H:Cr contacts when used in combination with A-II. A possible justification for this improvement in friction performance can be adsorption of GMO-derived films, comprising majorly of the hydroxyl group, on active sites of a-C:H:Cr coatings and asperities; thus, direct contact of surfaces was avoided, resulting in low levels of friction (Topolovec-Miklozic et al., 2008).

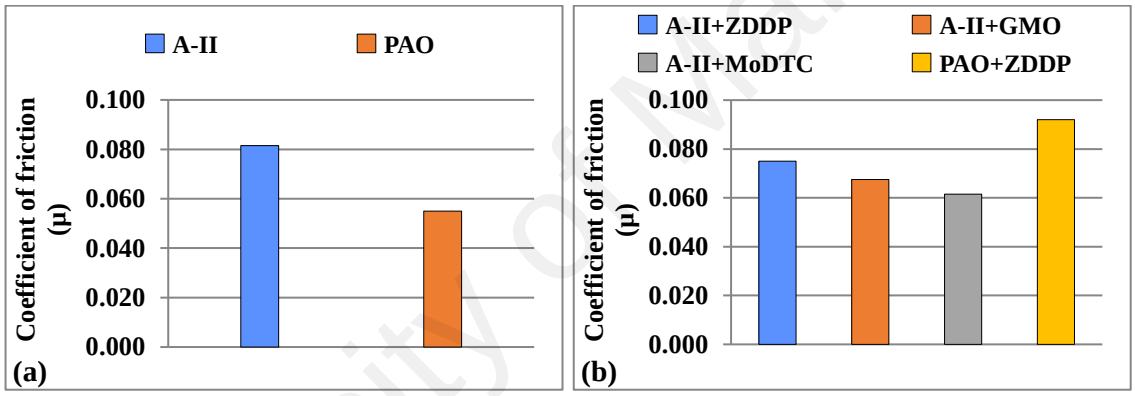

Figure 2.14: Average values of coefficient of friction for a-C:H:Cr/a-C:H:Cr contact with (a) base oils and (b) formulated lubricants
(Tasdemir, Tokoroyama, et al., 2013, 2014; Topolovec-Miklozic et al., 2008)

Although formulation of ZDDP in PAO badly influenced the friction performance, it significantly improved the wear characteristics of a-C:H:Cr/a-C:H:Cr contact. As shown in **Figure 2.15**, a very low wear coefficient of 0.40×10^{-8} mm^3/Nm was observed when ZDDP was mixed with PAO, and this value was about three times less than that of additive-free PAO. Tribochemical interactions of ZDDP with DLC coatings resulted in the formation of a tribofilm with either a patchy or pad-like structure. It is reported in the literature that ZDDP-derived films with a patchy structure have no beneficial effect on the wear performance (Topolovec-Miklozic et al., 2008). Regarding

self-mated a-C:H:Cr contacts, ZDDP-derived tribofilm with a pad-like structure was formed on sliding surfaces because of decomposition of ZDDP (Tasdemir, Tokoroyama, et al., 2014). This tribofilm has pads of different shapes compared with those formed on other doped DLC coatings, yet it resulted in a significant reduction in wear because of its inherent antiwear characteristics (Tasdemir, Tokoroyama, et al., 2014).

Both GMO and MoDTC have positive effects on the friction performance, whereas ZDDP increases the wear resistance of a-C:H:Cr/a-C:H:Cr contacts. Since, wear coefficients of other base oils and additives are unavailable in the literature, the effectiveness of ZDDP, when mixed with other base oils, cannot be assessed. Future studies should investigate the tribological performance, especially wear characteristics, of self-mated a-C:H:Cr contacts with A-II, A-III, and M in combination with most widely used additives, such as MoDTC, GMO, and AP.

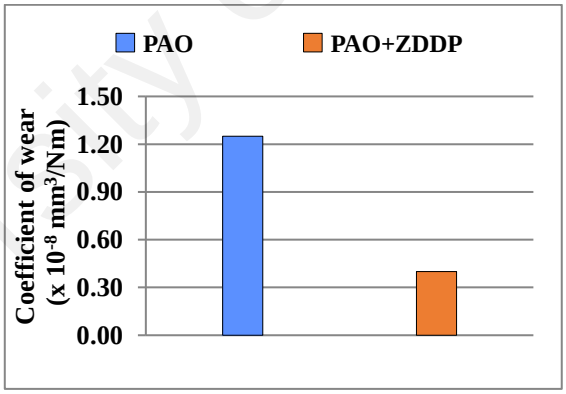

Figure 2.15: Average values of coefficient of wear for a-C:H:Cr/a-C:H:Cr contact with PAO (with and without additives)
(Tasdemir, Tokoroyama, et al., 2013, 2014)

2.4.6 Summary

MoDTC improved the friction performance of all the considered contacts primarily because of the formation of MoS_2. However, dependence of wear coefficients on the type of DLC and base oil was observed when MoDTC was used as an additive. In a-C:H:Ti/a-C:H:Ti contact, a positive effect on wear was observed with PAO+MoDTC, whereas the opposite was true for a-C:H:W and a-C:H:WC when A-III+MoDTC was used as a

lubricant. An increase in wearing out of the tungsten-doped DLC coatings with MoDTC additivated lubricants can be attributed to the formation of WS_2 along with MoS_2, which had adverse effects on the wear performance. No change in the wear coefficient of a-C:H:Si was detected when MoDTC was mixed with A-III.

In most of the cases, ZDDP proved to be beneficial in enhancing wear performance of the contacts, with the exceptions of a-C:H:W and a-C:H:Si coatings when tested with RO+ZDDP and A-III+ZDDP, respectively. The positive effect of ZDDP on wear resistance can be attributed to the prevention of coating spallation, delamination, graphitization, and formation of pad-like ZDDP-derived tribofilm, which comprised zinc, phosphorus, and sulfur, on the interacting surfaces. RO+ZDDP was unable to resist the formation of tungsten-rich transfer layer from the beginning until the end, which resulted in escalated wear of a-C:H:W/a-C:H:W contact. In symmetrical Si-DLC contacts, additivation of ZDDP with A-III appeared to be adversely affecting the running-in behavior, and most of the material loss occurred during this period. Overall, a negative effect of ZDDP on friction performance was observed, but the opposite behavior was also noticed in some cases. When a-C:H:Ti, a-C:H:W, a-C:H:Si, and a-C:H:Cr coatings were used in combination with M+ZDDP, PAO+ZDDP, A-III+ZDDP, M+ZDDP, and A-II+ZDDP, respectively, friction remained at the same level as that of non-additivated base oils. Comparatively, DLC coatings doped with tungsten showed an improvement in friction characteristics with ZDDP additivated lubricants. This finding can be attributed to the formation of WS_2, which acts as a solid lubricant and well-known for its lubricious properties. An increase in friction levels of a-C:H:Si coatings was also realized when M+ZDDP and PAO+ZDDP were used as lubricants separately.

In case of a-C:H:W/a-C:H:W contact tested with PAO+ZDDP, no tribofilm was detected. A tungsten-rich transfer layer formed between the contact because of delamination, and this layer reduced the further wearing of the DLC-coated surfaces.

Although many studies have been conducted using GMO as an additive that proved it to be very effective in improving the tribological performance of non-doped DLCs in both symmetrical and asymmetrical contacts, very few investigations have determined whether it has synergistic or antagonistic correlations with self-mated doped DLC contacts. The main mechanism behind the improvement in tribological performance caused by GMO is the adsorption of the hydroxyl group on the sliding surfaces, which passivates the dangling carbon bonds of DLC coatings, especially non-hydrogenated non-doped ones. GMO-derived tribofilm, formed as a result of additive-material tribochemical interaction, possesses low shear strength and offers low friction between the sliding surfaces (Tasdemir, Wakayama, et al., 2013a). A similar friction reduction mechanism was observed when AII+GMO lubricant was used in symmetrical a-C:H:Cr contacts. Given that the wear coefficient has not been calculated by researchers, effects of GMO on the wear coefficient of doped DLC contacts have yet to be explored.

Another lubricant additive that was investigated extensively to explore its tribological benefits is AP. In all instances, an increase in friction was observed with AP additivated oils. Possible reasons for this detrimental effect on friction can be increased surface activity and prevention of material transfer between the interacting surfaces. Similar to ZDDP, AP also proved to be helpful in augmenting the wear resistance of self-mated doped DLCs. A reduction in wear coefficients of a-C:H:Ti/a-C:H:Ti, a-C:H:W/a-C:H:W, and a-C:H:Si/a-C:H:Si contacts was observed when M+AP was used as a lubricant. This result can be attributed to the replacement of adhesive wear by polishing wear and prevention of coating spallation/delamination.

2.5 Tribological interaction between non-doped DLC coatings and conventional lubricant additives

2.5.1 ta-C/ta-C contact

A lot of experimental investigations were carried out on ta-C by different researchers using various test conditions and lubricant formulations (Kano et al., 2005; Tasdemir, Tokoroyama, et al., 2014; Tasdemir, Wakayama, et al., 2013a, 2013b; Vengudusamy, Green, et al., 2011; Vengudusamy et al., 2012, 2013a; Vengudusamy, Mufti, et al., 2011). The primary objective of those studies was to explore the tribological characteristics and analyze the suitability of ta-C coatings for various industrial applications. Tasdemir, Tokoroyama, et al. (2014), Tasdemir, Wakayama, et al. (2013a) and Tasdemir, Wakayama, et al. (2013b) used PAO as a base oil, GMO as a friction modifier and ZDDP as an antiwear additive to see the impact of formulated and additive-free versions of PAO on friction and wear performance of symmetrical ta-C contacts. Vengudusamy, Green, et al. (2011), Vengudusamy, Mufti, et al. (2011), Vengudusamy et al. (2012) and Vengudusamy et al. (2013a) investigated the influence of sp^3 content and formulated lubricants on the tribological behavior of ta-C coatings. A similar study was conducted by Kano et al. (2005) using GMO as a friction modifier in PAO.

In **Figure 2.16a**, average friction coefficients of ta-C/ta-C contacts tested with base oils are compared. Results show that friction values obtained with PAO are relatively lower than those obtained with additive-free A-III. This effect can be attributed to tribologically beneficial interaction between symmetrical ta-C contact and PAO. Another viable justification can be occurrence of graphitization phenomenon at higher extent with PAO compared to A-III. This hypothesis is also supported by higher wear rates of ta-C/ta-C contact observed in combination with PAO (**Figure 2.17a**). Those experimental investigations in which A-III was used as base oil (Vengudusamy, Green, et al., 2011; Vengudusamy et al., 2012, 2013a; Vengudusamy, Mufti, et al., 2011), values of applied

load and test temperature were around 31N and 100ºC whereas 5N of load and 80ºC temperature were used in the studies which used PAO as a lubricant (Tasdemir, Wakayama, et al., 2013a, 2013b). In the literature, inverse relation of applied load and temperature with coefficient of friction has been established by different researchers (Al Mahmud et al., 2014b; Erdemir, Bindal, Fenske, Zuiker, & Wilbur, 1996; Forsberg, Gustavsson, Renman, Hieke, & Jacobson, 2013; Kano et al., 2005; Kim & Kim, 2013; Ouyang et al., 2009). Even with higher values of applied load and test temperature, A-III was not able to achieve friction values comparable to that of PAO**.** From these observation, it can be concluded that friction characteristics of PAO with symmetrical ta-C contacts is better than A-III in additive-free form.

Figure 2.16b shows friction performance of ta-C/ta-C tribopair when used in combination with formulated lubricants. Highest values of friction were observed with different blends of A-III base oil whereas PAO formulated with ZDDP demonstrated the lowest value. Although additives improved the friction performance of A-III but still the values were higher than additive-free PAO and its formulated versions. Formulation of GMO in PAO+ZDDP lubricant deteriorated its friction performance and resulted in highest value of friction among the PAO oils. A similar behavior was also seen in case of PAO+GMO which resulted in an increase in value of friction as compared to additive-free PAO. This negative influence of GMO on friction performance can be attributed to passivation of dangling carbon bonds in ta-C coating by hydroxyl group causing suppression in graphitization phenomenon (Kalin et al., 2007; Tasdemir, Wakayama, et al., 2013b). ZDDP proved to be effective in lowering the friction of symmetrical ta-C contacts irrespective of the base oil. This can be attributed to tribochemical interaction between ZDDP and ta-C coated interacting surfaces resulting in formation of white-colored ZDDP-derived tribofilm having a patchy structure and comprised of phosphorus, sulfur and zinc containing compounds. Formulation of A-III with MoDTC resulted in

negligible change in the friction characteristics of self-mated ta-C coatings because of the formation of tribofilm containing higher MoO_3/MoS_2 ratio.

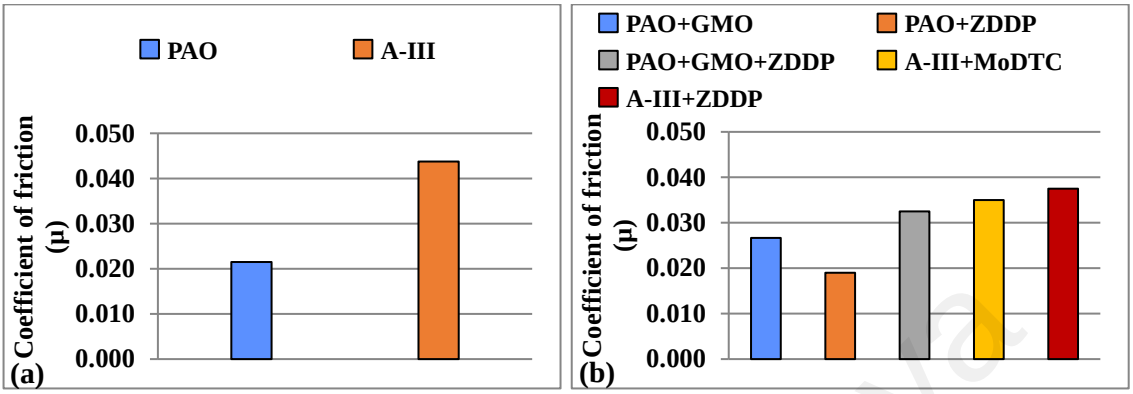

Figure 2.16: Average values of coefficient of friction for ta-C/ta-C contact with (a) base oils and (b) formulated lubricants
(Kano et al., 2005; Tasdemir, Tokoroyama, et al., 2014; Tasdemir, Wakayama, et al., 2013a, 2013b; Vengudusamy, Green, et al., 2011; Vengudusamy et al., 2012, 2013a; Vengudusamy, Mufti, et al., 2011)

Wear coefficients of ta-C/ta-C contacts in combination with formulated and additive-free lubricants are shown in **Figure 2.17**. Contrary to friction results, high values of wear coefficients were observed with PAO compared to A-III **(Figure 2.17a**). It is mentioned in the literature that coatings with higher hardness/elastic modulus ratios have better wear properties compared to lower ones (Neuville & Matthews, 2007; Vengudusamy, Mufti, et al., 2011). Although, ta-C coatings used in combination with PAO have high hardness/elastic modulus in comparison to those tested with A-III, still better wear performance was observed with latter. As stated earlier, occurrence of graphitization phenomenon to higher extent in the presence of PAO can be attributed to accelerated wear of ta-C-coated surfaces. Higher tribotest temperature in case of A-III can be another viable justification for better wear performance. In experimental investigations, it was also found that there is a strong influence of counterbody material on the wear properties of DLC coatings. When ta-C/steel contact was investigated in combination with PAO, complete delamination of DLC coating was observed but when steel counterbody was replaced with

ta-C, no such behavior was seen resulting in significant decrease in wear (Tasdemir, Wakayama, et al., 2013b). This behavior can be attributed to strong affinity of carbon atoms towards ferrous surfaces and graphitization of DLC coating (Komanduri & Shaw, 1975; Shimada et al., 2004). As a result of graphitization, carbon atoms diffuses into steel counterbodies resulting in higher wear rates of ta-C coated surface (Tasdemir, Wakayama, et al., 2013b).

Formulation of PAO with lubricant additives resulted in decreased wear as compared to the additive-free oil (**Figure 2.17b**). Formulation of PAO with GMO substantially reduced the wear of self-mated ta-C from 3.60 x 10^{-8} mm^3/Nm to 2.20 x 10^{-8} mm^3/Nm. This effect can be attributed to the passivation of dangling carbon bonds within the structure of DLC coating by the hydroxyl group of GMO and suppression of graphitization phenomenon (Tasdemir, Wakayama, et al., 2013b, 2014). Because of this hindrance in graphitization, very high value of COF was also observed with PAO+GMO lubricant. It is mentioned in the literature that graphitization can be concealed to an appreciable extent by mixing different lubricant additives in the base oils even at high test temperatures (Kalin et al., 2007; Kosarieh et al., 2013b; Vengudusamy et al., 2014a).When ZDDP was used as an additive in PAO, additive-derived tribofilm was formed at ta-C/ta-C interface but it resulted in only slight reduction in wear (Tasdemir, Wakayama, et al., 2013b). When both GMO and ZDDP was mixed with PAO, wear coefficient of self-mated ta-C contact became higher than PAO+GMO but less than that of PAO+ZDDP. Presence of ZDDP in PAO+GMO lubricant not only affects the wear reducing capability of GMO but also not able to perform any tribochemical interaction with ta-C coating. Contrary to wear performance of formulated versions of PAO, an increase in wearing out of ta-C coated surfaces was seen with A-III+MoDTC. This increase can be attributed to the formation of MoO_3 which usually shear off quite easily during sliding motion due to its weak adhesion with the interacting surfaces

(Vengudusamy et al., 2012). Although ZDDP resulted in very minor decrease in wear when mixed with PAO however, it proved to be very effective in reducing wear of ta-C/ta-C contact in combination with A-III.

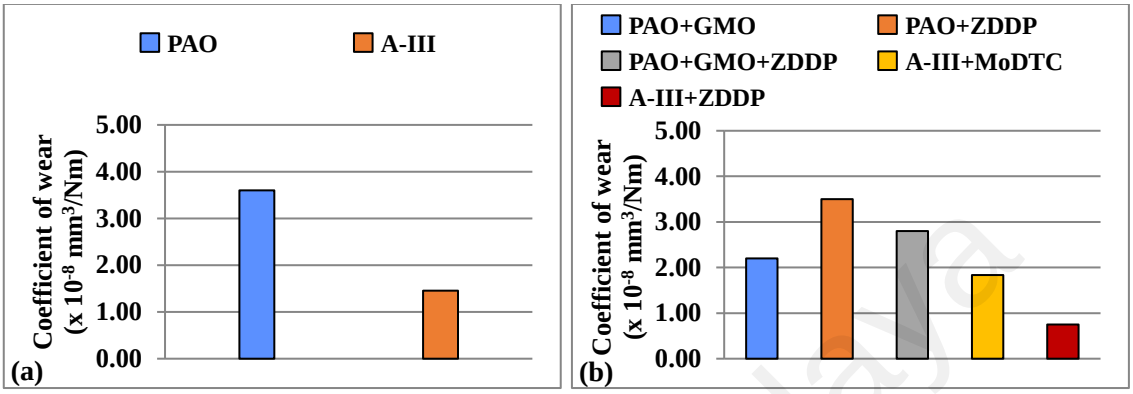

Figure 2.17: Average values of coefficient of wear for ta-C/ta-C contact with (a) base oils and (b) formulated lubricants
(Kano et al., 2005; Tasdemir, Tokoroyama, et al., 2014; Tasdemir, Wakayama, et al., 2013a, 2013b; Vengudusamy, Green, et al., 2011; Vengudusamy et al., 2012, 2013a; Vengudusamy, Mufti, et al., 2011)

From these observations, it can be concluded that most of the lubricant additives, which are primarily designed for metals, can also improve the intrinsic tribological performance of self-mated ta-C coatings irrespective of base oil type. Among formulated lubricants, A-III+ZDDP is proved to be the ideal formulation for ta-C/ta-C contacts as it not only improved the wear-resistance but also helped in reducing friction. PAO+ZDDP lubricant is also one of the viable options to be used in combination with symmetrical ta-C contacts especially for those applications in which extremely low friction coefficients are desirable.

2.5.2 a-C:H/a-C:H contact

It is one of the most widely investigated DLC coatings. Many tribological studies were carried out by different researchers on symmetrical a-C:H contacts to comprehend their compatibility with conventional lubricant additives (de Barros'Bouchet et al., 2005;

Equey et al., 2008a, 2008b; Kalin et al., 2010; Kalin et al., 2007; Kalin & Vižintin, 2006a, 2006b; Kalin et al., 2004; Kalin et al., 2006; Tasdemir, Tokoroyama, et al., 2013, 2014; Vengudusamy, Green, et al., 2011; Vengudusamy et al., 2012, 2013a, 2013b; Vengudusamy, Mufti, et al., 2011).

Among additive-free base oils, PAO offered lowest friction between a-C:H-coated sliding surfaces whereas highest values were observed with M and SO **(Figure 2.18a)**. In addition to the composition and physicochemical properties of a base oil, there is a strong dependence of tribological parameters of a contact on tribotest conditions. It is reported in the literature that friction is inversely proportional to applied load, sliding velocity, sliding distance and temperature (Al Mahmud et al., 2014b; Forsberg et al., 2013; Kalin et al., 2007; Kalin & Vižintin, 2006b; Kim & Kim, 2014; Ouyang & Sasaki, 2005; Ouyang et al., 2009; Tasdemir, Wakayama, et al., 2014; Vengudusamy, Green, et al., 2011; Vengudusamy, Mufti, et al., 2011; Yasuada, 2003). This variation in friction performance of a-C:H/a-C:H contacts in combination with base oils can also be attributed to different operating conditions and test equipment employed by researchers. In case of M and SO, the total sliding distance was kept at 100 m whereas it was 288 m for PAO and 720 m for A-II and A-III base oils. Since, a considerable amount of sliding is required for tribochemical interactions and achieving steady state coefficient of friction, therefore, inadequate sliding distance can be a possible reason for high friction values obtained with M and SO. Tribological evaluation of a-C-H/a-C-H contacts in combination with A-II and A-III oils were conducted using identical tribotest conditions and almost similar values of friction coefficients were achieved.

Generally, mixing of PAO with different lubricant additives resulted in increased friction of a-C:H/a-C:H tribopair (**Figure 2.18b**). Although, MoDTC improved the friction behavior and running-in behavior when used in combination with but the values

of friction obtained with PAO+MoDTC were greater than average friction coefficient calculated for additive-free PAO. A similar behavior was also observed with PAO+MoDTC+ZDDP lubricant but it was more effective as compared to PAO+MoDTC in reducing friction of self-mated a-C:H coating. This difference in friction performance can be attributed to higher ratio of MoS_2/MoO_3 formed in case of PAO+MoDTC+ZDDP compared to PAO+MoDTC. Presence of ZDDP in PAO+MoDTC lubricant helps in complete decomposition of MoDTC and aggravates the formation of MoS_2 by supplying sufficient amount of sulfur**.** It was also observed that MoDTC-derived tribofilm rich in MoS_2 only forms on the contact area as a result of sliding whereas no such compounds were detected outside the wear track. Contrary to PAO+MoDTC+ZDDP results, deterioration in friction performance of a-C:H coating and an increase in friction coefficient was observed when only ZDDP was formulated with PAO. Although, weakly adhered ZDDP-derived tribofilm was formed on the a-C:H coated surfaces but it did not play any role in enhancing friction characteristics. A possible reason for this behavior can be making and breaking of tribofilm during sliding due to which average coefficient of friction value remain on the higher side. It was also observed that tribofilm formed on a-C:H-coated surfaces had different structure from that formed on sliding steel surfaces. Weak adhesion of ZDDP-derived tribofilm with a-C:H coated surfaces can be attributed to the absence of ferrous-based compounds such as FeO, Fe_2O_3, Fe_3O_4 and ferrous sulfide (FeS) in a-C:H/a-C:H contact that promote binding between ZDDP-derived polyphosphate glass and interacting surfaces. Another feasible justification for increase in friction can be adsorbtion and tribochemical interaction between ZDDP and interacting surfaces which prevents the formation of a-C:H-derived transfer film possessing low shear strength. Highest value of friction was observed when PAO was formulated with GMO whereas butyl-triphenylphosphorothionate (b-TPPT) additive gave the lowest friction value among the variants of PAO. The ineffectiveness of ester-containing oil

(PAO+GMO) in reducing friction of a-C:H/a-C:H pair can be attributed to inability of GMO to interact with a-C:H coated surfaces. Another possible justification can be different intrinsic/extrinsic conditions and test equipment used by researchers. It is mentioned in the literature that GMO forms tribofilms on DLC coatings by adsorbing on the interacting surfaces and passivates the dangling carbon bonds with hydroxyl group (Topolovec-Miklozic et al., 2008). Since, most of the dangling carbon atoms in a-C:H are passivated with hydrogen atoms during the deposition process therefore, hydroxyl group was not able to find any active sites to interact with the a-C:H coated surfaces. Although, b-TPPT additive tribochemically interacted with a-C:H-coated surfaces and a patchy tribofilm, comprised of phosphorus and sulfur, was observed on the contact areas but it was not able to substantially reduce the friction compared to additive-free PAO due to weak adhesion with the interacting surfaces. On the other hand, AP additive was not able to tribochemically interact with a-C:H/a-C:H contact and no evidence of any tribofilm was found using X-ray Photoelectron Spectroscopy (XPS) and Time-of-Flight Secondary Ion Mass Spectrometry (ToF-SIMS). As a result, increase in friction coefficient from 0.040 to 0.105 was observed when PAO+AP was used as a lubricant. The unavailability of sulfur in the structure of AP, that plays a key role in the formation of ZDDP- and b-TPPT-derived tribofilms, can be a viable justification for this behavior. When M was formulated with AP and ZDDP separately, an increase in friction was observed as compared to additive-free M. A sulphate and phosphate-based tribochemical film was detected when M+ZDDP lubricant was used in combination with self-mated a-C:H coating. Moreover, a depletion in S/P ratio after tribological tests confirmed the tribochemical reaction between ZDDP and DLC-coated surfaces but all these interactions had adverse effects on the friction performance. This behavior can be attributed to the hindrance in the phenomenon of graphitization due to the presence of ZDDP. Contrary to that, an increase in ratio between D and G peaks (I_D/I_G) ratio and transformation from

diamond to graphitic phase was observed with Raman spectroscopy when additive-free M was used as a lubricant. Although, no tribochemical interaction was detected between M+AP lubricant and a-C:H coating however, AP played its role in suppressing graphitization of a-C:H coating like ZDDP that results in higher value of coefficient of friction. Reduction in friction was observed when A-II and A-III base oils were formulated with MoDTC. As stated earlier, formation of tiny crystalline MoS_2 with a thickness of few nanometers due to the decomposition of MoDTC in the contact area can be attributed to this improvement in friction performance. GMO and ZDDP also reduced the friction of self-mated a-C:H coatings when formulated with A-II and A-III respectively whereas a slight increase in friction was observed when ZDDP was used as an additive in A-II. A formation of ZDDP-derived tribofilm composed of zinc, phosphorus and sulfur was confirmed by EDS and XPS when A-III+ZDDP was used as a lubricant. It is believed that tribochemical interaction between A-III+ZDDP and a-C:H/a-C:H contact were responsible for improvement in friction performance. When ZDDP was mixed with A-II, thick phosphate film, which is generally formed on steel/steel contact, was not observed. Instead, a very thin tribochemical film was formed on the contact area which was not able to play any role in enhancing friction characteristics of self-mated a-C:H coating. In case of A-II+GMO, reduction in friction coefficient can be attributed to formation of viscous layer due to tribochemical reaction and adsorbtion of additive that prevents asperities of interacting surfaces from coming into contact with each other.

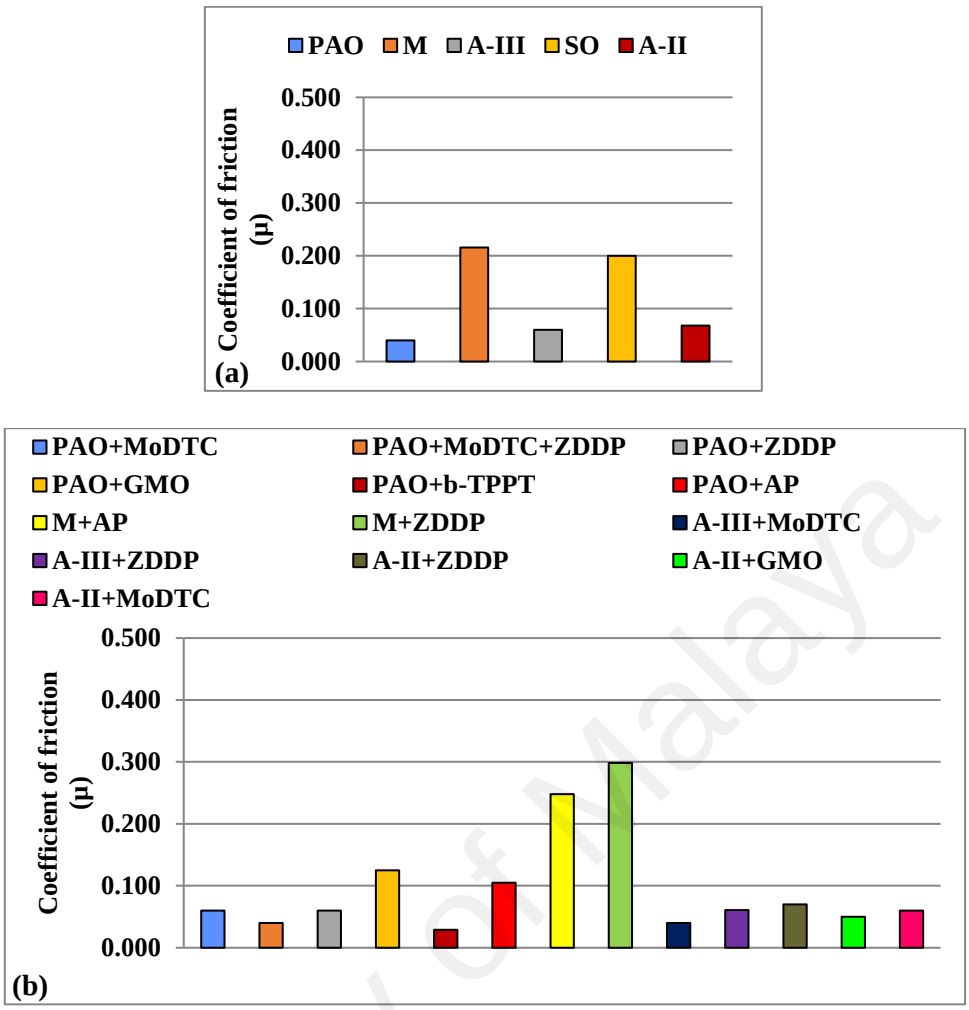

Figure 2.18: Average values of coefficient of friction for a-C:H/a-C:H contact with (a) base oils and (b) formulated lubricants
(de Barros'Bouchet et al., 2005; Equey et al., 2008a, 2008b; Kalin et al., 2010; Kalin et al., 2007; Kalin & Vižintin, 2006a, 2006b; Kalin et al., 2004; Kalin et al., 2006; Tasdemir, Tokoroyama, et al., 2013, 2014; Vengudusamy, Green, et al., 2011; Vengudusamy et al., 2012, 2013a, 2013b; Vengudusamy, Mufti, et al., 2011)

A bar graph comparison of wear coefficients of symmetrical a-C:H contacts in combination with formulated and additive-free lubricants is given in **Figure 2.19**. From the results presented in **Figure 2.19a**, it can be clearly seen that A-III offered significantly less wear of interacting surfaces compared to other base oils whereas highest value of wear coefficient was observed with M. Wear coefficient of self-mated a-C:H when SO was used as lubricant is greater than PAO and A-III but less than that of M. Extreme wearing of a-C:H-coated surfaces with M can be attributed to graphitization of carbon

coating under boundary-lubricated conditions whereas no such behavior was observed with PAO and A-III. An increase in I_D/I_G ratio, which shows occurrence of graphitization phenomenon, was confirmed by Raman spectroscopy. Due to graphitization, diamond phase of a-C:H coating was transformed into softer graphite material which is more prone to wearing and can be removed quite easily due to sliding resulting in aggravated wear coefficients. Although, tribological investigation of a-C:H/a-C:H contact was carried out using same test conditions and equipment yet significant difference in the wear coefficients of M and SO was observed. SO proved to be more efficient in enhancing wear characteristics compared to M. This behavior can be attributed to high concentration of unsaturated molecules and polar components (fatty acids) in the structure of SO which makes it more interactive with the sliding surfaces compared to saturated and non-polar base oils such as M (Kalin et al., 2008; Velkavrh, Kalin, & Vizintin, 2008).

A substantial improvement in wear performance of symmetrical a-C:H contacts was observed with additives irrespective of lubricant formulation (**Figure 2.19b**). When PAO was mixed with MoDTC, almost 10 times reduction in wear was realized compared to additive-free PAO whereas PAO+MoDTC+ZDDP resulted in more than 100 times decrease in wear. No wear debris were found in the wear tracks when both MoDTC and ZDDP were used in combination with PAO. It is interesting to note that MoDTC also has the ability to improve the wear resistance of a-C:H coating by suppressing graphitization in addition to reducing friction between the interacting surfaces by forming MoS_2. Addition of ZDDP in PAO+MoDTC lubricant not only provide sufficient sulfur for MoS_2 formation but also tribochemically decomposed into zinc phosphate [$Zn_3(PO_4)_2$] and played a vital role in overcoming asperities breakage. Lubricant additives such as AP and ZDDP, when mixed with M, significantly scaled down wear in a-C:H/a-C:H contact compared to additive-free version of M. An amorphous and soft tribochemical layer was formed on DLC-coated surfaces when AP additive was used, which was plastically

deformed during rubbing. Although, no signs of tribochemical interaction between M+ZDDP lubricants and interacting surfaces were found with EDS and Fourier Transform Infrared Spectroscopy (FTIR) yet, it was proved to be more effective in reducing wear compared to M+AP lubricant. Formulated versions of A-III base oil (A-III+MoDTC and A-III+ZDDP) further improved the resilient wear behavior of self-mated a-C:H coatings observed with additive-free A-III. Negligible wear of a-C:H coated surfaces was realized when A-III+MoDTC was used as a lubricant. Presence of sulfides and oxides in the contact area was confirmed by ToF-SIMS whereas neither molybdenum nor its compounds were found outside the wear tracks. Formation of MoDTC-derived tribochemical compounds, especially MoS_2, not only improved the friction performance of a-C:H/a-C:H contacts but also proved to be helpful in augmenting wear resistance. A tribochemical interaction took place between A-III+ZDDP and a-C:H coating resulting in the formation of additive-derived tribochemical compounds comprised of sulfur, phosphorus and zinc on the interacting surfaces. An increase in concentration of these tribo-compounds was seen with a decrease in hydrogen content of a-C:H coatings. Vengudusamy et al. (2013b) conducted a study to see the influence of tribofilm on the magnitude of adhesive forces between the interacting a-C:H-coated surfaces. A decrease in adhesive force was perceived with an increase in hydrogen concentration of a-C:H coatings. Contact areas with higher concentration of tribochemical compounds offered less adhesive force compared to those without tribofilm. Effect of hydrogen concentration on the surface energies of a-C:H coating was also observed. Coatings with higher hydrogen content and subsequently higher surface energies are more susceptible to interact tribochemically with lubricant additives. In addition, capability of adsorbing additive molecules also increases with an increase in surface energy.

In light of the above discussion, it can be safely stated that lubricant additives exhibit different tribological behavior when used in combination with various base oils even with

same type of DLC-coated interacting surfaces. Formulated versions of PAO and A-III especially those containing MoDTC and ZDDP resulted in extraordinary tribological performance of a-C:H/a-C:H contacts. Contrary to that, M-based lubricants not only resulted in high friction coefficients but also unable to provide sufficient wear protective tribofilms on a-C:H coated interacting surfaces.

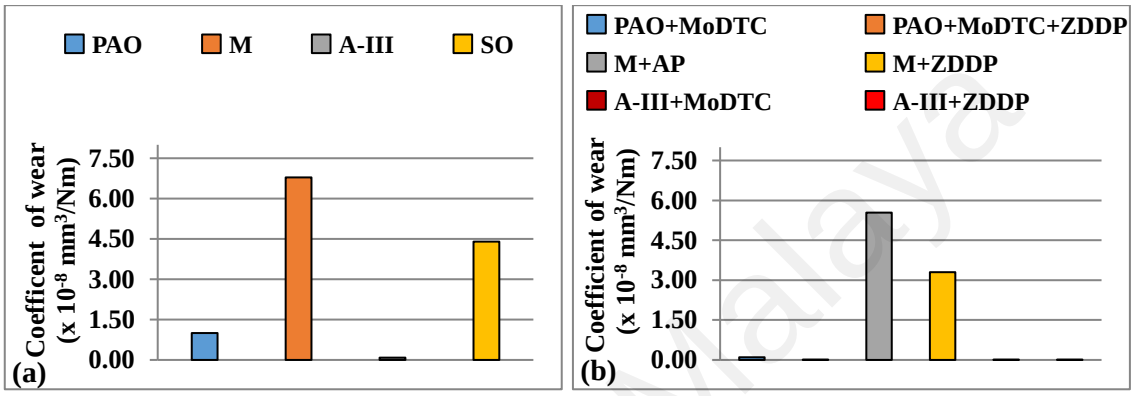

Figure 2.19: Average values of coefficient of wear for a-C:H/a-C:H contacts with (a) base oils and (b) formulated lubricants
(de Barros'Bouchet et al., 2005; Equey et al., 2008a, 2008b; Kalin et al., 2010; Kalin et al., 2007; Kalin & Vižintin, 2006a, 2006b; Kalin et al., 2004; Kalin et al., 2006; Tasdemir, Tokoroyama, et al., 2013, 2014; Vengudusamy, Green, et al., 2011; Vengudusamy et al., 2012, 2013a, 2013b; Vengudusamy, Mufti, et al., 2011)

2.5.3 a-C/a-C contact

Unlike ta-C and a-C:H coatings, tribological performance of symmetrical a-C contact is not frequently examined in the literature. Only few studies have been carried out using PAO and A-III base oils in formulated and additive-free forms (Tasdemir, Tokoroyama, et al., 2014; Vengudusamy, Green, et al., 2011; Vengudusamy et al., 2012, 2013b).

As compared to PAO, A-III base oil exhibited better friction results when used in combination with a-C/a-C contacts (**Figure 2.20a**) whereas an opposite behavior was observed in case of ta-C and a-C:H coatings. Higher values of load and temperature were applied while evaluating A-III in combination with a-C/a-C, compared to PAO. It is mentioned in the literature that friction between the interacting surfaces increases with a

decrease in temperature and applied load (Al Mahmud et al., 2014b; Forsberg et al., 2013), therefore, low friction coefficient achieved with A-III can be attributed to different tribotest conditions deployed in experimental studies carried out by various researchers. Average value of steady state friction coefficient of 0.050 was obtained with A-III after 2 hours of sliding. At the start of tribotest, lower level of friction (0.035) was observed between the interacting surfaces which went to higher value as a result of subsequent sliding (Vengudusamy et al., 2013b). A viable justification for this behavior can be higher sp^2 content in a-C coating initially as compared to sp^3 which makes it more graphitic in nature (Vengudusamy et al., 2013b). If we compare the friction values of a-C/a-C contact in combination with A-III base oil with other non-doped DLC coatings, we came to know that this value is greater than that of ta-C (0.044), but less than those of a-C:H (0.060) and ta-C:H (0.070) under same operating and tribotest conditions. In contrast, PAO was unable to lubricate the a-C-coated sliding surfaces in the similar way as it does for ta-C/ta-C and a-C:H/a-C:H contacts and resulted in highest value of friction coefficient among non-doped DLC coatings. This degradation in friction performance can be attributed to total delamination of a-C coated pin during tribotesting due to its poor load-carrying capacity and adhesion with the substrate which subsequently converted a-C/a-C contact to a-C/steel contact.

In **Figure 2.20b**, friction coefficients of a-C/a-C contacts with different formulated lubricants are presented. MoDTC proved to be beneficial in reducing friction between the a-C-coated sliding surfaces when used in combination with A-III and a decrease of around 20% in friction coefficient was observed. Like earlier state, reduced friction observed in case of MoDTC can be attributed to the formation of MoS_2 which acts as a solid lubricant (Vengudusamy et al., 2012). Due to the presence of molybdenum-derived compounds between sliding surfaces, nature of contact changed from DLC on DLC to DLC on MoS_2 and hence, ease in sliding was seen (Vengudusamy et al., 2012). Contrary to A-

III+MoDTC, an adverse effect on the friction performance of a-C/a-C tribopair was realized when A-III and PAO were formulated with ZDDP separately. Although, ZDDP-derived tribofilm was detected on the sliding surfaces but no positive outcome of it was observed on friction coefficient. One possible reason for this behavior can be catastrophic effect of tribochemical compounds on the low friction characteristics of graphitic a-C coating. PAO+ZDDP was not able to prevent complete delamination of a-C-coated pin and similar peeling-off behavior was observed which was seen in case of additive-free version of PAO.

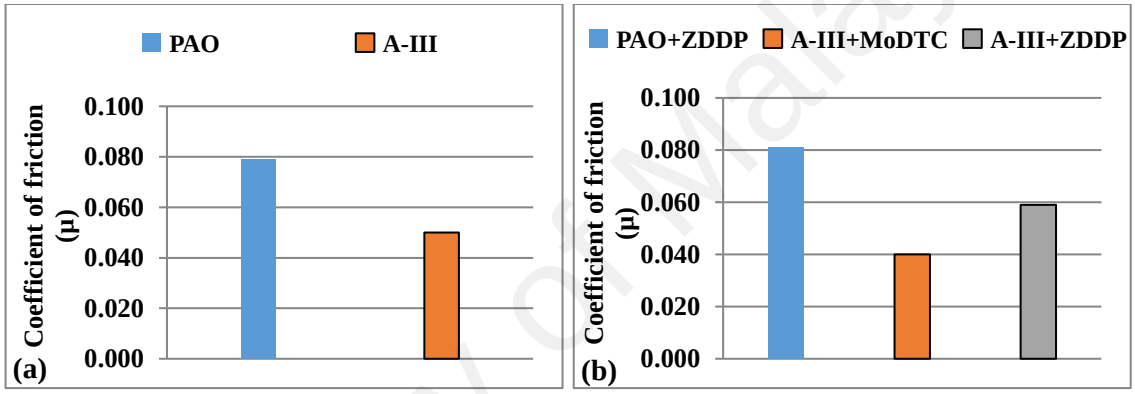

Figure 2.20: Average values of coefficient of friction for a-C /a-C contacts with (a) base oils and (b) formulated lubricants
(Tasdemir, Tokoroyama, et al., 2014; Vengudusamy, Green, et al., 2011; Vengudusamy et al., 2012, 2013b)

When PAO was used as a lubricant in self-mated a-C/a-C contact having pin-on-disk geometric configuration, no significant wear of DLC-coated disk was found after 1 hour of sliding. Contrary to that, DLC coating was completely delaminated from the pin due to its poor adhesion with the substrate material (AISI 52100 chrome steel) (Tasdemir, Tokoroyama, et al., 2014). Although, heavier load was applied (31 N compared to 5 N) yet no such behavior was observed in case of additive-free A-III rather significantly lower wear coefficient of 0.08 x 10^{-8} mm^3/Nm was seen (**Figure 2.21a**). This variation in adhesion strength of a-C coating with the substrates having different geometric shapes

can be attributed to dissimilar deposition techniques and parameters deployed by the manufacturers of DLC coatings resulting in diversified mechanical properties such as hardness, elastic modulus, concentration of hydrogen and sp^3/sp^2 ratio.

ZDDP was not able to adequately perform its primary role of antiwear agent and proved to be ineffective in improving the wear resistance of a-C/a-C tribopair, irrespective of the base oil (**Figure 2.21b**). Although, ZDDP-derived tribofilm was formed on interacting surfaces with both PAO+ZDDP and A-III+ZDDP lubricants but no substantial effect of these tribochemical interactions was seen on the wear behavior a-C. Formulation of PAO with ZDDP was not able to maintain the structural integrity of a-C coating and complete delamination of the coating material from the substrate was seen at the end of sliding test. Similarly, mixing of ZDDP with A-III base oil resulted in further increase in wear as compared to its additive-free version. Although, MoDTC is primarily a friction modifier, yet lowest value of wear coefficient was observed with A-III+MoDTC lubricant. Reduction in wear observed with MoDTC was due to the reduction in disk wear whereas ball wear remained almost at the same level. Opposite behavior was observed when ZDDP was used as additive, i.e., disk wear was increased and ball wear remained the same. The reason behind change in wear coefficients of disks when different additives were used is still unknown and needs to be investigated in the future studies.

Based on the aforementioned findings, it can be stated that lubricants additives have the ability to influence the tribological behavior of a-C/a-C contacts considerably. ZDDP, which is primarily an antiwear additive, was not able to perform its role and resulted in high wear and friction coefficients of self-mated a-C coatings compared to additive-free PAO and A-III. On the other hand, MoDTC not only improved the friction behavior of a-C coatings but also substantially reduced the wear of a-C-coated interacting surfaces when mixed with A-III. In order to further evaluate the compatibility of a-C/a-C contact

with various additives (GMO, AP etc.) and base oils (M, A-II, SO), there is a need to perform more tribological investigations using formulated lubricants.

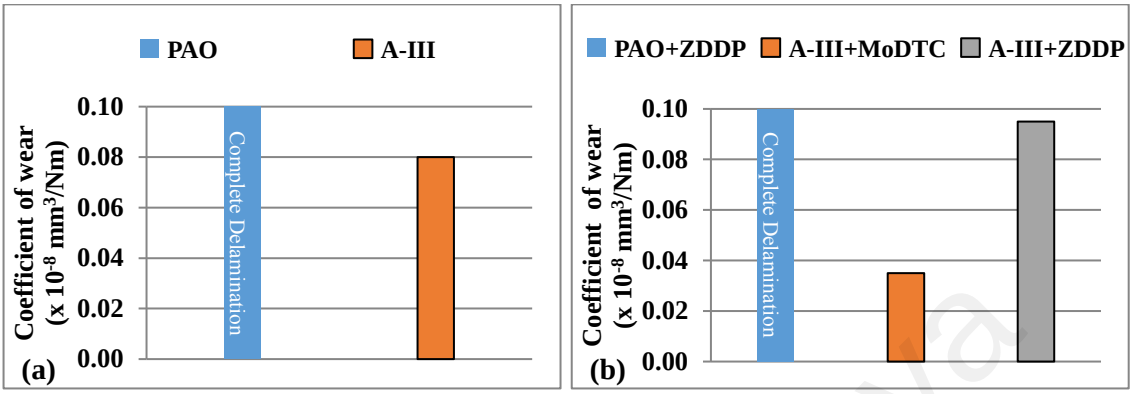

Figure 2.21: Average values of coefficient of wear for a-C /a-C contacts with (a) base oils and (b) formulated lubricants
(Tasdemir, Tokoroyama, et al., 2014; Vengudusamy, Green, et al., 2011; Vengudusamy et al., 2012, 2013b)

2.5.4 ta-C:H/ ta-C:H contact

It is not a common type of DLC coating and very few tribological investigations were carried out on its symmetrical contact. Although, a lot of studies were performed in 1990s to analyze how its deposits on various substrates (Morrison et al., 1997; Morrison, Rodil, Ferrari, Robertson, & Milne, 1999; Rodil & Muhl, 2004; Schwan et al., 1995) but afterwards, researchers did not pay much attention to evaluate tribological characteristics of this DLC type.

Recently, Vengudusamy et al. (2012) conducted an experimental study to reveal the tribological characteristics of ta-C:H coating under lubricated conditions using formulated and additive-free versions of A-III base oil (**Figure 2.22**). They used MoDTC as lubricant additive and observed it to be tribologically beneficial for ta-C:H/ta-C:H tribopair. A slight decrease in coefficient of friction (0.07 to 0.06) was realized with A-III+MoDTC lubricant compared to additive-free A-III. Like previously discussed, this advantageous role of MoDTC in terms of friction can be attributed to tribochemical

interaction between ta-C:H coated surfaces and MoDTC resulting in the formation of MoS_2 (Vengudusamy et al., 2012). In contrast, friction coefficient was increased from 0.05 to 0.06 when A-III+MoDTC was used instead of additive-free A-III in ta-C:H/steel contact. This rise in friction level can be attributed to accelerated wearing out of ta-C:H-coated disk during tribotesting which not only increases the surface roughness but also degrades the friction performance of the contact (Vengudusamy et al., 2012)

Although, MoDTC is primarily a friction modifier, yet it was able to significantly reduce the wear coefficient of symmetrical ta-C:H contact. Almost 50% decrease in wear (0.10×10^{-8} mm^3/Nm to 0.06×10^{-8} mm^3/Nm) was observed with A-III+MoDTC lubricant compared to additive-free A-III (**Figure 2.23**). Contrary to ta-C:H/ta-C:H contact, an increase in wearing out of interacting surfaces was observed with MoDTC-containing lubricant when AISI 52100 chrome steel ball was used as counterbody. It is mentioned in the literature that MoO_3, which is formed as a result of incomplete tribochemical decomposition of MoDTC, drastically affects the wear characteristics of a contact by passivating the dangling carbon bond and promoting oxidative wear (Shinyoshi et al., 2007). Presence of steel counterbody promotes the formation of MoO_3 by forming ferrous oxide (FeO), ferric oxide (Fe_2O_3) and magnetite (Fe_3O_4). This drastic effect of MoDTC on wear characteristics of DLC/steel can be mitigated to an appreciable extent by using sulfur-containing antiwear additives in combination with MoDTC-containing lubricant (Haque et al., 2009). Antiwear additive such as ZDDP provides continuous supply of sulfur for complete decomposition of MoDTC resulting in high MoS_2/MoO_3 ratio.

In order to perceive the suitability of ta-C:H coating for industrial applications, there is a need to further investigate its tribological characteristics in combination with formulated and additive-free lubricants under various operating conditions.

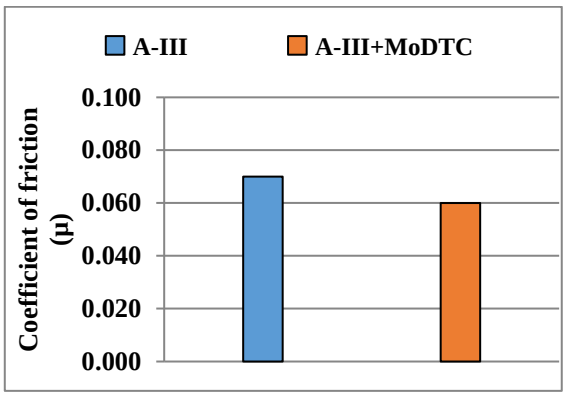

Figure 2.22: Average values of coefficient of friction for ta-C:H/ta-C:H contact with A-III (with and without additive)
(Vengudusamy et al., 2012)

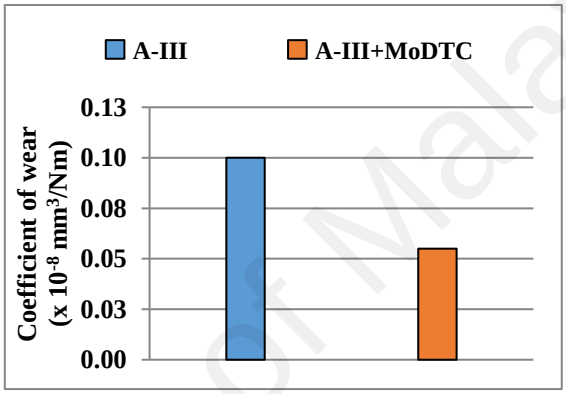

Figure 2.23: Average values of coefficient of wear for ta-C:H/ta-C:H contact with A-III (with and without additive)
(Vengudusamy et al., 2012)

2.5.5 Summary

ZDDP, an antiwear additive, proved to be effective in further enhancing the wear resistance of DLC coatings irrespective of the base oil. The improvement in wear characteristics can be attributed to the formation of ZDDP-derived tribofilms comprised of phosphates and sulphates. Hindrance in graphitization due to the presence of ZDDP resulting in prevention of delamination and coating spallation can be another viable justification for low wear coefficients. The only exception to this observation was a-C/a-C contact which showed a slight increase in wear coefficient when A-III+ZDDP was used as lubricant. This deterioration in wear performance can be associated to antagonistic correlation between base oil, additive and DLC-coated interacting surfaces. Contrary to wear results, ZDDP-additivated lubricants either increased or unable to make any changes

in friction characteristics of most of the DLC coatings. It is believed that running-in behavior of most DLC coatings is generally negatively influenced due to the presence of ZDDP additive (Vengudusamy, Green, et al., 2011). Only PAO+ZDDP and A-III+ZDDP showed a slight decrease in friction coefficients compared to their non-additivated versions when used in combination with self-mated ta-C coating. Although, ZDDP-derived tribofilm was also formed on ta-C/ta-C contact when tested with PAO+ZDDP and A-III+ZDDP but instead of strongly adhered pad-like structure, it was thin, patchy and easily removal with acetone or benzene.

A decrease in friction coefficients of symmetrical DLC contacts was observed when MoDTC was used as friction modifier in combination with A-III whereas opposite behavior was observed with PAO and A-II base oils. In most of the cases, it is the formation of MoS_2, as a result of tribochemical decomposition of MoDTC, which acts as solid lubricant and played a vital role in achieving low levels of friction. An increase in friction coefficients of ta-C/ta-C and a-C:H/a-C:H contacts when PAO+MoDTC and A-II+MoDTC were used as lubricants respectively, can be attributed to incomplete decomposition of MoDTC and formation of MoO_3 instead of MoS_2 in higher ratios. It is widely accepted that MoO_3 is ineffective in overcoming friction due to its sharp edge crystalline structure. When ZDDP was mixed with MoDTC-additivated PAO lubricant, a-C:H/a-C:H contact showed better friction characteristics compared to PAO+MoDTC and PAO+ZDDP lubricants. This effect can be attributed to the continuous supply of sulfur from ZDDP which resulted in complete decomposition of MoDTC and formation of MoS_2. Although, MoDTC is primarily a friction modifier but it also proved to be effective in overcoming wear of DLC coatings. Only exception to this observation was ta-C/ta-C contact which showed an increase in wear coefficient when A-III+MoDTC was used as lubricant. This can be attributed to suppression in phenomenon of graphitization due to the presence of MoDTC.

GMO is another conventional lubricant additive which has been widely investigated in combination with DLC coatings. Although, GMO is considered to be a friction modifier but it was not effective in overcoming the friction losses of most of most of the DLC coatings. Instead, an improvement in wear resistance was observed to some extent. When GMO was used as an additive in PAO with self-mated ta-C DLC coating, an enhancement in wear behavior was observed whereas level of friction between the sliding surfaces was increased. A similar deterioration in friction performance was also observed in case of a-C:H/a-C:H contact when PAO+GMO was used as lubricant. This change in tribological characteristics can be attributed to passivation of dangling carbon bonds by the hydroxyl group. Another viable justification for this behavior can be suppression of graphitization phenomenon due to the presence of GMO. It is mentioned in the literature that graphitization substantially affect the structural integrity of DLC coatings making them soft and more vulnerable to excessive wearing (Ouyang & Sasaki, 2005). On the other hand, graphitization usually results in decreased friction and facilitates sliding because of low shear strength possessed by graphitic layer compared with diamond. A deterioration in the tribological characteristics of ta-C/ta-C contact was observed when ZDDP was additivated with PAO+GMO lubricant. Among PAO-additivated lubricants, highest value of friction was observed when PAO+GMO+ZDDP was used. In addition to that, presence of ZDDP also affected the wear characteristics of PAO+GMO and increase in wear coefficients of ta-C/ta-C contact was observed. Although, GMO was able to passivate the active sites on ta-C coated surfaces but no ZDDP-derived tribofilm was detected when PAO+GMO+ZDDP was used. GMO performed its primary role of friction modifier when additivated with A-II and used in combination with symmetrical a-C:H contacts and an improvement in friction behavior was observed. A viable justification for this outcome can be adsorbtion of hydroxyl group and formation of GMO-derived tribochemical species on interacting surfaces.

2.6 Evaluation of DLC coatings for cam/tappet interfaces

A lot of studies were carried out by researchers to evaluate the suitability of DLC coatings for various tribopairs of automotive engines by simulating the contact using tribometers. However, there are only few experimental investigations in which DLC-coated engine parts were used and tested in the original environment of the engine under realistic running conditions. Some of the automotive components and assemblies which were considered by researchers for the application of DLC coatings include piston/cylinder assembly (Cho et al., 2009; Etsion et al., 2006; Tung & Gao, 2003), cam/tappet interface (Gangopadhyay et al., 2012; Gangopadhyay et al., 2011; Kano, 2006; Lawes et al., 2010; Mabuchi et al., 2007; Schamel et al., 1997; Yasuada, 2003), piston ring/cylinder interface (Cho et al., 2009; Etsion et al., 2006; Tung & Gao, 2003), gears (Kalin & Vižintin, 2005; Snidle & Evans, 2009) and bearings (Franklin & Baranowska, 2007; Vanhulsel et al., 2007).

In one of the studies, Dobrenizki et al. (2016) analyzed the influence of zirconium-doped DLC coating (a-C:H:Zr) and a-C:H on the friction and wear behavior of tappet/camshaft interface. In order to do so, they used one tappet/one cam friction test rig using series-production tappets, cams and valve springs so that experimental data can be related to the actual engine (**Figure 2.24**). Above-mentioned coatings were only applied to the tappets whereas uncoated camlobes were used. Mineral-oil based SAE 0W20 and PAO-based SAE 5W30 containing GMO, MoDTC and ZDDP were used as lubricants. A significant reduction in friction losses and improvement in wear-resistance was observed when DLC-coated tappets were used regardless of camshaft speed, lubricant temperature and lubricant formulation. When DLC-coated tappets were analyzed by Raman spectroscopy and XPS, no signs of any additive-derived tribofilm was seen. This observation shows that improvement in tribological performance of DLC-coated tappet/uncoated cam was due to inherent low-friction and high wear resistance

characteristics of DLC coatings and not because of the tribochemical interaction of additives with DLC-coated tappets.

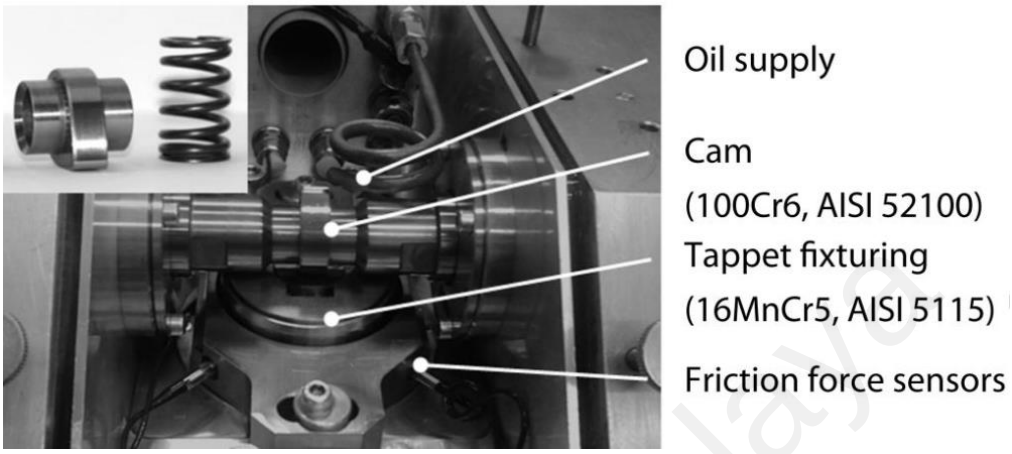

Figure 2.24: One tappet/one cam friction test rig
(Dobrenizki et al., 2016)

In another experimental investigation, Durham and Kidson (2014) tested the suitability of DLC coatings for cam/tappet interface using cylinder head of commercial diesel engine under fired and motored condition (**Figure 2.25**). Four different types of DLC coatings which include a-C:H, a-C:H:Si, a-C:H:Ti coating and a-C:H:W were deposited on the tappets of commercial diesel engine and tested against uncoated camshafts. Low sulfated ash, phosphorus and sulfur SAE 10W40 was used for wear tests whereas three different versions of SAE 10W30 lubricants containing organic friction modifiers and additive packages were used for friction tests. Significant reduction in friction was seen when DLC-coated tappets were used instead of uncoated ones against uncoated camshafts irrespective of lubricant formulation. After 300 hours of wear testing, only a-C:H was able to withstand test conditions whereas a-C:H:Ti was completely delaminated from the tappets. Delamination of coating was also observed when a-C:H:Si-coated tappets were used but only on the central region. Although, a-C:H:W was also able to sustain itself during testing but its thickness was substantially reduced. On the other hand, substantial

decrease in wearing-out of uncoated camshaft was seen when DLC-coated tappets were used against it instead of uncoated one irrespective of DLC coating type.

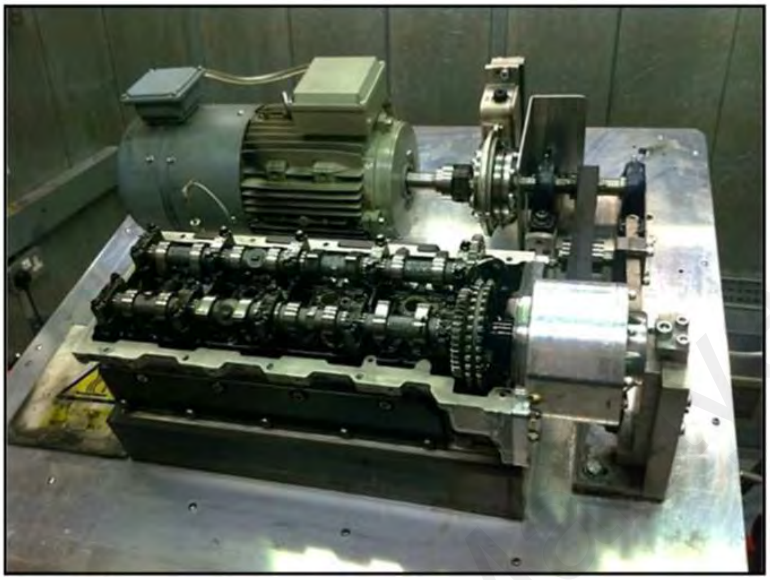

Figure 2.25: Lubrizol's tribometer using OM646LA engine head (Durham & Kidson, 2014)

Suitability of multi-layered DLC coating (CrN + a-C:H:W + a-C:H) for tappets of 2.0 liters supercharged gasoline engine was analyzed by Kong et al. (2016) under motored and fired conditions in the presence of SAE 5W40 lubricant (**Figure 2.26**). A significant reduction of 33% in the valve train friction was observed when DLC-coated tappets were used instead of uncoated ones at an engine speed of 2000 RPM. Not only this, remarkable improvement in wear-resistance was also seen with DLC-coated tappets. No signs of coating delamination or peeling-off was noticed after 450 hours of standard durability cycle test.

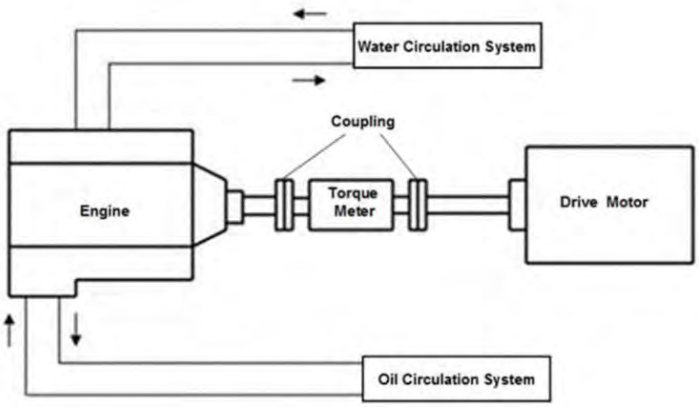

Figure 2.26: Test rig capable of running 2.0 liters supercharged gasoline engine under motored and fired conditions
(Kong et al., 2016)

In order to simulate the cam/tappet interface of automotive engine, single cam tribometer was used by Mistry, Morina, and Neville (2012) (**Figure 2.27**). AISI 52100 chrome steel shims were coated with a-C:H and tested against uncoated cast iron cams in the presence of PAO-based lubricants formulated with detergents, dispersants, ZDDP and MoDTC. Although, no signs of MoS_2, MoO_3 and zinc sulfide (ZnS) were seen on the shim surface in Raman spectra, still improvement in tribological improvement was seen. Highest friction was observed when ZDDP-containing PAO was used as lubricant whereas PAO+MoDTC+ZDDP resulted in lowest value of friction coefficient. Significant reduction in wear of DLC-coated shims was observed when MoDTC and ZDDP containing PAO was used as lubricant instead of its additive-free version.

In another study, Kano (2006) used ta-C-coated follower against uncoated camshaft in the presence of GMO-containing PAO using cylinder head of commercial engine. Friction was reduced by 45% when ta-C-coated follower was used instead of uncoated one at an engine speed of 2000 RPM. In order to see the durability of coating, cylinder head was operated at 4000 RPM for 300 hours but no signs of coating delamination were noticed.

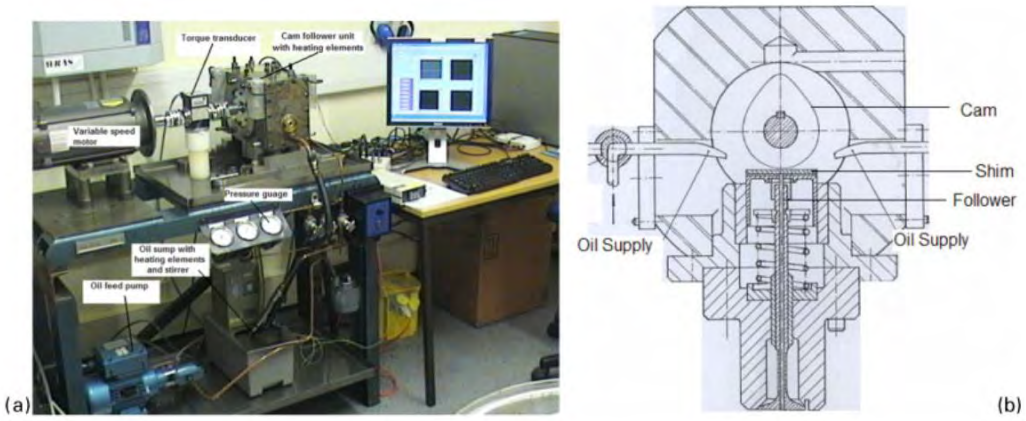

Figure 2.27: Single cam tribometer: (a) major components; (b) cam and shim assembly
(Mistry et al., 2012)

Mutafov, Lanigan, Neville, Cavaleiro, and Polcar (2014) investigated the suitability of a-C:H:W for cam/tappet interface of automotive engine using engine test bench under fired condition in the presence of SAE 5W40 fully formulated engine oil (**Figure 2.28**). Engine was operated at different running conditions after which tappets were removed for analysis. Presence of thick additive-derived tribofilm, comprised of elements and compounds typical of engine oil and additives, on DLC-coated tappets was confirmed by Raman spectroscopy and ToF-SIMS. As a result, significant improvement in wear resistance of tappets was seen compared to uncoated ones. This observation shows that conventional additives can tribochemically interact with DLC-coated valve train components and improve its tribological performance by reducing friction and wear.

Figure 2.28: Engine test bench

2.6.1 Summary

Various types of DLC-coating were used by researchers for analyzing their suitability for cam/tappet interface under motored and fired conditions. In almost all of the studies, DLC coatings was only applied to the tappets/followers whereas uncoated camshaft was used. Although, various types of lubricants were tested which include fully-formulated lubricants and PAO-based lubricants but researchers did not consider bio-lubricants during their investigations. Improvement in friction and wear characteristics of cam/tappet interface was observed by all the researchers irrespective of lubricant and DLC coating type used. Not only this, decrease in wearing out of uncoated camshaft was also observed when DLC-coated tappets were used. When tappets were analyzed using material characterization techniques such as Raman spectroscopy, XPS and ToF-SIMS, additive-derived tribofilms were not detected in most of the cases which shows that improvement in tribological characteristics of cam/tappet interface was due to the inherent low-friction and high wear resistance of DLC coatings. When durability test was carried out on a-C:H, a-C:H:Si, a-C:H:Ti and a-C:H:W- coated tappets in the presence of SAE 10W30, only a-C:H was able to withstand 300 hours of testing, a-C:H:Ti was completely delaminated, a-C:H:Si was partially delaminated whereas decrease in

thickness of a-C:H:W coating was seen. These observations show that a-C:H and a-C:H:W coatings are most suitable for cam/tappet interface of direct acting valve train assembly of automotive engine.

CHAPTER 3: RESEARCH METHODOLOGY

3.1 Introduction

In this chapter, details of experimental set-ups, which include a four-ball wear tester, universal wear testing machine and direct acting valve train test rig, are discussed along with the test conditions and procedures. In addition to that, specifications of the materials used in this research work are also given. These materials include conventional and bio base oils, conventional lubricant additives, substrate materials, engine components and various types of DLC coatings. Moreover, optical, spectroscopic and mechanical material characterization techniques used in this study to investigate the mechanisms responsible for a particular tribological behavior are also deliberated.

3.2 Tribotesting using four-ball wear tester and universal wear testing machine

In order to analyze the potential of an oil as lubricant base stock and while formulating lubricants for a particular industrial application, various types of tribometers are used in industry as well as in academia. These tribometers are capable of simulating numerous types of contacts and operating conditions used in industrial applications according to the requirements. In order to do the tribotesting, certain set of rules and specifications are mentioned in ASTM standards. Tribometers which were used in this study include four-ball wear tester (ASTM D2783) and universal wear testing machine (ASTM G133).

3.2.1 Four-ball wear tester

Four-ball wear tester is one of the most widely used tribometer in industry during the developmental phase of lubricants. Schematic diagram of four-ball wear tester used in this study is shown in **Figure 3.1**.

Figure 3.1: Four-ball wear tester

AISI 52100 chrome steel balls were used to simulate ball-on-ball geometric configuration details of which will be discussed in **section 3.2.1.2**. Steel balls and machine components (ball holder, clamps, test-oil cup etc.) were washed with toluene to remove antirust coatings, contaminants and residual lubricant layers before and after each test. Lint free industrial wipes were used to remove traces of toluene before putting them in test-oil cup and spindle. One of the balls was tightened into the spindle of the machine while other three balls were assembled in test-oil cup and tightened by applying torque of around 2.8 to 5.6 Nm with the help of wrench. Three balls at the bottom were held stationary and pressed against the top ball establishing three different point contacts which proved to be very useful for carrying out statistical analysis such as calculation of mean wear scar diameter and error bars. Test-oil cup was then filled with lubricant sample in such a way that it stays 3 mm above the top surface of balls and placed inside the machine.

Although, ball-on-ball contact associated with four-ball wear tester, does not replicate any contact present in the engine but still it is widely used in the automotive industry during the developmental stage of lubricants to determine their tribological and extreme pressure characteristics. The four-ball wear tester was originally developed by shell as a screening test to assess the capability of lubricating oils to prevent wear in highly loaded contacts. It turned out to be a suitable and cost-effective test to assess the effectiveness of antiwear and extreme pressure additives; and was accepted by the oil community as a standard screening test and incorporated in various national standards [ASTM, German Institute for Standardization (DIN)].

In this study, four-ball wear tester was used to evaluate extreme pressure characteristics and load-carrying capacity of lubricant samples by conducting the sliding tests according to the procedure described in ASTM D-2783 standard. Extreme pressure characteristics and load carrying capacity of lubricants are related to their ability to decrease wear of the parts exposed to very high pressures and prevent lubricant starvation conditions. Some of the important test conditions which are mentioned in the above-mentioned ASTM standard and used in the tests are shown in **Table 3.1**. In order to compare the extreme pressure characteristics of lubricant samples, wear scar diameter of lower three balls were calculated. After the completion of test duration, lubricant was drained form the test-oil cup and scar area was cleaned with a tissue. While balls were still clamped, assembly was placed on a custom-made base of microscope that was specially designed for four-ball machine. For each wear scar, two measurements were taken to calculate mean value. One measurement was taken along a radial line from the center of the holder whereas second reading was taken along a line 90° from the first measurement.

Table 3.1: Tribotest conditions for evaluating extreme pressure characteristics of lubricants using four-ball wear tester

Physical Quantity	Specifications
Temperature	18 - 35 °C
Speed	1760 ± 40 RPM
Duration	10 seconds
Load	40, 50, 63, 80, 100, 126, 160, 200, 250 kg

The parameters which were calculated during extreme pressure tests include last non-seizure load, initial seizure load and weld point. These parameters are defined below:

i Last non-seizure load

It is the value of last load at which the measured scar diameter is not more than 5 % above the compensation line.

ii *Initial seizure load*

It can be defined as the value of applied load at which a significant increase in the value of wear scar diameter is observed due to momentary breakdown of lubricating film.

iii *Weld point*

It is the lowest value of applied load at which the rotating ball welds to the three stationary balls due to collapsing of lubricant film at the contact.

3.2.1.2 Substrates and counterbodies

(a) ***AISI 52100 chrome steel balls***

AISI 52100 chrome steel balls were used in four-ball wear tester to evaluate the tribological compatibility between additives and TMP on steel/steel contact. The above-mentioned balls were commercially available ball bearings acquired off-the-shelf from an

Italian vendor (RGP International) and used as received. Physical and material properties of the above-mentioned balls are given in **Table 3.2** whereas chemical composition is presented in **Table 3.3**.

Table 3.2: Physical and mechanical properties of AISI 52100 chrome steel balls

Properties	**Specifications**
Grade	AISI 52100
Diameter	12.70 mm
Hardness	60-66 HRC
Average surface roughness	0.02 - 0.03 μm

Table 3.3: Chemical composition of AISI 52100 chrome steel balls

Element	**Weight percentage (wt.%)**
Iron	96.800 - 97.150
Carbon	0.950 - 1.100
Silicon	0.350
Manganese	0.200 - 0.500
Phosphorus	0.025
Sulfur	0.025
Chromium	1.300 - 1.600

3.2.1.3 Lubricants and their composition

In this research work, 10 different lubricants were used, out of which 2 were additive-free base oils whereas rest of the 8 were formulated lubricants. A lot of experimental studies were carried out by researchers to investigate tribological compatibility of vegetable oils with conventional lubricant additives in combination with various types of DLC coatings. In most of these studies, rapeseed and sunflower oils, formulated with conventional additives, were used as bio-lubricants. Although, few of the researchers also considered palm oil in combination with DLC coatings but without conventional additives

(Al Mahmud et al., 2015; Al Mahmud et al., 2014a). To address this research gap, there is need to investigate tribological characteristics of formulated palm oil-based lubricants with DLC coatings. Due to this reason, palm oil was selected as biodegradable and renewable base oil. In order to see its potential to be used as lubricant base-stock, its tribological performance was compared with that of PAO, which is most widely used conventional base oil in engine lubricants. In order to improve the thermo-oxidative stability and low temperature characteristics of palm oil, it was chemically modified by transesterification process. Chemical equation of the reaction is shown in **Figure 3.2**. During the synthesis of TMP, palm oil was first converted into its methyl ester and then reacted with trimethylolpropane. The rationale for selecting trimethylolpropane [2-ethyl-2-hydroxymethyl-1,3-propanediol] as polyol was its low melting point compared to others. During the transesterification process, ester (-COOR-) group from palm methyl ester was replaced by hydroxyl (-OH-) group of trimethylolpropane. Transesterification reaction was conducted in 500 ml three-necked reactor equipped with a reflux condenser, a thermometer, and a sampling port. The condenser was coupled to a vacuum line with a relief valve, an accumulator, and a vacuum trap. During the synthesis, the reactor was immersed in a temperature-controlled silicon oil bath and the solution was agitated with a magnetic stirrer. A 200-ml of methyl ester and a known amount of trimethylolpropane were placed in the reactor and the mixture was heated to the operating temperature before a catalyst was added. Vacuum was gradually applied after catalyst addition to avoid the spillover of reaction materials. Sodium methoxide was used as the catalyst because it minimizes the saponification of esters. Samples were taken at pre-determined time intervals for the gas chromatographic analysis of product yield. After the reaction was completed, the catalyst was separated from the product mixture by vacuum filtration whereas distillation was conducted to remove unreacted methyl esters from the final product.

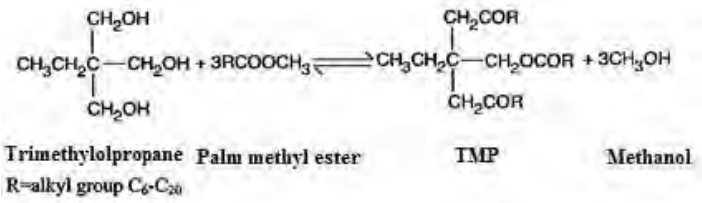

Figure 3.2 Chemical equation for synthesis of TMP

Since, valve train assembly mostly operates in boundary lubrication regime, therefore, antiwear additives and friction modifiers (GMO, MoDTC and ZDDP) were used to further enhance the tribological performance of base oils. Other additives such as detergents, dispersants, antioxidants were not considered while formulating lubricants so that effectiveness of tribologically relevant additives can be analyzed in isolation. PAO was purchased from Ineos, USA whereas lubricant additives were acquired from Adeka, Japan. In order to study the tribological performance of each additive independently, without the influence of others, formulated lubricants were prepared by mixing additives at a concentration of 1.0 wt.% in each base oil separately. A precision weighing balance with a least count of 0.1 milligram was used for accurate weight measurements. Initially, a beaker containing base oil was heated to 80°C using a magnetic stirrer at 150 rpm and then additive was added to it. The solution was then magnetically stirred until additive was fully dissolved in the base oil to get a homogenous mixture. These base oils and above-mentioned formulated lubricants were used in universal wear testing machine with ball-on-flat geometric configurations. Beside these 6 formulated lubricants, 2 more lubricants were formulated by mixing 3.0 wt.% of additives i.e. 1.0 wt.% of each additive in 97.0 wt.% of each base oil. These 2 lubricants containing all of the three additives were used in the universal wear testing machine with a pin-on-plate geometric configuration and cylinder head testing along with additive-free base oils. Formulation details of the lubricants used in this study are shown in **Table 3.4**.

Table 3.4: Formulation details of lubricants used in this research work

Lubricant name	PAO conc. (wt.%)	TMP conc. (wt.%)	GMO conc. (wt.%)	MoDTC conc. (wt.%)	ZDDP conc. (wt.%)
PAO	100	-	-	-	-
TMP	-	100	-	-	-
PAO+GMO	99	-	1	-	-
TMP+GMO	-	99	1	-	-
PAO+MODTC	99	-	-	1	-
TMP+MODTC	-	99	-	1	-
PAO+ZDDP	99	-	-	-	1
TMP+ZDDP	-	99	-	-	1
PAO+GMO+MoDTC+ZDDP (P+G+M+Z)	97	-	1	1	1
TMP+GMO+MoDTC+ZDDP (T+G+M+Z)	-	97	1	1	1

(a) ***Physicochemical properties***

In order to gauge the potential of an oil to be used as lubricant, it is very important to thoroughly analyze its physicochemical properties. Some of the most important physicochemical properties are discussed below:

i Viscosity

It represents resistance to the flow of lubricant and depends on operating conditions such as temperature, pressure as well on fluid film thickness (Mobarak, Niza Mohamad, et al., 2014). If the viscosity of a lubricant is very low, there is high probability of metal-to-metal contact during sliding especially at higher temperatures. Contrary to that, if a

lubricant is too viscous, a lot of input energy is wasted in overcoming the lubricant's shear strength resulting in higher value of coefficient of friction.

ii VI

Another important performance parameter of lubricant is VI which relates viscosity with temperature and represents changes in viscosity as a result of changing temperature. An ideal lubricant is the one which has high VI due to which it maintains its viscosity over a wide range of temperatures.

iii Density

Density of a lubricant is also critical to its tribological performance. It represents ratio of lubricant's mass to volume. If the density of lubricant is too high, it will be difficult for it to be spread on the interacting surface especially at lower operating temperatures. In addition to that, it is recommended for a lubricant to have a density lower than that of water so that if some moisture content get mixed with the lubricant, it settles down at the bottom and filters out through the drain valve while lubricant remains at the top.

Kinematic viscosities and densities of all the lubricants considered in this study were measured using Anton Paar SVM 3000 stabinger viscometer according to ASTM D7042-2012 standards whereas VI was calculated through ASTM D2270 by measuring the values of kinematic viscosities at 40°C and 100°C.

3.2.2 Universal Wear Testing Machine

Reciprocatory sliding tests were conducted to analyze the tribological compatibility of conventional lubricant additives with TMP and various types of DLC coatings. When camshaft rotates, camlobe makes line contact with the tappet. Cam nose translates over the tappet's top source in a linear motion and pushes the tappet downward. In addition to

that, tappet also rotates inside its bore because cams are slightly off-centered relative to the tappet center to facilitate and ensure continuous rotation of tappets in their bores, reducing friction and ensuring even wear. In order to simulate that complex combination of linear and rotational motion of tappet, reciprocating tests were carried out. In order to estimate the effectiveness, friction and wear coefficients of DLC/DLC contacts, obtained with TMP-based lubricants were compared with those of PAO-based ones. In addition to that, tribological performance of above-mentioned lubricants on DLC/DLC contacts was also compared with those of steel/steel and steel/cast iron contacts. Moreover, influence of steel counterbody presence in the contact on tribochemical interactions between conventional additives and DLC coatings was also investigated by using DLC/steel and DLC/ cast iron contacts. In order to understand the mechanism behind a particular tribological behavior of DLC-lubricant pair, material characterization techniques were deployed after carrying out tribotests details of which will be discussed in **section 3.2.2.4**. Ball-on-plate and pin-on-plate geometric configurations were tested using universal wear testing Machine (Cameron Plint TE99)(**Figure 3.3**). Tribotests with ball-on-plate geometric configuration were carried out to see the tribological compatibility of single-additive containing lubricants and DLC coatings so that performance of each additive can be analyzed in isolation without the influence of other additives. On the other hand, pin-on-plate geometric configuration was used to simulate cam/tappet interface of direct acting valve train of a commercial diesel engine. Since, fully-formulated lubricants are used in cars therefore, multi-additive containing lubricants were used in addition to additive-free base oils during pin-on-plate tribotests.

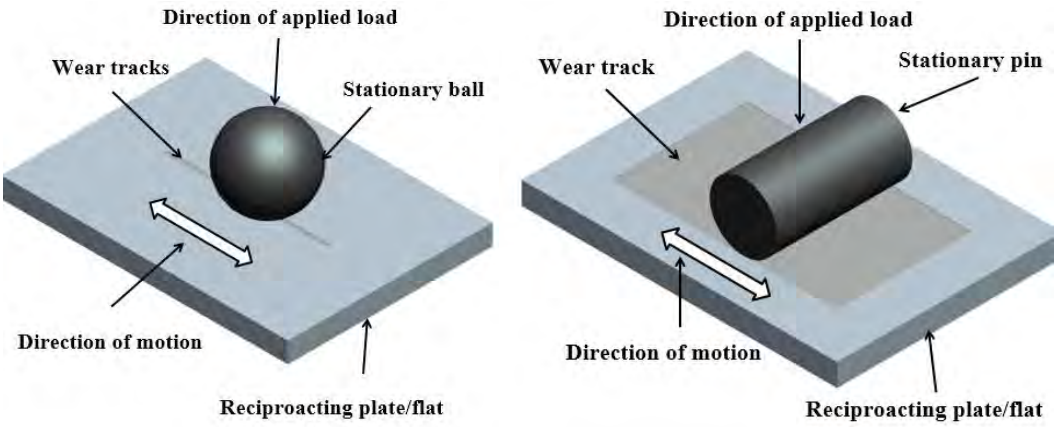

Figure 3.3: Ball-on-plate and pin-on-plate geometric configurations simulated using universal wear testing machine

In universal wear testing machine, a variable speed motor is connected to sliding carriage through connecting rod which converts rotational motion into reciprocatory motion. Oil sump is mounted on sliding carriage. In both of the above-mentioned contacts, AISI 52100 chrome steel plates were clamped in oil sump and then filled with lubricant sample in such a way that its top surface is completely covered with lubricant. The lubricant is then heated inside the oil sump using electric resistance heating and required temperature is achieved with the help of a thermocouple and control system. A Linear Variable Differential Transformer (LVDT) sensor was used to determine the frictional force between the interacting surfaces. In order to calculate coefficient of friction, frictional force was divided by normal applied load. Wear characteristics of contact was characterized by calculating wear coefficients of interacting surfaces. Wear coefficients of ball and pin were calculated by measuring the wear scar diameter (WSD) and wear track width respectively using SEM and converting them into wear volume by using Microsoft® Excel®-based mathematical equation. In order to calculate wear volume of plate, Surftest SJ-210 mechanical stylus profilometer was deployed to obtain the depth profile of wear track using area under the curve method and then multiplying it

by the stroke length i.e. 10 mm. Wear volume was then divided with applied load and total sliding distance to get coefficient of wear. A specially-designed data acquisition (DAQ) system was used for establishing a communication between DAQ hardware and sensors. A fully labelled-3D model of universal wear testing machine is shown in **Figure 3.4**. In ball-on-flat configuration, AISI 52100 chrome steel balls were used as counterbody and slid against plates whereas BS 1452 cast iron pins were used in pin-on-plate geometric configuration. Counterbodies were clamped to the loading arm with the help of a specially designed holder. Tribotest conditions such as temperature, load, sliding speed etc. for the above-mentioned tests were selected in such a way that they replicate the original conditions of cam/tappet interface of direct acting valve train assembly of commercial diesel engine (**Table 3.5**). Similar conditions were also used by other researchers while evaluating cam/tappet interface (Haque et al., 2007; Haque, Morina, Neville, Kapadia, & Arrowsmith, 2008; Kosarieh et al., 2013a; Yang, Neville, Brown, Ransom, & Morina, 2014). Since, cam/tappet interface mostly operates in boundary lubrication regime (Riaz Ahmad Mufti, Zahid, Qureshi, Aslam, et al., 2015) therefore, tribotesting using universal wear testing machine was carried out in boundary lubrication regime. The calculation of the dimensionless film parameter, the lambda ratio (λ), was based on the starting average surface roughness of interacting surfaces. This parameter was used to describe the lubrication regime and was calculated using the Dowson and Hamrock minimum film thickness equation.

$$\lambda = \frac{\boldsymbol{Film\ thickness}}{\boldsymbol{Surface\ roughness}} = \frac{h_{min}}{\sqrt{R^2 a_1 + R^2 a_2}} \qquad \textbf{3.1}$$

Where,

h_{min} = minimum film thickness

Ra_1 = Surface roughness of plate

Ra_2 = Surface roughness of ball

Before each test, plates, balls and pins were cleaned with acetone in ultrasonic bath whereas surfaces were washed with cyclohexane and kept in desiccator before carrying out surface analysis. Since, test matrix was huge and a lot of coating/lubricant combinations were analyzed therefore, each test was only conducted twice to see the repeatability and reproducibility of the results and to calculate the standard deviations. If results were not repeatable for a particular test and there was considerable difference between test 1 and test 2 results, it was carried out for the 3rd and 4th time as well in order to obtain a good statistical representation.

Table 3.5: Tribotest conditions for evaluating tribological performance parameters of steel/steel, steel/cast iron, DLC/steel, DLC/cast iron and DLC/DLC contacts using universal wear testing machine

Physical Quantities	**Specifications**	
	Ball-on-plate configuration	**Pin-on-plate configuration**
Temperature	90 °C	90 °C
Speed	0.04 m/s	0.04 m/s
Duration	120 min	120 min
Stroke length	10 mm	10 mm
Load	10 N	615 N
Maximum hertzian contact pressure	700 MPa	700 MPa
Total sliding distance	288 m	288 m

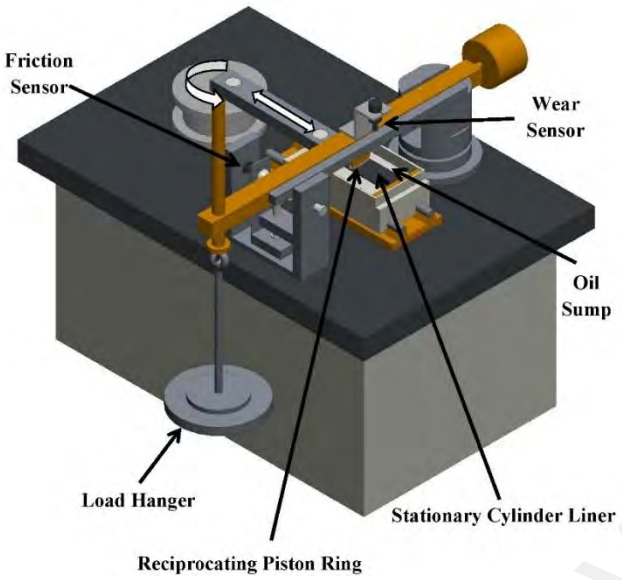

Figure 3.4: Fully labelled-3D model of universal wear testing machine

3.2.2.1 Substrates and counterbodies

(a) ***AISI 52100 chrome steel plates***

AISI 52100 chrome steel plates were procured in bulk form and then cut into required shape and size i.e. 100.00 mm length, 30.00 mm width 3.00 mm thickness, using milling and surface grinding machines. In order to make the hardness and surface finish of these plates comparable with tappets, heat treatment and grinding/polishing procedures were carried out respectively.

Heat treatment of plates was carried out in multiple steps. First of all, annealing of the plates was done by heating the plates in electric furnace at a temperature of 850°C for 45 minutes. Red hot plates were then quenched in heat treatment oil for 2 minutes, which was pre-heated to 55°C. After that, tempering process was performed in electric oven at 180°C for 3 hours to improve toughness and ductility of plates. In the end, plates were cleaned by removing oil, dirt and oxide layer from the surfaces with the help of wire brush prior to grinding and polishing process.

Grinding of the plates was performed with 200, 360, 600, 1000, 1500 and 2000 grit sized sand papers using double disc polishing machines. In order to remove the scratches made by the sandpapers, polishing of the plates was done by using polishing clothes in combination with diamond suspension of 1 μm size and silicon carbide suspension of 0.01 μm size. After carrying out the above-mentioned procedure, plates with an average surface roughness of 0.02 – 0.023 μm were achieved. Physical and material properties of the above-mentioned plates are given in **Table 3.6** whereas chemical composition is given in **Table 3.7**.

Table 3.6: Physical and mechanical properties of AISI 52100 chrome steel plates

Properties	**Specifications**
Grade	AISI 52100
Length	100.00 mm
Width	30.00 mm
Thickness	3.00 mm
Hardness	60 - 66 HRC
Average surface roughness	0.02 - 0.03 μm

Table 3.7: Chemical composition of AISI 52100 chrome steel plates

Element	**Weight percentage (wt.%)**
Iron	96.800 - 97.150
Carbon	0.950 - 1.100
Silicon	0.350
Manganese	0.200 - 0.500
Phosphorus	0.025
Sulfur	0.025
Chromium	1.300 - 1.600

(b) ***AISI 52100 chrome steel balls***

AISI 52100 chrome steel balls were used as counterbodies against AISI 52100 chrome steel plates during tribotests with ball-on-plate geometric configuration. Details of balls are already discussed in **section 3.2.1.2(a)**. The only difference between the balls used in four-ball wear tester and universal wear testing machine was the diameter. Instead of 12.7 mm, balls used in universal testing machine were of 15 mm diameter. In case of steel/steel and DLC/steel contacts, uncoated-balls were used in combination with uncoated and DLC-coated plates respectively whereas DLC-coated balls were used against DLC-coated plates for simulating DLC/DLC contacts.

(c) ***BS1452 cast iron pin***

BS1452 cast iron rods were acquired in the form of cylinders from the local vendor. In order to achieve surface roughness comparable to that of engine camlobes, cast iron rods were grinded and polished before cutting them into required shape and size using lathe machine i.e. diameter of 10 mm and length of 10 mm.

Grinding of the rods was performed with 200, 360, 600, 1000, 1500 and 2000 grit sized sand papers by clamping them in the turret of lathe machine. In order to remove the scratches made by the sandpapers, polishing of the rods was done by using polishing clothes in combination with diamond suspension of 1 μm size and silicon carbide suspension of 0.01 μm size. After carrying out the above-mentioned procedure, an average surface roughness of 0.02 – 0.023 μm was achieved.

BS1452 cast iron pins were used against AISI 52100 chrome steel plates to analyze the effectiveness of additives on various types of DLC coatings using universal wear testing machine with pin-on-plate geometric configuration. In case of steel/cast iron and DLC/cast iron contacts, uncoated-pins were used in combination with uncoated and DLC-coated plates respectively whereas DLC-coated pins were used against DLC-coated plates

for simulating DLC/DLC contacts. Physical and material properties of the above-mentioned rollers are presented in **Table 3.8** whereas chemical composition is shown in **Table 3.9**.

Table 3.8: Physical and mechanical properties of BS1452 cast iron pins

Properties	**Specifications**
Grade	BS1452
Diameter	10.00 mm
Length	10.00 mm
Hardness	22 – 32 HRC
Average surface roughness	0.02 - 0.03 μm

Table 3.9: Chemical composition of BS1452 cast iron pins

Element	**Weight percentage (wt.%)**
Iron	92.25 - 94.00
Carbon	2.90 - 3.65
Silicon	2.10 - 2.90
Manganese	0.60 - 0.80
Phosphorus	0.30
Sulfur	0.10

3.2.2.2 Lubricants and their composition

During tribotesting using universal wear testing machine, single-additive containing and multi-additive containing lubricants were used to investigate the tribological compatibility between additives and various types of DLC coatings. In addition to that, additive-free base oils were also tested so that effectiveness of additives can be analyzed..

3.2.2.3 DLC coatings specifications

In order to select the optimum DLC coating for cam/tappet interface of direct acting valve train application, three different types of DLC coatings were selected on the basis of literature review which include ta-C, a-C:H and a-C:H:W. All of these coatings are commercially available and belongs to Balinit series of Oerlikon Balzers. Balinit series of DLC coatings are specially designed for industrial applications where low friction coefficients and wear protection of interacting components are of prime interest. These coatings have thickness of 2 - 3 μm and deposited on the substrate using physical vapor deposition (PVD) and plasma-assisted chemical vapor deposition (PACVD) techniques. Other important details of each DLC coating used in this research work are discussed in the subsequent sections.

(a) ***ta-C***

ta-C used in this research work is commercially available with the name of Balinit Hard Carbon. It is one of the most widely investigated DLC coating in the literature. It lies in the category of non-doped DLC coatings. Some of the distinguished features of this coating include ultra-high hardness, high thermal stability, resistance against abrasive as well as adhesive wear. It was deposited on plates, balls and pins through PVD process using hybrid magnetron sputtering technique which is a combination of Filtered Cathodic Vacuum Arc (FCVA) and magnetron sputtering. Some of the important properties of ta-C coating are listed in **Table 3.10**

Table 3.10: Properties of ta-C

Properties	**Values**
Deposition technique	FCVA combined with magnetron sputtering
Interlayer	-
Thickness	2 - 3 µm
Average surface roughness	0.02 - 0.03 µm
Hardness	40 - 50 GPa
Maximum service temperature	500 ºC
Color	Black rainbow
Hydrogen content	<1.0 wt.%

(b) ***a-C:H:W***

As the name suggest, a-C:H:W falls in the category of doped-DLC coatings. Since, DLC coatings are considered to be chemically inert due to their low surface energies therefore, they are generally doped with metals such as tungsten to improve their ability to interact with lubricant additives and environmental species (Cui et al., 2012). In this way, ultra-low friction, extreme wear resistance, high hardness of DLC coatings and chemical reactivity of metals can be combined in a single material. Due to these reasons, W-DLC was selected, among various types of DLC coatings, to evaluate its tribological compatibility with conventional additives and TMP. The above-mentioned coating is commercially available with the name of Balinit C star.

A PVD process was used to deposit a-C:H:W with a CrN interlayer on plates, balls and pins. Prior to deposition, mirror-polished substrates were cleaned with acetone and ethyl alcohol in ultrasonic bath for 30 minutes and rinsed using distilled water. After that, substrates were placed on the turntable and loaded into the deposition chamber of PVD sputtering machine where pressure was maintained at 2 x 10^{-5} Pa. In order to evaporate the water molecules, substrates were heated to 200 ºC. Before performing deposition,

surfaces of the substrates were bombarded with Ar^+ plasma in a glow discharge mode for 30 minutes to remove the contaminants and iron oxide layer. The bias voltage was kept at –200 volts during the sputter etching process. CrN interlayer was firstly deposited on the substrates by ion beam arc evaporation. Nitrogen gas was fed into the deposition chamber through an anode layer ion source where it reacts with chromium ions produced by an arc evaporator with an arc current of 60 A and deposited as CrN interlayer on the substrate surface. Due to its hardness and toughness, CrN interlayer provides additional load bearing capacity, enhance the corrosion resistance of the coated components and improve the adhesion between substrate and top a-C:H:W layer. After the deposition of CrN interlayer, a-C:H:W coating was deposited on the substrate by ion beam deposition combined with DC magnetron sputtering. A high negative potential was applied to the tungsten target, which was used as sputtering source whereas ethyne (C_2H_2) was used as reactive gas. A stream of positively charged argon ions was then accelerated towards the tungsten target and bombarded on them to evaporate the tungsten source. A carbon precursor (C_2H_2) was then introduced into the chamber and reacted with sputtered tungsten particles evaporated from the coating material. During the deposition, discharge voltage of the ion source and chamber pressure were kept at 330 V and 0.2 Pa respectively whereas flow rates of argon and ethyne were maintained at 160 cm^3/min and 60 cm^3/min respectively. The concentration of tungsten in a-C:H:W was controlled by the sputtering current of tungsten target. In order to keep the thickness of the coating uniform, substrates were rotated at constant speeds at several axes during the deposition process. In this way, compact, defect-free, homogenous and thin layer of a-C:H:W coating, with desired composition, was deposited on the substrate surface. The total thickness of this coating was approximately 2-3 μm which also include 0.1-0.2 μm thick CrN interlayer. Some of the important properties of a-C:H:W coating are listed in **Table 3.11**.

Table 3.11: Properties of a-C:H:W

Properties	**Values**
Deposition technique	PVD combined with ion sputtering
Interlayer	CrN
Thickness	2 - 3 µm
Average surface roughness	0.02 - 0.03 µm
Hardness	12 - 15 GPa
Maximum service temperature	300 ºC
Color	Anthracite

(c) ***a-C:H***

Like ta-C coating, a-C:H belongs to non-doped category of DLC coatings and widely investigated in the past to comprehend their compatibility with lubricant additives formulated in conventional base oils. The commercial name of a-C:H coating used in this project is Balinit DLC star. This coating also has a CrN interlayer like Balinit C star coating due to which it has enhanced load carrying capacity and suitable for components bearing extreme loads. Balinit DLC star was coated using PACVD combined with ion sputtering. A hard and tough CrN layer was deposited on the substrate initially by sputtering. A carbon precursor, rich in hydrogen, was introduced into the chamber to build a-C:H coating on top of CrN layer. Some of the important properties of a-C:H coating are shown in **Table 3.12**.

Table 3.12: Properties of a-C:H

Properties	**Values**
Deposition technique	PACVD combined with ion sputtering
Interlayer	CrN
Thickness	2 - 3 µm
Average surface roughness	0.02 - 0.03 µm
Hardness	15 - 25 GPa
Maximum service temperature	300 ºC
Color	Black

3.2.2.4 Surface characterization techniques

In order to investigate the mechanisms responsible for a particular tribological behavior of DLC-lubricant pairs, various surface characterization techniques were deployed in this research. After tribotests and cylinder head testing, sliding surfaces and engine components were washed with cyclohexane and kept in desiccator before carrying out surface analysis. Surface characterization techniques which were used in this research work are discussed below.

(a) ***Raman spectroscopy***

In order to quantify the extent of graphitization, broad Raman spectra of DLC-coated plates after 2 hours of sliding against uncoated and DLC-coated balls and pins were acquired from 1000 cm^{-1} to 2500 cm^{-1} wavelength. The extent of graphitization can be realized from an increase in I_D/I_G indicated by the maximum disordered D-peak (I_D) intensity and the maximum graphite G-peak (I_G) intensity in the Raman spectra (Tasdemir, Wakayama, et al., 2013b). Intensity of D-peaks (I_D) and G-peaks (I_G) are usually measured at 1380 cm^{-1} and 1560 cm^{-1} wavelengths respectively (Ferrari & Robertson, 2000). Renishaw InVia Raman microscope with 514 nm diode laser in combination with 50X magnification was used for this purpose. The laser power was kept

at 10% to concentrate only on DLC coating and minimize the influence of substrate material while obtaining Raman spectra. Other related parameters such as resolution, spectra accumulation and collection time were kept at 2400 lines/nm, 2 and 60 seconds respectively. For each surface, three Raman spectra were obtained to achieve a good statistical representation. The software Renishaw WiRE 4™ was used to analyze the resulting spectra by a peak pick function to determine the peaks automatically.

(b) ***Field emission scanning electron microscope/energy dispersive x-ray spectroscopy (FESEM/EDS)***

In order to calculate wear coefficients of uncoated and DLC-coated balls and pins, Zeiss UltraPlus field emission scanning electron microscope (FESEM) was used. FESEM differs from optical microscope in such a way that it uses focused beam of electrons instead of photons (light rays) to produce images of a sample. The chemical composition of elements deposited on balls, pins and tappets, as a result of tribochemical interaction with additives, was investigated using Oxford Instruments energy dispersive x-ray spectroscopy (EDS) analysis system integrated with FESEM. FESEM was operated at an electron acceleration voltage of 10 Kev while obtaining micrographs and performing EDS analysis so that it captures data only from the coating and electron beam do not penetrate till the substrate material.

(c) ***Surface profiler***

Surface profiles of uncoated and DLC-coated plates and tappets after testing under lubricated conditions were measured using Surftest SJ-210 mechanical stylus profilometer (Mitutoyo, Kanagawa, Japan). For each plate, three measurements were taken i.e. one at the top, second at the middle and third at the bottom of the wear track to obtain statistically representative and repeatable results. Scan length was adjusted to 2.5 mm and 12.5 mm for ball-on-plate and pin-on-plate geometric configurations respectively

so that the topography of the whole wear track width can be measured whereas scan speed was set at 0.25 mm/s. Average surface roughness (R_a) values of plates and tappets were calculated using surface profile data.

3.3 Cylinder head testing of Mercedes Benz OM646LA diesel engine using direct acting valve train test rig

In order to analyze the suitability of TMP-based lubricants and various types of DLC coatings (**section 3.2.2.2**) for cam/tappet interface of direct acting valve train application, a number of tests were carried out using cylinder head of Mercedes-Benz OM646LA diesel engine (**Figure 3.5**). OM 646LA is a four-cylinder, twin cam engine with eight inlet and eight exhaust valves. Some of the important specification of OM646LA engine are shown in **Table 3.13**.

Table 3.13: Specifications of OM646LA diesel engine

Manufacturer	Daimler
Displacement	2148 cubic centimeter (cc)
Fuel	Common rail diesel direct injection
Induction	Turbocharged
Number of cylinders	4
Cylinders configuration	In-line
Emission compliance level	Euro IV
Exhaust post-treatment method	Oxidation catalyst converter (Oxy-Cat) / Diesel Particulate Filter (DPF)

Tribological performance of uncoated cam/uncoated tappet interface is compared with those of DLC-coated ones under lubricated conditions. Out of three types, only two DLC coatings were selected and carry forward, on the basis of tribological performance during tribotesting phase, to coat camlobes and tappets. Since, DLC/cast iron contacts shows inferior tribological properties compared to DLC/DLC contacts, therefore, only DLC-

coated components (DLC-coated tappets and DLC-coated camlobes) are considered during cylinder head testing.

Figure 3.5: Cylinder head of Mercedes Benz OM646LA engine

In order to investigate the effects of lubricant rheology and DLC coatings on tribological performance parameters of cam/tappet interface, tests were carried out at lubricant temperatures (40ºC and 90°C) and three different camshaft speeds (400 RPM, 800 RPM and 1200 RPM). Four lubricants were used for the tests, out of which two were base oils (TMP and PAO) and two were multi-additive containing lubrications (P+G+M+Z and T+G+M+Z). For each lubricant, new cam/tappet pair was used. During the tests, lubricant pressure was maintained at 2 bars via a feedback PID motor controller. Before starting the tests, lubricant was heated at the required temperature and circulated through the cylinder head lubricant circuit for 2 hours. For each lubricant and cam/tappet pair, tests were first carried out at temperature of 40ºC and camshaft speed of 1200 RPM. After 30 minutes of running, readings of friction torque and rotational speed of tappets were taken using National Instruments (NI) DAQ hardware and Laboratory Virtual Instrument Engineering Workbench (LabVIEW) software. After that, camshaft speed was reduced to 800 RPM and then 400 RPM and above-mentioned procedure was repeated

for taking readings. After carrying out tests at 40°C, lubricant temperature was increased to 90ºC and cylinder head was soaked for 2 hours so that all the components reached at the same temperature. Same procedure was repeated for taking friction torque and rotational speed of tappet reading at 1200 RPM, 800 RPM and 400 RPM of camshaft. After that, uncoated cam/tappet pair was replaced with a-C:H-coated pair and then a-C:H:W-coated pair and same procedure was repeated. Details of the test matrix for cylinder head testing are shown in **Table 3.14**.

Table 3.14: Test matrix for cylinder head testing

Test No.	Lubricant	Tribopair	Lubricant temperature	Camshaft speed
New uncoated camlobe/uncoated tappet pair and fresh additive-free PAO				
1.	PAO	Uncoated cam/uncoated tappet	40 ºC	1200 RPM, 800 RPM and 400 RPM
2.	PAO	Uncoated cam/uncoated tappet	90 ºC	1200 RPM, 800 RPM and 400 RPM
Change of uncoated camlobe/uncoated tappet pair with a new a-C:H-coated camlobe/a-C:H-coated tappet pair				
3.	PAO	a-C:H-coated camlobe/a-C:H-coated tappet	40 ºC	1200 RPM, 800 RPM and 400 RPM
4.	PAO	a-C:H-coated camlobe/a-C:H-coated tappet	90 ºC	1200 RPM, 800 RPM and 400 RPM
Change of a-C:H-coated camlobe/a-C:H-coated tappet pair with a new a-C:H:W-coated camlobe/a-C:H:W-coated tappet pair				
5.	PAO	a-C:H:W-coated camlobe/a-C:H:W-coated tappet	40 ºC	1200 RPM, 800 RPM and 400 RPM
6.	PAO	a-C:H:W-coated camlobe/a-C:H:W-coated tappet	90 ºC	1200 RPM, 800 RPM and 400 RPM
New uncoated camlobe/uncoated tappet pair and fresh additive-free TMP				
7.	TMP	Uncoated cam/uncoated tappet	40 ºC	1200 RPM, 800 RPM and 400 RPM

Table 3.14 continued

Test No.	Lubricant	Tribopair	Lubricant temperature	Camshaft speed
8.	TMP	Uncoated cam/uncoated tappet	90 ºC	1200 RPM, 800 RPM and 400 RPM
Change of uncoated camlobe/uncoated tappet pair with a new a-C:H-coated camlobe/a-C:H-coated tappet pair				
9.	TMP	a-C:H-coated camlobe/a-C:H-coated tappet	40 ºC	1200 RPM, 800 RPM and 400 RPM
10.	TMP	a-C:H-coated camlobe/a-C:H-coated tappet	90 ºC	1200 RPM, 800 RPM and 400 RPM
Change of a-C:H-coated camlobe/a-C:H-coated tappet pair with a new a-C:H:W-coated camlobe/a-C:H:W-coated tappet pair				
11.	TMP	a-C:H:W-coated camlobe/a-C:H:W-coated tappet	40 ºC	1200 RPM, 800 RPM and 400 RPM
12.	TMP	a-C:H:W-coated camlobe/a-C:H:W-coated tappet	90 ºC	1200 RPM, 800 RPM and 400 RPM
New uncoated camlobe/uncoated tappet pair and fresh T+G+M+Z				
13.	T+G+M+Z	Uncoated cam/uncoated tappet	40 ºC	1200 RPM, 800 RPM and 400 RPM
14.	T+G+M+Z	Uncoated cam/uncoated tappet	90 ºC	1200 RPM, 800 RPM and 400 RPM
Change of uncoated camlobe/uncoated tappet pair with a new a-C:H-coated camlobe/a-C:H-coated tappet pair				

Table 3.14 continued

Test No.	Lubricant	Tribopair	Lubricant temperature	Camshaft speed
15.	T+G+M+Z	a-C:H-coated camlobe/a-C:H-coated tappet	40 ºC	1200 RPM, 800 RPM and 400 RPM
16.	T+G+M+Z	a-C:H-coated camlobe/a-C:H-coated tappet	90 ºC	1200 RPM, 800 RPM and 400 RPM
Change of a-C:H-coated camlobe/a-C:H-coated tappet pair with a new a-C:H:W-coated camlobe/a-C:H:W-coated tappet pair				
17.	T+G+M+Z	a-C:H:W-coated camlobe/a-C:H:W-coated tappet	40 ºC	1200 RPM, 800 RPM and 400 RPM
18.	T+G+M+Z	a-C:H:W-coated camlobe/a-C:H:W-coated tappet	90 ºC	1200 RPM, 800 RPM and 400 RPM
New uncoated camlobe/uncoated tappet pair and fresh P+G+M+Z				
19.	P+G+M+Z	Uncoated cam/uncoated tappet	40 ºC	1200 RPM, 800 RPM and 400 RPM
20.	P+G+M+Z	Uncoated cam/uncoated tappet	90 ºC	1200 RPM, 800 RPM and 400 RPM
Change of uncoated camlobe/uncoated tappet pair with a new a-C:H-coated camlobe/a-C:H-coated tappet pair				
21.	P+G+M+Z	a-C:H-coated camlobe/a-C:H-coated tappet	40 ºC	1200 RPM, 800 RPM and 400 RPM
22.	P+G+M+Z	a-C:H-coated camlobe/a-C:H-coated tappet	90 ºC	1200 RPM, 800 RPM and 400 RPM

Table 3.14 continued

Test No.	Lubricant	Tribopair	Lubricant temperature	Camshaft speed
Change of a-C:H-coated camlobe/a-C:H-coated tappet pair with a new a-C:H:W-coated camlobe/a-C:H:W-coated tappet pair				
23.	P+G+M+Z	a-C:H:W-coated camlobe/a-C:H:W-coated tappet	40 ºC	1200 RPM, 800 RPM and 400 RPM
24.	P+G+M+Z	a-C:H:W-coated camlobe/a-C:H:W-coated tappet	90 ºC	1200 RPM, 800 RPM and 400 RPM

3.3.1 Substrates and counterbodies

Valve train components, which include tappets and camshafts, were acquired from Shahnawaz Pvt. Ltd., Pakistan for cylinder head testing (**Figure 3.6**). Since, original camshaft of OM646LA cylinder head consists of 8 camlobes and its practically not possible to use the new camshaft for each DLC-lubricant combination, therefore, a specially-designed camshaft was used to evaluate the tribological performance of only one cam/tappet pair at a time. A complete assembly of above-mentioned camshaft is shown in **Figure 3.7**. It consists of slip rings, drive sprocket, torque tube, bearings, camlobes, washer and nut. Camlobes were taken out from the original camshaft using lathe machine (**Figure 3.8**). Thickness of each camlobe was kept exactly the same so that every camlobe makes contact with the tappet at the same offset distance from its rotational axis. A hole was drilled in each camlobe so that it can be inserted into the camshaft. The center point of the hole was selected in such a way that position of camlobe matches with the original camshaft and it was kept same for each camlobe. In order to restrict the relative motion between camlobe and camshaft during operation, a hole was made on the side face of the camlobe and pin was extruded on the camshaft. While assembling the

camshaft, camlobe was inserted in such a way that pin of the camshaft sits inside the side hole of the camlobe. In this way, rotational position of camlobe was fixed relative to the camshaft. Uncoated tappets and camlobes were sent to Oerlikon Balzers for deposition of various types of DLC coatings.

Figure 3.6: Camshaft and tappets of Mercedes Benz OM646LA cylinder head

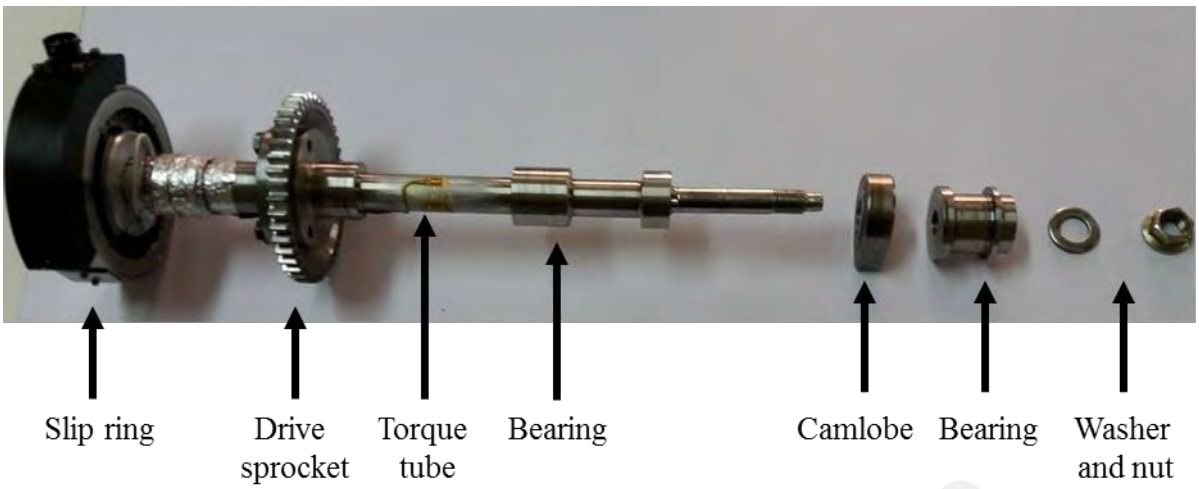

Figure 3.7: Complete assembly of specially-designed camshaft

Figure 3.8: Cutting of original camshaft to take out camlobes using lathe machine

3.3.2 Lubricants and their composition

Since, fully-formulated lubricants are used in engines, therefore only multi-additive containing lubricants are considered during cylinder head testing. In order to analyze the tribological compatibility of conventional lubricant additives with TMP and DLC coatings and their effectiveness in further enhancing the tribological performance of the cam/tappet interface, additive-free TMP was PAO were also used as lubricants for reference. Multi-additive lubricants and their composition details are already disused in **section 3.2.1.3.**

3.3.3 Direct acting valve train test rig

In order to operate the cylinder head under realistic running conditions of the engine, direct acting valve train test rig was used (**Figure 3.9**). A feedback-controlled variable speed induction motor was connected to the camshaft to run it at different speeds. The speed of the motor was controlled with the help of a controller, DAQ system and customized software developed using LabVIEW. A Bellow coupling, capable of transmitting the back-lash free torque and compensating for shaft misalignments (radial, axial and angular), was used to connect output shaft of the motor with the camshaft of the cylinder head. Another motor was used to run the lubricant pump. Pressure and flow rate of the lubricant was controlled by varying the speed of the motor with the help of DAQ system. The Cylinder head was assembled in oil sump, made from sheet metal, which was then bolted on the valve train test rig. It was also used to contain the lubricant coming out of the cylinder head, from which it is transferred to the external sump by gravity flow. Lubricant heating and cooling unit was used to heat the lubricant at different temperatures and maintain its temperature. Heating of the lubricant was carried out indirectly. Initially, heat transfer oil was heated by lubricant heating and cooling unit and then heat was transferred to the lubricant using in-line plate heat exchanger. A thermocouple was connected at the oil inlet to the cylinder head gallery to monitor the lubricant temperature.

All the lubricant pipes were insulated to reduce heat loss. Analog pressure gauge was used to monitor the pressure of the lubricant entering into the cylinder head. In addition to that, piezo-resistive pressure transducer was also used to convert the pressure into voltage so that pressure of the lubricant entering into the cylinder head can be monitored and controlled using computer software. A feedback PID controller was used to maintain lubricant pressure and temperature throughout the test run. External sump, which is basically an insulated double walled container capable of maintaining the temperature of the oil, was used as lubricant reservoir from which lubricant is pumped into the cylinder head.

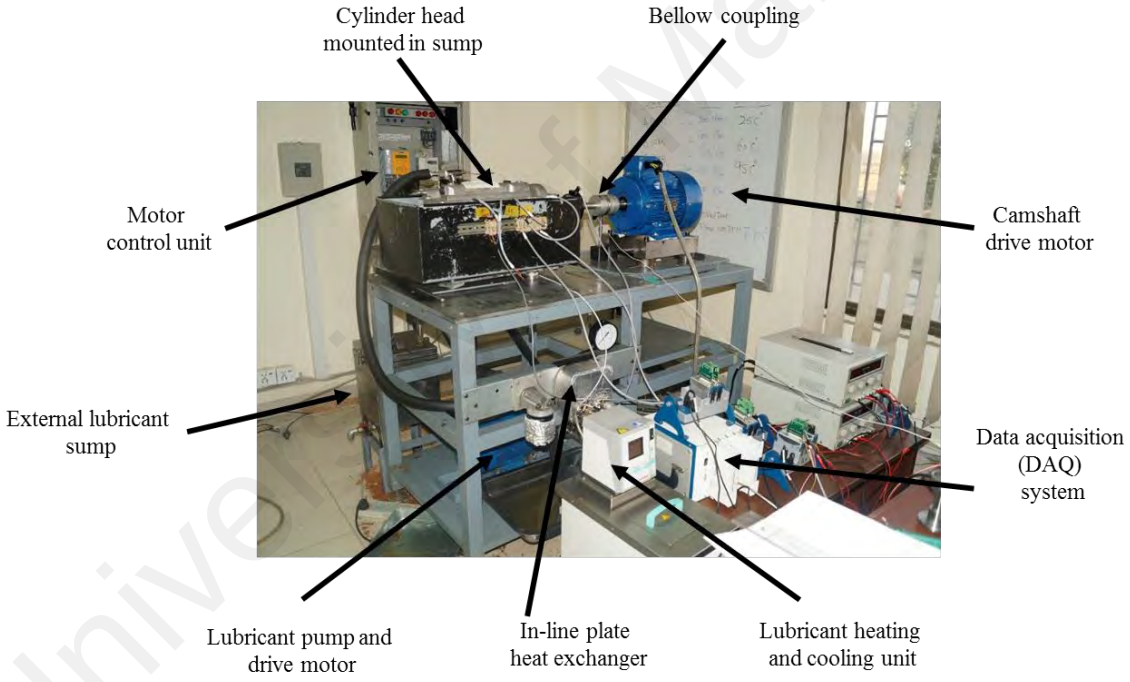

Figure 3.9: Direct acting valve train test rig

3.3.4 Instrumentation of cylinder head of OM 646LA Mercedes Benz diesel engine

3.3.4.1 Tappet rotation measurement

An innovative measurement technique was used for real time monitoring of rotational speed of one tappet on an exhaust camshaft of direct acting valve train. The most attractive

feature of this technique is its ability to work without making any modifications in the cylinder head. The rotational speed of the tappet was measured using a giant magnetoresistance (GMR) magnetometer chip which works on the principle of giant magnetoresistive effect. A large change in electrical resistance occurs when GMR material is exposed to external magnetic field is known as giant magnetoresistive effect. Magnetometer chip, which is one of the many variants of GMR sensors, acts as a magnetic switch. It gives high signal when exposed to external magnetic field and low signal when magnetic field is removed from the near vicinity of the sensor. Some of the advantages of using GMR magnetometer sensors include its miniature size (1.1mm× 1.1mm× 0.45 mm), low power requirements and low cost (**Figure 3.10**). Magnetometer sensors are easy to install, and there is no adverse effect of high oil temperature on the performance of the sensor since they are designed to operate continuously in the temperature range from -40°C to 125°C.

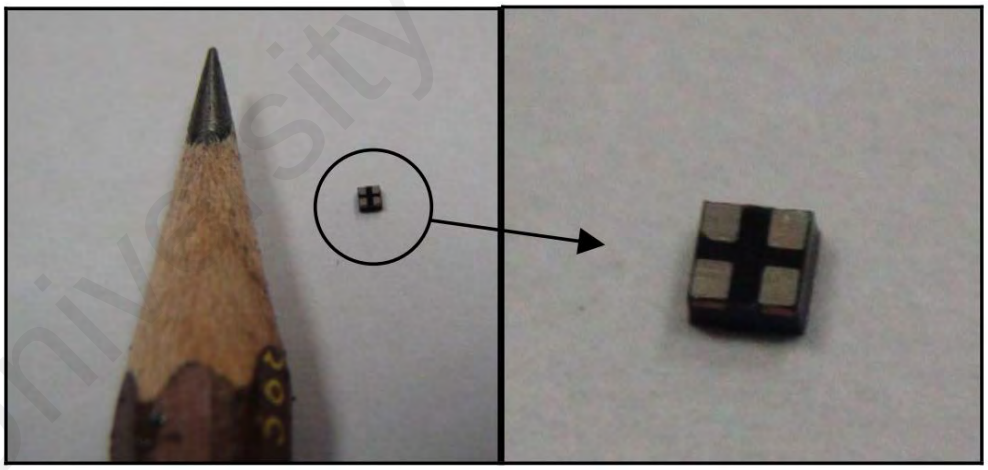

Figure 3.10: Giant magnetoresistance (GMR) magnetometer chip and its size comparison

Figure 3.11: Giant magnetoresistance (GMR) magnetometer chip mounted on Printed Circuit Board (PCB)

To install the magnetometer chip in the Mercedes Benz OM646LA cylinder head for measuring the tappet rotation speed, it was first mounted on a specially designed 3 mm diameter PCB with voltage supply and signal wires coming out of it (**Figure 3.11**). The chip was then mounted on the top of the valve spring retainer using epoxy resin (**Figure 3.12**). As the magnetometer chip works in the presence of an external magnetic field, an Alnico [alloy of iron, aluminum (Al), nickel (Ni) and cobalt (Co)] magnet of diameter 5 mm and 1.6 mm thick was mounted on the inner surface of the tappet using epoxy resin (**Figure 3.12**). The thickness of the magnet was selected based on the availability and the clearance space between the tappet and the spring retainer. For the Mercedes Benz OM646LA cylinder head, it was approximately 3.5 mm.

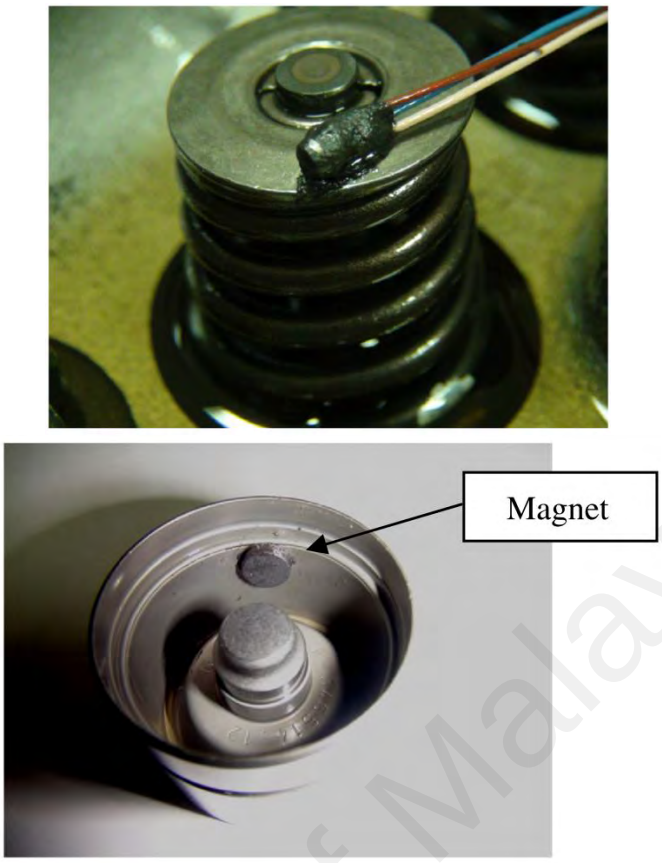

Figure 3.12: GMR magnetometer mounted on valve spring retainer and Alnico magnet on inner surface of tappet

3.3.4.2 Camshaft friction torque measurement

A strain gauge-based torque tube was used to monitor the friction torque of cam/tappet interface (**Figure 3.13**). The torque tube was designed in such a way that it can be easily integrated with the specially-designed camshaft manufactured to evaluate the tribological performance of only one cam/tappet pair. The strain gauges were temperature compensated so that the effects of temperature drift on the output signal could be minimized. Since, torsional stiffness and strain gauge sensitivity are critical aspects of torque tube design, therefore it was designed in such a way that it has required sensitivity as well as high torsional rigidity to minimize the undesirable torsional vibrations. High quality slip rings (Michigan Scientific B6-2 slip ring assembly) were used to transfer the signal from the torque tube to the DAQ system (**Figure 3.14**). As the signal from the

strain gauge bridge is of the order of millivolts, therefore, Fylde 379TA high performance transducer amplifier was used to amplify the signal so that it can be easily ready by DAQ system (**Figure 3.15**). Some of the salient features of above-mentioned amplifier are its high signal/noise ratio, high frequency response, low drift with time and high frequency capability. In order to maintain a high signal/noise ratio, the signal from the transducer was magnified 300 times before transmitting it to the DAQ system.

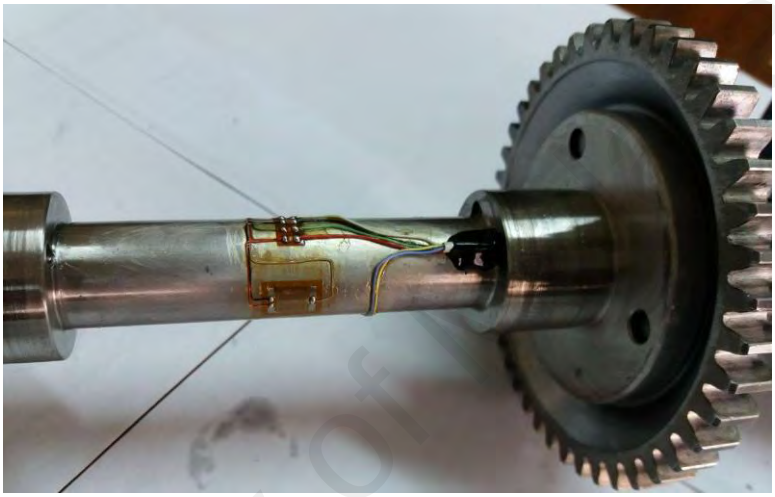

Figure 3.13: Strain-gauge-based torque tube integrated with camshaft

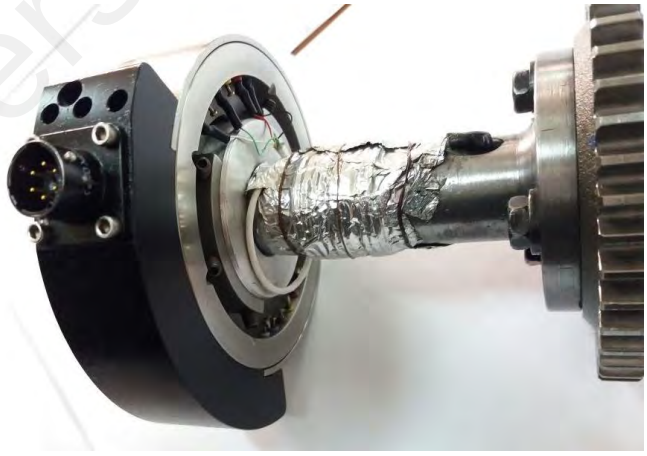

Figure 3.14: Michigan Scientific B6-2 slip ring assembly

Figure 3.15: Fylde 379TA high performance transducer amplifier

To synchronize the reading of the camshaft torque output with cam angle, an optical encoder with 720 pulses per revolution and a once per revolution index mark, referenced to top dead center, was attached to the end of the camshaft. The optical encoder incremental pulse was used as an external clock for sampling the channels. The encoder ungated index mark was also recorded along with the other channels for cam position information. The analogue channels were sampled simultaneously as the DAQ system does not work in multiplex mode but rather each channel has its own analogue to digital converter. All channels were digitally recorded with 12-bit resolution. In order to get high repeatability and reproducibility, data was averaged for 20 cycles and then transferred for analysis.

In order to convert the output voltage of the torque tube into friction torque, it was calibrated using customized calibration bench over the range of drive torque expected in the cylinder head testing (**Figure 3.16**). Specially-designed adapters were used so that one end of the camshaft, integrated with the torque tube, can be held stationary by bolting it to the fixed support whereas a torque can be applied to the other end using a simple bar and weight hanging arrangement. Self-aligning frictionless ball bearings, attached to the calibration bench, were used to hold the camshaft. The friction torque of the ball bearings was assumed to be negligible in comparison to the applied torque. By measuring the output voltage on the amplifier for each applied torque, a relationship was established

between torque and the output voltage. The calibration was carried out in both clockwise and anti-clock wise directions over a torque range of 20 Nm.

Figure 3.16: Customized calibration bench for torque tube

3.3.4.3 Wear measurement

(a) ***Tappet wear measurement***

In order to measure the wear of tappets after testing, a Nanovea PS50 profilometer was used. The above-mentioned equipment has a repeatability of 15 nm and resolution of 2.7 nm as per the manufacturer's specification. It is a 2D non-contact type optical profilometer based on chromatic confocal technology (Axial Chromatism). With the help of above-mentioned equipment, surface profile of each tappet was scanned before and after cylinder head testing, using a physical wavelength which directly relates to its

topography therefore, there was no influence of light reflection in the measurements. Surface profiles of tappets (before and after cylinder head testing) were superimposed on each other and wear profile was calculated by subtracting the two profiles using Microsoft® Excel® model. Wear profile was then converted into the wear volume by multiplying it with the area of the tappet's top surface (3.142 x16.5 mm x 16.5 mm).

In order to maintain the same reference line to study the tappet wear, a specially-designed jig was used (**Figure 3.17**). The purpose of the jig was to hold and lock the tappet in the same position every time it is scanned using profilometer. Otherwise the profilometer cannot give the repeatable results because there will be a different line on which profilometer will scan the tappet surface. To hold the tappet firmly and exactly in the same position every time it is scanned with profilometer, bore diameter of the jig was machined in such a way that tappet can only slide fit into it whereas its depth was made exactly the same as the height of the tappet. Tappet's rotational degree of freedom was constrained by inserting a pin into the lubricant hole of the tappet. Two legs were made at the bottom of the jig so that it can be placed exactly at the same position on the profilometer stage during scanning.

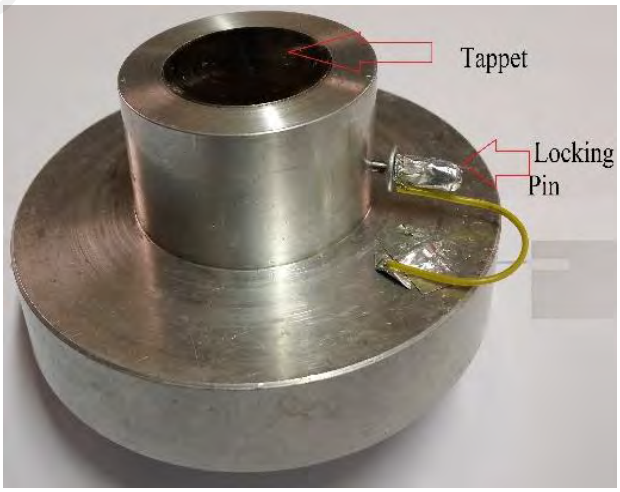

Figure 3.17: A specially-designed jig for holding the tappet during surface profilometry

(b) ***Camlobe wear measurement***

Camlobe nose wear was measured using AMETEK Solartron VG/20/S LVDT and a specially-designed jig (**Figure 3.18**). The purpose of the jig was to hold the LVDT in the same position and at the same point every time it is placed over the camshaft to measure the change in cam lift after cylinder head testing. Since, there is a clearance of 30 μm between the camshaft and its bearings, therefore it wobbles during its operation. In order to cope-up with this situation and take the accurate reading of camlobe nose wear without any errors, LVDT jig was designed in such a way that the entire assembly lifts with the wobble of the camshaft without any relative motion. The width of each leg of the jig was kept according the width of bearings on which it is to be clamped (**Figure 3.18**). In order to prevent the LVDT surface from damage, Teflon screw was used to hold it inside the jig. Spring washers were used while clamping the jig on the bearings to leave clearance for camshaft wobble and screws were only hand tight for easily rotation of camshaft during taking measurements. During the calibration of LVDT, a linear relation was found between the its output voltage and displacement. NI DAQ hardware and LabVIEW-based software was used to calculate camlobe nose wear by analyzing the difference in camlobes profile/camlift, before and after cylinder head testing.

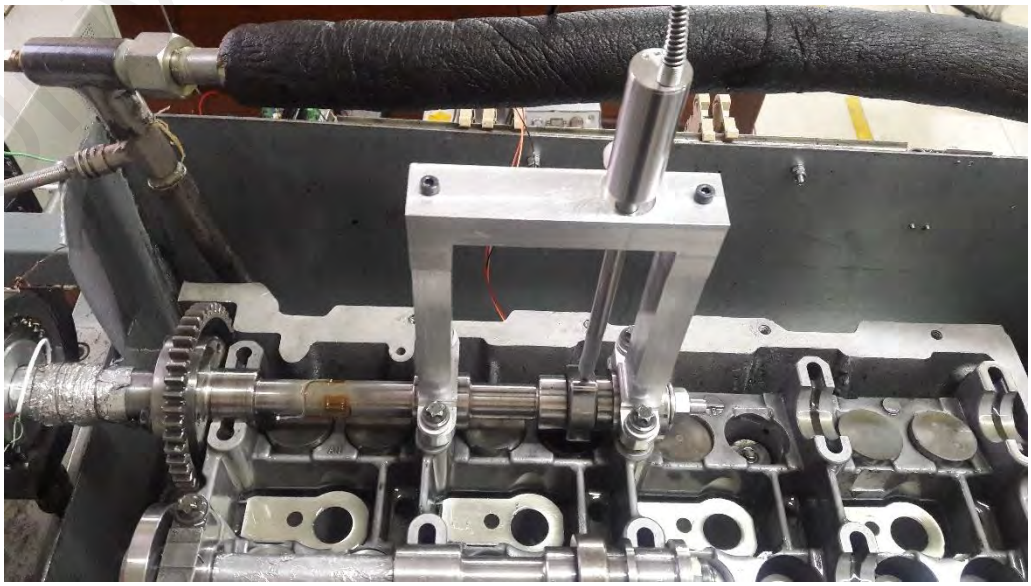

Figure 3.18: LVDT and its jig clamped on the camshaft bearings

(c) ***DAQ system***

DAQ system based on LabVIEW software and NI hardware was used for this research work. During the tests, engine speed, oil temperature, and pressure were monitored continuously. To measure the rotational speed of the tappets, DAQ system based on NI cDAQ-9174 with a digital module, an analog output module, and i3 computer was used. The NI cDAQ-9174 has counter channel that was programmed to measure the tappet speed. The sensor output signal was connected to the counter via the digital module NI 9401 to measure the time required by the tappet to complete one revolution, which was then converted into revolutions per minute. The analog module NI 9263 was used to power the sensor. One of the main reasons for having the power supply and measuring modules in the same chassis of cDAQ-9174 was to reduce the electric noise. In order to measure the camlobe nose wear, a specially-designed LabVIEW-based software was used in combination with NI cDAQ-9174 chassis with analogue input DAQ card NI 9215 and i5 computer. The LVDT was powered using a stable constant DC power supply of 10V.

3.3.5 Surface characterization techniques

In order to investigate the mechanisms responsible for a particular tribological behavior, SEM/EDS and surface roughness analysis was carried out on tappets after cylinder head testing. Surface characterization techniques are already discussed in ample detail in **section 3.2.2.4**.

CHAPTER 4: RESULTS AND DISCUSSION

4.1 Introduction

In this chapter, results of tribological experimental carried out on various DLC coatings in combination with PAO-based and TMP-based lubricants are presented. The main objective of those experiments was to validate the suitability of TMP as engine lubricant base oil and find out the most suitable DLC coating for cam/tappet interface of direct acting valve train assembly of passenger car diesel engine. In order to achieve these objectives, tribological compatibility of conventional lubricant additives with TMP was investigated by carrying out extensive tribotesting and cylinder head testing in combination with steel/steel, DLC/DLC and DLC/steel contacts. The results obtained with formulated versions of TMP were compared with those of PAO-based lubricants to quantify the improvement or degradation in key tribological parameters.

4.2 Physicochemical properties of PAO-based and TMP-based lubricants

The first step, in analyzing the potential of any oil to be used as lubricant, is to investigate its physicochemical properties in both additive-free and formulated forms. Some of the most important physicochemical properties of additive-free and formulated versions of TMP are shown in **Table 4.1**. For comparison purpose, physicochemical properties of PAO-based lubricants are also tabulated.

In **Table 4.1**, it can be seen that kinematic viscosity of TMP at 100ºC is comparable with that of PAO. In addition to that, densities of above-mentioned base oils are also analogous to each other. However, TMP has better VI compared to PAO which shows that former has greater viscosity stability over wide range of temperature compared to latter. Moreover, no significant effect was seen on the physicochemical properties of base oils when they were formulated with conventional lubricant additives irrespective of their type.

Based on the physicochemical properties, it can be stated that tribological properties of TMP and PAO-based lubricants can be compared with each other in order to analyze the compatibility of lubricant additives and various types of DLC coatings.

Table 4.1: Physicochemical properties of PAO-based and TMP-based lubricants

Lubricants	**Kinematic viscosity @ 100°C (cSt)**	**Viscosity Index (VI)**	**Density @ 15°C (g/cm^3)**
PAO	9.852	135.400	0.835
TMP	9.333	194.500	0.917
PAO+GMO	9.987	135.700	0.835
TMP+GMO	9.418	193.000	0.918
PAO+MODTC	9.934	135.900	0.836
TMP+MODTC	9.699	193.500	0.919
PAO+ZDDP	9.979	134.700	0.837
TMP+ZDDP	9.394	192.200	0.918
P+G+M+Z	9.981	135.340	0.838
T+G+M+Z	9.835	193.235	0.920

4.3 Tribotesting using four-ball wear tester for comparing extreme pressure and load carrying capacity of PAO-based and TMP-based lubricants

A comparison of wear scar diameters of steel balls obtained at different values of applied loads under lubricated conditions is presented in **Table 4.2**. Among the base oils, TMP demonstrated superior extreme pressure characteristics compared to PAO. Although, value of LNSL and ISL were same for both base oils but WL for TMP was 10 kg higher than PAO (**Table 4.3**). Not only this, values of Wear Scar Diameters (WSDs) for TMP remained on the lower side throughout the applied load range (**Figure 4.1a**). A decreasing trend was observed in the difference between WSD values of TMP and PAO

with an increase in value of applied load. At 40 kg, WSD value obtained with PAO was almost double compared to that of TMP but difference reduced to only 12.75 % at an applied load of 100 kg. Enhanced load-carrying capacity of TMP can be attributed to the presence of polar components in its structure. Polar molecules of TMP such as carboxyl group of fatty acids forms a monomolecular layer and attach on the chemically reactive steel surfaces as a result of physisorption (Stachowiak & Batchelor, 2014). This thin layer of lubricant separates the contacting surfaces and prevents metal-to-metal contact. Due to non-polar structure of PAO, no such behavior was seen in case of PAO (Kalin et al., 2008).

Table 4.2: Wear scar diameters of balls with additive-free and formulated lubricants at different values of applied load

Lubricants	Wear Scar Diameters (mm) at different values of applied load (kg)											
		40	**50**	**63**	**80**	**100**	**110**	**120**	**140**	**150**	**160**	**170**
TMP	Ball 1	0.41	0.46	1.78	2.06	2.55	2.94	Weld				
	Ball 2	0.41	0.44	1.76	2.08	2.63	2.94					
	Ball 3	0.42	0.43	1.78	2.05	2.63	2.93					
	Mean	0.41	0.44	1.78	2.06	2.60	2.94					
	Standard Deviation	0.0048	0.0159	0.0111	0.0188	0.0449	0.0064					
PAO	Ball 1	0.88	1.00	2.41	2.79	2.99	Weld					
	Ball 2	0.91	1.07	2.33	2.82	2.96						
	Ball 3	0.87	1.02	2.33	2.81	2.99						
	Mean	0.89	1.03	2.36	2.81	2.98						
	Standard Deviation	0.0198	0.0346	0.0436	0.0174	0.0175						
TMP+GMO	Ball 1	0.13	1.68	1.76	2.22	2.79	2.98	Weld				
	Ball 2	0.13	1.70	1.80	2.41	2.88	2.96					
	Ball 3	0.14	1.67	1.78	2.43	2.84	2.86					
	Mean	0.14	1.68	1.78	2.35	2.84	2.93					
	Standard Deviation	0.0024	0.0147	0.0211	0.1157	0.0463	0.0675					
PAO+GMO	Ball 1	0.14	0.18	0.18	2.50	2.83	Weld					
	Ball 2	0.13	0.17	0.21	2.48	2.90						
	Ball 3	0.14	0.18	0.21	2.48	2.87						
	Mean	0.14	0.18	0.20	2.49	2.86						
	Standard Deviation	0.0042	0.0064	0.0170	0.0107	0.0359						

Table 4.2 continued

Lubricants	Wear Scar Diameters (mm) at different values of applied load (kg)											
		40	**50**	**63**	**80**	**100**	**110**	**120**	**140**	**150**	**160**	**170**
TMP+MoDTC	Ball 1	0.14	0.14	1.87	2.18	Weld						
	Ball 2	0.13	0.13	1.89	2.24							
	Ball 3	0.14	0.14	1.89	2.19							
	Mean	0.14	0.14	1.88	2.20							
	Standard Deviation	0.0042	0.0042	0.0106	0.0333							
PAO+MoDTC	Ball 1	0.14	0.22	0.29	2.26	2.44	2.75	2.94	3.34	Weld		
	Ball 2	0.13	0.25	0.27	2.23	2.45	2.73	2.88	3.35			
	Ball 3	0.14	0.22	0.28	2.24	2.44	2.74	2.95	3.31			
	Mean	0.14	0.23	0.28	2.24	2.44	2.74	2.92	3.33			
	Standard Deviation	0.0041	0.0145	0.0126	0.0163	0.0065	0.0058	0.0376	0.0183			
TMP+ZDDP	Ball 1	0.13	0.18	0.24	2.01	2.16	2.35	2.56	2.97	3.16	3.30	Weld
	Ball 2	0.13	0.18	0.23	2.04	2.10	2.34	2.54	2.99	3.16	3.33	
	Ball 3	0.13	0.18	0.25	2.00	2.14	2.35	2.54	2.99	3.16	3.31	
	Mean	0.13	0.18	0.24	2.02	2.13	2.35	2.55	2.98	3.16	3.31	
	Standard Deviation	0.0020	0.0026	0.0109	0.0212	0.0274	0.0054	0.0121	0.0081	0.0032	0.0105	
PAO+ZDDP	Ball 1	0.20	0.22	0.23	0.23	0.30	0.33	0.36	0.37	Weld		
	Ball 2	0.21	0.22	0.24	0.25	0.29	0.33	0.35	0.36			
	Ball 3	0.21	0.21	0.25	0.25	0.31	0.33	0.37	0.36			
	Mean	0.21	0.22	0.24	0.24	0.30	0.33	0.36	0.36			
	Standard Deviation	0.0064	0.0042	0.0111	0.0121	0.0063	0.0042	0.0064	0.0024			

Table 4.2 continued

Lubricants	Wear Scar Diameters (mm) at different values of applied load (kg)											
		40	**50**	**63**	**80**	**100**	**110**	**120**	**140**	**150**	**160**	**170**
T+G+M+Z	Ball 1	0.22	0.23	1.99	2.10	2.15	2.20	2.24	2.84	2.93	3.27	Weld
	Ball 2	0.22	0.22	2.01	2.0	2.20	2.21	2.24	2.88	2.99	3.37	
	Ball 3	0.21	0.23	2.04	2.07	2.17	2.19	2.23	2.81	3.02	3.18	
	Mean	0.22	0.23	2.01	2.09	2.18	2.20	2.23	2.84	2.98	3.27	
	Standard Deviation	0.0064	0.0024	0.0231	0.0147	0.0246	0.0104	0.0065	0.0336	0.0449	0.0925	
P+G+M+Z	Ball 1	0.19	0.23	0.22	0.26	2.42	2.42	2.54	3.00	Weld		
	Ball 2	0.18	0.23	0.23	0.25	2.46	2.46	2.60	3.05			
	Ball 3	0.19	0.22	0.24	0.27	2.41	2.41	2.58	3.00			
	Mean	0.19	0.22	0.23	0.26	2.43	2.43	2.57	3.02			
	Standard Deviation	0.0063	0.0063	0.0064	0.0085	0.0246	0.0246	0.0281	0.0298			

Table 4.3: LSNL, ISL, JBWL and WL values for additive-free and formulated lubricants

Lubricants	LNSL (kg)	ISL (kg)	WL (kg)
TMP	50	63	120
PAO	50	63	110
TMP+GMO	40	50	120
PAO+GMO	63	80	110
TMP+MoDTC	50	63	100
PAO+MoDTC	63	80	150
TMP+ZDDP	63	80	170
PAO+ZDDP	140	150	150
T+G+M+Z	50	63	170
P+G+M+Z	80	100	150

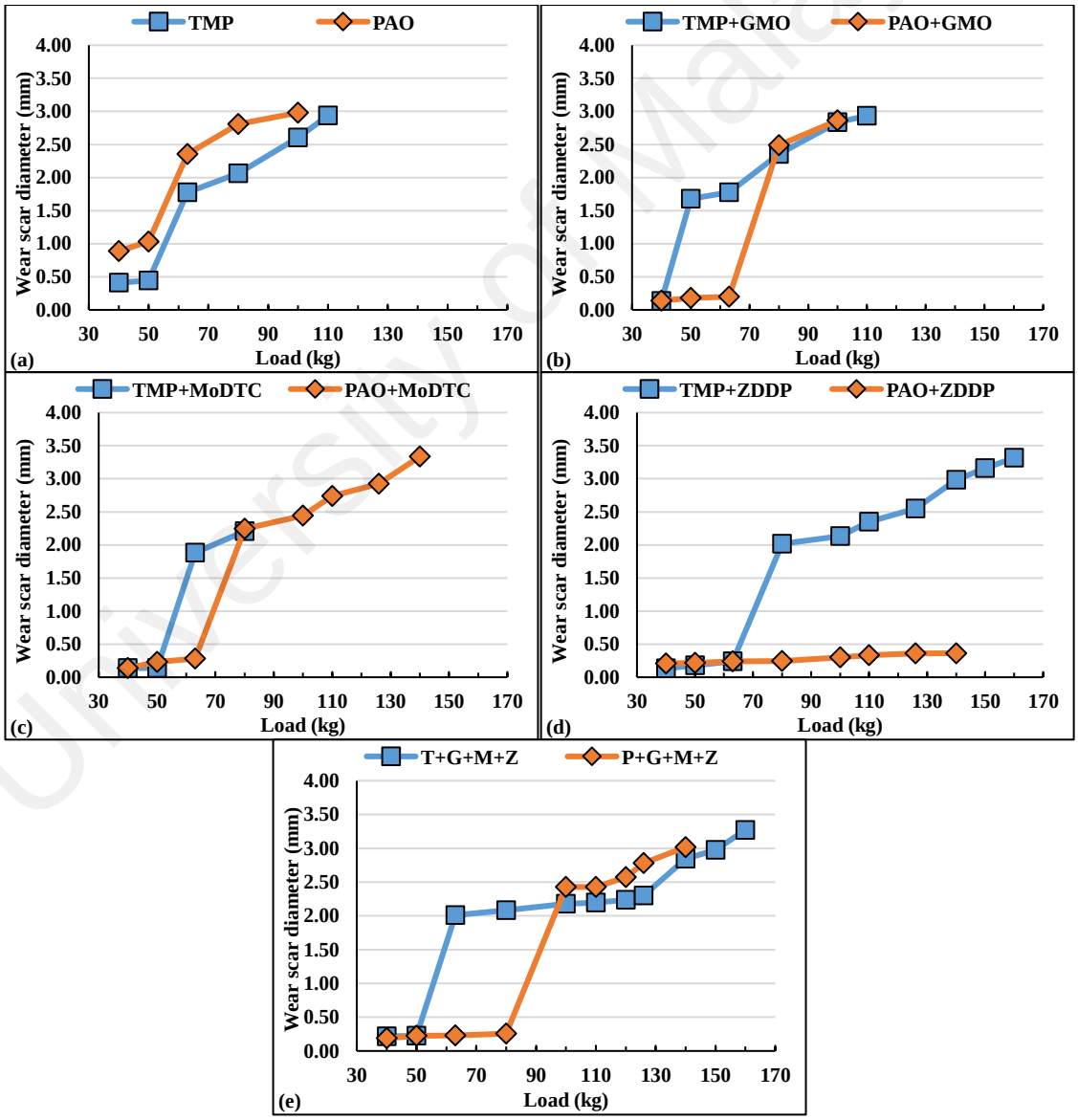

Figure 4.1: Mean values of wear scar diameters plotted against applied load for PAO-based and TMP-based lubricants

A significant change in extreme pressure characteristics of base oils was seen when lubricant additives were used and values of WSDs were decreased especially at lower values of applied loads. ZDDP, which is primarily an antiwear/extreme pressure additive, proved to be most effective in enhancing load carrying capacity irrespective of base oil type (**Figure 4.1d**). Among single-additive containing lubricants, highest value of WL (170kg) was obtained with TMP+ZDDP whereas PAO+ZDDP resulted in very low values of WSDs. No significant wear was observed on balls till 140kg (0.36 mm) in the presence of PAO+ZDDP, but when the load was increased further to 150kg, welding occurred. This behavior shows that ZDDP was able to form a lubricant film that prevented the interacting surfaces from coming into direct contact with each other resulting in very low values of WSDs till 140kg (Vengudusamy, Green, et al., 2011). When a load of 150 kg was applied, lubricant film raptured resulting in metal-to-metal contact and eventually welding occurred. Contrary to ZDDP, GMO was not able to further augment the extreme pressure behavior of base oils in terms of WL and values remained at the same level (**Table 4.3**). When TMP+GMO was used instead of TMP, LNSL and ISL values were reduced from 50 kg and 63 kg to 40 kg and 50 kg, respectively. Not only this, values of WSDs were also increased with the formulation of GMO in TMP at most of the applied loads. On the contrary, GMO proved to be more effective when mixed with PAO. Initial seizure occurred at 80 kg instead of 63 kg and a reduction in values of WSDs was observed when PAO+GMO was used instead of additive-free PAO. Like GMO, formulation of MoDTC also deteriorated the load carrying characteristics of TMP and resulted in lowest value of WL (100kg) among all the tested lubricants (**Table 4.3**). Although, values of WSDs obtained with TMP MoDTC were lower than those obtained with additive-free TMP, but at heavier applied loads, opposite behavior was observed. Contrary to that, MoDTC appeared to be more compatible with PAO and resulted in increase in values of LNSL, ISL and WL from 50 kg, 63 kg and 110 kg to 63 kg, 80 kg

and 150 kg respectively. In addition to that, value of WSDs were also significantly reduced throughout the range of applied loads when PAO+MoDTC was used instead of PAO. At lower values of applied loads, P+G+M+Z provided better lubrication to the contact and resulted in lower values of WSDs at 40kg, 50kg, 63kg and 80kg of applied loads compared to T+G+M+Z (**Figure 4.1e**). Not only this, LNSL and ISL were also notably high when multi-additive containing PAO was used. Contrary to that, T+G+M+Z was able to provide better load carrying capability at medium to heavy range of applied loads and exhibited higher value of WL compared to P+G+M+Z. In case of T+G+M+Z, additives only played their role when applied load was increased beyond 80kg whereas effectiveness of additives was seen even at an applied load of 40kg when mixed in PAO It is mentioned in the literature that there is a threshold value of load below which additives can be play their role in enhancing tribological performance of a contact(Gangopadhyay, Zdrodowski, & Simko, 2014).

From the above-mentioned observations, it can be concluded that TMP is more suitable than PAO in those industrial applications which involve lighter applied loads and where lubricant additives cannot be used. Moreover, lubricant additives which are actually optimized for conventional base oils such as PAO are also compatible with TMP to some extent. The only exception to this finding was MoDTC which deteriorated the inherent extreme pressure characteristics of TMP.

4.4 Tribotesting using universal wear testing machine with ball-on-plate geometric configuration in combination with single-additive containing lubricants

4.4.1 Friction analysis

Transient friction behavior and average friction coefficient values of steel/steel, DLC/DLC and DLC/steel contacts in combination with PAO-based and TMP-based

lubricants are shown **Figure 4.2** and **Figure 4.3** respectively. Further details of friction behavior of each contact in combination with additive-free and formulated lubricants are discussed below.

4.4.1.1 Steel/steel contact

TMP-based lubricants displayed lower levels of friction compared to PAO-based ones irrespective of their formulation. In additive-free form, TMP facilitates the sliding of interacting steel surfaces and offered 12% less friction as compared to PAO because of its superior lubricity. Deterioration in friction behavior of steel/steel contact was observed when formulated lubricants were used instead of additive-free base oils. The only exception to this finding was seen when MoDTC-containing lubricants were used. Among the formulated lubricants, the lowest friction coefficient value was achieved with TMP+MoDTC (0.044) followed by PAO+MoDTC (0.052). Both GMO and ZDDP were not able to further enhance the friction performance of steel/steel contact. Rather an increase of around 4-22% in value of friction coefficient was realized when above-mentioned additives containing lubricants were used instead of their respective base oils. At the start of tribotest, PAO+ZDDP showed a low friction coefficient value but were unable to maintain that level and ended up at highest value of friction at the end of 2 hours of sliding (**Figure 4.2a**). This can be attributed to either the inability of these additives to interact tribochemically with the interacting steel surfaces or formation of weakly-adhered tribofilms under the selected tribotest conditions. Raman spectroscopy and SEM/EDS analysis were carried out on plates and balls respectively to investigate the actual cause of this tribological behavior which will be discussed in the subsequent **section 4.4.3** and **section 4.4.4**.

4.4.1.2 ta-C/ta-C contact

Contrary to steel/steel contact, the self-mated ta-C contact demonstrated better friction performance when additive-free PAO was used as a lubricant compared to TMP. When average friction coefficient values of steel/steel and ta-C/ta-C contacts in combination with base oils were compared, it was observed that the latter demonstrated almost 21-38% less friction than the former. Deterioration in the friction characteristics of ta-C/ta-C contacts was observed when formulated lubricants were used. The only exception to this finding was witnessed when PAO+MoDTC was used as additive. When PAO was mixed with GMO, insignificant change in friction coefficient was seen whereas an increase in friction between ta-C-coated surfaces was observed when TMP+GMO was used as lubricant. Since, friction reducing mechanism of GMO involves chemical adsorbtion of its negatively-charged hydroxyl group on chemically active sites of interacting surfaces, therefore, no interaction of GMO-containing lubricants was seen with chemically unreactive ta-C-coated surfaces (Tasdemir, Wakayama, et al., 2014). Like GMO, ZDDP was also not able to play any role in reducing friction of a self-mated ta-C contact.

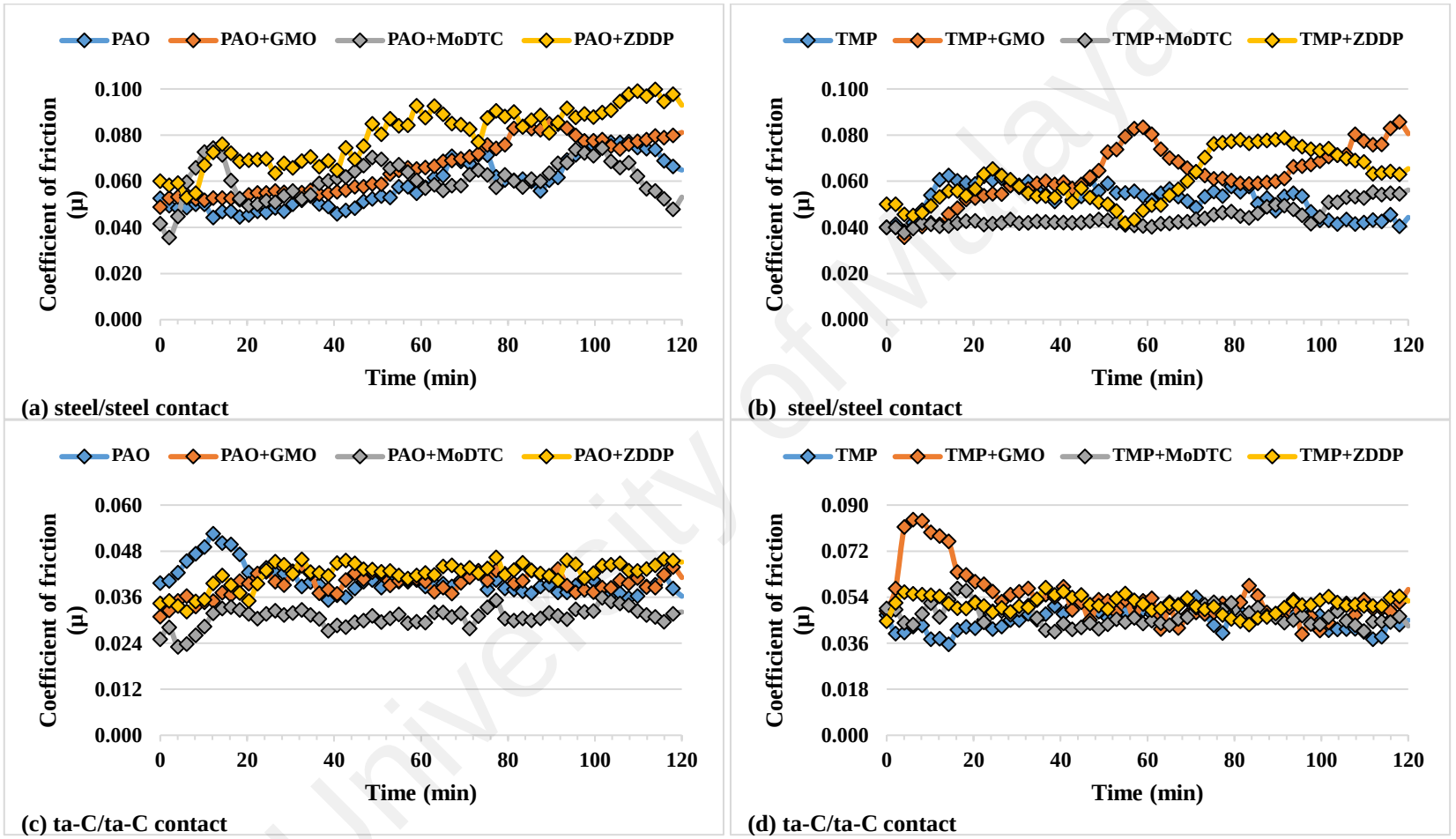

Figure 4.2: Transient friction behavior of steel/steel, DLC/DLC and DLC/steel contacts in the presence of PAO-based and TMP-based lubricants

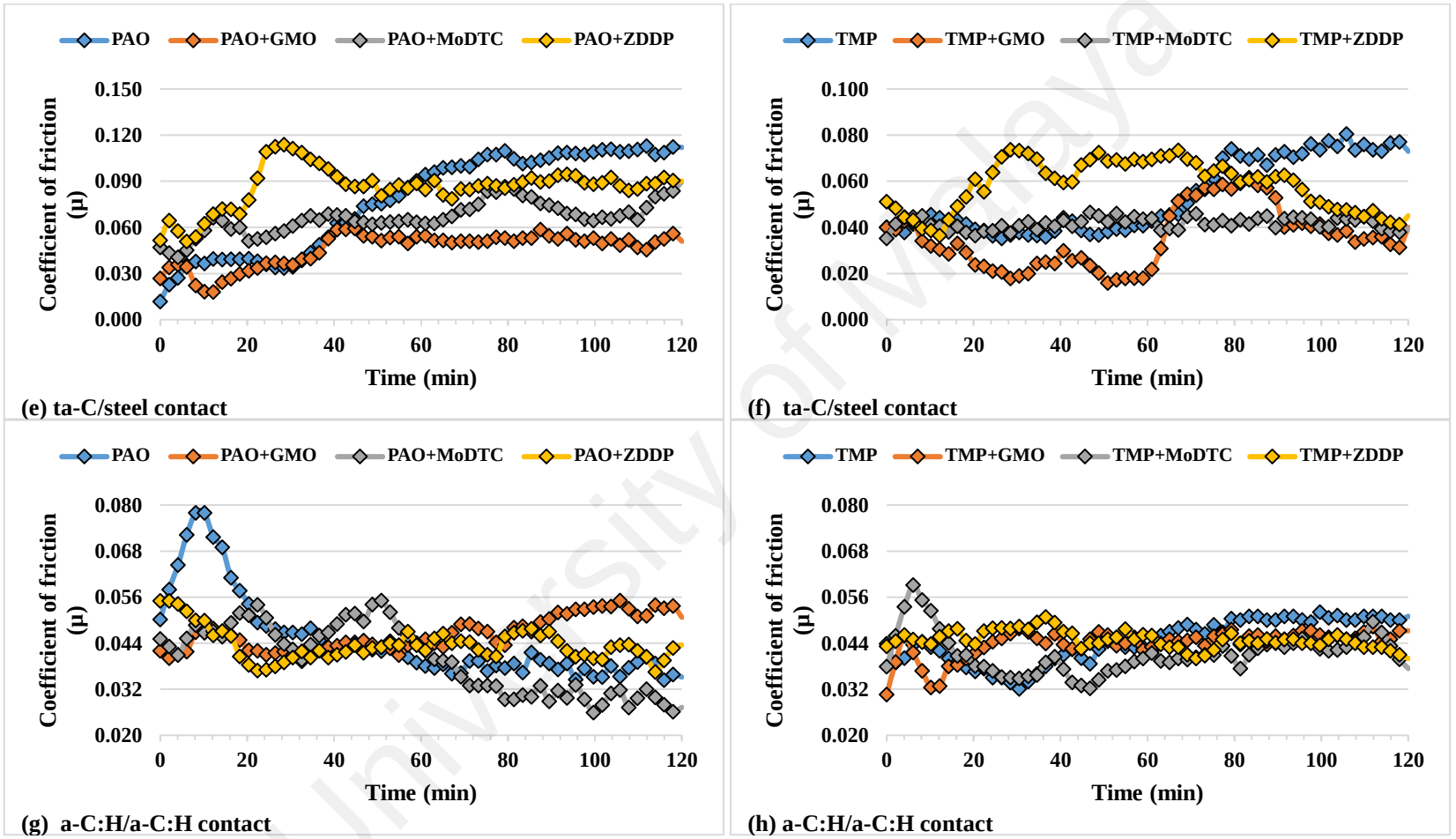

Figure 4.2 continued

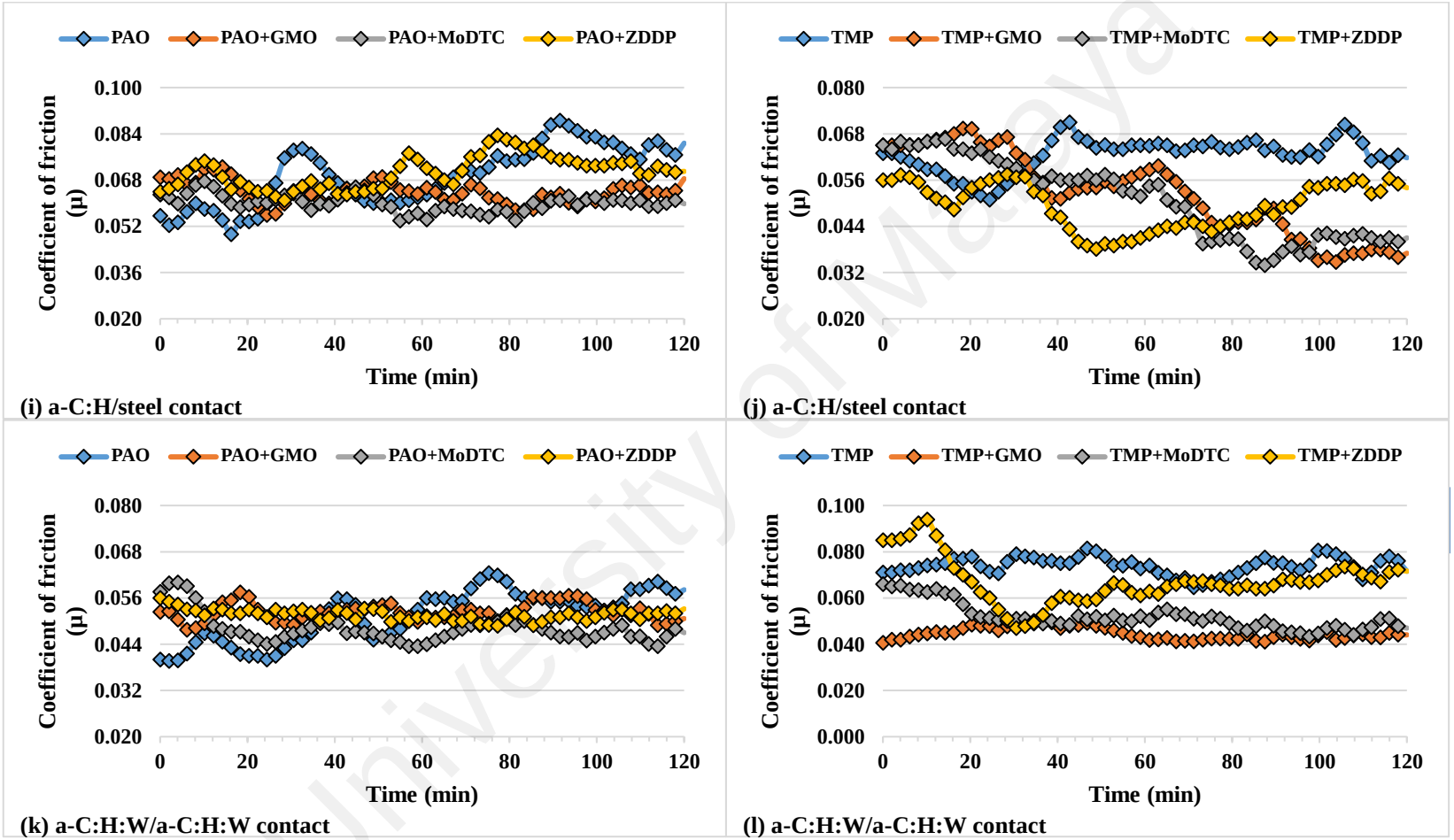

Figure 4.2 continued

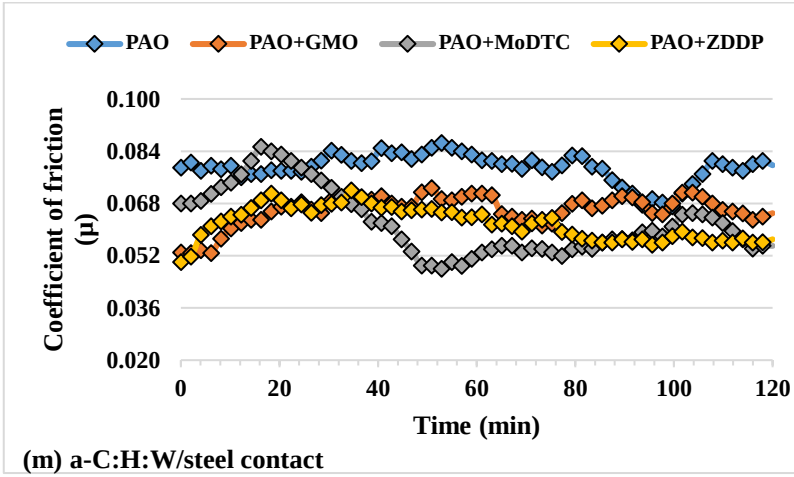

(m) a-C:H:W/steel contact

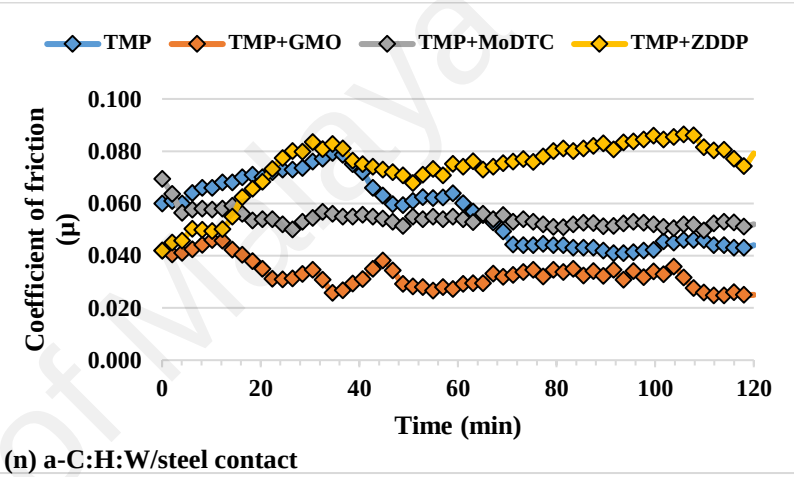

(n) a-C:H:W/steel contact

Figure 4.2 continued

4.4.1.3 ta-C/steel contact

Among the base oils, biodegradable and renewable TMP offered lower level of frictional forces between the sliding surfaces compared to conventional and non-degradable PAO. This enhanced friction performance of TMP can be attributed to its polar structure due to which its molecules attached on the metallic surfaces such as steel and facilitates sliding of the interacting surfaces whereas PAO is not capable of doing so because of its neutral chemical structure (Kalin et al., 2008). Additives were able to further enhance the friction characteristics of ta-C/steel contact irrespective of their type and base oil used. GMO-containing lubricants were proved to be most effective in reducing the frictional force and offered the lowest friction coefficients when mixed with PAO and TMP separately. This friction reduction behavior of GMO can be attributed to its hydroxyl functional group which attaches itself to the metallic surfaces and helps in effectively lubricating the contact (Tasdemir, Wakayama, et al., 2013a). A possible justification for lowest value of friction coefficient achieved with TMP+GMO among the formulated lubricants can be polar nature of both base oil and additive due to which lubricant never slips out of the sliding surfaces and prevents lubricant starvation condition throughout the course of sliding (Henderson & Maggi, 2008; Waara, Hannu, Norrby, & Byheden, 2001). Although, MoDTC was also able to reduce friction levels compared to additive-free base oils but not to an extent of GMO. Lubricants containing ZDDP as an additive were not able to make any significant difference in friction behavior of ta-C/steel contact.

4.4.1.4 a-C:H/a-C:H contact

In comparison to steel/steel contacts, a-C:H/a-C:H contacts resulted in considerably lower friction coefficients irrespective of lubricant formulation. In most of the cases, additives resulted in further improvement in friction performance of base oils irrespective of their type. The only exception to this finding was PAO+GMO which resulted in slight

increase (2.22%) in friction coefficient value compared to additive-free PAO. MoDTC-containing lubricants proved to be most-effective with a-C:H/a-C:H contacts and lowest value of friction coefficient was observed with PAO+MoDTC (0.040) followed by TMP+MoDTC (0.041). Effectiveness of MoDTC in further enhancing the friction performance of a-C:H/a-C:H contacts was also observed by other researchers as well (de Barros'Bouchet et al., 2005; Vengudusamy et al., 2012). Although, ZDDP also resulted in decrease in friction coefficient but not to the extent of MoDTC.

4.4.1.5 a-C:H/steel contact

Deterioration in friction performance was observed when uncoated steel balls were used instead of a-C:H-coated ones in combination with a-C:H-coated plates. A similar behavior was also observed in ta-C/steel contact. Among the base oils, TMP demonstrated better friction performance in combination with a-C:H/steel contact compared to PAO resulted in a 10% lower friction coefficient value. Lubricant additives were proved to be more effective in the presence of ferrous-counterbody and eloquent decrease in friction levels were observed when formulated lubricants were used. This improvement can be attributed to chemically reactive nature of ferrous surface compared to a-C:H coating due to which tribochemical interaction between contact and additives was promoted (Kalin & Vižintin, 2006a). Lowest friction coefficient values were observed when MoDTC was used whereas PAO+ZDDP resulted in highest value among additive-containing lubricants. It is interesting to note that conventional lubricant additives which are actually optimized to interact with conventional base oils performed better when mixed with TMP compared to PAO.

4.4.1.6 a-C:H:W/a-C:H:W contact

Among base oils, high value of average friction coefficient (45.1%) was observed when TMP was used as lubricant instead of PAO. A similar friction behavior was also

seen in case of ta-C/ta-C and a-C:H/a-C:H contacts. This shows that additive-free TMP can only outperform PAO in the presence of ferrous counterbody. Sight deterioration in friction behavior of a-C:H:W/a-C:H:W contacts was observed when formulated versions of PAO were used with the exception of PAO+MoDTC. Contrary to that, additives (GMO and ZDDP) were able to further enhance the friction behavior of TMP. Among the formulated lubricants, lowest friction coefficient was observed when TMP+GMO was used as lubricant whereas TMP+ZDDP resulted in highest levels of friction between the sliding surfaces.

4.4.1.7 a-C:H:W/steel contact

When uncoated steel balls were used against a-C:H:W-coated plates in combination with base oils, opposite behavior was observed compared to a-C:H:W/a-C:H:W contact and TMP outperformed PAO in reducing friction between interacting surfaces. This improved friction performance can be attributed to the attachment of polar components of TMP on ferrous-counterbody which resulted in facilitated sliding of the interacting surfaces (Kalin et al., 2006). A similar friction behavior was also seen in ta-C/steel and a-C:H/steel contact. When friction coefficients of symmetrical a-C:H:W contact were compared with those of a-C:H:W/steel contact, it was observed that presence of ferrous-counterbody deteriorated the friction behavior of the contact. When additives were used in combination with base oils, significant improvement in friction behavior of a-C:H:W/steel contact was seen irrespective of lubricant formulation. Only exception to this finding was seen when TMP+ZDDP was used as lubricant and friction coefficient was increased from 0.057 to 0.074. Among formulated lubricants, lowest friction coefficient was observed with TMP+GMO followed by TMP+MoDTC.

In summary, lowest friction coefficient values were observed with a-C:H/a-C:H contacts followed by ta-C/ta-C and a-C:H:W/a-C:H:W contacts. An increase in friction

coefficient values was seen when uncoated steel balls were used instead of DLC-coated ones against DLC-coated plates. Among the base oils, TMP proved to be more effective when one of the interacting surfaces was ferrous-based whereas symmetrical DLC contacts resulted in lowest levels of friction between sliding surfaces in the presence of additive-free PAO. Since, DLC coatings are chemically inert, therefore, polar component of TMP was not able to adsorb on the contact area when both surfaces were coated with DLC coating due to the unavailability of active sites resulting in high friction coefficients (Vercammen et al., 2004). Among the formulated lubricants, TMP+GMO, PAO+MoDTC and TMP+MoDTC resulted in lower values of friction coefficients whereas deterioration friction performance was observed with PAO+ZDDP and TMP+ZDDP with most of the considered contacts.

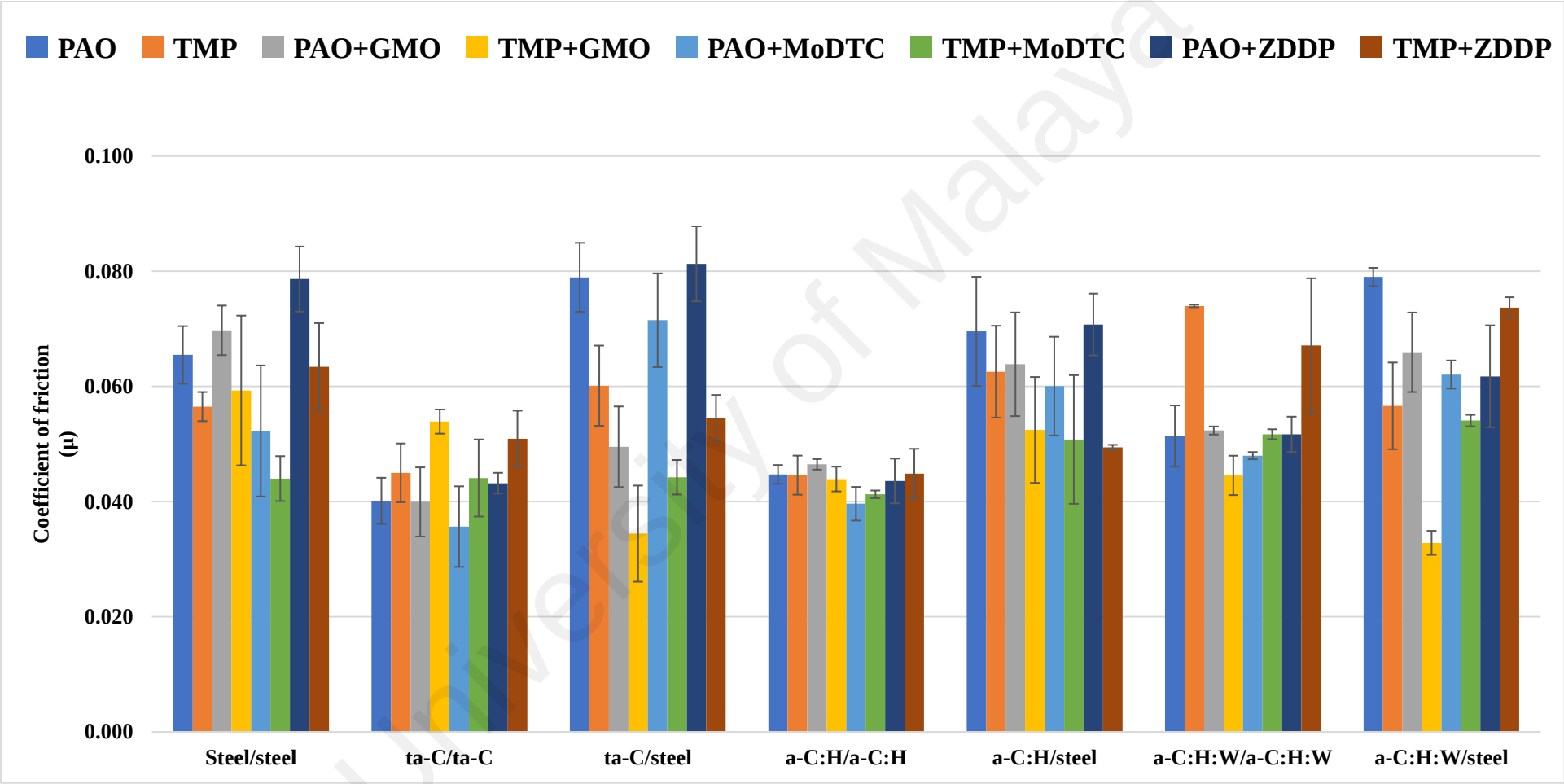

Figure 4.3: Average friction coefficient values of steel/steel, DLC/DLC and DLC/steel contacts in the presence of PAO-based and TMP-based lubricants

4.4.2 Wear analysis

Wear coefficients of uncoated and DLC-coated balls and plates after 2 hours of sliding against each other are shown in **Figure 4.4** and **Figure 4.5** respectively. Further details of wear behavior of each contact in combination with additive-free and formulated lubricants are discussed below.

4.4.2.1 Steel/steel contact

Among the base oils, additive-free PAO proved to be more effective in providing wear protection to the interacting surfaces compared to TMP. Significant reduction in wear coefficient of steel balls was observed when formulated lubricants were used instead of additive-free ones. Only exception to this finding was seen when TMP+MoDTC was used as lubricant instead of additive-free TMP and wear coefficient of ball was increased from 1.68×10^{-7} mm^3/Nm to 1.76×10^{-7} mm^3/Nm. Although, ZDDP is primarily an antiwear additive and played its role to some extent but it was not able to provide the optimum surface protection to interacting steel surfaces when mixed with PAO. In case of PAO-based lubricants, the lowest wear coefficient of ball was observed with PAO+GMO followed by PAO+ZDDP and PAO+MoDTC. Contrary to that, TMP+ZDDP proved to be most effective among TMP-based lubricants and resulted in lowest wear coefficient of ball followed by TMP+GMO. An improvement in wear resistance of steel plates was also seen with most of the formulated lubricants. The only exceptions to this finding was observed when PAO+MoDTC and TMP+GMO were used as lubricants instead of their respective base oils. Among formulated lubricants, the lowest wear coefficient of plate was also observed with PAO+GMO followed by PAO+ZDDP, similar to wear behavior of ball.

4.4.2.2 ta-C/ta-C contact

Similar to steel/steel contacts, additive-free PAO outperformed TMP in providing surface protection and resulted in significantly lower values of wear coefficients of balls and plates. Among the additives, ZDDP was able to perform its primary role and resulted in lowest wear coefficient of ball irrespective of base oil type whereas MoDTC was proved to be least effective. Although, improvement in wear behavior of balls was observed when formulated lubricants were used irrespective of additive type, but opposite behavior was seen in plates. Most of the formulated lubricants either deteriorated the wear characteristics of their additive-free versions or maintained wear coefficients of plates at the same level. The only exception to this finding was GMO which played its role to appreciable extent in moderating wearing rates of plates, irrespective of base oil type. Among PAO-based lubricants, PAO+MoDTC and PAO+ZDDP resulted in higher wear coefficient of plates compared to additive-free PAO whereas ZDDP proved to be ineffective in further augmenting the wear performance of TMP.

4.4.2.3 ta-C/steel contact

Similar to friction results, additive-free TMP offered better wear resistance to uncoated steel balls and ta-C-coated plates compared to PAO. This improved wear performance of ta-C/steel contact in the presence of TMP can be attributed to adsorbtion of its molecules on the contact area resulting in mitigation of asperity-breakages due to direct contacts (Zulkifli et al., 2016). Formulation of base oils with additives resulted in improved wear performance of ta-C/steel contact irrespective of lubricant formulation. Optimum wear protection to ta-C/steel contact was provided by ZDDP and lowest values of wear coefficients of balls and plates were observed when ZDDP-containing lubricants were used. This behavior can be attributed to the formation of ZDDP-derived tribofilms, as a result of tribochemical interaction, which strongly-adhered and stayed on the contact during the complete course of sliding and provided maximum wear protection. The actual

cause of wear-reducing mechanism of ZDDP-containing lubricants will be discussed in **section 4.4.3** and **section 4.4.4**. A similar type of tribofilm, rich in sulfur and phosphorus was also observed by other researchers when ta-C/steel contact was lubricated with PAO+ZDDP (Okubo, Tadokoro, & Sasaki, 2015). MoDTC, which is primarily a friction modifier, was also proved to be effective in enhancing the wear characteristics of balls compared to additive-free base oils but not to the extent of GMO.

4.4.2.4 a-C:H/a-C:H contact

Significant improvement in the wear resistance of ball-on-plate contact was observed when a-C:H-coated surfaces were used instead of uncoated steel ones. In additive-free form, TMP proved to be more effective in providing protection to interacting surfaces and resulted in 55% and 70% reduction in wear coefficient of ball and plate respectively, compared to PAO respectively. Contrary to friction results, additives were proved to be ineffective and resulted in deteriorated wear resistance of a-C:H-coated balls. The only exception to this finding was TMP+ZDDP, which further improved the wear characteristics of TMP and offered maximum surface protection to a-C:H-coated balls among formulated lubricants. Additives also proved to be ineffective in further augmenting the wear behavior of a-C:H-coated plates, when formulated with TMP. A similar trend was also seen in wear behavior of a-C:H-coated plates when TMP-based lubricants were used. Only GMO was able to further improve the wear characteristics of TMP resulting in lowest wear coefficient value of plate among all the lubricants considered. Contrary to TMP-based lubricants, most of additives played their role in further augmenting the wear resistance of a-C:H-coated plate when used in combination with PAO. Among PAO-based lubricant, lowest value of wear coefficient of plate was observed with PAO+GMO followed by PAO+ZDDP whereas significant increase in wearing out of the DLC-coated plate was observed in the presence of PAO+MoDTC

4.4.2.5 a-C:H/steel contact

Among the base oils, PAO proved to be more effective in mitigating the wear of interacting surfaces compared to TMP. A substantial decrease in wear coefficient values of uncoated balls and a-C:H-coated plates was observed when formulated lubricants were used. The only exception to this finding was witnessed when PAO+MoDTC was used as lubricant resulting in the highest wear coefficient value of a-C:H-coated plate among tested lubricants. Among PAO-based lubrications, optimum surface protection to a-C:H/steel contact was provided by PAO+ZDDP whereas TMP+GMO proved to be most effective in further enhancing the wear behavior of a-C:H/steel contact in TMP-based lubricants.

4.4.2.6 a-C:H:W/a-C:H:W contact

On comparing wear characteristics of the a-C:H:W/a-C:H:W contact with those of steel/steel contact, it can be seen that deposition of DLC-coating resulted in better wear protection to interacting surfaces especially a-C:H:W-coated balls. The only exception to this finding was witnessed when PAO+MoDTC was used as the lubricant. Similar to friction results, additive-free PAO proved to be more effective in protecting the a-C:H:W-coated ball from excessive wear compared to TMP. Superior wear performance of ta-C-coated ball in combination with PAO was also observed in the ta-C/ta-C contact whereas opposite behavior was seen in the self-mated a-C:H contact. Additives were proved to be effective when mixed with TMP whereas no improvement in wear behavior of a-C:H:W-coated ball was observed when formulated versions of PAO were used. ZDDP, when used in combination with TMP, effectively performed its primary role of an antiwear additive and provided maximum protection to interacting surfaces among formulated lubricants. Contrary to that, eloquent increase in wear coefficient of ball was observed when PAO+ZDDP was used instead of additive-free PAO. A similar trend was also witnessed with other PAO-based lubricants. Contrary to the wear behavior of a-C:H-coated balls,

TMP provided more wear protection to a-C:H:W-coated plate and resulted in a wear coefficient value which was one-third compared to that of PAO. A similar wear behavior was also seen in the ta-C/steel and a-C:H/a-C:H contact. Formulation of TMP with additives resulted in improved wear performance of a-C:H-coated plates whereas opposite behavior was seen when PAO-based lubricants were used. The only additive which proved to be effective in reducing the wear coefficient of the a-C:H:W-coated plate, in combination with PAO, was GMO (1.53×10^{-9} mm^3/Nm to 3.79×10^{-10} mm^3/Nm).

4.4.2.7 a-C:H:W/steel

A significant increase in the wear coefficient of the ball was seen when an uncoated steel ball was used as a counterbody instead of a a-C:H:W-coated ball against a a-C:H:W-coated plate. In most of the cases, deterioration in wear performance of the a-C:H:W/steel contact was so immense that it resulted in a higher wear coefficient of ball compared to those of steel/steel contact. The only exception to this finding was seen when ZDDP-containing lubricants were used and the lowest values of wear coefficient of ball were observed. Among base oils, PAO outperformed TMP in providing surface protection to the uncoated steel ball during its sliding against a-C:H:W-coated plate. PAO+MoDTC also amplified the wear of the uncoated steel ball compared to additive-free PAO, but not to the extent of the symmetrical a-C:H:W contact. On the other hand, MoDTC was able to improve the wear protection of a-C:H:W-coated ball when mixed with TMP, but no such behavior was seen when an uncoated steel ball was used as a counterbody against a a-C:H:W-coated plate. GMO was able to improve the inherent wear characteristics of TMP and resulted in improved wear protection of uncoated-steel ball when used in combination with TMP whereas opposite behavior was seen when it was mixed with PAO. Contrary to the wear results of an uncoated steel ball, a-C:H:W-coated plates resulted in lower wear coefficient values in the presence of additive-free TMP compared

to PAO. An improvement in the wear resistance of a a-C:H:W-coated plate was witnessed when uncoated steel ball was used as counterbody instead of a a-C:H:W-coated ball. Exceptions to these findings were TMP+MoDTC and TMP+ZDDP which resulted in high wearing rates of a-C:H:W-coated plates compared to symmetrical a-C:H:W contacts. Among all the additives, MoDTC proved to be least ineffective in further augmenting the wear resistance of plates irrespective of base oil type. Rather an eloquent increase in wear coefficient values was observed especially when MoDTC was used in combination with TMP. Lowest wear coefficient of a-C:H-coated plate was observed when TMP+ZDDP was used as lubricant followed by TMP+GMO and PAO+GMO.

In summary, a-C:H coating was proved to be most effective in protecting the interacting surfaces from excessive wear whereas ta-C/ta-C contact showed highest values of wear coefficient of ball and plate. Among the base oils, PAO outperformed TMP in providing surface protection of uncoated and DLC-coated balls and plates with most of the considered contact. Similarly, TMP+ZDDP and PAO+GMO further enhance the wear characteristics of balls and plates respectively. A significant difference in wear coefficient values of balls and plates was observed irrespective of lubricant formulation. This variance implies that balls and plates wear-out at different rates under the same test conditions. This can be attributed to the non-polar nature of PAO due to which it was not able to form surface-protective film during the course of sliding and its slippage from the contact resulting in direct asperity contacts and accelerated wearing out of the interacting surfaces (Kalin et al., 2008; Wu et al., 2016).

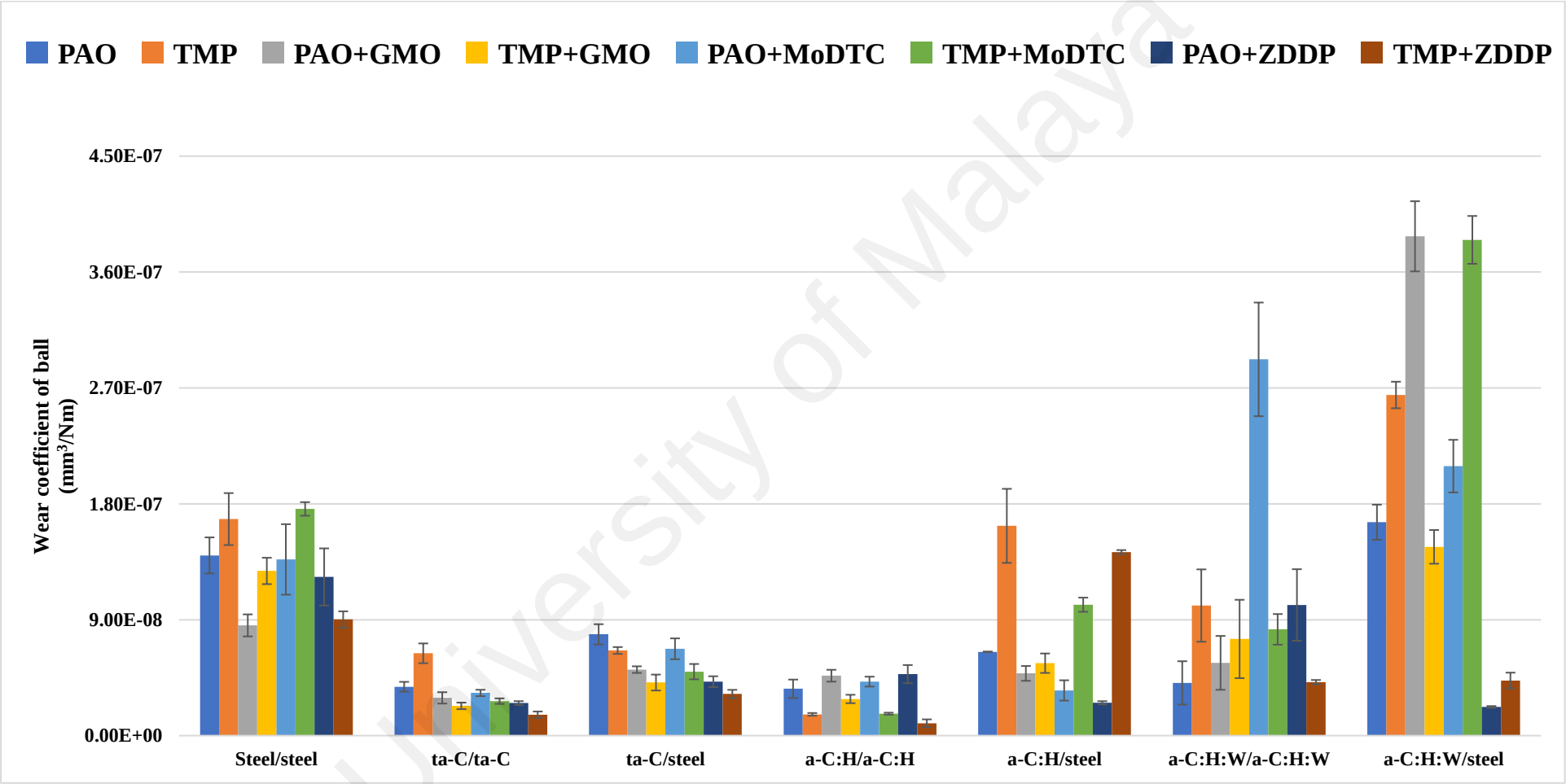

Figure 4.4: Wear coefficient values of uncoated and DLC-coated balls of steel/steel, DLC/DLC and DLC/steel contacts in the presence of PAO-based and TMP-based lubricants

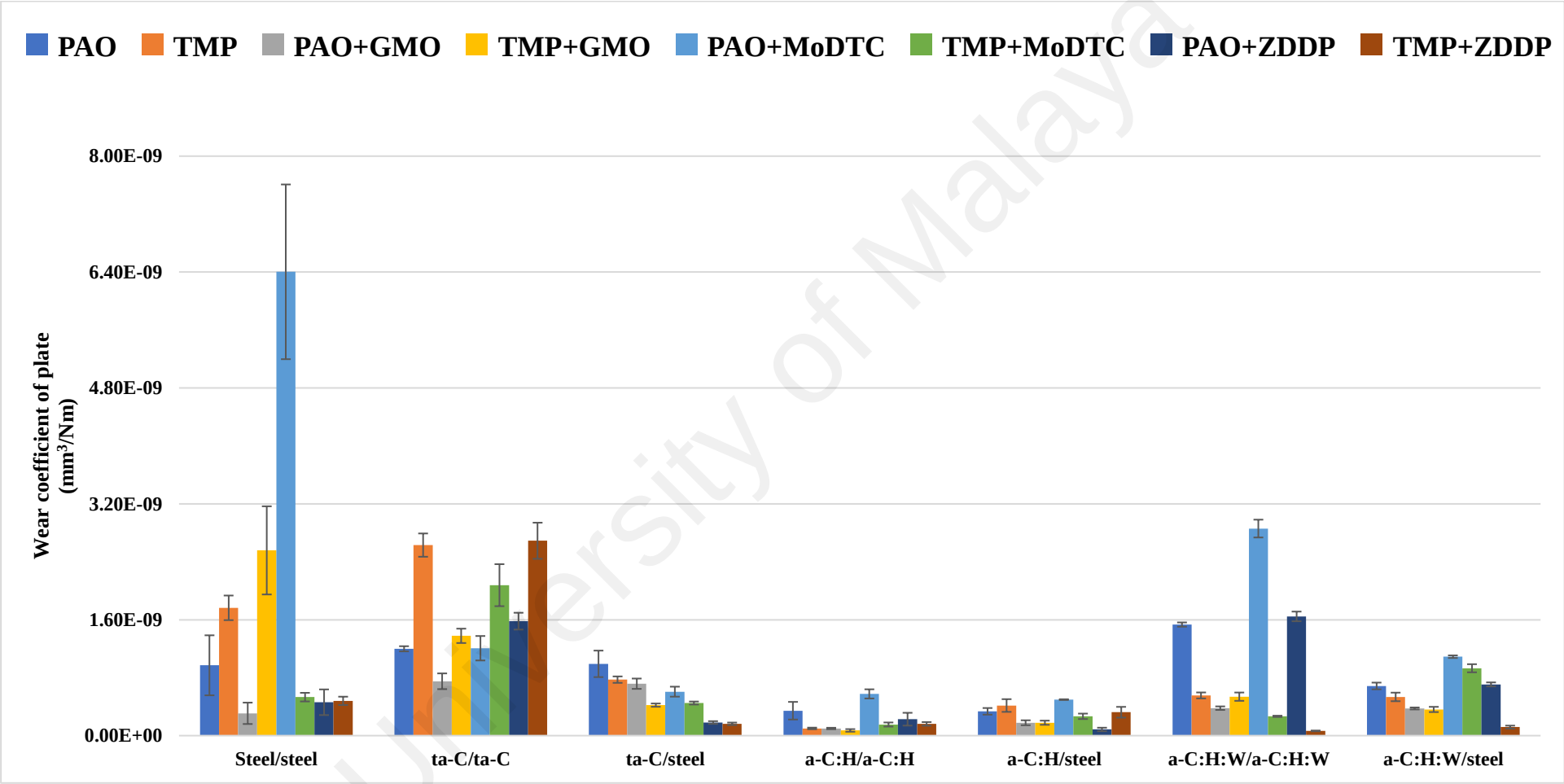

Figure 4.5: Wear coefficient values of uncoated and DLC-coated plates of steel/steel, DLC/DLC and DLC/steel contacts in the presence of PAO-based and TMP-based lubricants

4.4.3 Raman spectroscopy analysis

I_D/I_G ratio of DLC-coated plates after 2 hours of sliding against DLC-coated and uncoated steel balls are shown in **Table 4.4**.

Table 4.4: I_D/I_G ratio of DLC-coated plates after 2 hours of sliding against DLC-coated and uncoated steel balls

Lubricants	**ta-C/ ta-C (I_D/I_G) 0.754**	**ta-C/ steel (I_D/I_G) 0.754**	**a-C:H/ a-C:H (I_D/I_G) 0.767**	**a-C:H/ steel (I_D/I_G) 0.767**	**a-C:H:W/ a-C:H:W (I_D/I_G) 0.840**	**a-C:H:W/ steel (I_D/I_G) 0.840**
TMP	Delamination	0.822	0.689	0.784	0.812	0.854
PAO	0.810	0.762	0.765	0.759	0.938	0.817
TMP+GMO	0.697	0.764	0.684	0.742	0.927	0.903
PAO+GMO	0.690	0.832	0.717	0.681	0.886	0.903
TMP+MoDTC	0.746	0.722	0.777	0.710	0.932	0.978
PAO+MoDTC	0.432	0.799	0.798	0.778	0.954	0.910
TMP+ZDDP	Delamination	0.810	0.793	0.800	0.796	0.869
PAO+ZDDP	0.659	0.693	0.759	0.745	0.922	0.897

4.4.3.1 ta-C/ta-C contact

Broad Raman spectra of ta-C-coated plates before and after 2 hours of sliding against ta-C-coated balls are shown in **Figure 4.6** and **Appendix Figure A-1**. In **Appendix Figure A-1**, it can be seen that Raman spectrum of TMP is different from rest of the spectra. This difference shows that ta-C coating was completely delaminated from the plate during sliding tests and Raman spectra shown in **Appendix Figure A-1e** is actually of steel surface. A similar Raman spectra was also observed by Al Mahmud et al. (2014b) due to the delamination of a-C:H coating. Complete delamination of ta-C coating in the presence of TMP was also confirmed by highest wear coefficient of plate among TMP-

based lubricants (**Figure 4.5**). Delamination of ta-C coating can be attributed to either inability of TMP to provide proper lubrication or removal of soft graphitic layer due to graphitization. Since, ta-C/ta-C contacts demonstrated one of the lowest values of friction coefficients with TMP among TMP-based lubricants, therefore, it can be assumed that removal of coating was due to high extent of graphitization (**Figure 4.3**). It is mentioned in the literature that graphitization adversely affects the structural integrity of DLC coatings due to which they become soft and more vulnerable to excessive wearing (Al Mahmud et al., 2014b; Kalin et al., 2010). Delamination of ta-C coating was also observed when TMP+ZDDP was used as lubricant resulting in Raman spectra similar to that of TMP. An increase in I_D/I_G ratio (from 0.754 to 0.810) was seen when PAO was used as lubricant resulting in occurrence of graphitization phenomenon but no signs of coating delamination were observed in Raman spectra **(Table 4.4)**. As a result, PAO resulted in low value of friction coefficients compared to TMP (**Figure 4.3**). Similar graphitization of ta-C-coating was also observed by (Tasdemir, Wakayama, et al., 2013b) with additive-free PAO. When formulated lubricants were used, a significant decrease in I_D/I_G ratio and suppression in graphitization was seen irrespective of lubricant formulation **(Table 4.4)**. It is widely accepted that additives have the ability to suppress the graphitization of DLC coating by passivating their dangling carbon bonds resulting in improved wear resistance (Kalin et al., 2007; Tasdemir, Wakayama, et al., 2013b, 2014). As a result of this suppression, friction coefficients of ta-C/ta-C contact was increased whereas wear coefficients of ta-C-coated plates were decreased with most of the formulated lubricants (**Figure 4.3** and **Figure 4.5**).

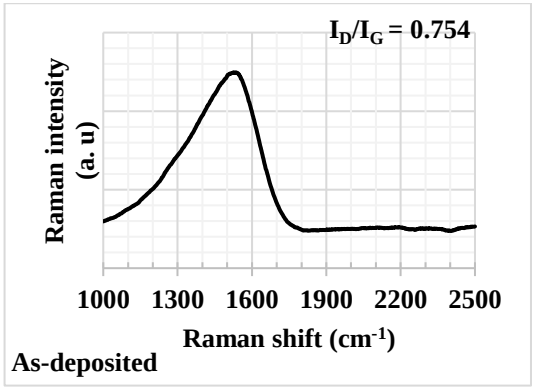

Figure 4.6: Raman spectrum of ta-C-coated plate before testing

4.4.3.2 ta-C/steel contact

Although, delamination of ta-C coating from the plate surface was observed when ta-C-coated balls were used against them but no such behavior was seen in the Raman spectra of ta-C-coated plates with uncoated steel counterbodies (**Appendix Figure A-2**). Increase in I_D/I_G as a result of surface graphitization of ta-C coating was seen with most of tested lubricants **(Table 4.4)**. Exceptions to this finding were seen when PAO+ZDDP and TMP+MoDTC were used as lubricant. On the contrary, occurrence of graphitization phenomenon in ta-C/ta-C contact was only witnessed when additive-free PAO was used as lubricant. This observation shows that presence of ferrous counterbody in the contact increases the chances of surface graphitization. A possible justification for this behavior can be presence of wear debris of steel ball on the contact area in large quantity which induces very high pressure on ta-C-coated plates resulting in the occurrence of pressure-induced graphitization (Kosarieh et al., 2013b).

4.4.3.3 a-C:H/a-C:H contact

Insignificant change in I_D/I_G ratio of a-C:H-coated plates were seen after 2 hours of sliding with additive-free and formulation lubricants compared to as-deposited value of 0.767 (**Table 4.4, Figure 4.7** and **Appendix Figure A-3**). The value either remained at the same level or decrease a bit. This observation shows that improved friction performance of symmetrical a-C:H contact compared to steel/steel contacts was not due to the surface graphitization (**Figure 4.3**). Rather, it was actually due to the inherent low friction and self-lubrication characteristics of a-C:H coating. However, few exceptions to this finding were observed especially with MoDTC-containing lubricants. When PAO+MoDTC and TMP+MoDTC were used as lubricant separately, I_D/I_G ratio was increased from 0.767 to 0.798 and 0.777 respectively **(Table 4.4)**. Therefore, slight improvement observed in friction performance of a-C:H/a-C:H contact in the presence of PAO+MoDTC and TMP+MoDTC can be attributed to surface graphitization (**Figure 4.3**). On the contrary, graphitization deteriorated the inherent wear resistance of a-C:H-coated plates and wear coefficient values were substantially increased (54 - 68%) compared to additive-free PAO and TMP (**Figure 4.5**). Occurrence of graphitization phenomenon was also seen with TMP+ZDDP resulting in highest wear coefficient of a-C:H-coated plate among TMP-based lubricants. It is widely accepted that graphitization adversely affects the structural integrity of DLC coatings due to which they become soft and more vulnerable to excessive wearing (Kalin et al., 2010).

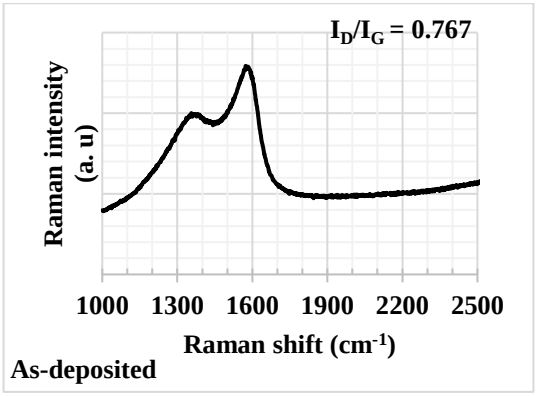

Figure 4.7: Raman spectrum of a-C:H-coated plate before testing

4.4.3.4 a-C:H/steel contact

No signs of surface graphitization were seen in the Raman spectra of PAO-based lubricants irrespective of their formulation (**Table 4.4** and **Appendix Figure A-4**). The only exception to this finding was observed when PAO+MoDTC was used as lubricant and I_D/I_G ratio was slightly increased from 0.767 to 0.778 **(Table 4.4)**. As a result of this structural transformation form diamond to graphite phase, lowest friction coefficient value of a-C:H/steel contact was realized with PAO+MoDTC among PAO-based lubricants (**Figure 4.3**). However, detrimental effects of graphitization were seen on the wear resistance resulting in accelerated wearing out of the a-C:H-coated plate and subsequently highest wear coefficient value among PAO-based lubricants (**Figure 4.5**). In **Appendix Figure A-4**, it can be seen that Raman spectrum of additive-free TMP is different from rest of the spectra. Since, highest wear coefficient values of uncoated steel ball and a-C:H-coated plate were observed with additive-free TMP (**Figure 4.4** and **Figure 4.5**), therefore this change in Raman spectrum shape can be attributed to influence of CrN and/or ferrous material, transferred from ball, in Raman spectra. In addition to that, increase in I_D/I_G ratio (from 0.767 to 0.784) was also observed when additive-free TMP was used as lubricant **(Table 4.4)**. Thus, better friction performance of a-C:H/steel contact in the presence of TMP compared to PAO can be attributed to surface

graphitization along with polar nature of TMP due to which its molecules adsorbed on the interacting sliding and facilitated the sliding (**Figure 4.3**). Similar to a-C:H/a-C:H contact, graphitization of a-C:H-coated plate was also seen in the presence of TMP+ZDDP (from 0.767 to 0.800) after 2 hours of sliding against uncoated steel ball **(Table 4.4)**. As a result, lowest friction coefficient and highest wear coefficient values of a-C:H/steel contact was seen with TMP+ZDDP among formulated TMP-based lubricants (**Figure 4.3**, **Figure 4.4** and **Figure 4.5**).

4.4.3.5 a-C:H:W/a-C:H:W contact

Structural transformation of a-C:H:W coating from diamond to graphite phase was observed in Raman spectra of a-C:H:W-coated plates irrespective of lubricant formation and I_D/I_G was increased from as-deposited value of 0.840 (**Table 4.4, Figure 4.8** and **Appendix Figure A-5**). Exception to this finding was observed when additive-free TMP and TMP+ZDDP were used as lubricants resulting in highest friction coefficient values of a-C:H:W/a-C:H:W contact (**Figure 4.3**). It is interesting to note that additives neither suppress the occurrence of graphitization phenomenon nor improve the friction performance of symmetrical a-C:H:W contact, when mixed with PAO. This observation shows that low friction coefficient values of a-C:H:W/a-C:H:W contact were because of surface graphitization instead of tribochemical interaction between additives and interacting surfaces. On the other hand, graphitization adversely effects the structural integrity of a-C:H:W coating and significant increase in wear coefficient values of plates were seen when formulated versions of PAO were used (**Figure 4.5**). A direct relation between extent of surface graphitization and wear coefficient values of plates was seen. Among the PAO-based lubricants, highest value of I_D/I_G ratio was observed with PAO+MoDTC resulting in accelerated wearing-out of a-C:H:W-coated plate compared to other lubricants. When TMP+GMO and TMP+MoDTC were used as lubricants, a significant decrease in friction coefficient value was seen compared to that of additive-

free TMP and reached the same level as that of PAO-based lubricants (**Figure 4.3**). ZDDP was able to play its primary role of antiwear additive when mixed with TMP and resulted in lowest wear coefficient of plate. This behavior can be attributed to suppression of graphitization and/or tribochemical interaction of ZDDP with sliding surfaces resulting in the formation of additive-derived tribofilm which will be discussed in **section 4.4.4**.

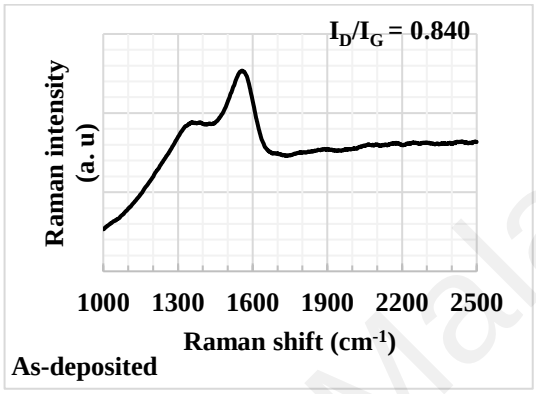

Figure 4.8: Raman spectrum of a-C:H:W-coated plate before testing

4.4.3.6 a-C:H:W/steel contact

Contrary to symmetrical a-C:H:W contacts, occurrence of graphitization phenomenon was observed when additive-free TMP was used as lubricant whereas no such behavior was observed with PAO (**Appendix Figure A-6**). As a result, TMP resulted in significantly lower friction coefficient value of a-C:H:W contact/steel contact compared to that of PAO (**Figure 4.3**). Although, additives are believed to suppress graphitization but no such behavior was seen in a-C:H:W/steel contacts irrespective of lubricant formulation. As a result, significant improvement in friction performance and deterioration in wear resistance of a-C:H:W-coated plates was seen when formulated lubricants were used especially those containing PAO as base oil. The only exception to this finding was seen with PAO+GMO which resulted in lowest wear coefficient value of a-C:H:W-coated plate among PAO-based lubricants. This can be attributed to adsorbtion of hydroxyl group of GMO on the surface asperities due to which transfer of DLC coating

from plate to uncoated steel balls was prohibited (Tasdemir, Wakayama, et al., 2014). As mentioned earlier, graphitization of a-C:H:W-coated plates was also occurred with TMP-based lubricants but insignificant change in the friction performance of a-C:H:W/steel contact was seen as a result of this. Rather, 30% increase in friction coefficient value was realized when TMP+ZDDP was used as lubricant instead of additive-free TMP. Exception to this finding was seen with 42% reduction in friction coefficient value with TMP+GMO compared to TMP. A direct relation between extent of graphitization and wear coefficient value was seen when TMP+MoDTC was used as lubricant. Among PAO-based lubricant, highest value of I_D/I_G ratio (0.978) was seen with TMP+MoDTC resulting in accelerated wearing-out of a-C:H:W-coated plate compared to other lubricants **(Table 4.4)**.

4.4.4 SEM/EDS analysis

4.4.4.1 Steel/steel contact

SEM micrographs of uncoated steel balls after 2 hours of sliding against uncoated steel plates in the presence of PAO-based and TMP-based lubricants are shown in **Figure 4.9** whereas EDS results showing atomic percentage of elements found on uncoated steel balls are presented in **Table 4.5**. Compared to formulated versions of PAO, additive-free PAO resulted in relatively clean and unaltered ball surface after 2 hours of sliding. As a result, PAO demonstrated better friction performance compared to most of its formulated versions. Although, few pits and scratch lines were seen at the middle of the micrograph but they appeared to be shallow. The dark spots appeared at the top represents oxidized surface. The presence of oxygen, which was also confirmed by EDS results, can be attributed to the formation of iron oxides (**Table 4.5**). When PAO+GMO was used as lubricant, very high content of oxygen was observed in EDS results compared to PAO (27.8%). Not only this, plenty of pits and deep grooves in the sliding direction were seen throughout the surface. It is mentioned in the literature that GMO results in ultra-low

friction coefficients when its hydroxyl group adsorbs on the interacting surfaces and forms viscous tribofilm on contact asperities. Since, no improvement in friction behavior of steel/steel contact was seen, therefore, it can be concluded that either GMO was not able to form any tribofilm on the contact area or it peels off during sliding. In **Figure 4.9c**, white-colored MoDTC-derived tribofilm can be clearly scene at the middle and top-right corner of the micrograph. It is widely accepted that tribochemical decomposition of MoDTC results in the formation of MoS_2 and MoO_3 (Neville, Morina, Haque, & Voong, 2007). If there is limited supply of sulfur available in the lubricant due to incomplete decomposition of MoDTC, some of the MoS_2 can also be oxidized and converted into MoO_3 during the course of sliding. Since, insignificant increase in the amount of oxygen was detected when PAO+MoDTC was used instead of PAO, therefore, it can be assumed that MoDTC-derived tribofilm formed on interacting surfaces was rich in MoS_2. As a result, lowest friction coefficient was observed among PAO-based lubricants when PAO+MoDTC was used (**Figure 4.3**). Contrary to friction results, PAO+MoDTC deteriorated the wear performance of contact resulting in accelerated wear of interacting surfaces especially plate (**Figure 4.4** and **Figure 4.5**). This depravation in wear behavior can be attributed to adhesive wear between the interacting surfaces which resulted in material transfer, formation of deep grooves and delaminated patches (**Figure 4.9c**). A lot of surface activity can be seen in micrograph associated with PAO+ZDDP (**Figure 4.9d**). The main wear mechanisms involved were pitting wear and brittle fracture which resulted in the formation of pits, surface cracks and scratch marks. Presence of zinc, phosphorus and sulfur detected on ball surface in EDS results shows that ZDDP-derived tribofilm was formed on the contact area. As a result, decrease in wear coefficient of interacting surfaces was seen when ZDDP-containing PAO was used as lubricant instead of additive-free PAO (**Figure 4.4** and **Figure 4.5**). Few signs of adhesive wear and scratch lines in the direction of sliding were observed in the micrograph of TMP (**Figure 4.9e**).

In micrograph of TMP+GMO, it can be clearly seen that no interaction between lubricant and sliding surfaces was established (**Figure 4.9f**). As a result, abrasive and adhesive wear were witnessed as predominant wear mechanisms which resulted in formation deep grooves and scratch lines on wear scar. Wear debris generated during sliding not only resulted in abrasive wear but also welded on the ball surface due to starved lubrication condition. A possible justification for inability of TMP+GMO to provide wear protection to ball surface can be its slippage during sliding resulting in metal-to-metal contact and inability to establish any lubricant tribofilm at the contact. High content of molybdenum and sulfur was found on ball surface in EDS analysis when TMP+MoDTC was used as lubricant which confirmed the formation of MoS_2. Formation of MoDTC-derived tribofilm as a result of its tribochemical decomposition of not only reduced friction between the interacting surfaces but also resulted in second lowest wear coefficient of plate among TMP-based lubricants (**Figure 4.3** and **Figure 4.5**) Although negligible amount of zinc, phosphorus and sulfur, were detected on ball surface after 2 hours of sliding in the presence of TMP+ZDDP compared to PAO+ZDDP, still, significant decrease in wear coefficient of ball and plate was observed resulting in lowest values among TMP-based lubricants. This observation shows that either no tribochemical interaction took place between ZDDP and interacting surfaces or ZDDP-derived tribofilm wiped out during sliding.

Table 4.5: Atomic percentage of elements found on uncoated steel balls after 2 hours of sliding against uncoated steel plates in the presence of PAO-based and TMP-based lubricants

Lubricants	Elements							
	Fe	**C**	**O**	**Cr**	**Zn**	**S**	**P**	**Mo**
PAO	85.6	2.5	10.7	1.2	-	-	-	-
PAO+GMO	58.7	12.1	27.8	0.9	0.3	-	-	0.2
PAO+MoDTC	74.9	3.5	13.5	0.7	-	2.5	0.3	4.6
PAO+ZDDP	59.4	8.21	25.9	0.8	2.2	1.0	2.4	-
TMP	70.8	14.1	13.5	0.8	0.2	0.1	0.3	0.2
TMP+GMO	74.1	14.3	10.5	0.6	-	-	0.3	0.2
TMP+MoDTC	61.7	10.4	18.9	0.9	-	2.3	0.4	5.4
TMP+ZDDP	79.5	4.21	13.7	1.0	0.6	0.4	0.5	-

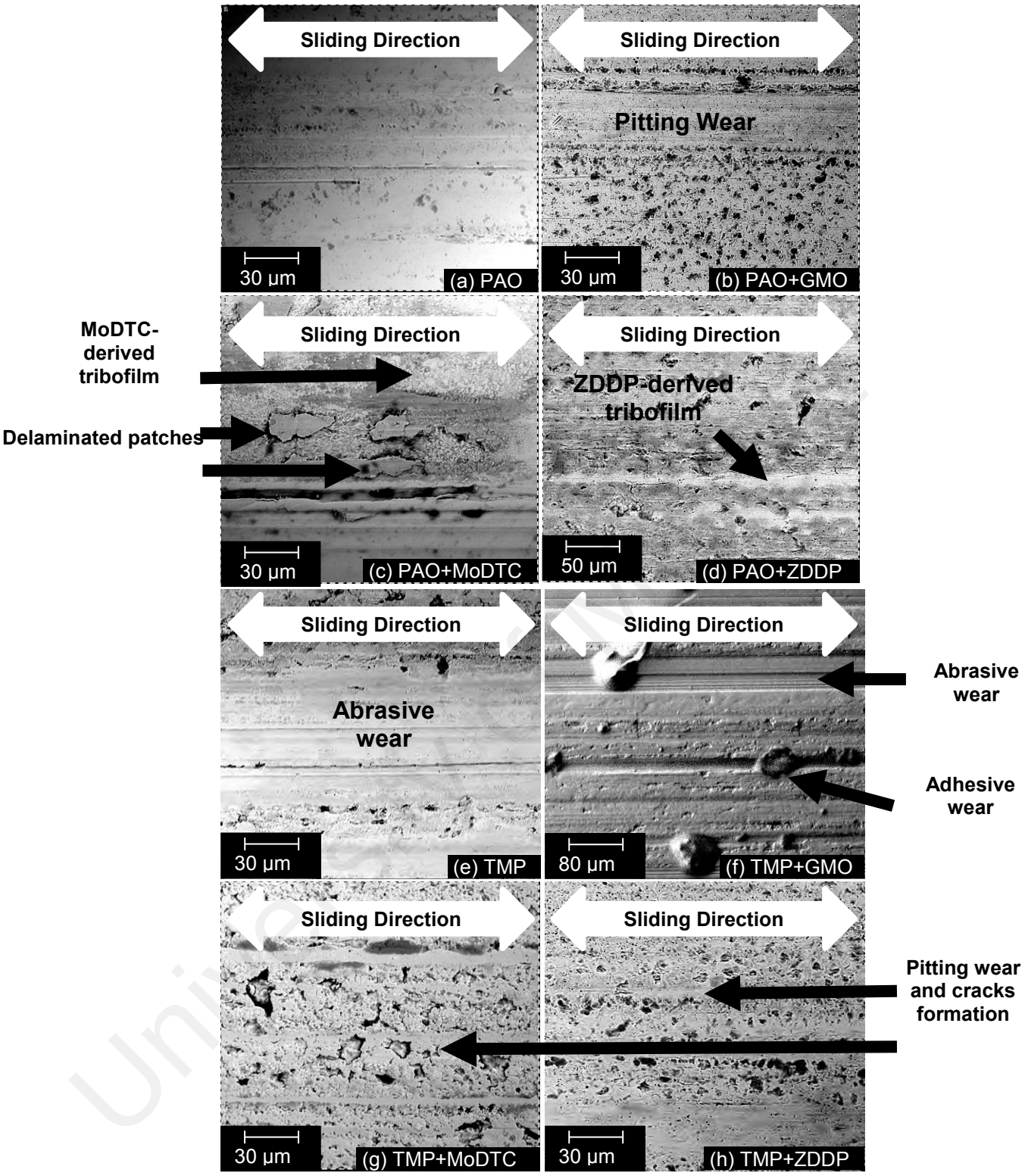

Figure 4.9: SEM micrographs of uncoated steel balls after 2 hours of sliding against uncoated steel plates in the presence of PAO-based and TMP-based lubricants

4.4.4.2 ta-C/ta-C contact

When TMP was used as lubricant, ta-C/ta-C contact was not able to sustain 2 hours of sliding and resulted in complete delamination of coating from ball surface (**Figure 4.10e**). Three distinct regions were observed in the micrograph of TMP. At the left, steel surface (dark-grey region) with scratch lines in the direction of sliding can be clearly seen whereas unaltered ta-C-coated surface (light-grey region) is evident at the right side. At the middle, bright region representing unaltered steel surface is clearly visible. When GMO was mixed with TMP, wear resistance of ta-C/ta-C contact was substantially increased resulting in unaltered and clean surface after 2 hours of sliding. This improvement in wear resistance of ta-C coating in the presence of TMP+GMO can be attributed to transfer of some of the coating material from ta-C-coated plate due to adhesive wear and adsorbtion of hydroxyl group from GMO resulting in increased oxygen content (**Figure 4.10** and **Table 4.6**). Although, improvement in wear performance of ta-C/ta-C contact was also observed when PAO+GMO was used as lubricant but no signs of tribochemical interaction or transfer layer can be seen in micrograph (**Figure 4.10b)**. Among ta-C/ta-C contact, lowest friction coefficient values were observed when MoDTC-containing lubricants were used (**Figure 4.3**). This can be attributed to the formation of white-colored MoDTC-derived tribofilm, composed of molybdenum, oxygen and sulfur, on ta-C-coated ball irrespective of the base oil (**Figure 4.10** and **Table 4.6**). As mentioned earlier, tribochemical decomposition of MoDTC resulted in the formation of MoS_2 which facilitates sliding due to its low shear strength. From this observation, it can be concluded that ta-C is capable of tribochemically interacting with conventional additives, especially MoDTC, even in the absence of ferrous-counterbody. Although, MoDTC is primarily a friction modifier and plenty of cracks/crevices were observed in the micrograph of TMP+MoDTC due to brittle fracture (**Figure 4.10g**), still significant reduction in wear coefficients of both interacting surfaces was observed

(**Figure 4.4** and **Figure 4.5**). As compared to PAO+MoDTC, higher concentration of oxygen and lower concentration of sulfur and molybdenum were observed in EDS result of TMP+MoDTC which shows that MoO_3 was formed in higher ratio in comparison to MoS_2 as a result of tribochemical decomposition of MoDTC.

Similar to MoDTC-containing lubricants, ZDDP was also able to interact with symmetrical ta-C contacts and resulted in lowest values of wear coefficient of balls. On the contrary, presence of ZDDP accelerated the wearing out of ta-C-coated plates. It is well-known that there is a threshold temperature below which additives cannot perform their intended temperature (Rizvi, 1999; Rowe, 1988). This disagreement in wear behavior of sliding surfaces under same tests conditions can be attributed to relatively high temperature of ball compared to plate during sliding, resulting in formation of strongly-adhered and stable ZDDP formed stable tribofilm. Although concentration of zinc and sulfur remained same for both PAO+ZDDP and TMP+ZDDP but phosphorus was present in higher concentration on ta-C-coated ball when latter was used as lubricant. Brittle fracture, resulting in cracks and crevices, was the predominant wear mechanism observed in the micrograph of TMP+ZDDP but polishing wear was also seen in addition to cracking of ta-C coating in the presence of PAO+ZDDP.

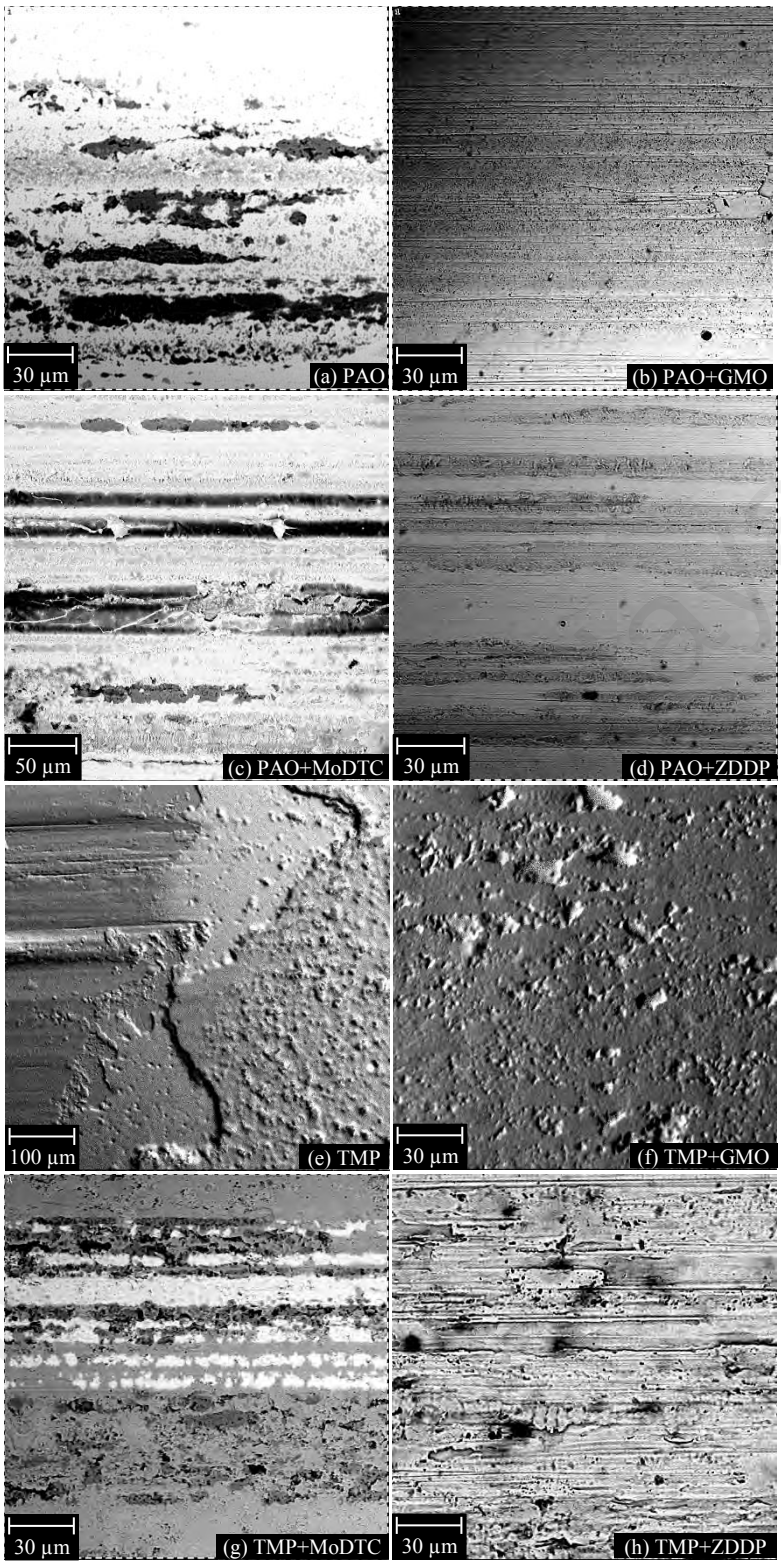

Figure 4.10: SEM micrographs of ta-C-coated balls after 2 hours of sliding against ta-C-coated plates in the presence of PAO-based and TMP-based lubricants

Table 4.6: Atomic percentage of elements found on ta-C-coated balls after 2 hours of sliding against ta-C-coated plates in the presence of PAO-based and TMP-based lubricants

Lubricants	Elements							
	Fe	**C**	**O**	**Cr**	**Zn**	**S**	**P**	**Mo**
PAO	9.1	74.4	15.4	0.8	-	-	0.1	0.2
PAO+GMO	2.1	89.3	7.2	0.8	0.2	0.2	0.1	0.1
PAO+MoDTC	1.6	85.4	8.8	0.8	-	1.4	0.1	1.9
PAO+ZDDP	1.8	73.1	20.8	0.6	2.5	0.5	0.7	-
TMP	19.5	69.2	9.9	0.9	0	0.2	0.2	0.1
TMP+GMO	1.7	79.7	17.8	0.7	0.1	-	-	-
TMP+MoDTC	6.3	76.2	13.9	0.8	-	1.2	0.1	1.5
TMP+ZDDP	1.3	77.4	15.3	1.1	2.6	0.5	1.8	-

4.4.4.3 ta-C/steel contact

A lot of surface deterioration was seen in the micrographs of PAO-based lubricants compared to those of TMP ones (**Figure 4.11**). As a result, ta-C/steel contacts resulted in high values of friction and wear coefficients when different variants of PAO were used (**Figure 4.3**, **Figure 4.4** and **Figure 4.5**). When additive-free PAO was used, abrasion was observed as the main wear mechanism which resulted in the formation of scratch lines in the direction of sliding especially in the lower part of the micrograph accompanied with few pits and grooves (**Figure 4.11a**). Although, few scratch lines and pits were also observed with TMP but the major difference between the two micrographs was the transfer of carbon material from ta-C-coated plate represented by black region in the middle (**Figure 4.11e**). High percentage of carbon observed in EDS results (**Table 4.7**), low friction coefficient value (**Figure 4.3**) and delamination of coating from the plate confirmed the transfer of carbon material from ta-C-coated plate (**Figure 4.11e**).

Micrographs of GMO-containing lubricants showed excessive abrasive wear represented by deep grooves and concentrated scratch lines throughout the scan area especially when TMP+GMO was used (**Figure 4.11b** and **Figure 4.11f**). In case of PAO+GMO, pitting was the other predominant wear mechanism in addition to abrasive wear. This excessive pitting can be attributed to adsorbtion of hydroxyl group from GMO, resulting in high content of oxygen in EDS analysis and lowest friction coefficient value of ta-C/steel contact among PAO-based lubricants. Those pits act as small reservoirs to maintain continuous supply of lubricant to the contact and prevent starvation conditions. Formation of white-colored MoDTC-derived tribofilm as a result of its tribochemical decomposition was observed in the micrograph of PAO+MoDTC especially at the middle and top regions (**Figure 4.11c)**. In addition to that, some of the coating material was also transferred to the steel ball from ta-C-coated plate and can be seen as black and grey-colored patches. Although, MoDTC-derived tribofilm was also observed in EDS results of TMP+MoDTC but it was mostly comprised of MoO_3 as sulfur was present in low percentage compared to oxygen (**Table 4.7)**. In case of ZDDP-based lubricants, additive-derived tribofilm composed of zinc, phosphorus and sulfur was observed on steel balls irrespective of base oil type (**Table 4.7**). When PAO+ZDDP was used as lubricant, patchy ZDDP-derived tribofilm was seen in micrograph (**Figure 4.11d)**. In addition to abundant cracks, crevices and wear debris; scratch lines were also observed in the direction of sliding. Compared to PAO+ZDDP, relatively clean and unaltered ball surface was seen in the micrograph of TMP+ZDDP and no signs of brittle fracture or wear debris were detected. As a result, TMP+ZDDP resulted in improved tribological performance when used as lubricant in ta-C/steel contact.

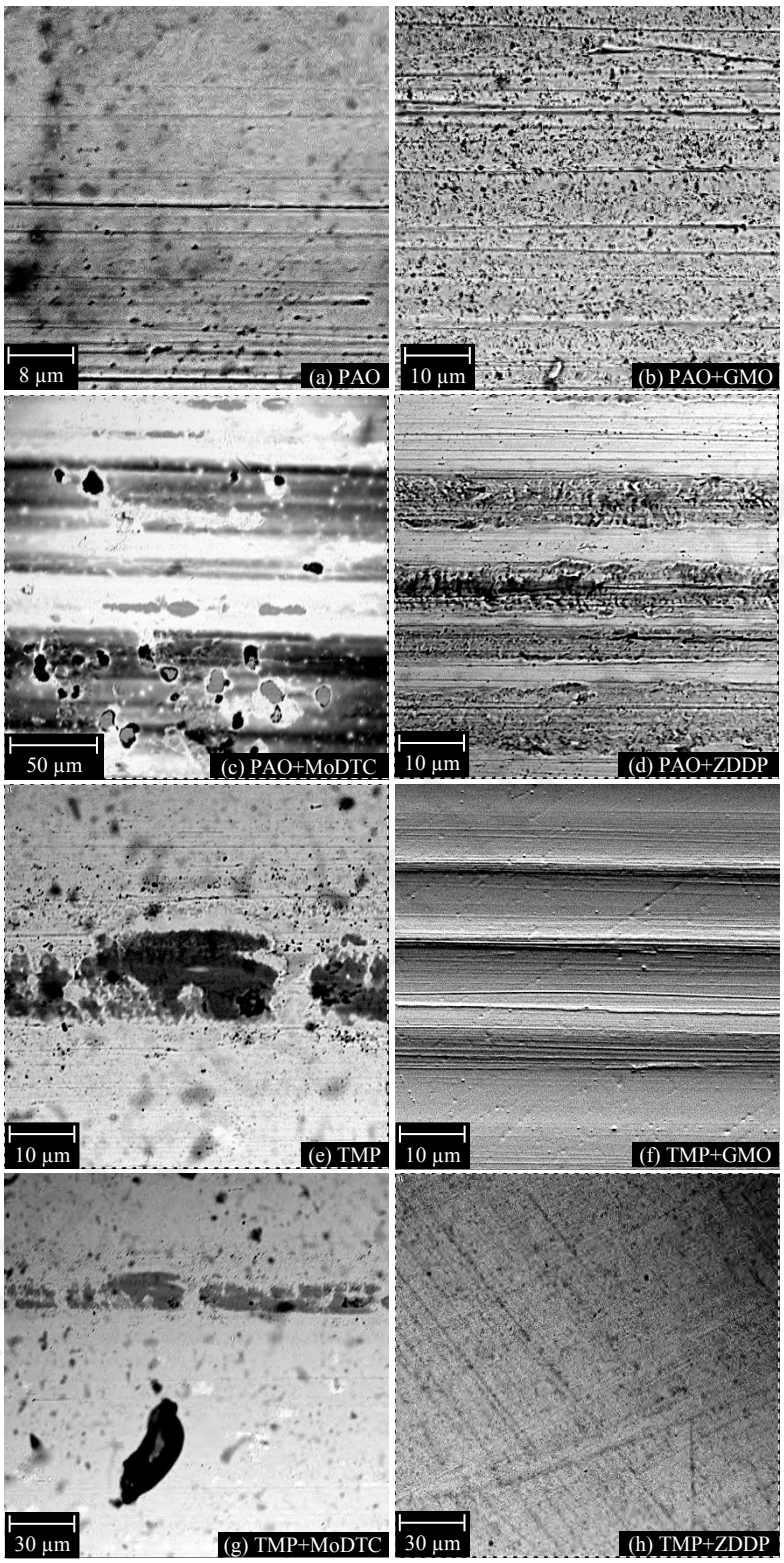

Figure 4.11: SEM micrographs of uncoated steel balls after 2 hours of sliding against ta-C coated plate in the presence of PAO-based and TMP-based lubricants

Table 4.7: Atomic percentage of elements found on uncoated steel balls after 2 hours of sliding against ta-C-coated plates in the presence of PAO-based and TMP-based lubricants

Lubricants	Elements							
	Fe	**C**	**O**	**Cr**	**Zn**	**S**	**P**	**Mo**
PAO	69.1	14.2	15.5	1.2	-	-	-	-
PAO+GMO	66.3	12.5	20.9	0.3	-	-	-	-
PAO+MoDTC	67.5	24.8	4.2	1.2	-	1.2	0.3	0.8
PAO+ZDDP	82.4	7.8	6.5	0.8	0.8	0.8	0.9	-
TMP	53.2	35.7	9.7	0.9	0.2	0	0.2	0.1
TMP+GMO	60.9	15.1	22.9	0.8	-	0.2	0.1	-
TMP+MoDTC	70.9	12.7	13.9	0.8	-	0.5	0.1	1.1
TMP+ZDDP	75.6	13.4	6.6	1.1	1.2	0.9	1.1	0.1

4.4.4.4 a-C:H/a-C:H contact

In SEM micrographs of PAO and PAO+GMO, white-colored CrN interlayer can be clearly seen (**Figure 4.12**). High percentage of chromium and nitrogen detected in EDS analysis also confirmed the exposed CrN interlayer as a result of top a-C:H coating delamination (**Table 4.8**). Compared to that, relatively unaltered surface can be seen in the micrographs of TMP and TMP+GMO with 97.34% and 90.10% of carbon. As a result, wear coefficient values of a-C:H-coated balls obtained with PAO and PAO+GMO were 55% and 40% higher than those of TMP and TMP+GMO respectively (**Figure 4.4**) but no significant change of delamination was seen in friction results (**Figure 4.3**). A possible justification for this behavior can be the presence of coating material on the contact area even after its delamination from the ball surface but when sliding parts were cleaned before carrying out material characterization, it was removed. Although, improvement in friction performance of a-C:H/a-C:H contact was seen when PAO+MoDTC was used as

lubricant (0.044 to 0.040) but no signs of MoDTC-derived tribofilm was seen in SEM micrograph and EDS results. Contrary to that, MoDTC was able to interact tribochemically with a-C:H-coated ball to some extent when mixed with TMP resulting in the formation of white-colored additive-derived tribofilm (**Figure 4.12g)**. EDS results also confirmed the formation of MoDTC-derived tribofilm. Although, zinc, phosphorus and sulfur were observed in EDS results but no significant change in the wear coefficient of a-C:H-coated ball was seen when PAO+ZDDP was used as lubricant instead of additive-free PAO but wear resistance of a-C:H-coated plate was substantially increased (**Figure 4.4** and **Figure 4.5**). This shows that ZDDP-derived tribofilm was originally formed on a-C:H-coated plate and some of it was transferred to ball surface at the end of 2 hours of sliding before which maximum wearing out of the ball surface was already occurred. Contrary to that, thick layer of ZDDP-derived tribofilm can be clearly seen on the micrograph of a-C:H-coated ball when TMP+ZDDP was used as lubricant resulting in lowest wear coefficient of ball among TMP-based lubricants (**Figure 4.12h)**.

Table 4.8: Atomic percentage of elements found on a-C:H-coated balls after 2 hours of sliding against a-C:H-coated plates in the presence of PAO-based and TMP-based lubricants

Lubricants	**Elements**											
	C	**Cr**	**N**	**P**	**S**	**Mo**	**Zn**	**Fe**	**O**	**Ar**	**Na**	**Cl**
PAO	68.7	23.7	6.7	-	-	-	-	-	0.9	-	-	-
PAO+GMO	50.2	27.3	10.8	-	-	-	-	-	11.1	0.6	-	-
PAO+MoDTC	88.4	-	5.1	-	-	-	-	-	5.4	1.1	-	-
PAO+ZDDP	34.7	31.6	15.9	1.1	0.6	-	2.2	6.8	6.5	0.6	-	-
TMP	97.4	-	-	-	-	-	-	-	1.3	1.3	-	-
TMP+GMO	90.1	6.1	-	-	-	-	-	-	2.5	1.3	-	-
TMP+MoDTC	71.1	-	-	0.5	0.2	0.3	-	-	14.7	0.2	1.0	0.5
TMP+ZDDP	71.2	8.3	3.1	2.51	1.5	-	3.3	7.6	1.50	0.9	-	-

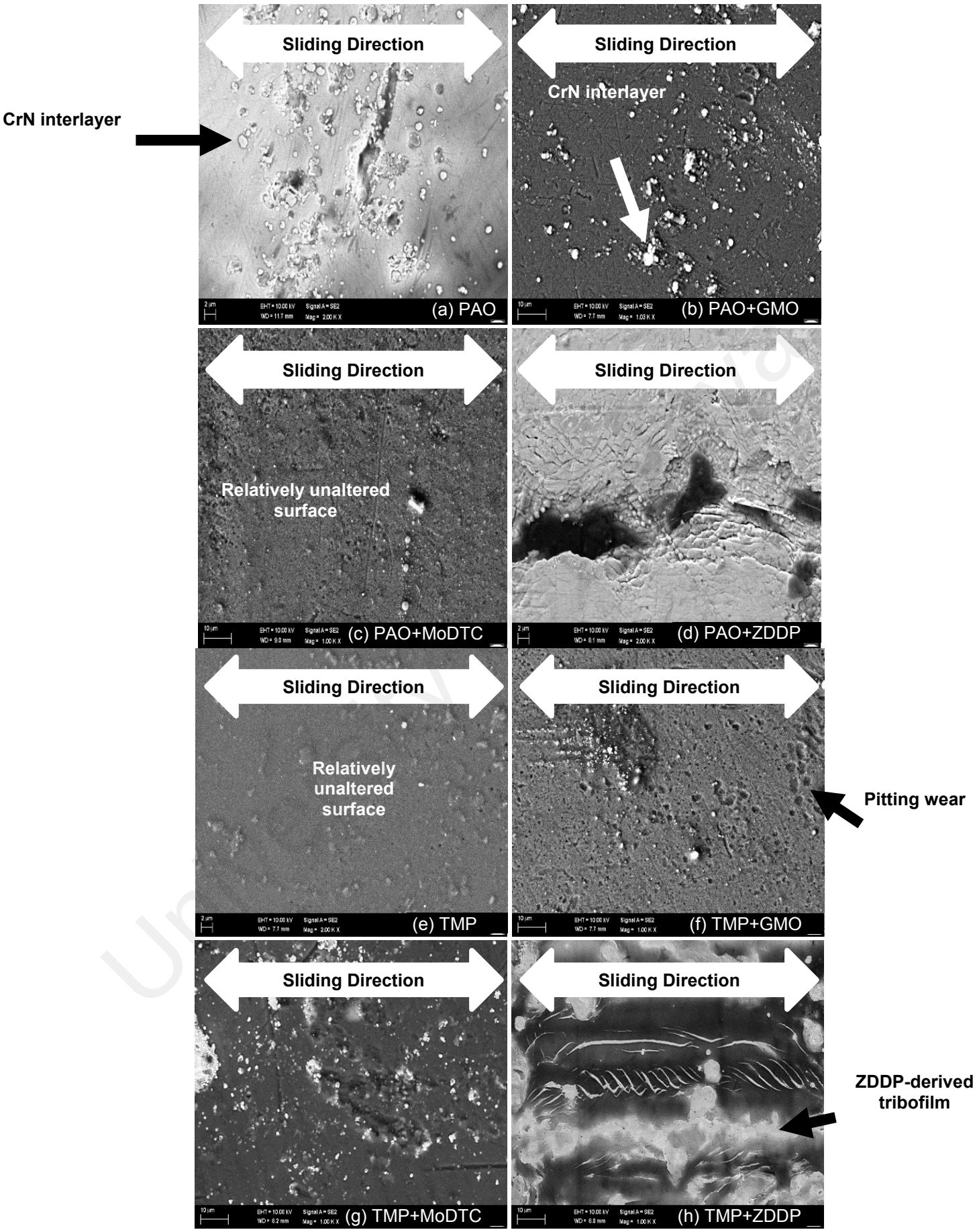

Figure 4.12: SEM micrographs of a-C:H-coated balls after 2 hours of sliding against a-C:H-coated plates in the presence of PAO-based and TMP-based lubricant

4.4.4.5 a-C:H/steel contact

Deep grooves were seen in the micrographs of PAO and PAO+GMO (**Figure 4.13a** and **Figure 4.13b**) due to abrasive wear whereas no such wear mechanism was observed with TMP-based lubricants (**Figure 4.13e** and **Figure 4.13f**). GMO was able to interact tribochemically with uncoated steel ball when mixed with TMP resulting in the formation of white-colored tribofilm and reduction of friction coefficient from 0.063 to 0.052 (**Figure 4.3**). Contrary to that, no signs of GMO-derived tribofilm was seen in the micrograph of PAO+GMO. MoDTC played its primary role and resulted in lowest friction coefficient values among formulated lubricant irrespective of base oil type (**Figure 4.3**). Not only this, reduction in wear coefficient of ball was also observed when PAO+MoDTC and TMP+MoDTC were used as lubricant instead of additive-free base oils (**Figure 4.4**). This improved tribological performance of a-C:H/steel contact in the presence of MoDTC-containing lubricant, especially PAO+MoDTC, can be attributed to the formation of tribofilm composed of molybdenum and sulfur (**Table 4.9**). Similar to MoDTC, ZDDP was able to tribochemically interact with sliding surfaces resulting in lowest wear coefficients values of a-C:H/steel contact among PAO-based lubricants (**Figure 4.4** and **Figure 4.5**). Formation of ZDDP-derived tribofilm, comprised of zinc, phosphorus and sulfur, was also confirmed by EDS analysis (**Table 4.9**). Contrary to PAO+ZDDP, no signs of any tribochemical interaction between additive and sliding surfaces was seen when TMP+ZDDP was used as lubricant. As a result, accelerated wearing of interacting surfaces was witnessed in the presence of TMP+ZDDP resulting in wear coefficient values which were 4 to 5 times higher than those of PAO+ZDDP.

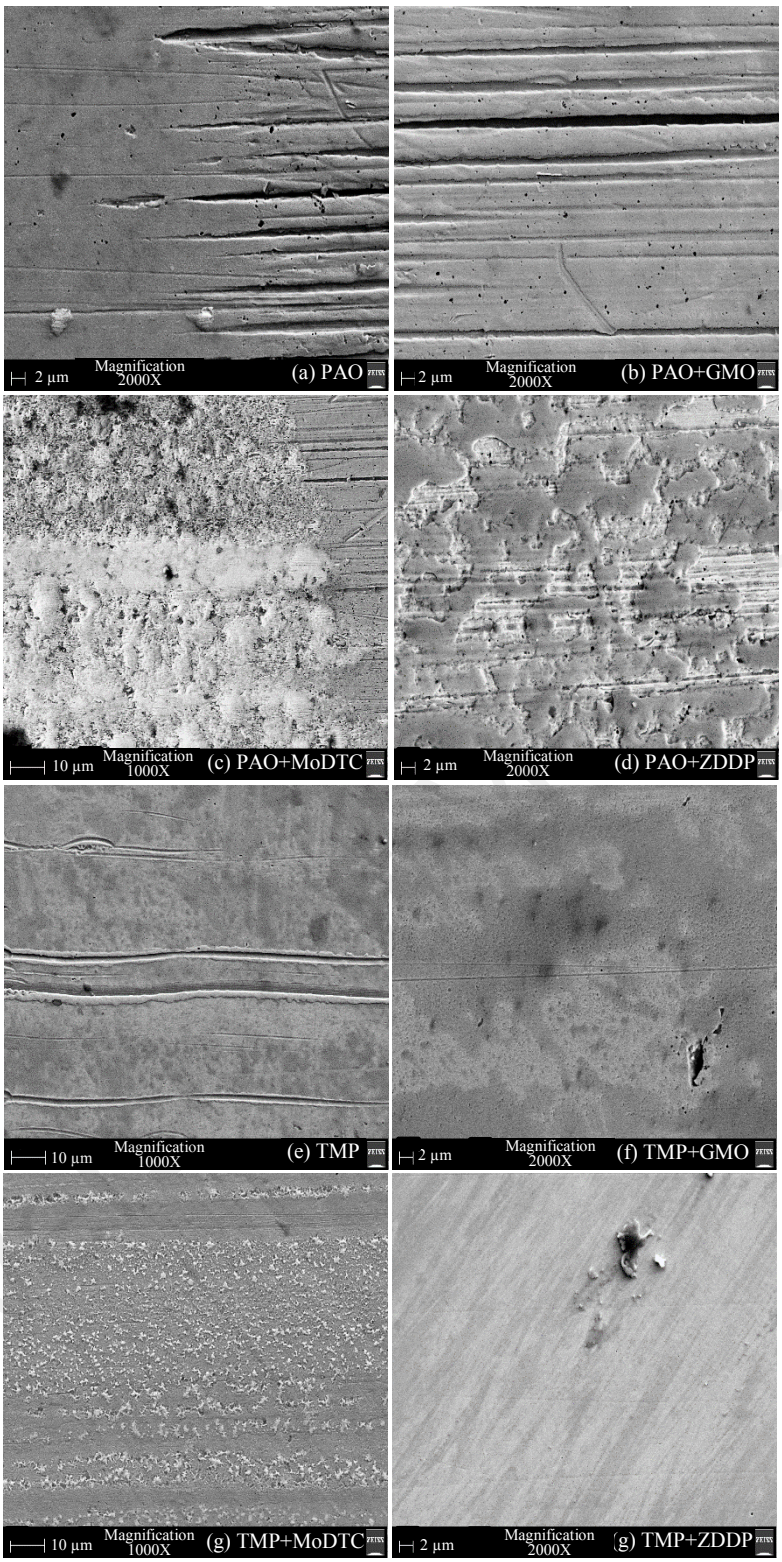

Figure 4.13: SEM micrographs of uncoated steel balls after 2 hours of sliding against a-C:H-coated plate in the presence of PAO-based and TMP-based lubricants

Table 4.9: Atomic percentage of elements found on uncoated steel balls after 2 hours of sliding against a-C:H-coated plates in the presence of PAO-based and TMP-based lubricants

Lubricants	Elements							
	C	**Cr**	**P**	**S**	**Mo**	**Zn**	**Fe**	**O**
PAO	15.3	-	-	-	-	-	84.7	5. 6
PAO+GMO	28.7	1.9	-	-	-	-	62.8	6.6
PAO+MoDTC	44.5	4.8	-	3.5	11.4	-	23.0	12.8
PAO+ZDDP	11.6	-	6.6	2.9	-	17.1	33.3	28.5
TMP	22.6	-	-	-	-	-	70.1	7.3
TMP+GMO	25.2	-	-	-	-	-	68.8	6.0
TMP+MoDTC	37.7	-	-	2.5	6.9	-	42.6	10.3
TMP+ZDDP	13.9	3.2	-	-	-	-	77.1	5.8

4.4.4.6 a-C:H:W/a-C:H:W contact

When additive-free TMP was used as lubricant, a-C:H:W-coated ball was not able to sustain 2 hours of sliding and resulted in delamination of top a-C:H:W coating and exposure of CrN interlayer (**Figure 4.14e**). EDS results show that some of the CrN interlayer was also exposed in the presence of PAO but not to the extent of TMP. Complete delamination of CrN interlayer and exposed ferrous substrate was not witnessed with any of the additive-free base oils. When PAO+ GMO was used as lubricant instead of additive-free PAO, deterioration in wear resistance and increase in wear coefficient of a-C:H:W-coated ball was seen (**Figure 4.3**). Delamination of top DLC layer and pitting was the predominant wear mechanism observed in the micrograph of PAO+GMO (**Figure 4.14b**). High concentration of chromium and nitrogen in EDS results also confirmed delamination of a-C:H:W layer. On the contrary, GMO improved the inherent wear characteristics of TMP and delamination of DLC coating was prevented

to appreciable extent. However, more pronounced pitting wear was seen with TMP+GMO compared to PAO+GMO ((**Figure 4.14f**). Highest wear coefficient values of a-C:H-coated ball and plate were seen when MoDTC-containing PAO was used as lubricant resulting in the complete delamination of a-C:H:W coating (**Figure 4.4** and **Figure 4.5**). Not only this, most of the CrN interlayer was also worn-out after 2 hours of sliding resulting in exposed ferrous substrate (49.8 % concentration). It is interesting to note that no change was seen in the friction performance of a-C:H:W/a-C:H:W was seen as a result of this delamination compared to additive-free PAO. Like state earlier, presence of coating material on the contact area after it was delaminated from the ball surface can be possible reason for this behavior. Another justification can be tribochemical interaction of MoDTC with exposed ferrous surfaces resulting in the formation of additive-derived tribofilm composed of MoS_2 and MoO_3. Presence of molybdenum and sulfur in large concentrations on ball surface in EDS analysis confirmed the presence of MoDTC-derived tribofilm (**Table 4.10**). Although, tribochemical interaction was also observed between MoDTC-containing TMP and interacting surfaces but no to the extent of PAO+MoDTC. However, a-C:H:W-coated surfaces were able to maintain their structural integrity after 2 hours of sliding and no signs of coating delamination was seen when TMP+MoDTC was used as lubricant. Grain-like appearance was observed in the micrograph of TMP+MoDTC but it was not as distinct as the cobblestone structure of as-deposited surface because of the polishing wear and presence of additive-derived tribofilm (**Figure 4.14g)**. As a result, significant improvement in tribological performance of a-C:H:W/a-C:H:W contact was seen when TMP+MoDTC was used as lubricant instead of additive-free TMP. Similar to MoDTC-containing TMP, TMP+ZDDP was also able to tribochemically interact with symmetrical a-C:H:W contact and resulted in lowest wear coefficient values of a-C:H:W-coated balls and plate (**Figure 4.4** and **Figure 4.5**). White-colored ZDDP-derived can be clearly seen in the micrograph

of TMP+ZDDP (**Figure 4.14h**). Presence of zinc, sulfur and phosphorus in EDS results also confirmed the formation of ZDDP-derived tribofilm. On the contrary, PAO+ZDDP accelerated the wearing out of interacting surfaces and high wear coefficient values were observed compared to additive-free PAO. Although, tribochemical interaction took place between TMP+ZDDP and sliding surfaces but not to the extent of PAO+ZDDP as per the EDS results.

Table 4.10: Atomic percentage of elements found on a-C:H:W-coated balls after 2 hours of sliding against a-C:H:W-coated plates in the presence of PAO-based and TMP-based lubricants

Lubricants	**Elements**										
	C	**W**	**Cr**	**N**	**P**	**S**	**Mo**	**Zn**	**Fe**	**O**	**Ni**
PAO	36.4	8.8	37.1	5.9	-	-	-	-	-	9.1	2.7
PAO+GMO	32.3	4.4	30.2	25.2	-	-	-	-	-	5.2	2.7
PAO+MoDTC	19.7	0.9	12.7	11. 9	-	2.5	6.3	-	49.8	8.1	-
PAO+ZDDP	32.9	12.3	22.0	12.9	-	1.3	-	0.9	-	11.3	6.4
TMP	9.3	4.7	43.8	34.7	-	-	-	-	-	4.8	2.7
TMP+GMO	59.4	25.8	3.9	-	-	-	-	-	-	3.6	7.3
TMP+MoDTC	57.3	19.8	5.5	-	-	0.7	2.8	-	-	8.5	5.4
TMP+ZDDP	49.8	12.9	12.3	8.8	1.4	2.8	-	3.2	-	8.8	-

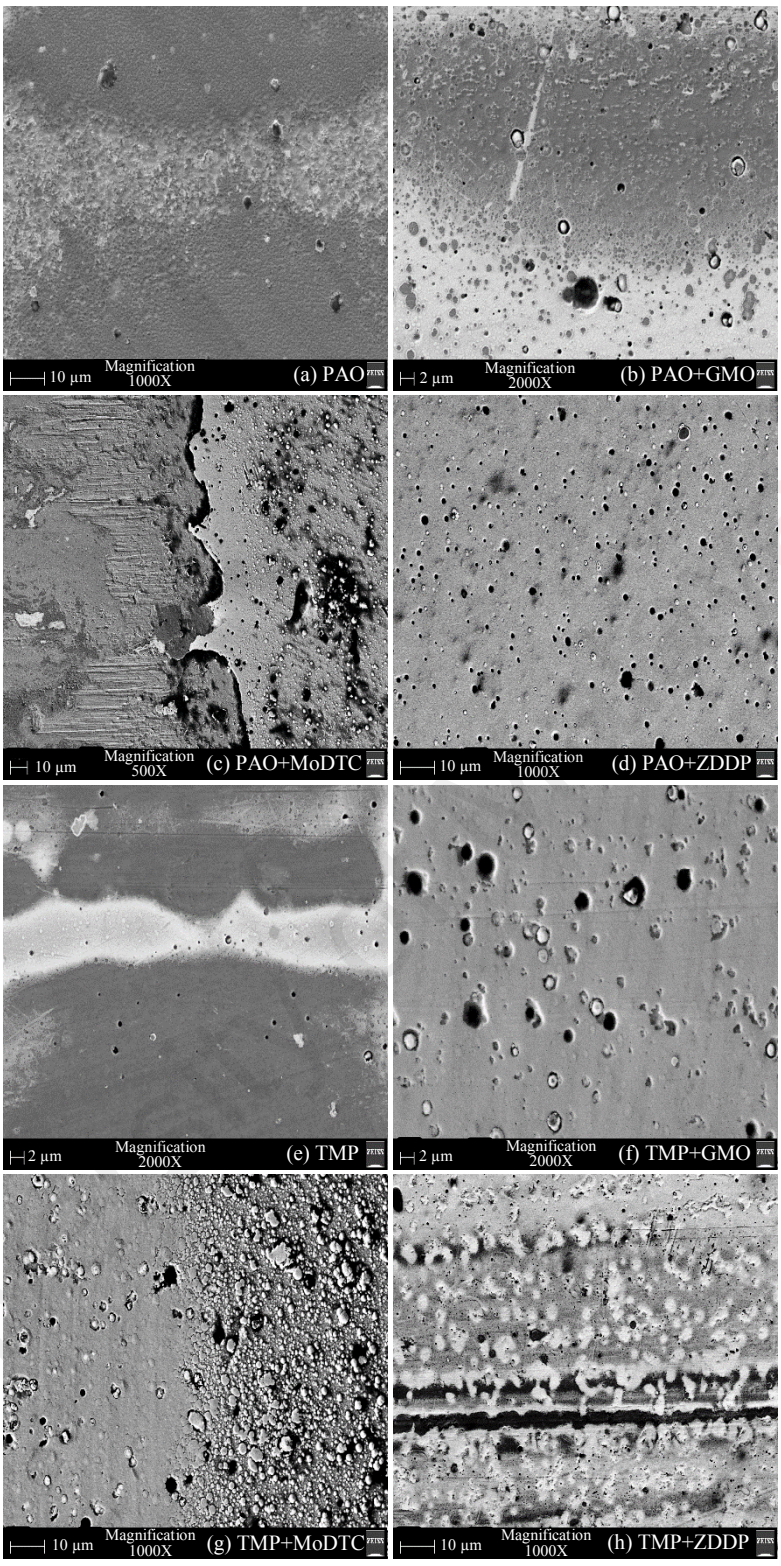

Figure 4.14: SEM micrographs of a-C:H:W-coated balls after 2 hours of sliding against a-C:H-coated plates in the presence of PAO-based and TMP-based lubricants

4.4.4.7 a-C:H:W/steel contact

A lot of surface deterioration was seen in the micrographs of uncoated steel balls when additive-free base oils were used as lubricants (**Figure 4.15a** and **Figure 4.15e**). Abrasion was observed as the main wear mechanism which resulted in the formation of scratch lines in the direction of sliding especially when additive-free TMP was used as lubricant. Although, few scratch lines and pits were also observed with PAO but the major difference between two micrographs was the transfer of carbon and tungsten from a-C:H:W-coated plate represented by black region in the middle. White-colored GMO-based tribofilm was observed on the micrographs of uncoated steel balls when GMO-based lubricants were used resulting in lowest friction coefficient values among formulated lubricants (**Figure 4.3**). Micrographs of GMO-containing lubricants showed excessive abrasive wear represented by deep grooves and concentrated scratch lines throughout the scan area especially when PAO+GMO was used (**Figure 4.15b**). In case of TMP+GMO, pitting was the other predominant wear mechanism in addition to abrasive wear (**Figure 4.15f**). This excessive pitting can be attributed to adsorbtion of hydroxyl group from GMO, resulting in high content of oxygen in EDS analysis (**Table 4.11**). Those pits act as small reservoirs to maintain continuous supply of lubricant to the contact and prevent starvation conditions. Similar to GMO, MoDTC-containing lubricants were also able to interact tribochemically with sliding surfaces resulting in the formation of MoDTC-derived tribofilm composed of molybdenum and sulfur. Although, reduction in friction coefficient of a-C:H:W/steel contact was witnessed as a result of MoDTC-derived tribofilm but it also resulted in accelerated wear of interacting surfaces. A possible justification for deterioration in wear performance can be consumption of tungsten and formation of WS_2 along with MoS_2 and MoO_3 as a result of tribochemical interaction and removal of weakly-adhered tribofilm as a result of sliding (Podgornik, Hren, & Vižintin, 2005; Yang et al., 2014). ZDDP was also able to tribochemically

interact with sliding resulted in the formation of tribofilm composed of sulfur, phosphorus and zinc. In case of TMP+ZDDP, tribofilm was also accompanied by transfer of coating material from a-C:H:W-coated plate whereas no such behavior was observed in the micrograph of PAO+ZDDP (**Figure 4.15d** and **Figure 4.15h**). Formation of ZDDP-derived tribofilm was also confirmed by EDS results as a result of which lowest wear coefficient value of ball were observed when ZDDP-containing lubricants were used. However, deterioration in friction performance of a-C:H:W/steel contact was seen in the presence of TMP+ZDDP.

Table 4.11: Atomic percentage of elements found on uncoated steel balls after 2 hours of sliding against a-C:H:W-coated plates in the presence of PAO-based and TMP-based lubricants

	Elements									
Lubricants	**C**	**W**	**Cr**	**P**	**S**	**Mo**	**Zn**	**Fe**	**O**	**Ni**
PAO	15.1	8.9	-	-	-	-	-	43.3	26.5	6.2
PAO+GMO	29.7	-	-	-	-	-	-	65.2	5.1	-
PAO+MoDTC	20.9	4.4	-	-	2.7	6.5	-	56.1	9.4	-
PAO+ZDDP	22.4	10.2	-	2.1	1.9	-	4.5	40.1	12.4	6.4
TMP	17.6	5.7	3.7	-	-	-	-	56.1	16.9	-
TMP+GMO	20.9	4.7	-	-	-	-	-	59.9	14.5	-
TMP+MoDTC	35.2	7.0	-	-	0.6	10.8	-	25.6	15.3	5.5
TMP+ZDDP	39.1	10.1	-	2.4	2.3	-	6.5	25.4	14.2	-

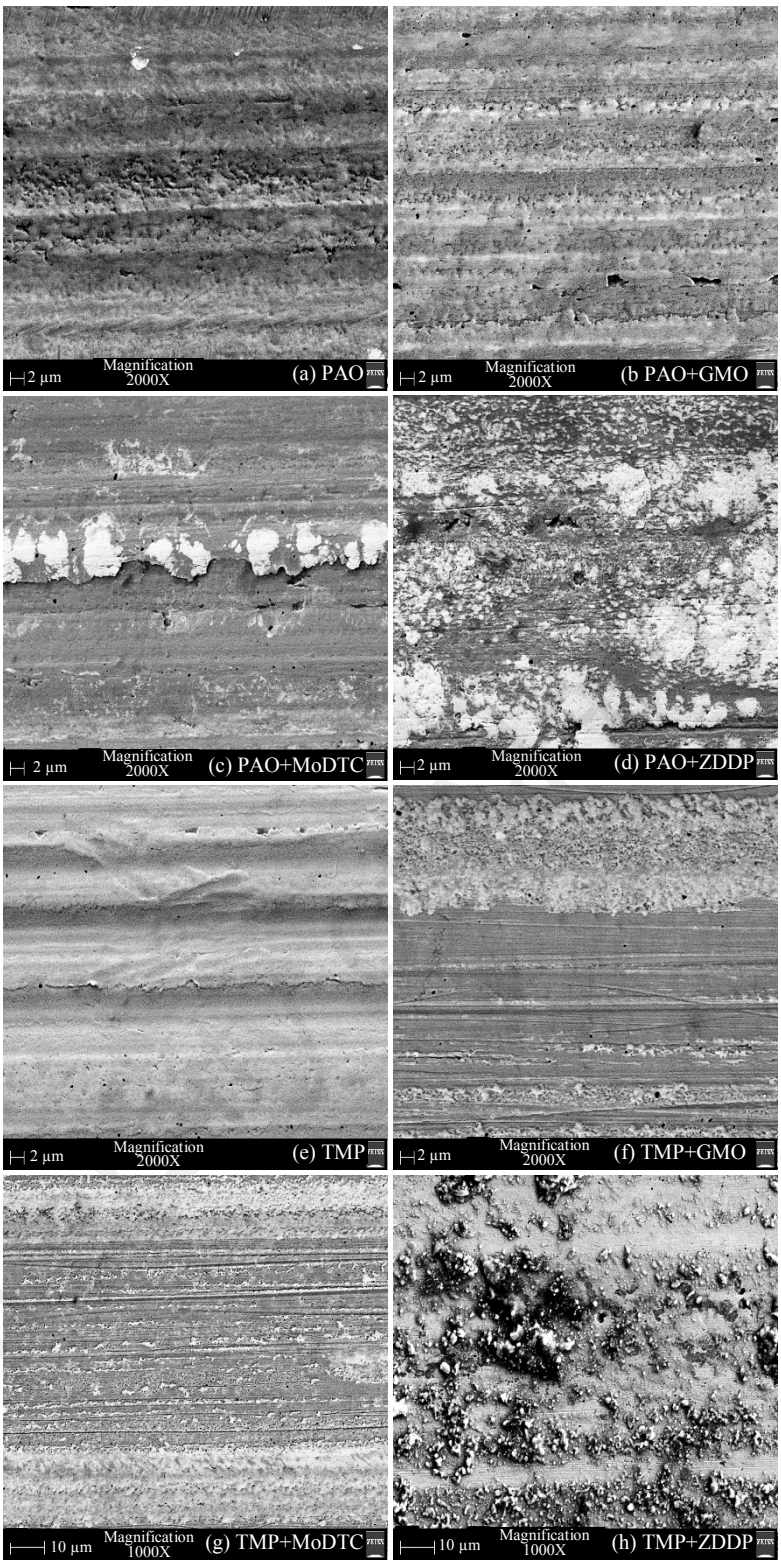

Figure 4.15: SEM micrographs of uncoated steel balls after 2 hours of sliding against a-C:H-coated plate in the presence of PAO-based and TMP-based lubricants

4.4.5 Surface roughness analysis

R_a values of uncoated and DLC-coated plates after 2 hours of sliding against uncoated and DLC-coated balls in the presence of PAO-based and TMP-based lubricants are presented in **Figure 4.23.**

4.4.5.1 Steel/steel contact

R_a value of uncoated steel plate was increased by 45% when additive-free TMP was used as lubricant instead of PAO due to chemical attack of fatty acids present in TMP and formation of non-reactive detergents (Bowden & Tabor, 2001). As a consequence of this deterioration, TMP resulted in high wear coefficients values (**Figure 4.4** and **Figure 4.5**). Although, TMP resulted in wider wear track (238 μm) on steel plate compared to that obtained with PAO (220 μm) but few deep grooves (2.5 μm) centred at 137 μm and 170 μm were observed with latter (**Figure 4.16**). A significant improvement in surface roughness value of steel plates was observed when additive-containing lubricants were used and only polishing wear was seen with most of the formulated lubrication. Exceptions to this finding was seen when PAO+MoDTC and TMP+GMO were used as lubricants resulting in severe roughening of steel plates. Among PAO-based lubricants, highest surface roughness value of 5.167 μm was seen with PAO+MoDTC whereas PAO+GMO resulted in lowest value (0.149 μm). When GMO was mixed with TMP, severe deterioration of plate surface was witnessed which resulted in highest surface roughness value among TMP-based lubricants. A possible hypothesis for ineffectiveness of TMP+GMO in protecting the interacting surfaces from deterioration can be polar nature of both base oil and additive due to which hydroxyl group of GMO attaches to the polar components of TMP instead of ferrous plate (Tasdemir, Wakayama, et al., 2013a).

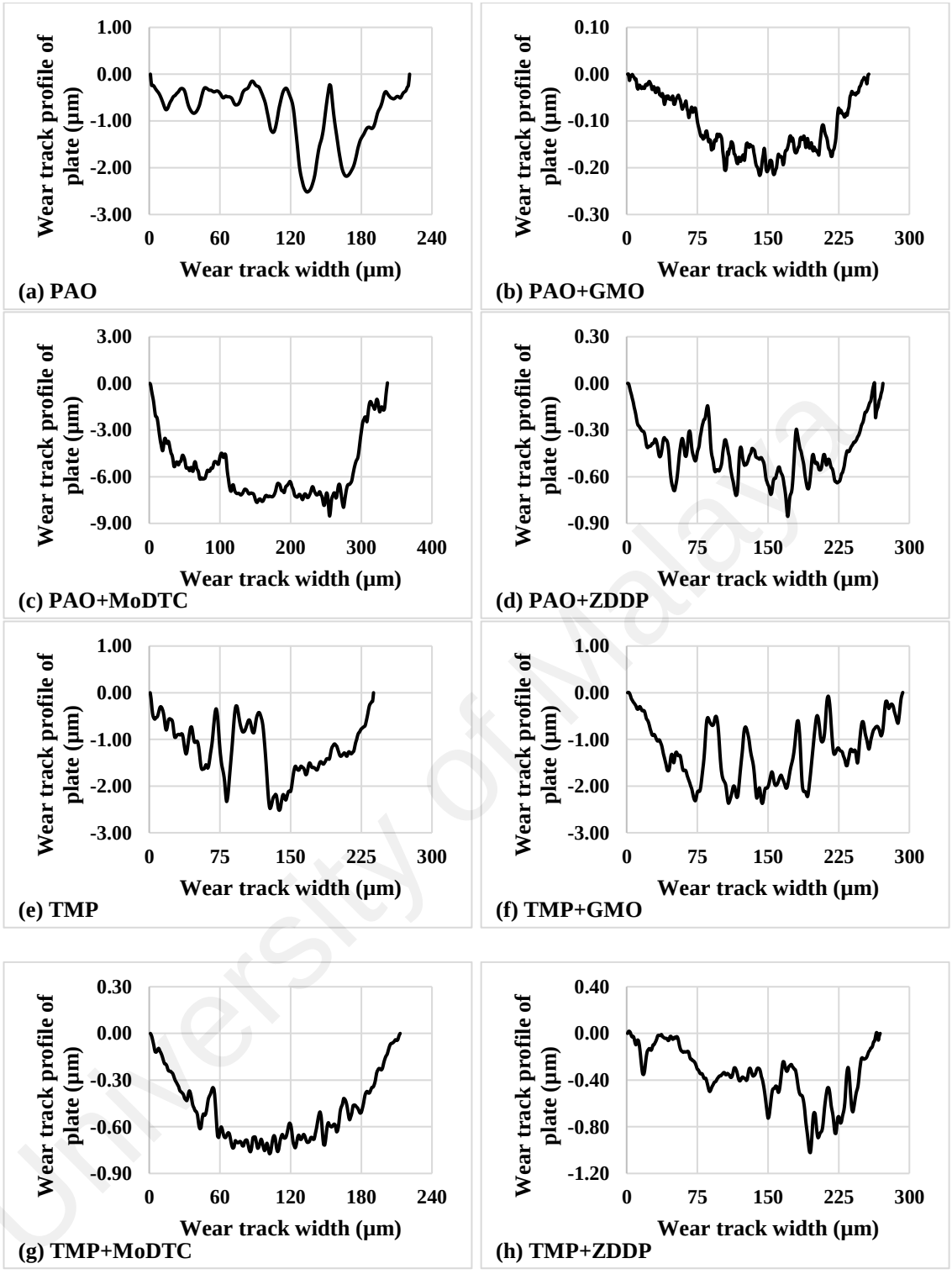

Figure 4.16: Wear track profiles of uncoated steel plates after 2 hours of sliding against uncoated steel balls in the presence of PAO-based and TMP-based lubricants

4.4.5.2 ta-C/ta-C contact

In **Figure 4.17**, it can be seen that ta-C-coated plates wear-out uniformly throughout the wear track width irrespective of lubricant formulation and maximum wear depth was seen at the centre of the wear track. Similar to steel plates, additive-free PAO was proved to be more effective in providing surface protection to ta-C-coated plates compared to TMP resulting in better tribological performance (**Figure 4.3**, **Figure 4.4** and **Figure 4.5**). Additives were proved to be more effective in protecting the ta-C-coated surface from severe roughening when mixed with TMP. GMO was the only additive which further improves the surface protection characteristics of both base oils resulting in lowest surface roughness values. Surface protective role of GMO can be explained by passivation of dangling carbon bonds of ta-C coatings by hydroxyl group (Tasdemir, Wakayama, et al., 2013a). This interaction resulted in the formation of GMO-based lubricant film due to which direct contact of the asperities was avoided. A similar behaviour was also observed by Tasdemir, Wakayama, et al. (2013b) while evaluating ta-C coating with PAO-based lubricants.

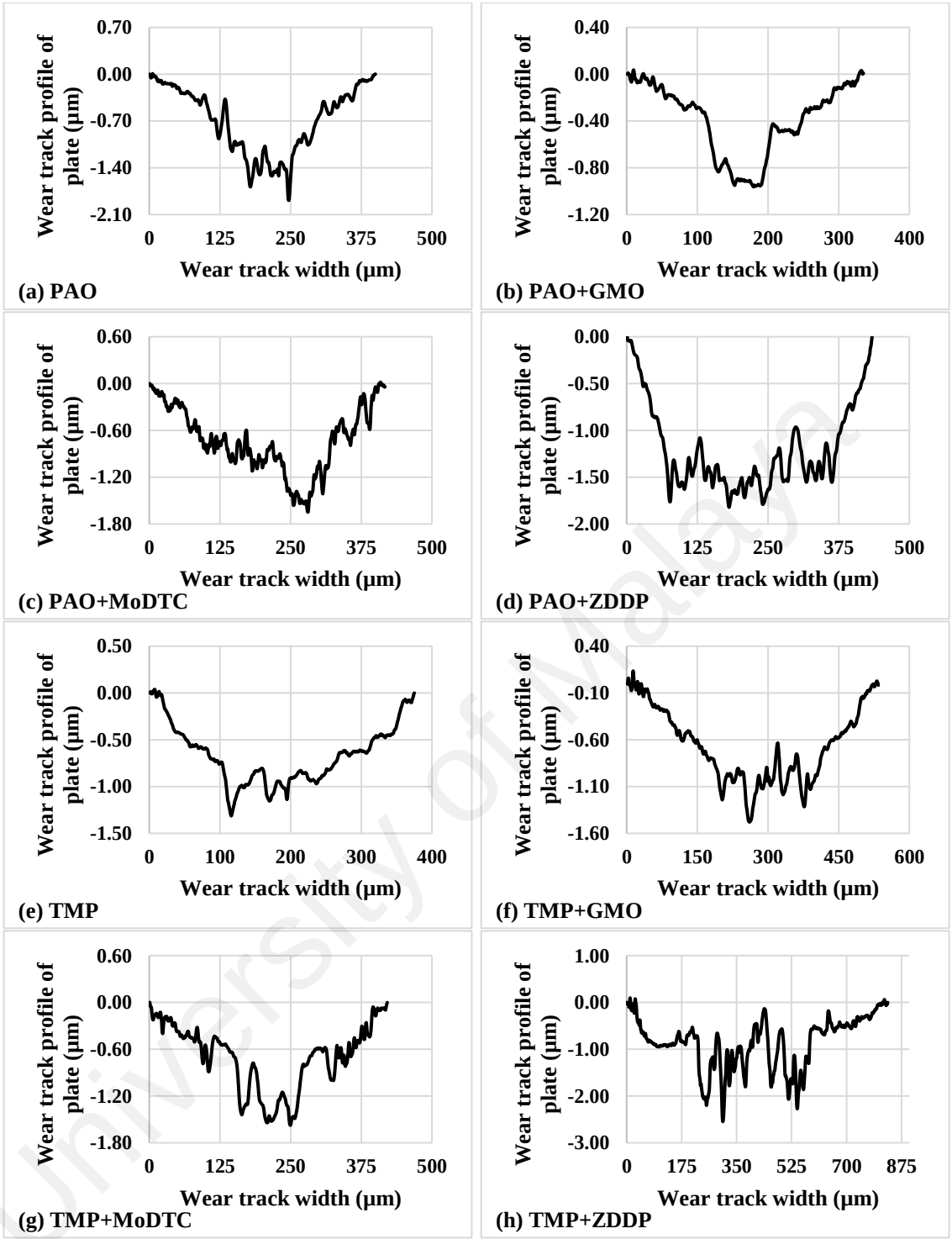

Figure 4.17: Wear track profiles of ta-C-coated plates after 2hours of sliding against ta-C-coated balls in the presence of PAO-based and TMP-based lubricants

4.4.5.3 ta-C/steel contact

Similar to steel/steel and ta-C/ta-C contacts, significantly high surface roughness value was seen when additive-free TMP was used compared to that of PAO. A clear difference

in the wear track profiles of PAO and TMP can be seen. Multiple deep grooves due to abrasive action of hard Fe_2O_3 particles was seen in the presence of PAO whereas delamination of coating material due to adhesion with uncoated steel ball was seen as predominant wear mechanism when TMP was used as lubricant. Additives were proved to be effective in preventing the deterioration of ta-C-coated plate when mixed with TMP resulting in eloquent decrease in surface roughness values but still values were higher than that of additive-free PAO. Among TMP-based lubricants, lowest surface roughness value was obtained with TMP+ZDDP. Surface protective role of ZDDP can be related to consumption of iron oxide particles by $Zn_3(PO_4)_2$ tribofilm due to which abrasive wear was minimized (Spikes, 2004). As a result, lowest wear coefficient values of ta-C-coated plate and uncoated cast iron pin was observed with TMP+ZDDP among tested lubricants (**Figure 4.4** and **Figure 4.5**). On the other hand, further deterioration of ta-C-coated surface was seen when formulated versions of PAO were used instead of additive-free PAO. Among PAO-based lubricants, highest surface roughness value was seen with MoDTC whereas PAO+ZDDP resulted in approximately same level of surface roughness as that of PAO. A possible hypothesis for severe deterioration of ta-C-coated plate in the presence of PAO+MoDTC can be formation of MoO_3 in higher concentration compared to MoS_2 as a result of tribochemical decomposition of MoDTC. It is mentioned in the literature that MoO_3 has sharp crystalline structure due to which it causes severe abrasion of the contact (Haque et al., 2007).

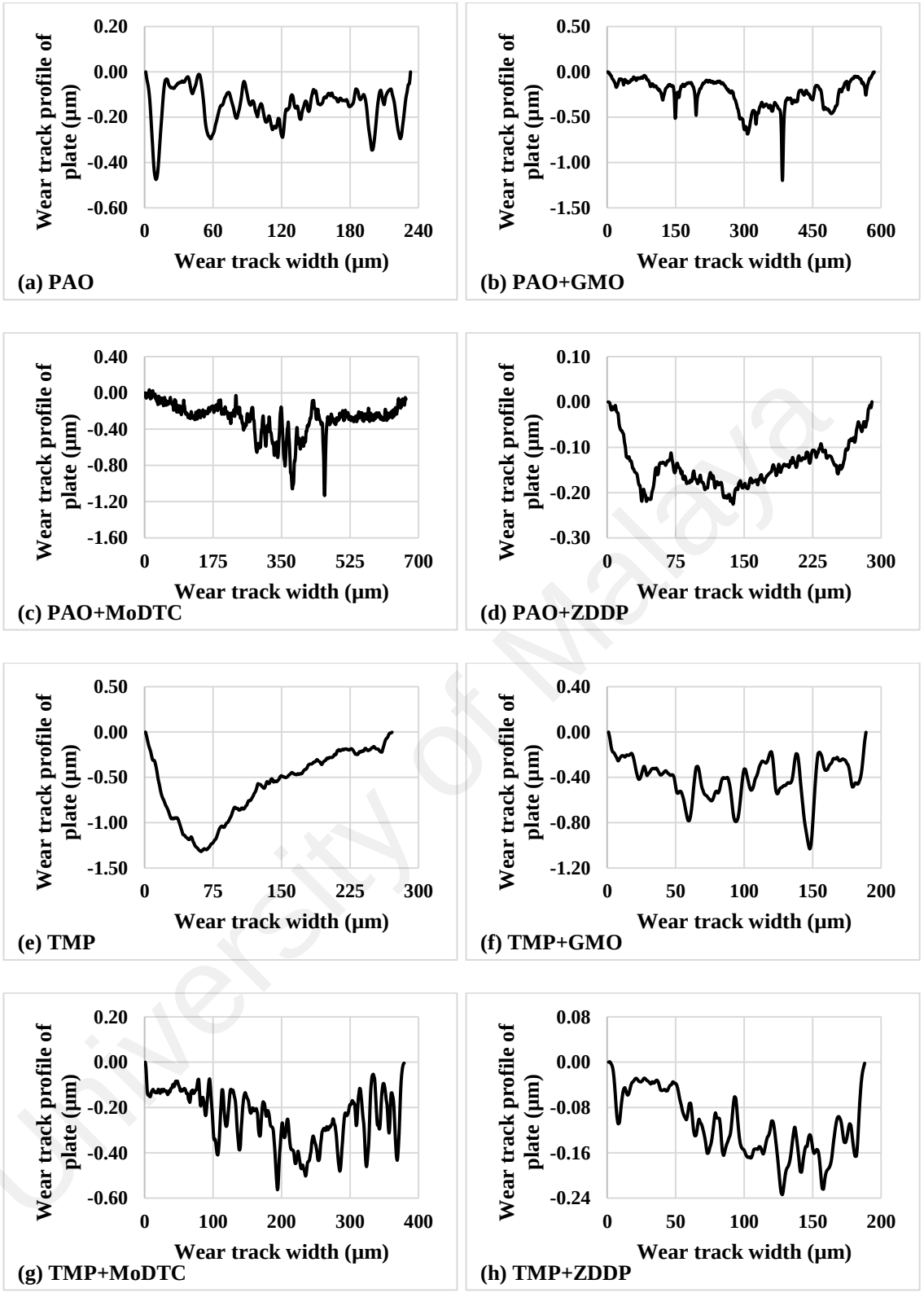

Figure 4.18: Wear track profiles of ta-C-coated plates after 2 hours of sliding against uncoated steel balls in the presence of PAO-based and TMP-based lubricants

4.4.5.4 a-C:H/a-C:H contact

Additive-free TMP proved to be most effective among TMP-based lubricants in protecting a-C:H-coated plate from deterioration and polishing wear was observed (**Figure 4.19e**). Contrary to that, delamination and formation of deep grooves as a result of abrasion were seen as predominant wear mechanisms when PAO was used as lubricant (**Figure 4.19a**). Although, accelerated wearing-out of interacting surfaces was seen with PAO compared to TMP as a result of severe surface deterioration but no effect of surface roughness values was seen on friction performance of a-C:H/a-C:H contact (**Figure 4.3**). Contrary to ta-C/ta-C and ta-C/steel contacts, increase in surface roughness was realized when formulated versions of TMP were used as lubricants but still values remained lower than most of the PAO-based lubricants. Similar to additive-free TMP, polishing was observed as predominant wear mechanism when PAO+GMO was used as lubricant and uniform wear depth was seen across the wear track width of a-C:H-coated plate. In wear track profiles of ZDDP-based lubricant, material removal was seen which can be attributed to either delamination of coating and/or plowing wear.

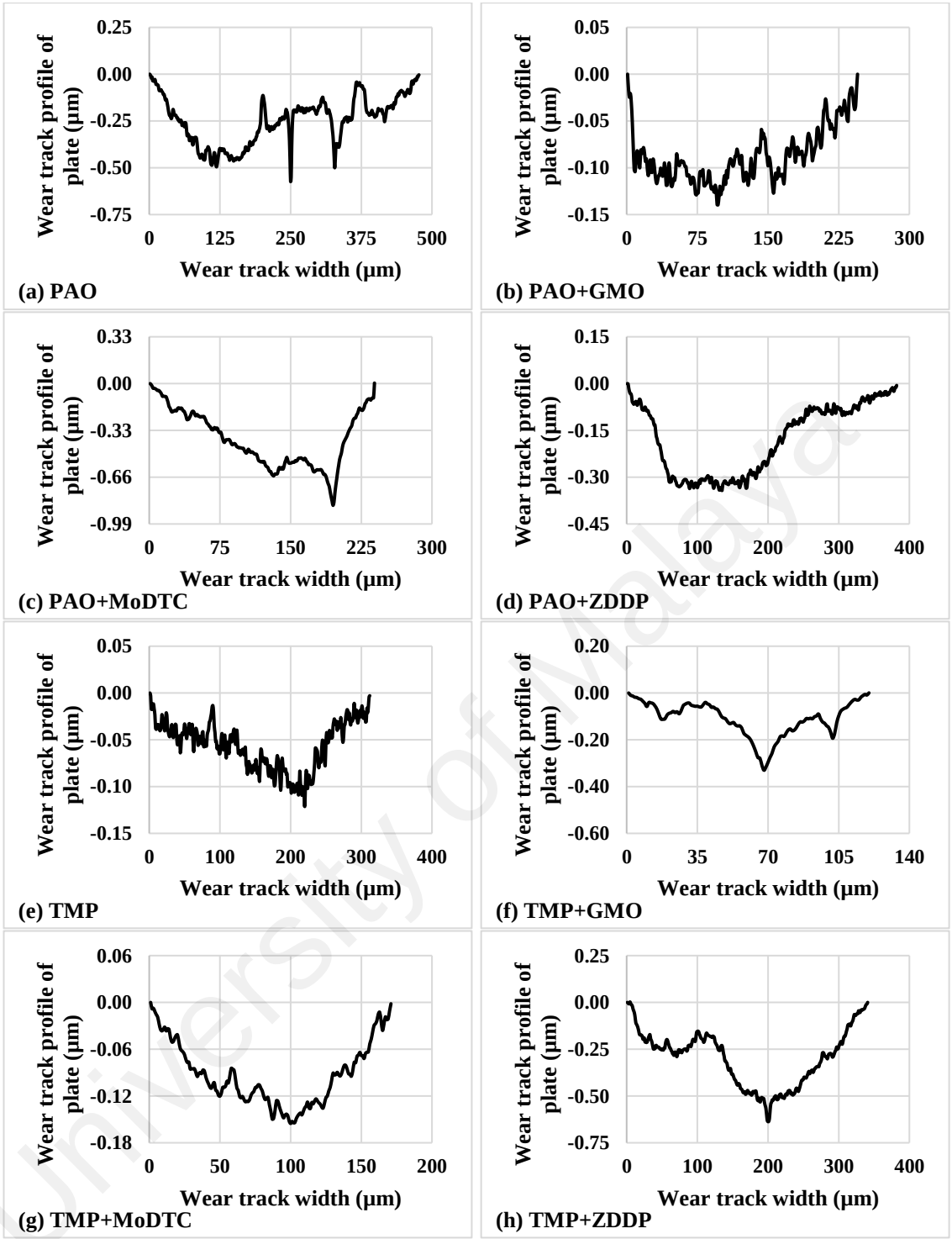

Figure 4.19: Wear track profiles of a-C:H-coated plates after 2 hours of sliding against a-C:H-coated balls in the presence of PAO-based and TMP-based lubricants

4.4.5.5 a-C:H/steel contact

Although, almost similar surface roughness values of a-C:H-coated plate were observed when additive-free PAO and TMP were used as lubricant separately but

significant difference in the wear track profiles can be seen (**Figure 4.20a** and **Figure 4.20e**). In case of PAO, delamination and plowing were witnessed as predominant wear mechanisms whereas abrasive wear occurred in the presence of TMP resulting in the formation of grooves especially in the middle of wear track width. GMO-based lubricants proved to be most effective in protecting the a-C:H-coated surface from roughening resulting in lowest surface roughness values (**Figure 4.23**). Shallow grooves due to abrasive wear were seen throughout the wear track width of a-C:H-coated plate when TMP+GMO was used as lubricant whereas polishing was witnessed as predominant wear mechanism with PAO+GMO with a deep groove of 0.37 μm depth due to abrasive action of wear debris. Among PAO-based lubricants, maximum surface deterioration was observed when PAO+MoDTC was used as lubricant whereas PAO+ZDDP resulted in lowest value. Uniform wearing-out of a-C:H-coated plate due to delamination/material removal was noticed in the presence of PAO+MoDTC whereas maximum wear was occurred in the centre of wear-track width with PAO+ZDDP.

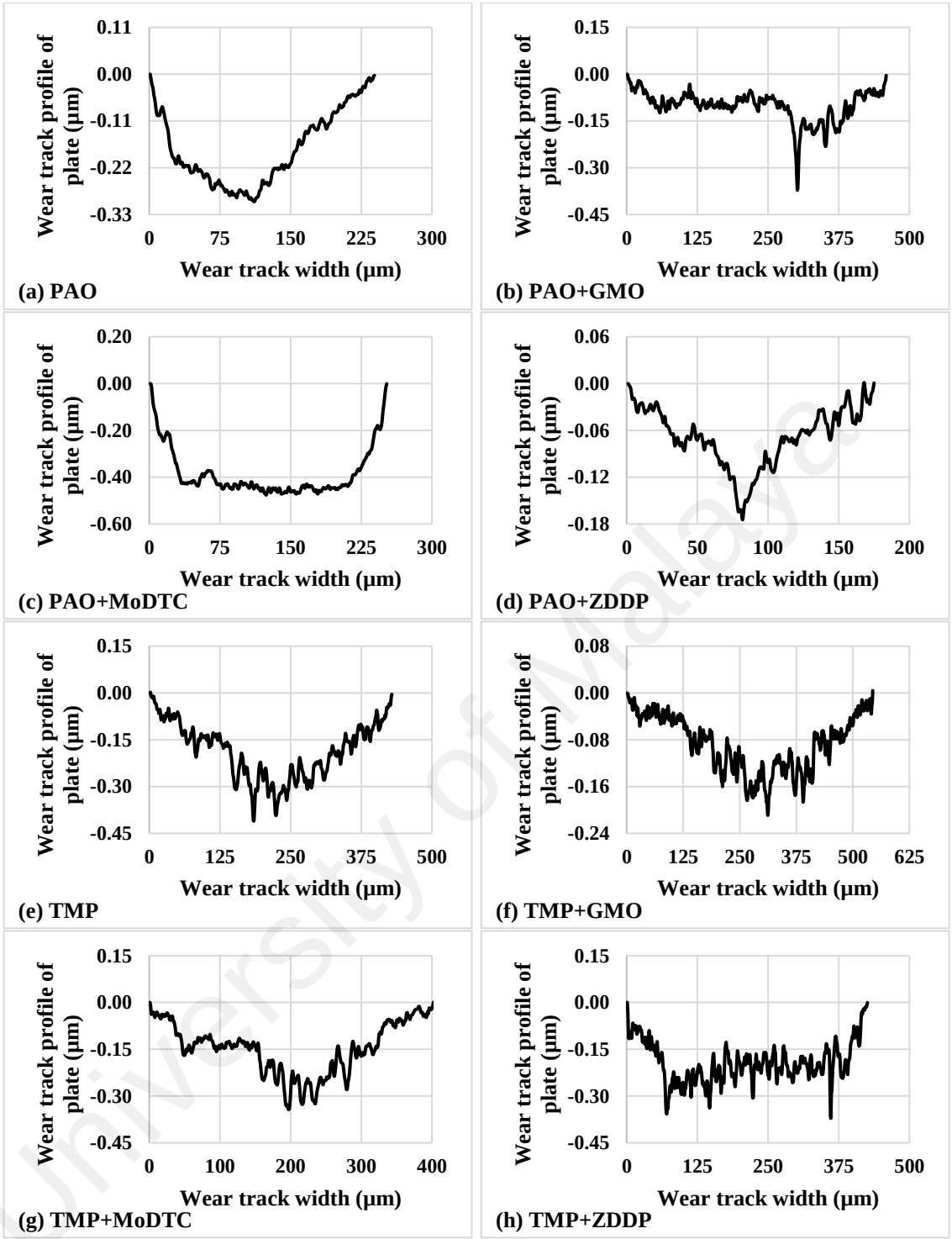

Figure 4.20: Wear track profiles of a-C:H-coated plates after 2 hours of sliding against uncoated steel balls in the presence of PAO-based and TMP-based lubricants

4.4.5.6 a-C:H:W/a-C:H:W contact

Similar to symmetrical a-C:H contact, significantly lower R_a value of a-C:H:W-coated plate was observed with additive-free TMP compared to PAO. As a result, three-times

more wear of a-C:H:W-coated plate was witnessed when PAO was used as lubricant instead of TMP (**Figure 4.5**). Formulated lubricants proved to be effective in protecting the plate surface from deterioration. Only exception to this finding was seen when PAO+MoDTC was used as lubricant resulting in highest surface roughness value among tested lubricants. Severe roughening of plate in the presence of PAO+MoDTC was also observed in ta-C/steel, a-C:H/a-C:H and a-C:H/steel contact (**Figure 4.23**). In case of PAO-based lubricant, coating spallation and plowing wear was observed as the main wear mechanism whereas TMP-based lubricant caused abrasive wear of a-C:H:W-coated plates which resulted in grooves formation throughout the wear track width. Maximum surface protection to a-C:H:W-coated plate was witnessed in the presence of TMP+ZDDP and polishing was observed as main wear mechanism with shallow scratch lines in the direction of sliding.

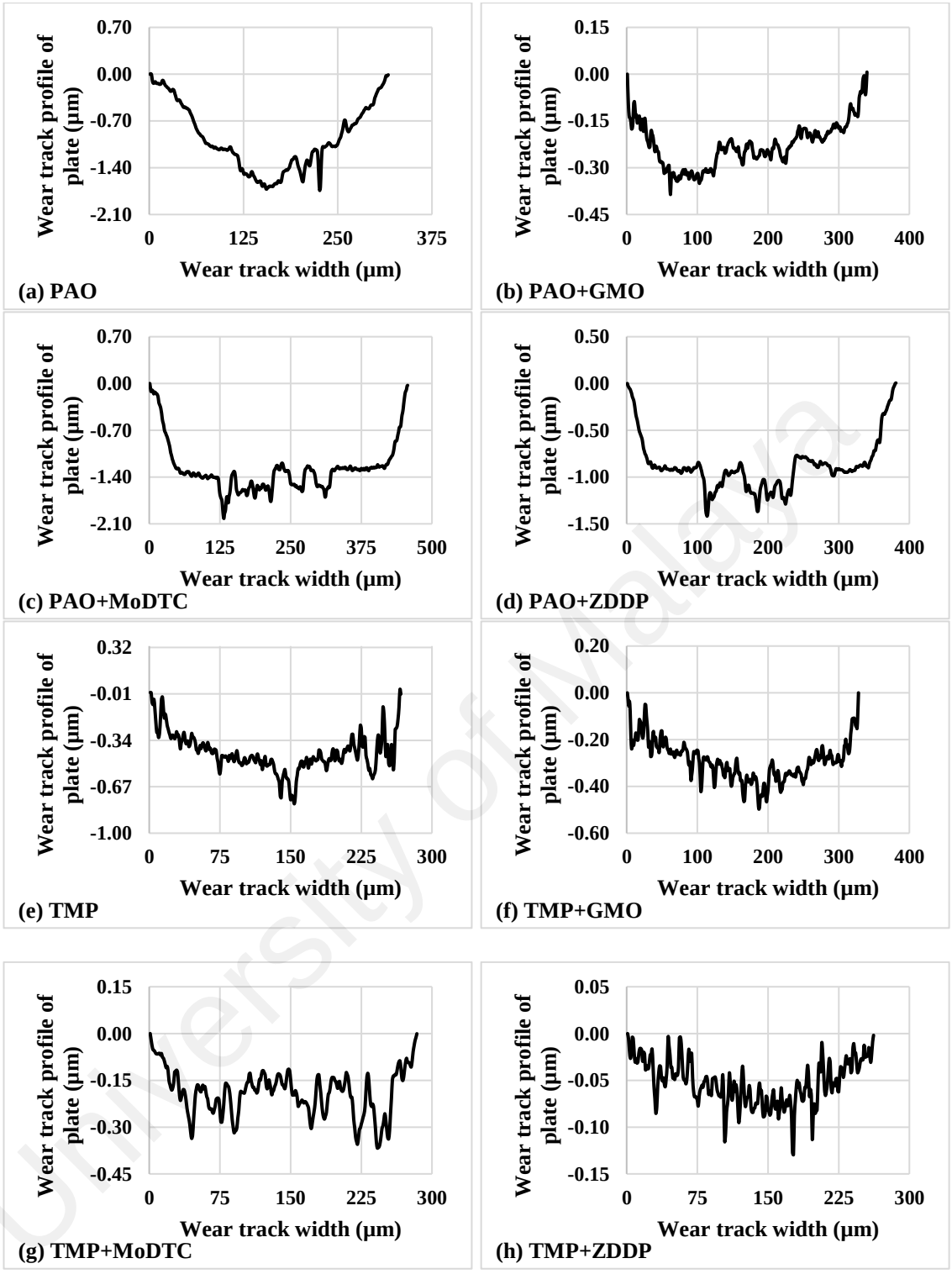

Figure 4.21: Wear track profiles of a-C:H:W-coated plates after 2 hours of sliding against a-C:H:W-coated balls in the presence of PAO-based and TMP-based lubricants

4.4.5.7 a-C:H:W/steel contact

Significant reduction in surface roughness value of a-C:H:W-coated plate was seen with additive-free PAO, when uncoated steel ball was used as counterbody instead of a-

C:H:W-coated one. However, insignificant change in the wear behaviour of TMP was observed. Abrasive wear, which resulted in the formation of grooves, was observed as main wear mechanism irrespective of lubricant formulation. Only exception to this finding was witnessed with PAO+GMO and instead of abrasion, polishing and plowing wear was seen as predominant modes of wear. It is interesting to note that maximum and minimum surface roughness values were observed when ZDDP-containing lubricants were used. Significant removal of coating material and very deep groove of around 1.70 μm at the wear track width of 30 μm can be seen in the wear track profile of PAO+ZDDP. On the other hand, only shallow scratch lines were seen when TMP+ZDDP was used as lubricant. Superior surface protection behaviour of TMP+ZDDP can be attributed to formation of ZDDP-derived tribofilm in higher concentration (**Table 4.11**) and lower extent of surface graphitization compared PAO+ZDDP.

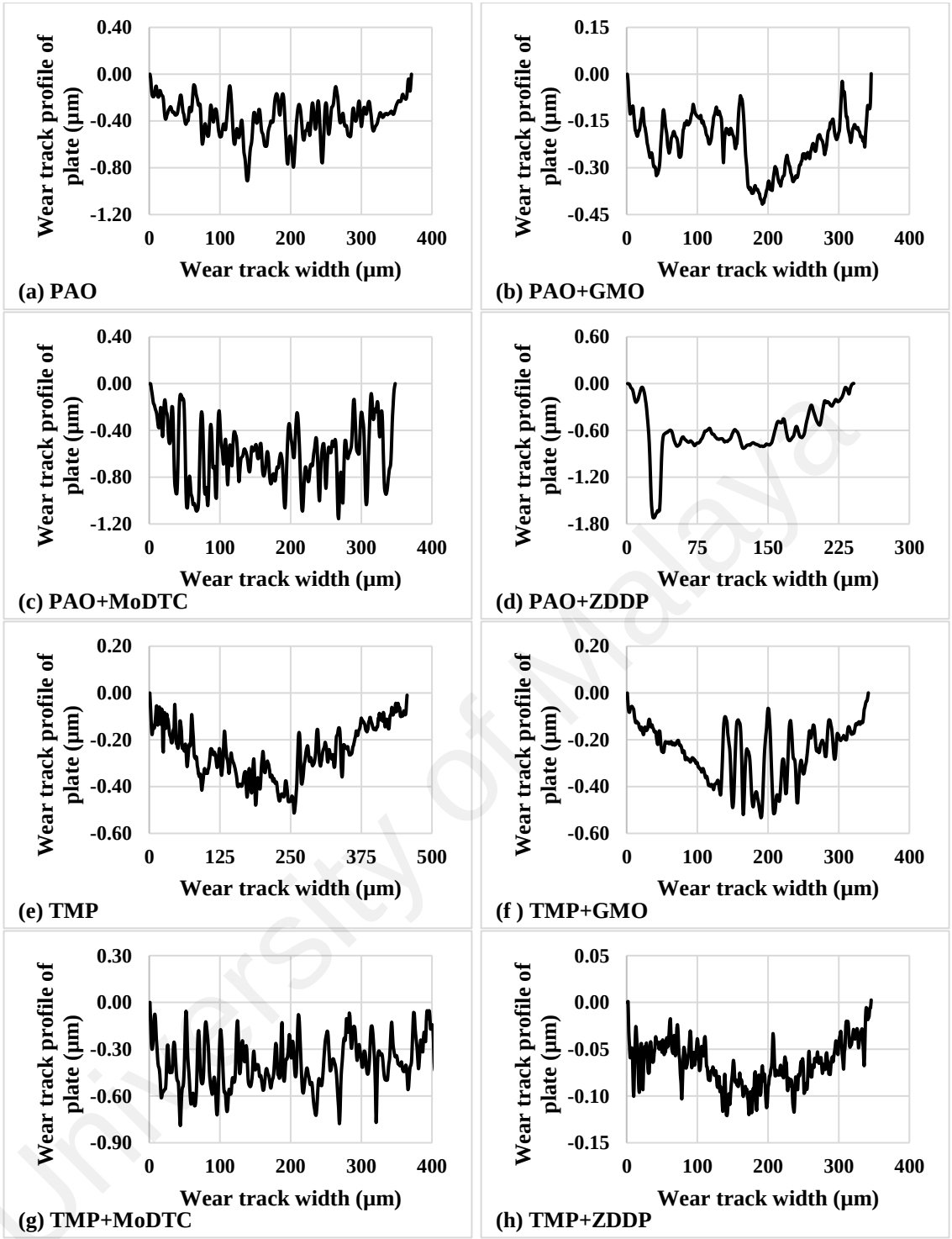

Figure 4.22: Wear track profiles of a-C:H:W-coated plates after 2 hours of sliding against uncoated steel balls in the presence of PAO-based and TMP-based lubricants

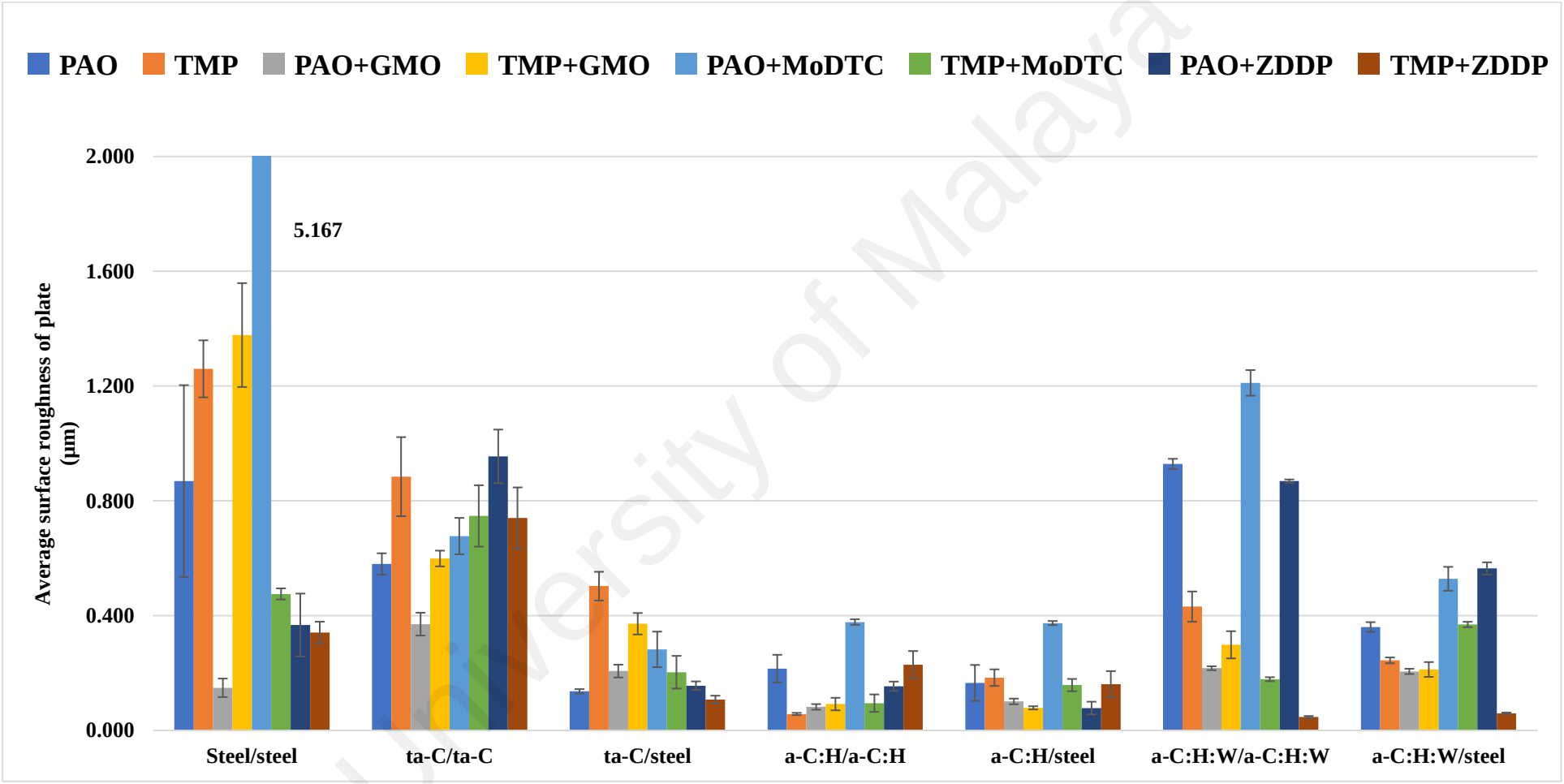

Figure 4.23: Average surface roughness of uncoated and DLC-coated plates of steel/steel, DLC/DLC and DLC/steel contacts in the presence of PAO-based and TMP-based lubricants

4.4.6 Summary

Significant improvement in friction characteristics was observed when DLC-coated surfaces were used and friction coefficients were reduced up to 45%. Additive-free TMP proved to be more effective in reducing friction of contact compared to PAO. An increase in coefficient of friction was observed when uncoated balls were used instead of DLC-coated ones as counterbodies against DLC-coated plates irrespective of their type. Lowest values of friction coefficients were observed with a-C:H/a-C:H and ta-C/ta-C contacts whereas steel/steel contacts resulted in highest values when single-additive containing lubricants were used as lubricant. In terms of friction, TMP+GMO was proved to be most effective lubricant whereas PAO+ZDDP appeared to be least effective in mitigating the wear.

Similar to friction results, an improvement in wear coefficient values of balls (up to 90%) were seen when DLC-coated surfaces were used instead of uncoated ones. Contrary to friction results, additive-free PAO appeared to be more effective in reducing wear of balls compared to PAO in most of the contacts. An increase in wear coefficient of balls was observed when uncoated balls were used instead of DLC-coated ones as counterbodies against DLC-coated plates irrespective of their type. Lowest values of wear coefficient of balls were observed with a-C:H/a-C:H contacts whereas a-C:H:W/steel contacts resulted in highest values when single-additive containing lubricants were used. In terms of wear of balls, TMP+ZDDP was proved to be most effective lubricant whereas additive-free TMP and TMP+MoDTC appeared to be least effective in mitigating the friction between ball and plate surface.

Contrary to friction and wear coefficient of balls, an increase in wear of DLC-coated plates was observed when DLC-coated balls were used against them against of uncoated steel balls irrespective of DLC type and lubricant formulation. Up to 90% reduction in

wear coefficient of plates was observed when DLC-coatings were deposited on them. Lowest values of wear coefficient of plates were observed with a-C:H/a-C:H contacts whereas steel/steel and ta-C/ta-C contacts resulted in highest values when single-additive containing lubricants were used. PAO+MoDTC appeared to be least effective in mitigating wear of uncoated and DLC-coated plates whereas PAO+GMO proved to be most effective lubricant.

Based on the above-mentioned observation, it can be concluded that conventional lubricant additives have tribological compatibility with TMP and various types of DLC coatings especially a-:C-H coating.

4.5 Tribotesting using universal wear testing machine with pin-on-plate geometric configuration in combination with multi-additive containing lubricants

4.5.1 Friction analysis

Transient friction behavior of steel/cast iron contact in the presence of PAO-based and TMP-based lubricants is shown in **Figure 4.24** whereas average friction coefficient values are presented in **Figure 4.25**.

4.5.1.1 Steel/cast iron contact

Among the base oils, TMP proved to be more effective in facilitating the sliding of uncoated cast iron pin on uncoated steel plate resulting in 10% reduction in friction coefficient value compared to PAO (**Figure 4.25**). At the start of the tribotesting, very low friction coefficient of steel/cast iron contact was observed when TMP was used as lubricant but after 6 minutes of sliding, an increase in friction was observed (**Figure 4.24a**). After 30 minutes of sliding, steady state coefficient of friction was achieved at the value of 0.131. Friction coefficient values were almost reduced to half when formulated lubricants were used instead of additive-free ones. Tribochemical interaction between

sliding surfaces and lubricant additives resulting in the formation of tribofilms can be attributed to this improvement in friction behavior which will be discussed further in **section 4.5.4**.

4.5.1.2 ta-C/ta-C contact

Significant difference in friction performance of ta-C/ta-C contact was observed in the presence of additive-free base oils (**Figure 4.24b** and **Figure 4.25**). TMP resulted in 37% less value of average friction coefficient compared to PAO. Although, ta-C coating is chemically unreactive compared to metallic surfaces but still polar components of TMP was able to interact with ta-C-coated surfaces and resulted in lower levels of friction between ta-C-coated surfaces. A friction reducing trend can be clearly seen in transient friction behavior of ta-C/ta-C contact in the presence of TMP right from the start of tribotest (**Figure 4.24b**). This trend continued till 30 minutes of sliding after which steady state friction level was achieved. Structural transformation of ta-C coating from diamond to graphite phase can be related to this behavior which will be discussed further in **section 4.5.3**. When GMO, MoDTC and ZDDP were used as additives in PAO in single formulation, an improvement in friction characteristics of ta-C/ta-C contact was observed and friction coefficient was reduced from 0.075 to 0.068. It is interesting to note that friction coefficient achieved with P+G+M+Z was still higher than that of additive-free TMP. Contrary to P+G+M+Z, additives were proved to be ineffective when mixed in TMP and deteriorated the friction performance of symmetrical ta-C contact. An eloquent increase of 64% in friction coefficient value was observed when formulated TMP was used instead of additive-free TMP. A possible justification for this behavior can be hindrance in the occurrence of graphitization phenomenon in the presence of lubricant additives which will be discussed further in **section 4.5.3**.

4.5.1.3 ta-C/cast iron contact

Similar to self-mated ta-C surfaces, additive-free TMP resulted in significantly lower friction coefficient value (0.034) of ta-C/cast iron contact compared to PAO (0.103) (**Figure 4.24c** and **Figure 4.25**). An increase in friction coefficient values was observed when uncoated cast iron pin was used as counterbody against ta-C-coated plate with most of the lubricant formulations. Only exception to this finding was seen when additive-free TMP was used as lubricant. Since, friction reducing mechanism of TMP is adsorbtion of its polar components on interacting surfaces therefore, presence of chemically reactive ferrous surface in the contact promoted the physisorption of lubricant molecules on the contact thus resulted in facilitated sliding. Formulation of PAO with additives resulted in improved friction performance and friction coefficient was reduced by almost 25%. This improvement can be attributed to tribochemical interaction between additives and interacting surfaces in the presence of PAO which facilitated the sliding and lower the friction level. Actual case of friction reduction will be discussed further in **section 4.5.3** and **section 4.5.4**. Contrary to that, deterioration in friction performance of ta-C/cast iron contact was seen when multi-additive containing TMP was used as lubricant and friction coefficient was increased from 0.034 to 0.100. Like stated before, hindrance of graphitization phenomenon and ineffectiveness of lubricant additives to interact with sliding surfaces in the presence of TMP can be possible reasons for this behavior. A similar deterioration in friction performance of ta-C/ta-C contact was also seen when T+G+M+Z was used as lubricant.

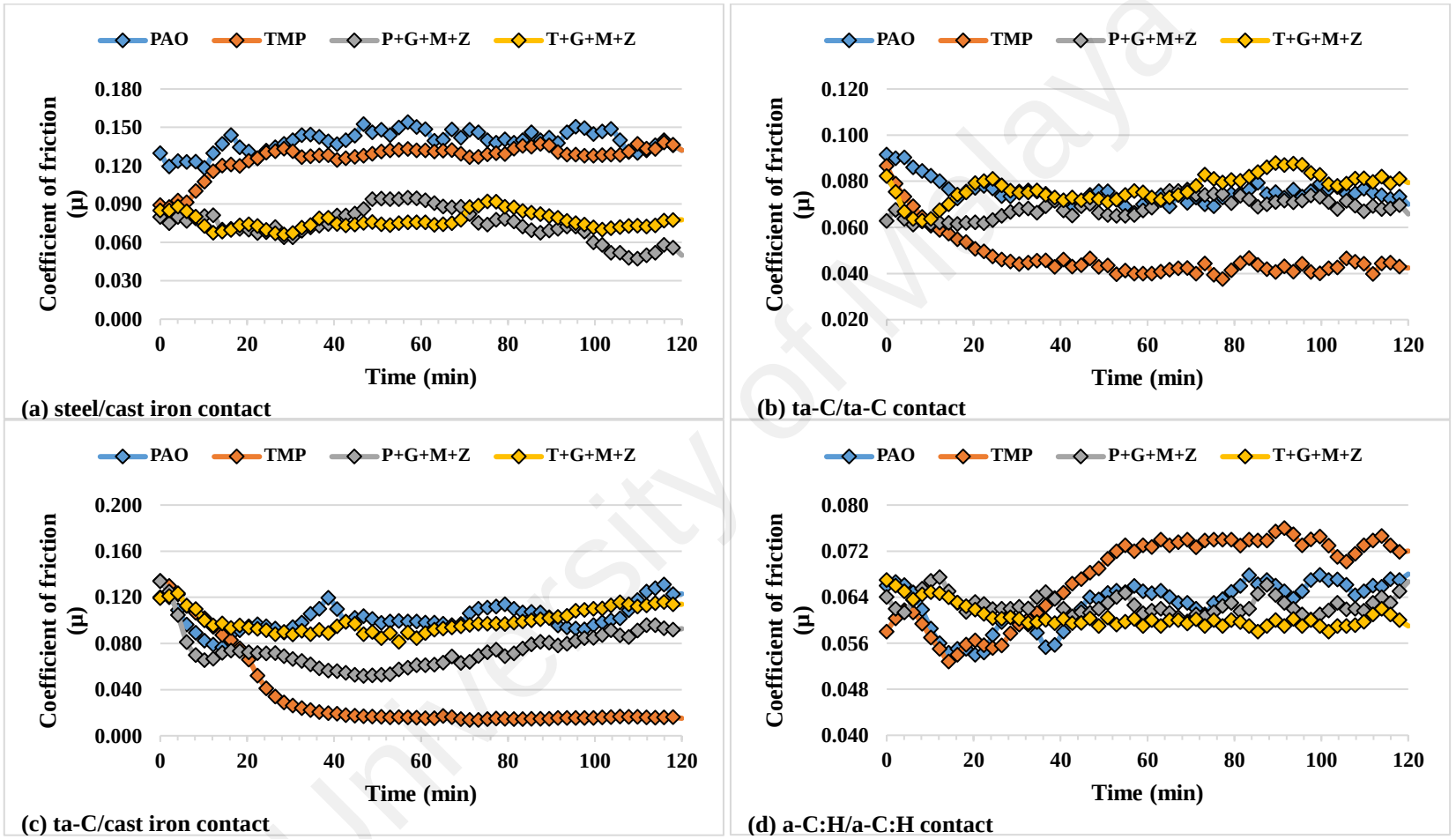

Figure 4.24: Transient friction behavior of steel/cast iron, DLC/DLC and DLC/cast iron contacts in the presence of PAO-based and TMP-based lubricants

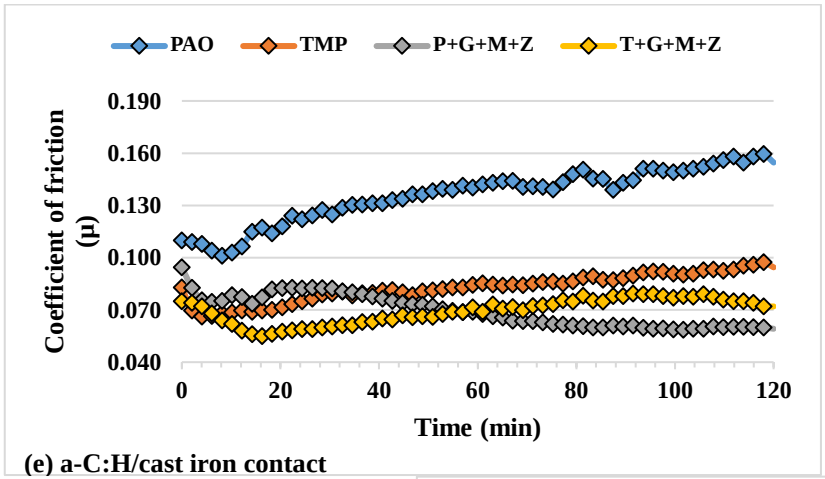

(e) a-C:H/cast iron contact

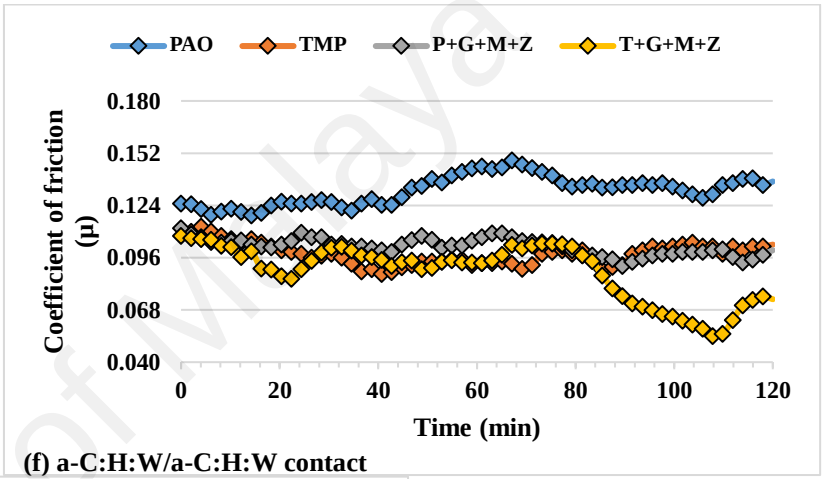

(f) a-C:H:W/a-C:H:W contact

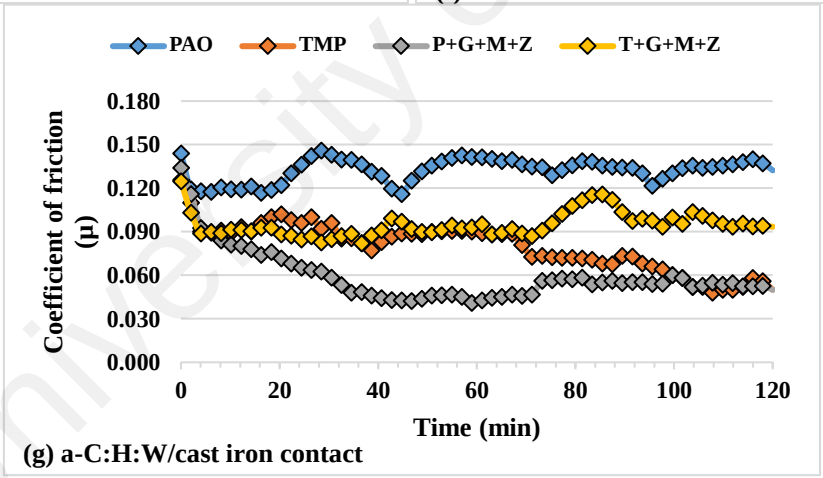

(g) a-C:H:W/cast iron contact

Figure 4.24 continued

4.5.1.4 a-C:H/a-C:H contact

Contrary to all other contacts considered in this study, a-C:H/a-C:H contact demonstrated better friction behavior in the presence of additive-free PAO and resulted in 8% lower friction coefficient value compared to TMP (**Figure 4.25**). At the start of the tribotest, TMP proved to be more effective in facilitating sliding compared to PAO but after 30 minutes of sliding, friction coefficient values were at the same level for both lubricants (**Figure 4.24d**). After that, deterioration in friction performance of a-C:H/a-C:H contact was seen especially in the presence of TMP. Only possible reason for this behavior can be inability of a-C:H-coated surfaces to graphitize at given test conditions. On comparing friction behavior of symmetrical a-C:H contact with those of others, it can be clearly seen that former resulted in lower friction coefficient values with most of the lubricant formulation. No change in friction performance of symmetrical a-C:H contacts was seen when P+G+M+Z was used as lubricant instead of additive-free PAO. Contrary to that, friction coefficient was reduced from 0.068 to 0.061 resulting in lowest friction coefficient value of self-mated a-C:H contact among all considered lubricants when TMP was used in combination with GMO, MoDTC and ZDDP. It is interesting to note that additives were proved to be more effective in PAO whereas severe deterioration in friction performance of ta-C/ta-C contact was seen when same additives were used with TMP. This observation shows that ta-C coating behaves differently from a-C:H coating as far as friction performance parameter is concerned.

4.5.1.5 a-C:H/cast iron contact

Deterioration in friction performance of the contact was witnessed when uncoated cast iron pin was used as counterbody instead of a-C:H-coated one against a-C:H plate, irrespective of lubricant formulation. However, friction coefficient values were still lower than those of steel/cast iron contact (**Figure 4.25**). Among the base oils, additive-free TMP proved to be more effective in facilitating the sliding and resulted in 40% lower

friction coefficient value compared to PAO. Significant improvement in friction performance of a-C:H/cast iron contact was witnessed when formulated lubricants were used instead of additive-free base oils. From transient friction behavior of a-C:H/cast iron contact in the presence of P+G+M+Z, it can be depicted that some tribochemical interaction took place between additives and sliding surfaces which resulted in reduced friction after 30 minutes of sliding (**Figure 4.24e**). Tribofilm formation as a result of tribochemical interaction will be discussed further in **section 4.5.4**. Although, friction coefficient of a-C:H/cast iron contact in combination with T+G+M+Z was significantly lower compared to P+G+M+Z at the start of tribotest and further reduction was seen till 15 minutes of sliding but after that friction coefficient value started to increase. This difference in friction behaviors of formulated lubricants will be investigated in **section 4.5.3** and **section 4.5.4**.

4.5.1.6 a-C:H:W/a-C:H:W contact

Deposition of a-C:H:W coating on uncoated steel and cast iron surfaces resulted in deteriorated friction characteristics of the contact especially when formulated lubricants were used (**Figure 4.25**). Like other contacts, additive-free TMP showed superior friction behavior compared to PAO due to its polar nature as a result of which it adsorbs on the interacting surface whereas no such behavior is associated with non-polar PAO. In **Figure 4.24f**, no significant improvement in friction behavior of the contact was seen during 2 hours of sliding with most of the lubricants and values either increased or remained at the same level. Only exception to this finding was witnessed when T+G+M+Z was used as lubricant and eloquent decrease in friction coefficient value was seen after 80 minutes of sliding resulting in lowest value among tested lubricant.

4.5.1.7 a-C:H:W/cast iron contact

Similar to a-C:H:W/a-C:H:W contact, TMP proved to be more effective in facilitating the sliding between a-C:H:W-coated plate and uncoated cast iron pin, resulting in 40% less friction coefficient value compared to that of PAO (**Figure 4.25**). On comparing friction coefficient values of a-C:H:W/a-C:H:W and a-C:H:W/cast iron contacts, it can be seen that presence of ferrous-counterbody further augment the friction characteristics of biodegradable base oil. Similar behavior was also seen when uncoated cast iron pin was used as counterbody instead of ta-C-coated one against ta-C-coated plate. Substantial improvement in friction behavior was observed when additive-containing PAO was used as lubricant and friction coefficient was reduced from 0.132 to 0.059. Contrary to that, deterioration in inherent friction characteristics of TMP was seen when additives were mixed with it. In **Figure 4.24g**, it can be seen that friction coefficient value of a-C:H:W/cast iron contact was decreased after 5 minutes of sliding in the presence of P+G+M+Z whereas no such behavior was witnessed with T+G+M+Z. This improvement in friction performance of P+G+M+Z can be attributed to either graphitization of a-C:H:W coating or tribochemical interaction of additives with interacting surfaces which will be discussed in **section 4.5.3** and **section 4.5.4.**

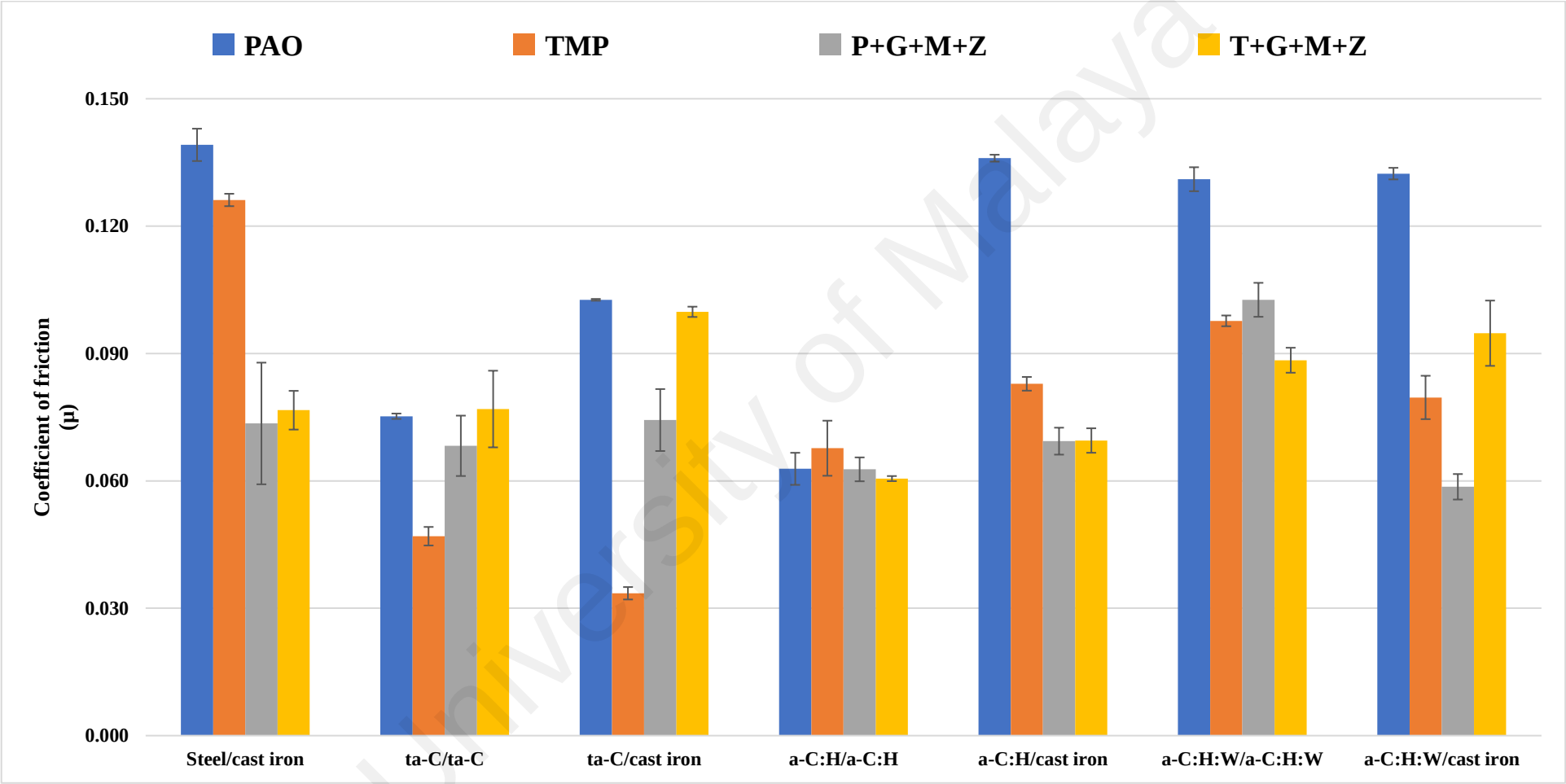

Figure 4.25: Average friction coefficient values of steel/cast iron, DLC/DLC and DLC/cast iron contacts in the presence of PAO-based and TMP-based lubricants

4.5.2 Wear analysis

Wear coefficient values of uncoated and DLC-coated pins and plates after 2 hours of sliding against each other in the presence of PAO-based and TMP-based lubricants are shown in **Figure 4.26** and **Figure 4.27** respectively.

4.5.2.1 Steel/steel contact

Accelerated wearing out of uncoated cast iron pins was observed compared to steel plates irrespective of lubricant formulation (**Figure 4.26** and **Figure 4.27)**. Similar to friction results, TMP proved to be more effective in mitigating the wear of steel plates compared to PAO whereas opposite trend was seen in wear behavior of cast iron pins. Eloquent decrease in wear coefficient of uncoated sliding surfaces was witnessed when formulated lubricants were used instead of additive-free base oils. Formation of additive-derived tribofilm as a result of tribochemical interacting between sliding surfaces and additives can be attributed to improved wear characteristics of steel/cast iron contact in the presence of P+G+M+Z and T+G+M+Z which will be further discussed in **section 4.5.4**.

4.5.2.2 ta-C/ta-C contact

Substantial increase in wear coefficient values was witnessed when ta-C-coated surfaces were used instead of uncoated ones irrespective of lubricant formulation. Similar wear behavior was also seen by Tasdemir, Wakayama, et al. (2013b) when they compared tribological performance of steel/steel, ta-C/ta-C and ta-C/steel contacts using additive-free and formulated versions of PAO as lubricants with pin-on-disc geometric configuration. Although, deterioration in wear resistance of both surfaces were observed but it was more aggravated in pin. Inability of ta-C-coating to sustain 2 hours of sliding was also seen in ball-on-plate geometric configuration (**Figure 4.4** and **Figure 4.5**). Since, no interlayer was used during deposition, therefore, lack of adhesion strength

between substrate and ta-C coating can be a possible reason for high wear coefficient values observed in symmetrical ta-C contacts. Another possible reason can be transformation of coating from diamond to graphite phase due to which it structural integrity was comprised and eventually it was peeled-off from the substrate during 2 hours of sliding. A significant reduction in wear coefficient values was observed when additive-containing lubricants were used irrespective of base oil type. Like steel/cast iron contacts, additives were proved to be more effective when mixed in TMP compared to PAO and wear coefficient of pin was reduced from 2.42 x 10^{-6} mm^3/Nm to 3.80 x 10^{-7} mm^3/Nm. Although, improvement in wear protection of ta-C-coated pin was also seen when P+G+M+Z was used as lubricant but not to the extent of T+G+M+Z. Compared to pins, plates proved to be wear-resistant irrespective of material combination and lubricant formulation. Contrary to wear coefficient of pins, additive-free TMP was able to provide better surface protection to ta-C-coated plates and resulted in wear coefficient value which was one-fourth compared to that of PAO. Although, additives were able to significantly reduce the wearing-out of ta-C-coated plates when used in combination with PAO but still the value was higher than that of additive-free TMP. When formulated version of TMP was used, further improvement in wear characteristics of ta-C-coated plates was observed resulting in lowest wear coefficient value among all the tested lubricants. On comparing wear coefficients of steel/cast iron contact with ta-C/ta-C contact, it can be seen that only additive-free TMP resulted in lower value of ta-C-coated plate compared to uncoated one whereas high wear rates of plates were observed with other lubricants.

4.5.2.3 ta-C/cast iron contact

Like ta-C/ta-C and steel/cast iron contacts, additive-free PAO outperformed TMP in providing wear protection to uncoated cast iron pin and resulted in 8% lower value of wear coefficient (**Figure 4.26**). When uncoated cast iron pins were used as counterbodies

instead of ta-C-coated pins against ta-C-coated plates, deterioration in wear performance was seen. A possible justification for this degradation can be the presence of hard wear debris, generated from ta-C-coated plate, between the sliding surfaces which acted as third-body and caused severe abrasion on uncoated cast iron pin surface. Although additives proved to be effective in mitigating the wearing-out of uncoated pins but still values were higher compared to those achieved with ta-C/ta-C in the presence of additive-free base oils. Similar to ta-C/ta-C contacts, additive-containing PAO was proved to be more effective compared to T+G+M+Z and was able to reduce the wear coefficient of pin from 6.58 x 10^{-6} mm^3/Nm to 3.45 x 10^{-6} mm^3/Nm. On the other hand, tremendous decrease in wear coefficient values of ta-C-coated plate was observed when ta-C-coated pins were replaced by uncoated cast iron pins (**Figure 4.27**). Not only this, wear coefficient of ta-C-coated plates were also comparatively lower than those of uncoated steel plates irrespective of lubricant formulation. The only exception to this finding was seen when T+G+M+Z was used as lubricant which resulted in highest value of wear coefficient of plate whereas lowest value was observed when additive-free TMP was used. Additives were proved to be effective in mitigating the wear of ta-C-coated plates when used in combination with PAO and resulted in approximately 36% decrease in wear coefficient value. Contrary to that, accelerated wearing-out of plates was observed when same additives were mixed in TMP and wear coefficient value was almost doubled. This observation shows that it is not necessary that additives which proved to be effective in one type of base oil will also show the same behavior in other base oils as well.

4.5.2.4 a-C:H/a-C:H contact

Compared to uncoated and ta-C-coated ones, a-C:H-coated surfaces proved to be more resilient against wear irrespective of lubricant formulation (**Figure 4.26** and **Figure 4.27**). Among the base oils, additive-free TMP outperformed PAO in providing surface protection to a-C:H-coated surfaces and prohibited them from wearing out at accelerated

rates. Further enhancement in wear resistance of a:C:H-coated pin and plate was observed when formulated PAO was used as lubricant resulting in substantial reduction in wear coefficient values. On the other hand, only slight reduction in wear coefficient of plate was witnessed when T+G+M+Z was used as lubricant instead of additive-free TMP. Contrary to that, deterioration in wear performance of a-C:H/a-C:H contact in terms of wear coefficient of pin was seen with formulated TMP but still value remained lower than those of steel/cast iron, ta-C/ta-C and ta-C/cast iron contacts.

4.5.2.5 a-C:H/cast iron contact

Although, a similar wearing trend was seen when a-C:H-coated pin was replaced by uncoated cast iron one as counterbody against a-C:H-coated plate but the magnitude of wear coefficient of pin was much higher compared to those of a-C:H/a-C:H contact with most of the considered lubricants (**Figure 4.26**). Similar to a-C:H/a-C:H contact, no improvement in wear behavior of uncoated cast iron pin was observed when formulated version of TMP was used as lubricant instead of additive-free TMP. Rather a slight increase in coefficient wear of pin was observed with T+G+M+Z compared to TMP. On the contrary, significant increase in wear resistance of pin was seen with additive-containing PAO resulting in lowest wear coefficient value of pin among a-C:H/cast iron contact. A similar behavior and lowest wear coefficient value was also seen in self-mated a-C:H contact with P+G+M+Z. Similar to wear behavior of pin, deterioration in wear performance of a-C:H-coated plates was also observed compared to a-C:H/a-C:H contact irrespective of lubricant formulation but wear coefficient values still remained lower than those of steel/cast iron contacts (**Figure 4.27**). Only exception to this finding was seen when additive-free TMP was used as lubricant plate of a-C:H/cast iron contact resulted in low wear coefficient value compared to symmetrical a-C:H contact.

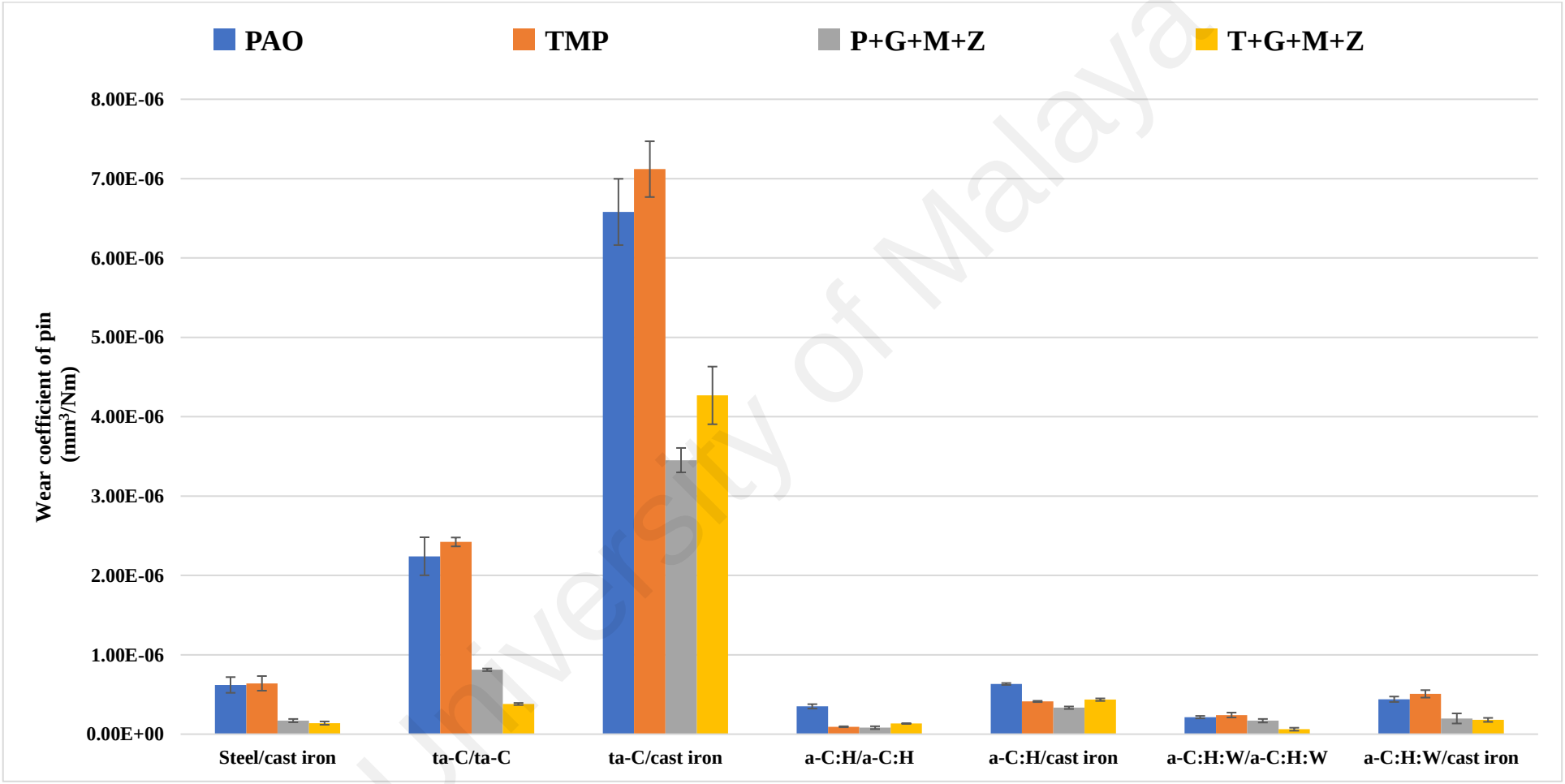

Figure 4.26: Wear coefficient values of uncoated and DLC-coated pins of steel/cast iron, DLC/DLC and DLC/cast iron contacts in the presence of PAO-based and TMP-based lubricants

4.5.2.6 a-C:H:W/a-C:H:W contact

Contrary to friction results, high wear coefficient values of interacting surfaces were observed with TMP compared to PAO (**Figure 4.25**, **Figure 4.26** and **Figure 4.27**). A possible reason for high wear coefficient values in the presence of TMP can be formation of organic acids due to the thermal decomposition of esters, which chemically attacked the interacting surfaces and formed soft oxide layer. This oxide layer possessed low shear strength due to which it facilitated the sliding between the interacting surfaces and resulted in low friction coefficients. However, it can be easily removed from the contact, due to its weak adhesion, by the scraping action of the counterbody and reformed by further chemical reaction resulting in accelerated wearing (N. H. Jayadas, Prabhakaran Nair, & G, 2007; Kržan & Vižintin, 2003). Another justification can be structural transformation of coating from diamond to graphite phase which will be discussed in **section4.5.3**. Mixing of base oils with additives substantially improved the wear resistance of interacting surfaces. Although, PAO also showed an increase in wear resistance of contact when formulated with GMO, MoDTC and ZDDP but not to an extent of TMP. Among the formulated lubricants, lowest wear coefficient values of a-C:H:W-coated pin and plate were observed with T+G+M+Z whereas TMP resulted in highest values.

4.5.2.7 a-C:H:W/cast iron contact

It is interesting to note that uncoated cast iron pins demonstrated different wear behavior compared to a-C:H:W-coated plates due to which difference in levels of wear coefficients of pins and plates can be clearly seen (**Figure 4.26** and **Figure 4.27**). Although same wear trend of interacting surfaces was observed but significantly high wear coefficients of uncoated cast iron pins were observed compared to a-C:H:W-coated plates irrespective of lubricant formulation. Similar to symmetrical a-C:H:W contact, high wear coefficient values of interacting surfaces were observed when additive-free

TMP was used as lubricant whereas T+G+M+Z resulted in lowest value. On comparing wear coefficients of symmetrical a-C:H:W contact with those of a-C:H:W/cast iron contact, it can be clearly seen that presence of ferrous counterbody deteriorated the wear resistance of the contact resulting in accelerated wearing-out of the interacting surfaces irrespective of lubricant formulation. High wear coefficient of a-C:H:W/cast iron contact compared to the symmetrical a-C:H:W contact can be related to strong affinity of carbon towards ferrous materials to form a covalent bond due to which material was transferred from a-C:H:W-coated plate and diffused into uncoated cast iron pin (Tasdemir, Wakayama, et al., 2013b). In an experimental investigation, Kalin et al. also observed excessive wearing of interacting surfaces in a-C:H:W/steel contact compared to a-C:H:W/a-C:H:W contact, when additive-free sunflower was used as lubricant (Kalin & Vižintin, 2006a).

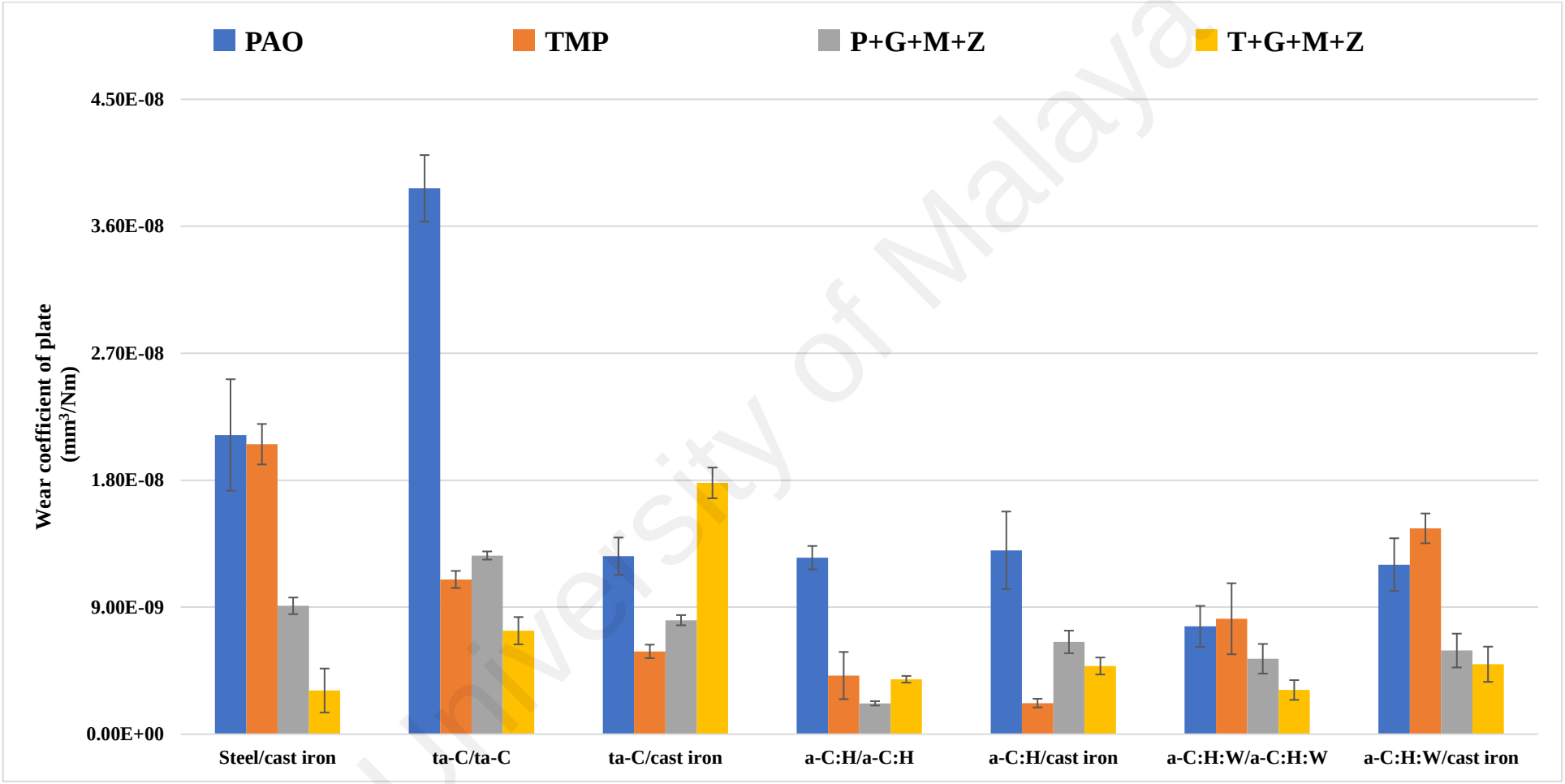

Figure 4.27: Wear coefficient values of uncoated and DLC-coated plates of steel/cast iron, DLC/DLC and DLC/cast iron contacts in the presence of PAO-based and TMP-based lubricants

4.5.3 Raman spectroscopy analysis

I_D/I_G ratio of DLC-coated plates after 2 hours of sliding against DLC-coated and uncoated steel balls are shown in **Table 4.12**.

Table 4.12: I_D/I_G ratio of DLC-coated plates after 2 hours of sliding against DLC-coated and uncoated cast iron pins

Lubricants	**ta-C/ ta-C (I_D/I_G) 0.754**	**ta-C/ steel (I_D/I_G) 0.754**	**a-C:H/ a-C:H (I_D/I_G) 0.767**	**a-C:H/ steel (I_D/I_G) 0.767**	**a-C:H:W/ a-C:H:W (I_D/I_G) 0.840**	**a-C:H:W/ steel (I_D/I_G) 0.840**
TMP	0.854	0.826	0.777	0.776	0.778	0.752
PAO	Delamination	0.802	0.803	0.727	0.777	Delamination
T+G+M+Z	0.759	0.716	0.723	0.726	0.891	0.792
P+G+M+Z	0.717	0.835	0.706	0.697	0.869	0.933

4.5.3.1 ta-C/ta-C contact

A clear difference can be seen in the Raman spectrum of PAO from the rest of the spectra (**Appendix Figure B-1**). This change in shape can be attributed to the delamination of ta-C coating from plate resulting in the influence of steel substrate on Raman spectrum. This hypothesis is also in accordance with the wear results which showed accelerated wearing out of ta-C-coated plate when additive-free PAO was used compared to other lubricants. When PAO was formulated with GMO, MoDTC and ZDDP, a significant improvement in wear resistance of ta-C-coated plate was seen and total delamination of coating was avoided. Not only this, wear coefficient of plate was reduced by 67% compared to that of additive-free TMP. Although, graphitization was not occurred when P+G+M+Z was used as lubricant but still 9% reduction in friction coefficient value was seen compared to that of PAO. Highest extent of graphitization was seen when additive-free TMP was used as lubricant and I_D/I_G ratio was increased from

0.754 (as-deposited ta-C coating) to 0.854 (**Table 4.12**). As a result, 38% reduction in friction coefficient value of ta-C/ta-C contact was realized when TMP was used as lubricant instead of PAO. Transient friction behavior of symmetrical ta-C contact showed a decreasing trend in friction coefficient value in the presence of TMP right from the start of tribotesting till 30 minutes, after which, steady state coefficient of friction at the level 0.04 was achieved (**Figure 4.24b**). This improvement in friction behavior can be attributed to formation of soft graphitic layer, as a result of structural transformation of ta-C coating from diamond to graphite phase, which facilitated the sliding of interacting surfaces. Hindrance in occurrence of graphitization phenomenon was seen when formulated version of TMP was used as lubricant. As a result, 64% increase in friction coefficient was realized compared to additive-free TMP. This observation shows that the main mechanism behind low friction coefficient of ta-C/ta-C contact was structural transformation of DLC coating. On the other hand, prevention of graphitization resulted in improved in wear resistance of ta-C/ta-C contact and significant decrease in wear coefficient values of interacting surfaces, especially ta-C-coated pin, was realized when T+G+M+Z was used as lubricant instead of additive-free TMP.

4.5.3.2 ta-C/cast iron contact

Occurrence of graphitization phenomenon and increase in I_D/I_G ratio of ta-C-coated plates were observed with most of the lubricant formulations (**Table 4.12**). The only exception to this finding was seen when T+G+M+Z was used as lubricant. It is interesting to that additives were able to prevent the structural transformation of ta-C coating from diamond to graphite phase when mixed with TMP but no such behavior was observed with P+G+M+Z. Rather I_D/I_G ratio was increased to 0.835 instead of 0.802 from 0.754 (as-deposited ta-C coating). Although, occurrence of graphitization phenomenon was more pronounced when TMP was used as lubricant compared to PAO but still former was able to protect ta-C-coated plate from wearing-out more efficiently compared to latter.

Not only this, 67% less friction was seen between interacting surfaces when TMP was used as lubricant compared to PAO (**Figure 4.25**). Similar to ta-C/ta-C contacts, eloquent increase in friction coefficient value of ta-C/cast iron was also seen when formulated version of TMP was used instead of additive-free TMP due to hindrance in the occurrence of graphitization phenomenon. Contrary to that, improvement in tribological performance of ta-C/cast iron contact was seen in combination with additive-containing PAO compared to additive-free PAO due to increase in I_D/I_G ratio.

4.5.3.3 a-C:H/a-C:H contact

Occurrence of graphitization phenomenon and increase in I_D/I_G ratio of a-C:H-coated plates was observed compared to as-deposited values of 0.767 when additive-free lubricants were used (**Table 4.12**, **Figure 4.7** and **Appendix Figure B-3**). Highest extent of graphitization was seen when PAO was used as lubricant resulting in lowest friction coefficient value of a-C:H/a-C:H contact. On the other hand, adverse effects of graphitization on the wear resistance of a-C:H-coated plates was seen in the presence of PAO resulting in three-times more wear of plate compared to that of additive-free TMP (**Figure 4.27**). Although, suppression in graphitization was seen when formulated TMP was used but still improvement in friction behavior of a-C:H/a-C:H contact was observed. This improvement in friction performance can be attributed to formation of additive-derived tribofilm which will be discussed in **section 4.5.4**. Hindrance in graphitization substantially improved the wear performance of the contact resulting in eloquent decrease in wear coefficient values when P+G+M+Z was used as lubricant instead of additive-free PAO (**Figure 4.26** and **Figure 4.27**). Although, graphitization suppression was also observed in the presence of T+G+M+Z but no improvement in wear behavior of interacting surfaces was seen. This behavior can be attributed to delamination of top a-C:H-coating from the pin surface and exposure of CrN interlayer due to which contact was changed from a-C:H/a-C:H to a-C:H/CrN.

4.5.3.4 a-C:H/cast iron contact

With most of the lubricants, graphitization of a-C:H-coated plates was not observed in Raman spectra (**Appendix Figure B-4**). The only exception to this finding was seen when additive-free TMP was used as lubricant and value of I_D/I_G ratio was increased from 0.767 to 0.0776 (**Table 4.12**). Although, structural transformation of a-C:H coating from diamond to graphite phase was seen in a-C:H/a-C:H contact when PAO was used as lubricant but no such behavior was seen with uncoated cast iron pins. As a result, 39% increase in friction coefficient value was seen when PAO was used as lubricant compared to TMP (**Figure 4.25**). Although, suppression in graphitization was seen when formulated version of TMP was used instead of additive-free one but still improvement in friction behavior of a-C:H/cast iron contact was observed. Tribochemical interaction of additives with interacting surfaces resulting in the formation of low-shear strength tribofilm can be a possible justification for improvement in friction behavior. Further details about composition of tribofilm will be discussed in **section 4.5.4**. A similar improvement in friction behavior was also seen with P+G+M+Z due to the formation of additive-derived tribofilm and friction coefficient was reduced by almost 50%. Not only this, wear coefficient values were also reduced to an appreciable extent when P+G+M+Z was used as lubricant instead of additive-free PAO. This variation in wear behavior of P+G+M+Z and T+G+M+Z will be further investigated in **section 4.5.4**. On the other hand, deterioration in wear performance of the contact was observed resulting in eloquent increase in wear coefficient values when T+G+M+Z was used as lubricant (**Figure 4.26** and **Figure 4.27**).

4.5.3.5 a-C:H:W/a-C:H:W contact

An increase in I_D/I_G ratio and occurrence of graphitization phenomenon was observed when formulated lubricants were used irrespective of base oil type (**Table 4.12**, **Appendix Figure B-5**). As a result, lowest friction coefficients were observed when

P+G+M+Z and T+G+M+Z were used as lubricants. In case of symmetrical DLC contacts, graphitization is not the only cause of friction reduction. Tribochemical interaction between lubricant additives and sliding surfaces also plays a vital role in determining tribological characteristics. When additive-free base oils were used, a decrease in I_D/I_G ratio and change in shape of Raman spectra was observed. This can be attributed to the delamination of top a-C:H:W layer from plate resulting in influence of exposed CrN interlayer or steel substrate on Raman spectra. This hypothesis is also in accordance with the wear results which showed accelerated wearing out of interacting surfaces when additive-free PAO and TMP base oils were used (**Figure 4.26** and **Figure 4.27**).

4.5.3.6 a-C:H:W/cast iron contact

When uncoated cast iron pins were used as counterbodies instead of a-C:H:W-coated ones, against a-C:H:W-coated plates, suppression in occurrence of graphitization was observed with most of the lubricants (**Table 4.12**, **Appendix Figure B-6**). The only exception to this finding was P+G+M+Z which showed highest level of graphitization resulting in substantial reduction in friction coefficient values compared to additive-free PAO (**Figure 4.25**). When additive-free base oils were used, a decrease in I_D/I_G ratio and change in shape of Raman spectra was observed. This can be attributed to the delamination of top a-C:H:W layer from plate resulting in influence of exposed CrN interlayer or steel substrate on Raman spectra. This hypothesis is also in accordance with the wear results which showed accelerated wearing out of interacting surfaces when additive-free PAO and TMP base oils were used.

4.5.4 SEM/EDS analysis

4.5.4.1 Steel/cast iron contact

When additive-free lubricants were used, severe cracks, wear debris, deep grooves and structural disintegration was observed on pin surface which resulted in extremely high

wear coefficients (**Figure 4.28a** and **Figure 4.28b)**. No such behavior was observed when formulated lubricants were used irrespective of base oil type (**Figure 4.28c** and **Figure 4.28d**). Additives not only decrease the wear coefficient of pins substantially but also resulted in relatively clean and unaltered surface after 2 hours of sliding (**Figure 4.26**). When P+G+M+Z was used as lubricant, only few deep scratch lines were observed on the pin surface accompanied by additive-derived tribofilm and shallow cracks. Formulated version of TMP was proved to be most effective in protecting the pin surface and no signs of surface deterioration was detected. This improved wear performance can be attributed to the formation of tribochemical film mostly composed of zinc compounds. In EDS results, higher concentration of oxygen was observed on cast iron pin irrespective of lubricant used (**Table 4.13**). These higher concentrations of oxygen can be associated with the formation of FeO, Fe_2O_3 and Fe_3O_4 which play an important role in the development of additive-derived tribofilm on the contact area (Quinn, Sullivan, & Rowson, 1984; Zulkifli, Kalam, Masjuki, Shahabuddin, & Yunus, 2013). As these oxide layers can be easily removed from the interacting surfaces during sliding therefore, higher wear coefficient of pin was observed when additive-free base oils were used. Another justification for higher concentration of oxygen in case of steel/cast iron contact especially in the presence of formulated lubricants is the adsorption of hydroxyl group from GMO and formation of highly viscous layer which not only prevents surface asperities from coming into direct contact with each other and reduces wear but also facilitates sliding. Presence of molybdenum, sulfur, phosphorus and zinc in EDS analysis of formulated lubricants shows MoDTC and ZDDP-derived tribofilm were also form on pin surface in addition to GMO-based tribofilm. As a result, significant improvement in tribological performance was witnessed in the presence of formulated lubricants (**Figure 4.25**, **Figure 4.26** and **Figure 4.27**)

Table 4.13: Atomic percentage of elements found on uncoated cast iron pins after 2 hours of sliding against uncoated steel plates in the presence of PAO-based and TMP-based lubricants

Lubricants	Elements						
	C	**P**	**S**	**Mo**	**Zn**	**Fe**	**O**
PAO	20.6	-	-	-	-	53.1	26.3
TMP	29.5	-	-	-	-	58.2	12.3
P+G+M+Z	18.2	0.4	0.7	4.3	1 4	58.5	17.9
T+G+M+Z	21.8	0.2	0.9	1.3	1.3	52.9	21.6

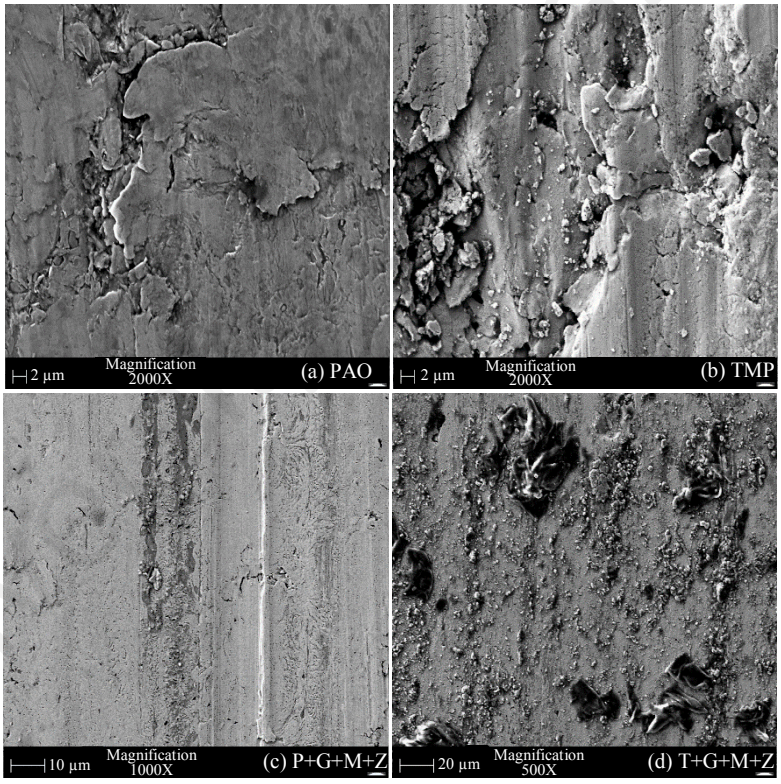

Figure 4.28: SEM micrographs of uncoated cast iron pins after 2 hours of sliding against uncoated steel plates in the presence of PAO-based and TMP-based lubricants

4.5.4.2 ta-C/ta-C contact

Delamination of ta-C-coating from the ball surface resulting in the exposure of ferrous substrate was observed in the presence of additive-free base oils. Some of the coating material transferred to the pin surface from ta-C-coated plate can be seen in micrograph

of PAO (**Figure 4.29a**). As a result, highest wear coefficient of plate was realized with PAO which was almost four times higher than TMP (**Figure 4.27**). In addition to delamination, abrasive wear resulting in shallow scratch lines in the direction of sliding and pitting wear were other wear mechanism seen in the micrographs of ta-C-coated pins. A significant improvement in the structural integrity of DLC coating was seen when formulated lubricants were used and presence of iron in EDS results was decreased from 27.2% and 20.6% of PAO and TMP to 14.7% and 9.8% (P+G+M+Z and T+G+M+Z) respectively (**Table 4.14**). Although, molybdenum, sulfur, phosphorus and zinc were detected in the EDS results of T+G+M+Z but instead of decrease, an increase in friction coefficient value of ta-C/ta-C contact was observed (**Figure 4.25**). It is believed that, ultra-low value of friction coefficient achieved with TMP was due to the graphitization of DLC coating which was also confirmed by Raman spectroscopy. Presence of additives in T+G+M+Z hindered the occurrence of graphitization phenomenon due to which deterioration in friction performance was seen. On the other hand, suppression of graphitization and formation of additive-derived tribofilm substantially augmented the wear performance of contact. As a result, lowest wear coefficient values of interacting surfaces were observed when T+G+M+Z was used as lubricant (**Figure 4.26** and **Figure 4.27**).

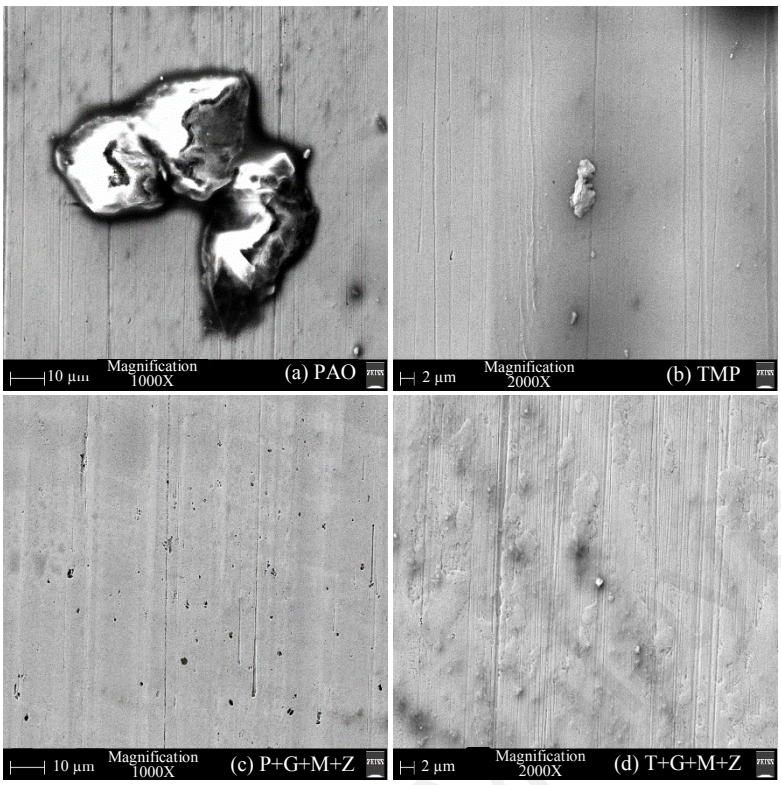

Figure 4.29: SEM micrographs of ta-C-coated pins after 2 hours of sliding against ta-C-coated plates in the presence of PAO-based and TMP-based lubricants

Table 4.14: Atomic percentage of elements found on ta-C-coated pins after 2 hours of sliding against ta-C-coated plates in the presence of PAO-based and TMP-based lubricants

Lubricants	Elements						
	C	**P**	**S**	**Mo**	**Zn**	**Fe**	**O**
PAO	66.9	-	-	-	-	27.2	5.9
TMP	62.9	-	-	-	-	20.6	16.5
P+G+M+Z	73.7	-	-	-	-	14.7	11.6
T+G+M+Z	57.4	13.4	1.2	1.1	2.9	9.8	14.2

4.5.4.3 ta-C/cast iron contact

Scratch lines can be clearly seen in the SEM micrograph of PAO (**Figure 4.30a**). Other wear mechanisms which were observed include pitting wear, formation of groves and

material removal due to adhesion. Although, deep scratch lines were also observed in the micrograph of TMP but predominant wear mechanism was brittle fracture which resulted in the formation of plentiful cracks and crevices (**Figure 4.30b**). Pin surface remained relatively clean and unaltered when formulated lubricants were used instead of additive-free base oils (**Figure 4.30c** and **Figure 4.30d**). As a result, significant improvement in wear resistance of uncoated cast iron pin were observed and wear coefficient values were reduced to almost half (**Figure 4.26**). Formation of ZDDP-derived tribofilm composed of zinc, phosphorus and sulfur can be a possible justification for improved wear behavior (**Table 4.15**). Transfer of carbon coating from ta-C-coated plate to uncoated cast iron pin can be seen in the micrograph of T+G+M+Z (**Figure 4.30d**). As a result, highest wear coefficient of plate was observed when T+G+M+Z was used as lubricant which was almost three-times higher than that of additive-free TMP (**Figure 4.27**). Similar to friction results of ta-C/ta-C contact, presence of additives deteriorated the inherent friction characteristics of TMP resulting in substantial increase in friction coefficient value of ta-C/cast iron contact (**Figure 4.25**). Like stated earlier, hindrance in graphitization phenomenon due to the presence of additives can be a possible justification for this behavior. On the other hand, P+G+M+Z reduced friction coefficient of ta-C/cast iron contact by 28% compared to additive-free PAO. This improvement in friction performance can be attributed to tribochemical decomposition of MoDTC into MoS_2 and MoO_3 during sliding.

Table 4.15: Atomic percentage of elements found on uncoated cast iron pins after 2 hours of sliding against ta-C-coated plates in the presence of PAO-based and TMP-based lubricants

Lubricants	Elements							
	C	**P**	**S**	**Mo**	**Zn**	**Fe**	**O**	**Si**
PAO	23.7	-	-	-	-	56.9	14.7	4.7
TMP	24.5	-	-	-	-	68.7	4.5	2.3
P+G+M+Z	18.8	2.6	2.6	3.5	4.3	57.5	7.1	3.6
T+G+M+Z	22.8	1.9	1.6	1.2	3.3	55.4	11.6	2.2

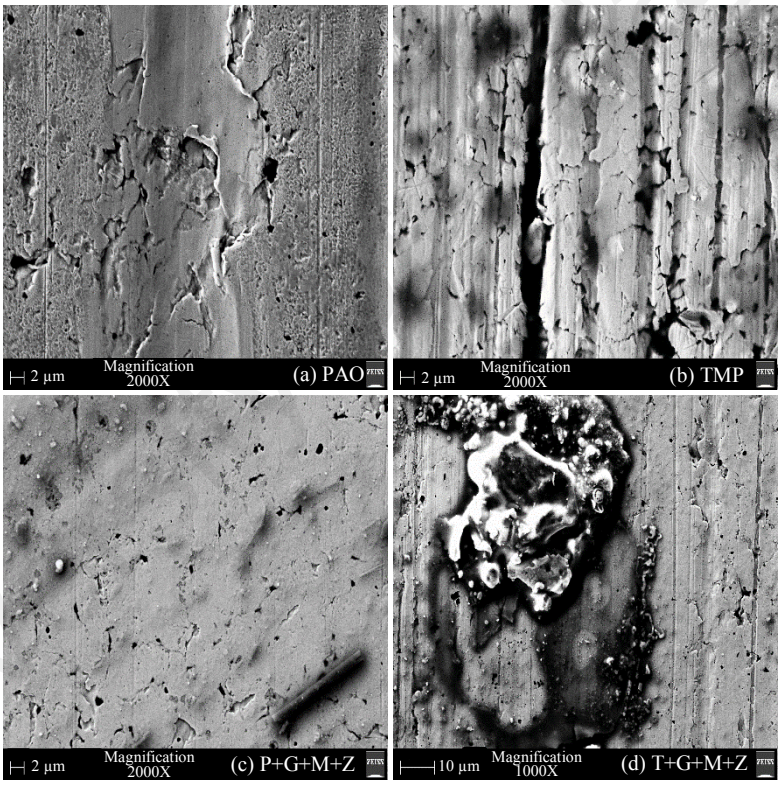

Figure 4.30: SEM micrographs of uncoated cast iron pins after 2 hours of sliding against ta-C-coated plates in the presence of PAO-based and TMP-based lubricants

4.5.4.4 a-C:H/a-C:H contact

In the SEM micrograph of PAO, delamination of top a-C:H coating resulting in exposure of CrN interlayer and ferrous substrate can be seen along with the scratch lines (**Figure 4.31**). As a result of this delamination, highest wear coefficients of a-C:H-coated

surfaces were realized when PAO was used as lubricant (**Figure 4.26** and **Figure 4.27**). Graphitization of a-C:H coating can be a possible justification for its delamination and accelerated wearing which was also confirmed by Raman spectroscopy. Decrease in friction coefficient value observed during 15 minutes of sliding can also be related to graphitization (**Figure 4.24d**). Since, graphite layers are soft and can be easily removed from the contact during sliding, therefore, increase in friction coefficient value during sliding after 60 minutes of sliding can be attributed to removal of graphite layer. Although, partial delamination of a-C:H coating and exposure of CrN interlayer was also occurred with additive-free TMP but not to the extent of PAO and no signs of ferrous substrate was seen in EDS results (**Table 4.16**). Other wear mechanisms which were seen in the micrograph of TMP include abrasive wear which resulted in the formation of deep scratch lines and pits. Significant improvement in wear behavior of symmetrical a-C:H contact was seen when P+G+M+Z was used as lubricant instead of PAO (**Figure 4.26** and **Figure 4.27**). This can be attributed to hindrance in graphitization phenomenon due to the presence of additives which was also confirmed by Raman spectroscopy. Another possible reason can be tribochemical interaction of additives with sliding surfaces resulting in the formation of tribofilm composed of molybdenum, sulfur, phosphorus and zinc (**Table 4.16**). Although, formation of tribofilm was also seen when T+G+M+Z was used as lubricant resulting in lowest friction coefficient value among tested lubricants but no substantial improvement in wear characteristics of the contact was witnessed (**Figure 4.25**, **Figure 4.26** and **Figure 4.27**). Major difference seen in the micrographs of formulated lubricants was the formation of pits in higher concentrations and removal of coating material in the presence of T+G+M+Z whereas no such phenomenon was seen with P+G+M+Z. On comparing the concentrations of additive-derived elements found on pin surface of steel/cast, ta-C/ta-C, ta-C/cast iron a-C:H/a-C:H contacts, it can be seen that very little tribofilm was formed on a-C:H-coated pin compared to others.

Table 4.16: Atomic percentage of elements found on a-C:H-coated pins after 2 hours of sliding against a-C:H-coated plates in the presence of PAO-based and TMP-based lubricants

Lubricants	Elements										
	C	**Cr**	**N**	**P**	**S**	**Mo**	**Zn**	**Fe**	**O**	**Cl**	**Na**
PAO	37.3	15.4	12.1	-	-	-	-	32.5	2.7	-	-
TMP	84.1	11.6	-	-	-	-	-	-	4.3	-	-
P+G+M+Z	72.2	6.1	4.8	0.9	0.6	0.4	1.2	-	12.9	0. 8	0.9
T+G+M+Z	51.1	27.6	8.9	0.2	0.9	1.2	0.2	-	9.9	-	-

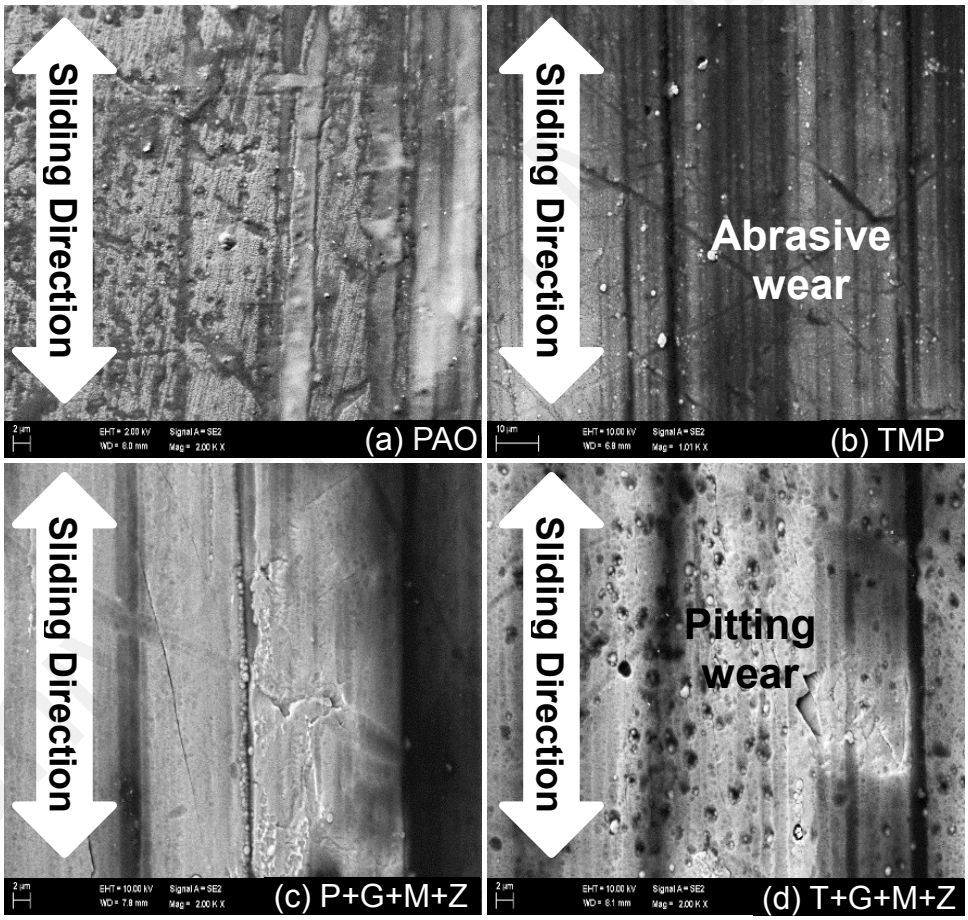

Figure 4.31: SEM micrographs of a-C:H-coated pins after 2 hours of sliding against a-C:H-coated plates in the presence of PAO-based and TMP-based lubricants

4.5.4.5 a-C:H/cast iron contact

Similar to symmetrical a-C:H contacts, highest friction and wear coefficient values of a-C:H/cast iron contact was seen when additive-free PAO was used as lubricant (**Figure 4.25**, **Figure 4.26** and **Figure 4.27**). This can be attributed to severe surface deterioration of uncoated cast iron pin in the presence of PAO. Surface fatigue and adhesion were observed as predominant wear mechanisms in the micrograph of PAO which resulted in formation of cracks, deep grooves and wear debris (**Figure 4.32a**). Contrary to that, micrograph of additive-free TMP remained unaltered and relatively cleaned (**Figure 4.32b)**. High content of carbon observed in EDS results of additive-free TMP can be related to residual lubricant layer on the pin surface even after thorough cleaning (**Table 4.17**). This shows that polar components of TMP were physisorbed on the interacting surfaces and adhered strongly to the pin surface. An eloquent decrease in friction and wear coefficient values of a-C:H/cast iron contact was seen when formulated version of PAO was used as lubricant. Not only this, brittle fracture was replaced by pitting wear as main wear mechanism. This can be attributed to tribochemical interaction of additives with the sliding surfaces. Formation of additive-derived tribofilm composed of molybdenum, sulfur, phosphorus and zinc was also confirmed by EDS results and can also be seen in the micrograph of P+G+M+Z (**Figure 4.32c** and **Table 4.17)**. Some scratch lines can also be seen in the micrograph of P+G+M+Z behind the white-colored tribofilm due to the abrasive action of wear debris of interacting surfaces, in addition to pitting wear. Although, above-mentioned elements were also seen in the EDS results of T+G+M+Z but in lower concentrations compared to that of P+G+M+Z. Inability of T+G+M+Z to form concentrated tribofilm on the contact area resulted in higher wear coefficient values of sliding surfaces compared to P+G+M+Z.

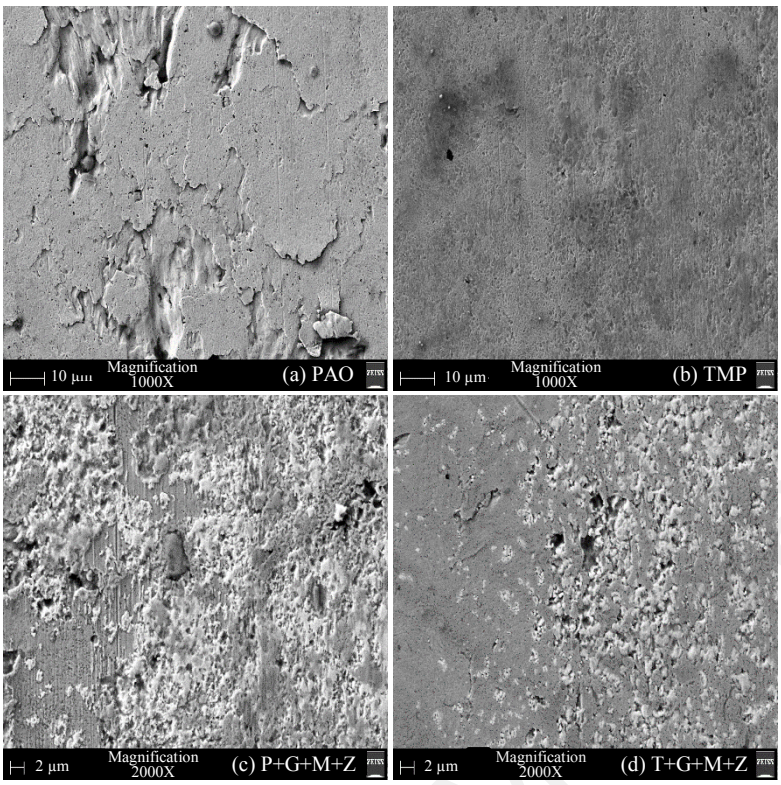

Figure 4.32: SEM micrographs of uncoated cast iron pins after 2 hours of sliding against a-C:H-coated plates in the presence of PAO-based and TMP-based lubricants

Table 4.17: Atomic percentage of elements found on uncoated cast iron pins after 2 hours of sliding against a-C:H-coated plates in the presence of PAO-based and TMP-based lubricants

Lubricants	Elements										
	C	W	Cr	N	P	S	Mo	Zn	Fe	O	Si
PAO	27.9	-	-	-	-	-	-	-	47.5	20.8	3.8
TMP	46.2	-	-	-	-	-	-	-	45.3	5.2	3.3
P+G+M+Z	31.8	-	-	3.1	1.4	2.0	8.9	2.2	34.2	13.9	2.5
T+G+M+Z	36.3	-	1.4	3.4	0.6	2.2	3.2	0.7	42.1	7.5	2.6

4.5.4.6 a-C:H:W/a-C:H:W contact

In SEM micrographs of a-C:H:W-coated pins, bright regions depict exposed CrN interlayer whereas dark regions represent top a-C:H:W layer (**Figure 4.33**). In the

presence of PAO-based lubricants, clear scratch lines in the direction of sliding can be seen which resulted in removal of a-C:H:W coating from certain areas. Small pits were formed in those regions in which there were no scratch lines due to abrasive wear. When PAO was used as lubricant, ploughing due to adhesion between a-C:H:W-coated surfaces was also seen which resulted in deep grooves and exposed ferrous-based substrate material (**Figure 4.33a**). Contrary to that, delamination of a-C:H:W coating was not observed when T+G+M+Z was used as lubricant and polishing was the predominant wear mechanism with few shallow scratch lines (**Figure 4.33d**). Although, some of the CrN interlayer was exposed in the presence of additive-free TMP due to abrasive wear of debris which resulted in formation of many micro-pits and ditches on the pin surfaces, but overall a-C:H:W layer was able to maintain its integrity till the end of 2 hours of sliding. In EDS results, presence of oxygen, chromium and nitrogen in large concentrations and small amounts of iron and tungsten on coated-pins depicts that most of the top a-C:H:W coating either delaminated or worn-out after 2 hours of sliding in the presence of PAO (**Table 4.18)**. Increase in oxygen concentration can be attributed to formation of FeO, Fe_2O_3 and Fe_3O_4 when ferrous-substrate was exposed due to delamination of DLC coating. In case of TMP-based lubricants especially T+G+M+Z, iron was not detected in EDS analysis whereas chromium and nitrogen were presented either in small concentrations or not at all. This shows that T+G+M+Z improved the wear-resistance of the contact due to which top layer of the coatings sustained 2 hours of sliding with exposure of CrN interlayer on few remote sites (**Figure 4.26** and **Figure 4.27**). Mixing of additives in PAO enhanced its inherent lubricity and total delamination of a-C:H:W coating was avoided. Although, an improvement in tribological performance of a-C:H:W/a-C:H:W contact was seen with formulated lubricants but elements associated with additive derived tribofilms (molybdenum, zinc, sulphur, phosphorus), were not seen in abundance on pin surface (**Figure 4.25**, **Figure 4.26** and **Figure 4.27**). A possible

justification for this behavior is making and breaking of tribofilm during tribotests due to its weak-adhesion with a-C:H:W-coated surfaces. Absence of ferrous-based compounds which promote binding between additive-derived tribofilm and contact surface can be attributed to this weak adhesion. Similar weakly-adhered tribofilms were also observed by Equey et al. (2008b) on symmetrical a-C:H contact in the presence PAO+ZDDP

Table 4.18: Atomic percentage of elements found on a-C:H:W-coated pins after 2 hours of sliding against a-C:H:W-coated plates in the presence of PAO-based and TMP-based lubricants

Lubricants	**Elements**									
	C	**W**	**Cr**	**N**	**P**	**S**	**Mo**	**Zn**	**Fe**	**O**
PAO	12.7	2.1	37.7	23.9	-	-	-	-	3.8	19.8
TMP	68.8	21.2	3.6	1.1	-	-	-	-	-	5.3
P+G+M+Z	49.8	12.9	17.6	8.8	0.3	0.9	0.7	0.2	-	8.8
T+G+M+Z	75.8	18.8	-	-	0.2	0.6	1.1	0.3	-	3.2

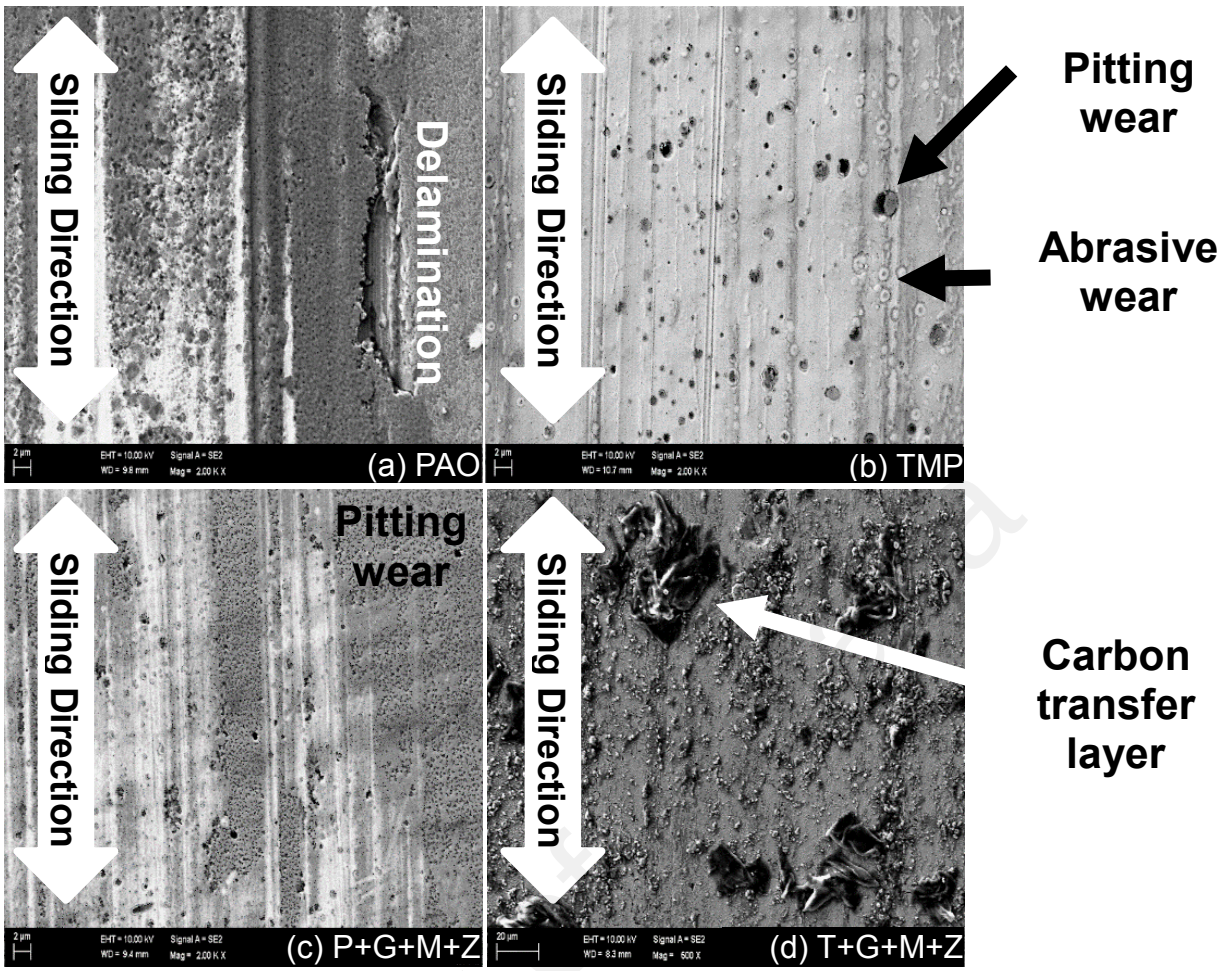

Figure 4.33: SEM micrographs of a-C:H:W-coated pins after 2 hours of sliding against a-C:H:W-coated plates in the presence of PAO-based and TMP-based lubricants

4.5.4.7 a-C:H:W/cast iron contact

A lot of surface deterioration was seen in the presence of PAO whereas no such effect was seen with other lubricants (**Figure 4.34**). This degradation can be attributed to adhesion and interlocking of asperities which resulted in transfer of material from one surface to another. A similar material transfer was also seen when formulated version of PAO was used but it was in the reverse order i.e. carbon was transferred from a-C:H:W-coated plate to cast iron pin (**Figure 4.34c**). This transfer of material resulted in lowest value of friction among tested lubricants (**Figure 4.25**). Another justification for this improved tribological performance can be attributed to formation of additive-derived tribofilm (**Table 4.19**). No such adhesive wear and transfer of material was observed

when additive-free TMP was used (**Figure 4.34b**). Instead, deep grooves due to abrasion and surface cracking were the main wear mechanisms observed. Similar cracks on the interacting surfaces were also observed by Zulkifli et al. (2016) in the presence of TMP due to localized plastic deformation which eventually leads to spall formation. In case of a-C:H:W/cast iron contact, lowest value of friction coefficient was observed when P+G+M+Z was used as lubricant followed by TMP, T+G+M+Z and PAO (**Figure 4.25**). This improved friction performance in the presence of P+G+M+Z can be attributed to tribochemical interaction between additives and interacting surfaces resulting in the formation of tribofilm comprised of phosphorus, sulphur, molybdenum and zinc. It is mentioned in the literature that presence of MoDTC and ZDDP in the lubricant results in decreased friction between the interacting surfaces due to the formation of MoS_2 (Khaemba, Neville, & Morina, 2016; Windom, Sawyer, & Hahn, 2011). During the tribotesting, MoDTC is tribochemically decomposed into MoS_2 and MoO_3. It is believed that MoS_2 facilitates the sliding due to its layered structure and low shear strength (Zahid et al., 2015). On the other hand, MoO_3, instead of reducing friction coefficient, increases the wearing-out of the interacting surfaces due to its sharp edge crystalline structure (Komori & Umehara, 2015). MoDTC can only plays its primary role of friction modifier if its decomposition results in higher concentration of MoS_2 compared to MoO_3 (Komori & Umehara, 2015). If ZDDP is present in MoDTC-containing lubricant, it supplies sulphur to MoDTC and amplifies the formation of MoS_2 (Tasdemir, Wakayama, et al., 2013a). Contrary to P+G+M+Z, when T+G+M+Z was used as lubricant, very little concentration of molybdenum was observed on pin surface which shows either very little or no tribochemical interaction at all between MoDTC and interacting surfaces. As a result, significant increase in coefficient of friction was observed with T+G+M+Z. Contrary to friction results, an eloquent improvement in wear behavior of a-C:H:W/cast iron contact, especially wear of pin, was observed with formulated version of TMP

instead of its additive-free version. This can be attributed to the formation of ZDDP-derived pad-like tribofilm on contact asperities due to which direct metal-to-metal contact was prevented (Spikes, 2004). A similar pad-like tribofilm was also observed by Tasdemir, Tokoroyama, et al. (2014) on various DLC contacts which resulted in higher levels of friction and reduction in wearing rate of interacting surfaces.

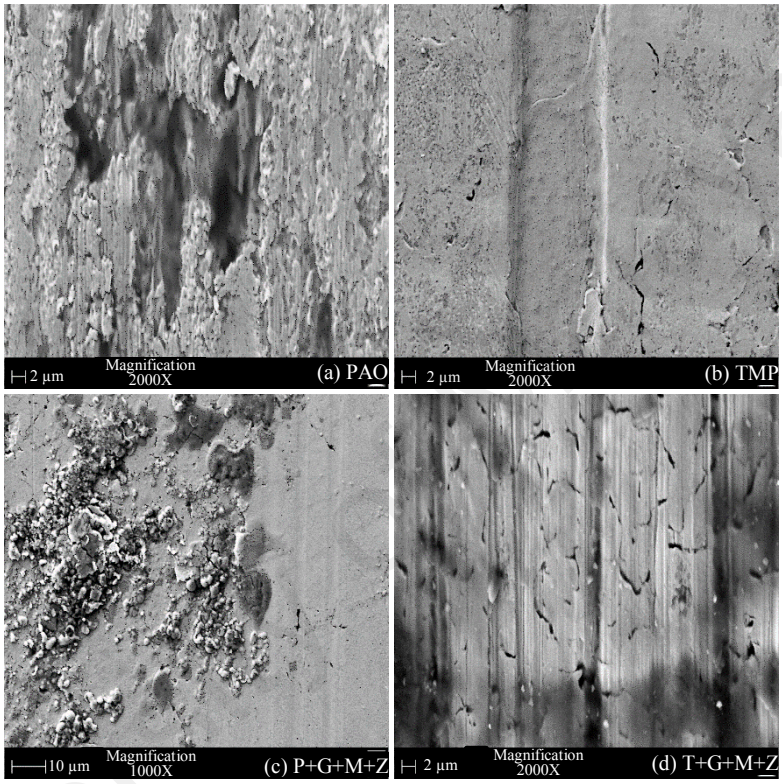

Figure 4.34: SEM micrographs of uncoated cast iron pins after 2 hours of sliding against a-C:H:W-coated plates in the presence of PAO-based and TMP-based lubricants

Table 4.19: Atomic percentage of elements found on uncoated cast iron pins after 2 hours of sliding against a-C:H:W-coated plates in the presence of PAO-based and TMP-based lubricants

Lubricants	**Elements**						
	C	**P**	**S**	**Mo**	**Zn**	**Fe**	**O**
PAO	56.6	-	-	-	-	35.2	8.2
TMP	25.7	-	-	-	-	61.8	12.5
P+G+M+Z	24.2	1.2	3.2	2.4	0.9	58.7	9.4
T+G+M+Z	43.3	2.1	1.3	0.2	3.4	42.5	7.2

4.5.5 Surface roughness analysis

R_a values of uncoated and DLC-coated plates after 2 hours of sliding against uncoated and DLC-coated pins in the presence of PAO-based and TMP-based lubricants are presented in **Figure 4.42.**

4.5.5.1 Steel/cast iron contact

TMP-based lubricants proved to be more effective in protecting the uncoated steel plates from surface deterioration compared to those containing PAO. When formulated lubricants were used, approximately 60% reduction in R_a values was observed compared to additive-free base oils. In **Figure 4.35,** clear difference can be seen in the wear depth values of wear track profiles of uncoated cast iron pins in the presence of additive-free and formulated lubricants which showed that additives were able to protect the uncoated steel plates from excessive earing and degradation by making tribofilms on the asperities. Formation of additive-derived tribofilm was also confirmed by SEM/EDS analysis (**Figure 4.28** and **Table 4.13**).

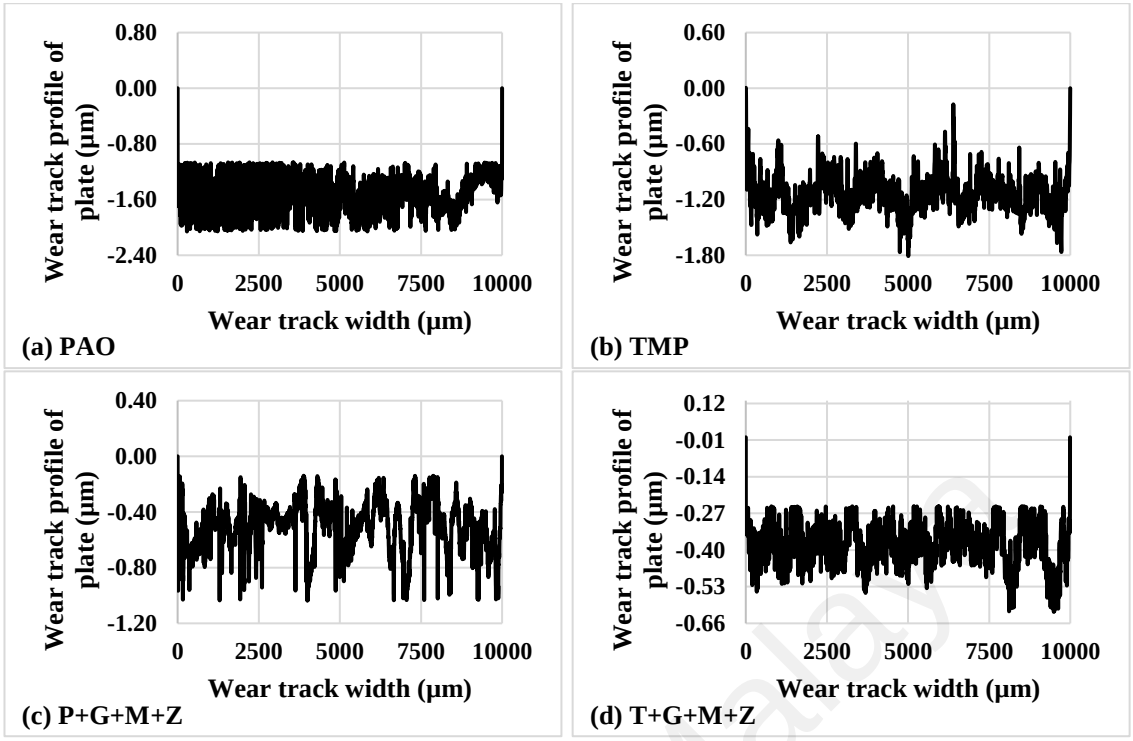

Figure 4.35: Wear track profiles of uncoated steel plates after 2 hours of sliding against uncoated cast iron pins in the presence of PAO-based and TMP-based lubricants

4.5.5.2 ta-C/ta-C contact

Similar to steel/cast iron contacts, aggravated surface deterioration of ta-C-coated plates was witnessed when additive-free PAO was used as lubricant instead of TMP (**Figure 4.36**). Although, 65% reduction in surface roughness value of plate was observed when ta-C-coated surfaces were used instead of ferrous-ones in the presence of TMP but no such behaviour was seen with PAO and value remained almost at the same level. This behaviour can be attributed to delamination of coating from the plate surface due to which contact was changed from ta-C/ta-C to steel/ta-C. Delamination of ta-C-coating in the presence of PAO was also confirmed by Raman spectroscopy. When formulated version of PAO was used, total delamination of ta-C coating from the plate surface was prevented due to which R_a value was reduced from 1.172 to 0.415. Maximum surface protection and lowest surface roughness value was observed when T+G+M+Z was used as lubricant. Significant difference in the wear track profiles of PAO-based and TMP-based lubricants

can be seen in **Figure 4.36** due to involvement of different wear mechanisms. In case of PAO-based lubricant, delamination of material and abrasive wear, resulting in material removal and formation of deep grooves in the direction of sliding, were seen as predominant wear mechanisms. On the other hand, polishing wear was witnessed when TMP and T+G+M+Z were used as lubricant accompanied by shallow scratch lines and grooves due to abrasive action of wear debris.

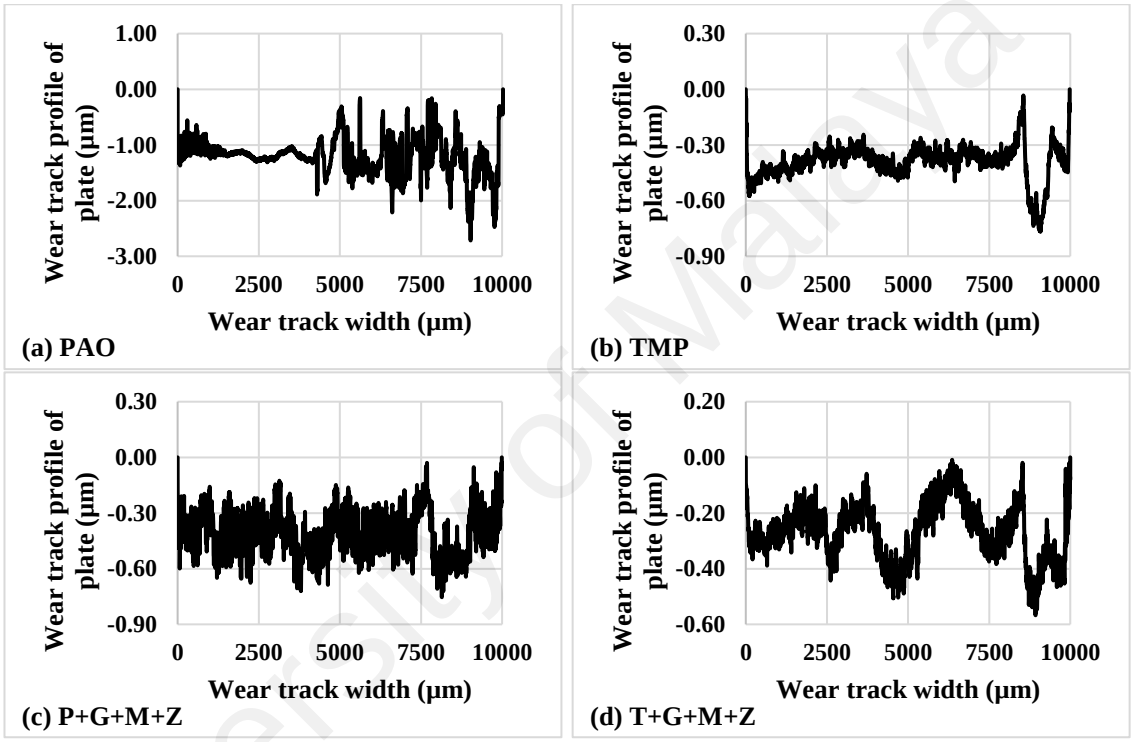

Figure 4.36: Wear track profiles of ta-C-coated plates after 2 hours of sliding against ta-C-coated plates in the presence of PAO-based and TMP-based lubricants

4.5.5.3 ta-C/cast iron contact

Similar to steel/cast iron and symmetrical ta-C contact contacts, additive-free TMP proved to be more effective in protecting the ta-C-coated plate from surface deterioration compared to PAO (**Figure 4.37**). As a result, lowest values of friction and wear coefficient of plates among tested lubricants were witnessed when TMP was used as lubricant (**Figure 4.25** and **Figure 4.27**). Although, additives played their role and

resulted in better protection of ta-C-coated plate when mixed with PAO but opposite behaviour was seen when formulated version of TMP was used. An increase of 160% in surface roughness value was observed with T+G+M+Z compared to additive-free TMP. Contrary to that, T+G+M+Z resulted in lowest surface roughness values of plate when used in combination with steel/cast iron and ta-C/ta-C contacts. In surface profile of ta-C-coated plates, extremely deep grooves (1.50 to 1.80 µm) can be clearly seen in the presence of T+G+M+Z compared to other lubricants. This behaviour can be attributed to abrasive action of deeply penetrated wear debris of either cast iron and/or ta-C coating during sliding. Polishing wear and formation of scratch lines accompanied with few wide grooves in the direction of sliding were observed as predominant wear mechanisms when lubricants other than T+G+M+Z were used in combination with ta-C/cast iron contact

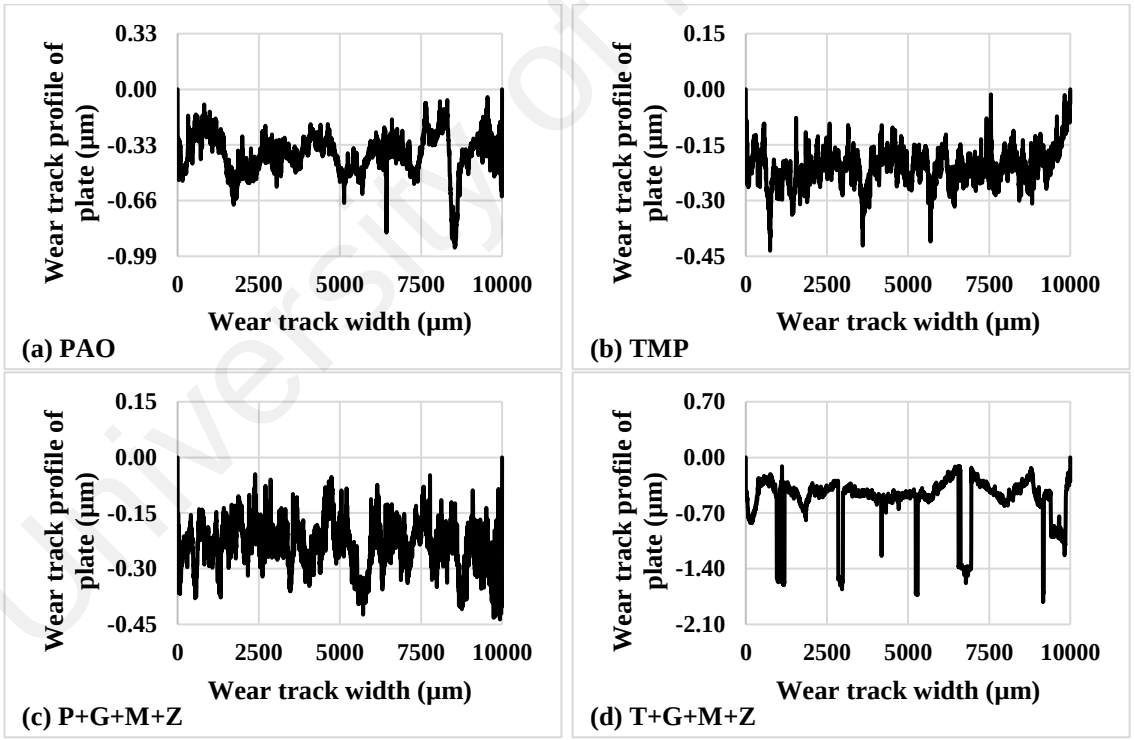

Figure 4.37: Wear track profiles of ta-C-coated plates after 2 hours of sliding against uncoated cast iron pins in the presence of PAO-based and TMP-based lubricants

4.5.5.4 a-C:H/a-C:H contact

In comparison to steel and ta-C-coated plates, a-C:H-coated plates proved to be more wear-resistant. Relatively unaltered surfaces and extremely low surface roughness values were seen after 2 hours of sliding (**Figure 4.38**). The only exception to this finding was seen when additive-free PAO was used resulting in almost three-times more surface deterioration compared to other lubricants. A direct relation between roughness values and wear coefficients of a-C:H-coated interacting surfaces was seen due to breaking of interlocking asperities whereas friction coefficient values of a-C:H/a-C:H contact remained unaffected (**Figure 4.25**, **Figure 4.26** and **Figure 4.27**). Ineffectiveness of PAO in protecting the plate surface from deterioration was also seen in steel/cast iron, ta-C/ta-C and ta-C/cast iron contacts. Lowest R_a value of a-C:H-coated plate was seen when formulated version of PAO was used as lubricant. Although, additives were also proved to be effective when mixed with TMP but not to the extent of P+G+M+Z. Polishing wear resulting in shallow scratch lines in the direction of sliding was seen with P+G+M+Z whereas material removal due to delamination and adhesive wear, accompanied with grooves, were observed as predominant wear mechanisms in other lubricants.

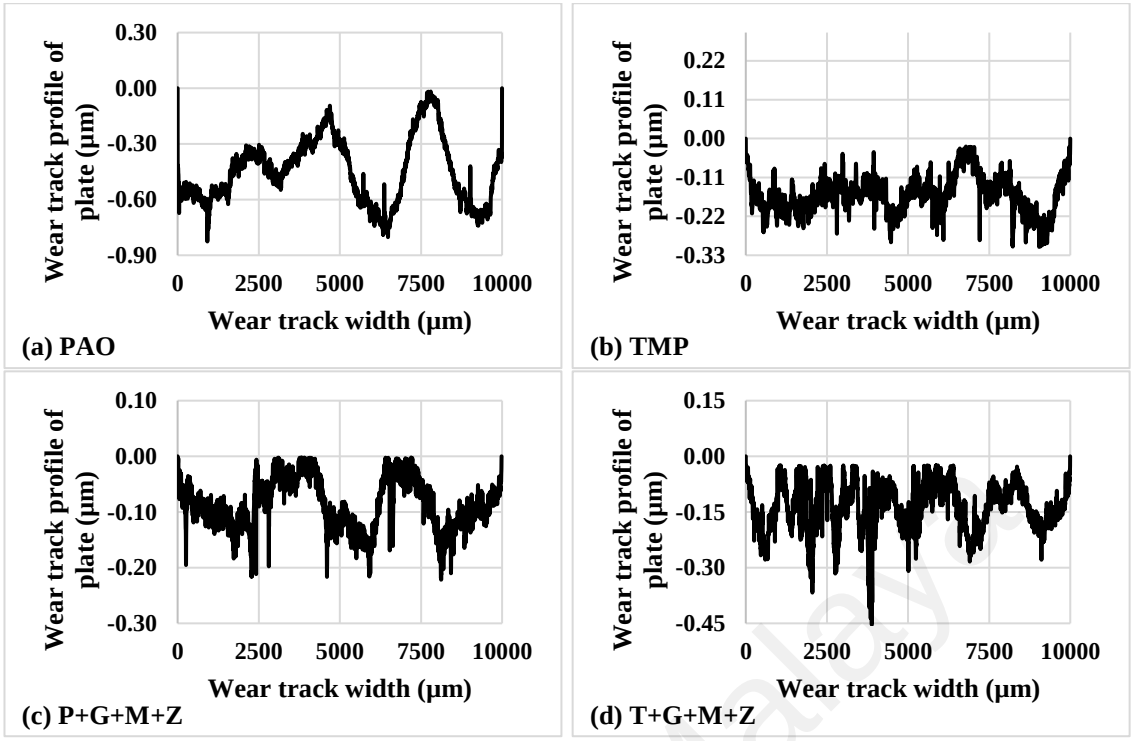

Figure 4.38: Wear track profiles of a-C:H -coated plates after 2 hours of sliding against a-C:H-coated pins in the presence of PAO-based and TMP-based lubricants

4.5.5.5 a-C:H/cast iron contact

An increase in surface roughness values of a-C:H-coated plates was seen when uncoated cast iron pins were used as counterbodies instead of a-C:H-coated ones (**Figure 4.42**). This behaviour can be attributed to higher affinity of carbon towards iron due to which increase in adhesive wear and diffusion of carbon atoms into the ferrous surface was witnessed (Gangopadhyay et al., 2011; Tasdemir, Wakayama, et al., 2013b). The only exception to this finding was seen when additive-free TMP was used as lubricant due to its polar nature with the help of which it adsorbed on the cast iron pin and prevented the adhesive wear. As a result, only polishing wear with few shallow grooves were seen on a-C:H-coated plates in the presence of TMP (**Figure 4.39**). A significant improvement in tribological performance of a-C:H/cast iron contact was witnessed due to better surface protection provided by TMP and lower values of friction and wear coefficients were observed compared to PAO (**Figure 4.25**, **Figure 4.26** and **Figure 4.27**). Similar to ta-

C/cast iron contact, increase in surface deterioration of a-C:H-coated plates was seen when formulated version of TMP was used instead of its additive-free one and polishing wear was replaced by delamination, adhesive wear and formation of deep grooves (**Figure 4.39**). Inability of T+G+M+Z, in providing surface protection to a-C:H/cast iron contact compared to additive-free TMP, can be attributed to competition between polar components of TMP and additive-derived tribofilm to adsorb on the cast iron pin. As a result, carbon diffuses onto the active sites on ferrous counterbody whenever it gets a chance thus, promoting adhesive wear between the interacting surfaces. Although, P+G+M+Z proved to be very effective in protecting a-C:H-coated plate from degradation compared to additive-free PAO but still R_a value remained at the same level as that of T+G+M+Z. However, formation of deep grooves and scratch lines in the direction of sliding due to abrasive wear were observed on the plate surface instead of adhesive wear when formulated version of PAO was used as lubricant instead of T+G+M+Z.

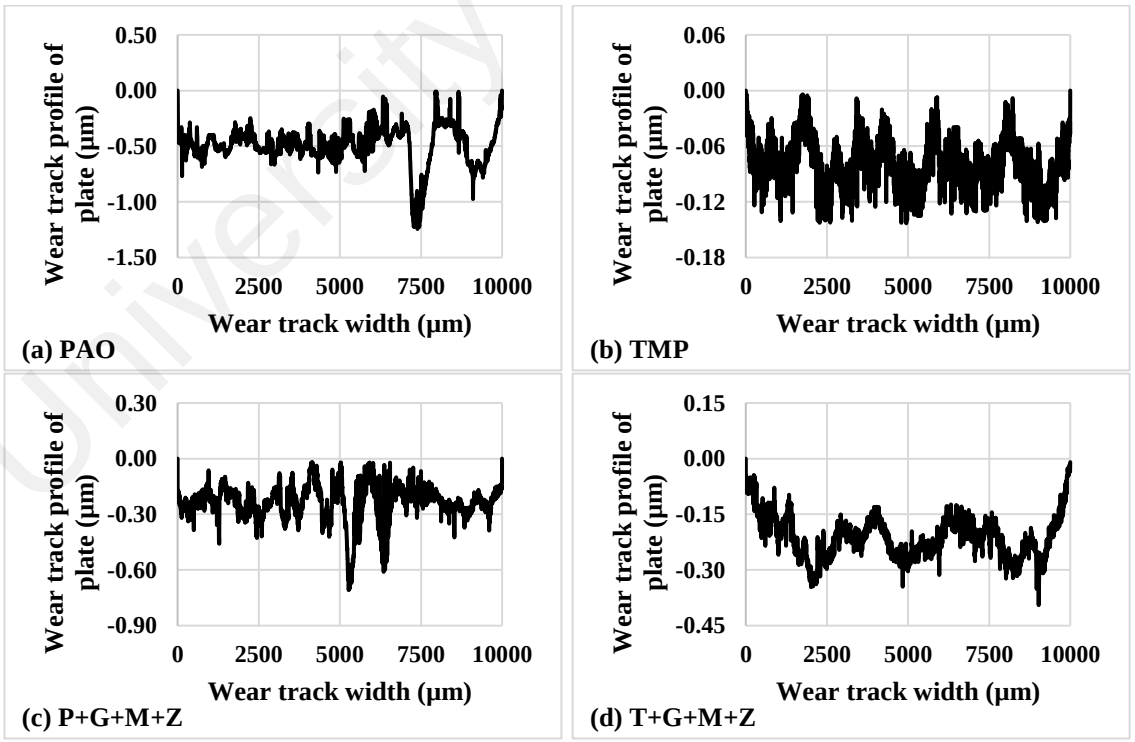

Figure 4.39: Wear track profiles of a-C:H-coated plates after 2 hours of sliding against uncoated cast iron pins in the presence of PAO-based and TMP-based lubricants

4.5.5.6 a-C:H:W/a-C:H:W contact

Among the base oils, severe roughening of a-C:H:W-coated plate was witnessed in the presence of TMP resulting in highest values of wear coefficient of sliding surfaces (**Figure 4.26** and **Figure 4.27**). Main wear mechanisms which were responsible for deterioration of a-C:H:W-coated surface include abrasive wear, plowing wear and pitting wear (**Figure 4.40**). As a result, considerable amount of coating was removed from the surface and deep grooves were formed. Although, abrasive wear and some delamination of coating was also seen in the presence of PAO but it was not as severe as witnessed in the case of TMP. Formulated lubricants were proved to be more effective in protecting the sliding surface from deterioration compared to additive-free base oils. Abrasive wear was replaced by polishing and pitting wear and no signs of delamination were observed when T+G+M+Z was used as lubricant instead of TMP resulting in lowest values of R_a and wear coefficients of interacting surfaces. Although, P+G+M+Z was also able to improve the structural integrity of a-C:H:W coating and delamination of coating was avoided but still few deep grooves were observed on the plate surface along with pitting wear. Although, a direct relation between R_a values of plates and wear coefficients of contact surfaces was seen but friction behavior of the contact appeared to be independent of it.

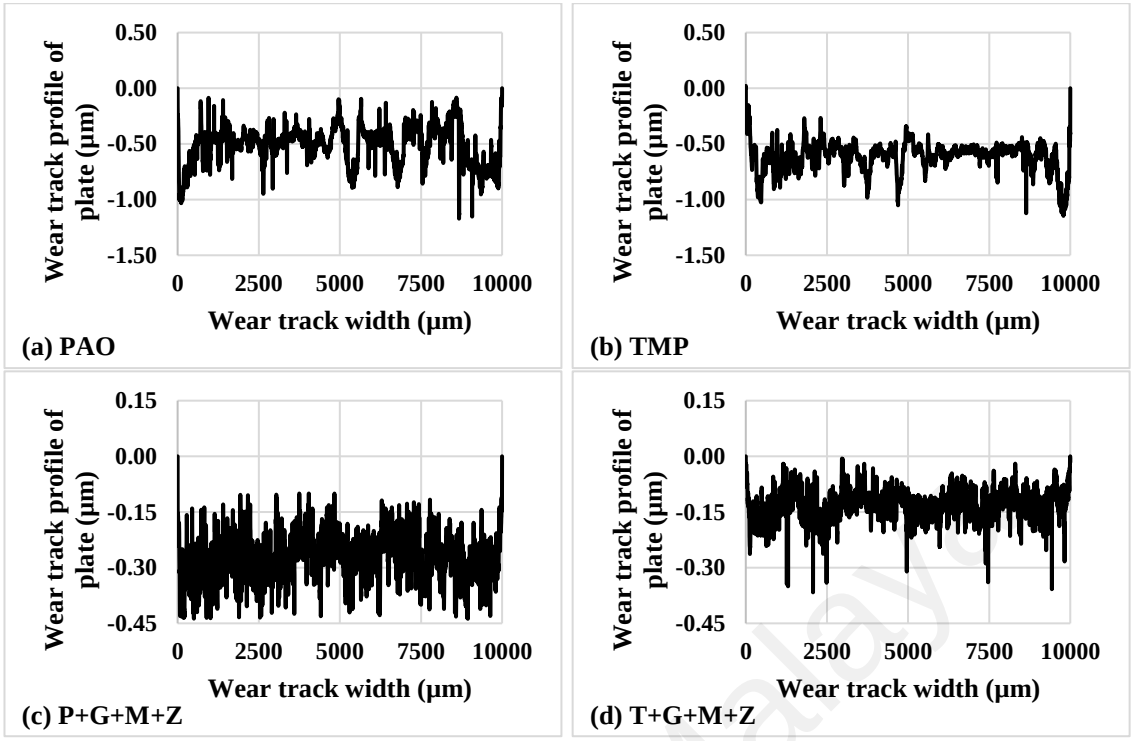

Figure 4.40: Wear track profiles of a-C:H:W-coated steel plates after 2 hours of sliding against a-C:H:W-coated pin in the presence of PAO-based and TMP-based lubricants

4.5.5.7 a-C:H:W/cast iron contact

A decrease in R_a values of a-C:H:W-coated plates was observed when uncoated cast iron pins were used instead of a-C:H:W-coated ones with most of the lubricant formulations and polishing wear was observed as predominant wear mechanism (**Figure 4.41**). Only exception to this finding was seen when T+G+M+Z was used as lubricant. Contrary to symmetrical a-C:H:W contact, TMP was proved to be more efficient in protecting the plate surface from deterioration compared to PAO in case of a-C:H:W/cast iron contact. Further improvement in inherent wear characteristics of TMP and reduction in R_a value of plates was witnessed when additives were mixed with it resulting in lowest surface roughness and wear coefficient values among tested lubricants. Similar trend was also seen in case of a-C:H:W/a-C:H:W contact

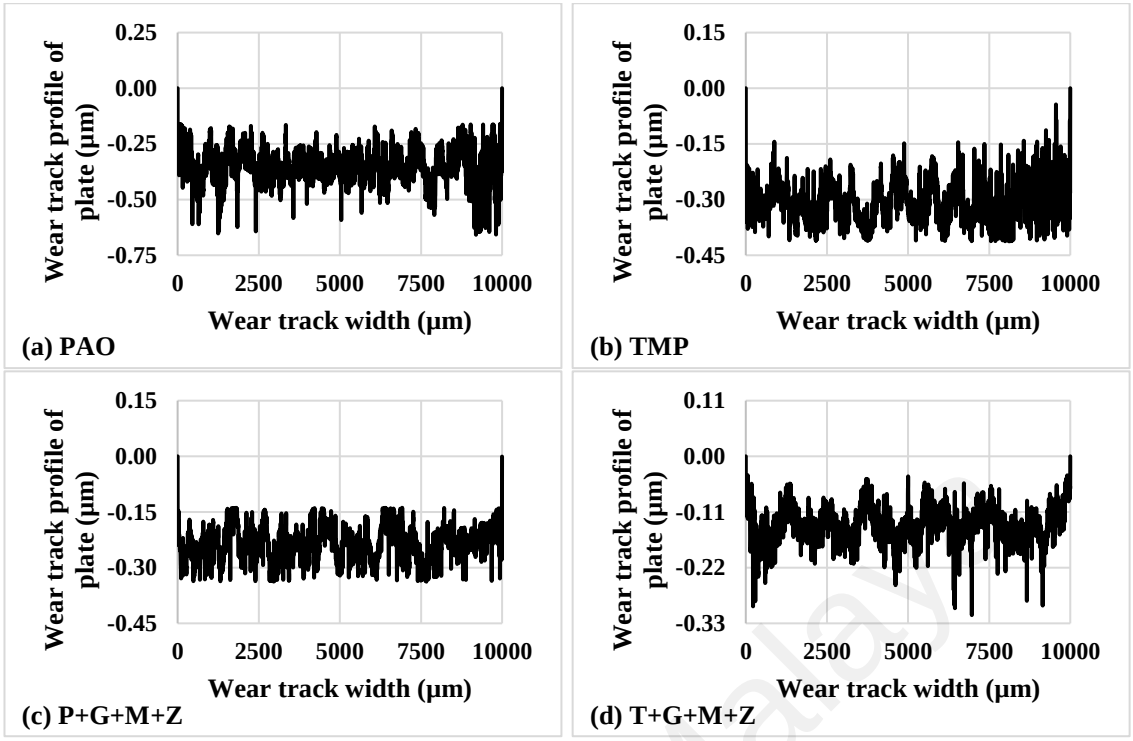

Figure 4.41: Wear track profile of a-C:H:W-coated steel plate after 2 hours of sliding against uncoated cast iron pins in the presence of PAO-based and TMP-based lubricants

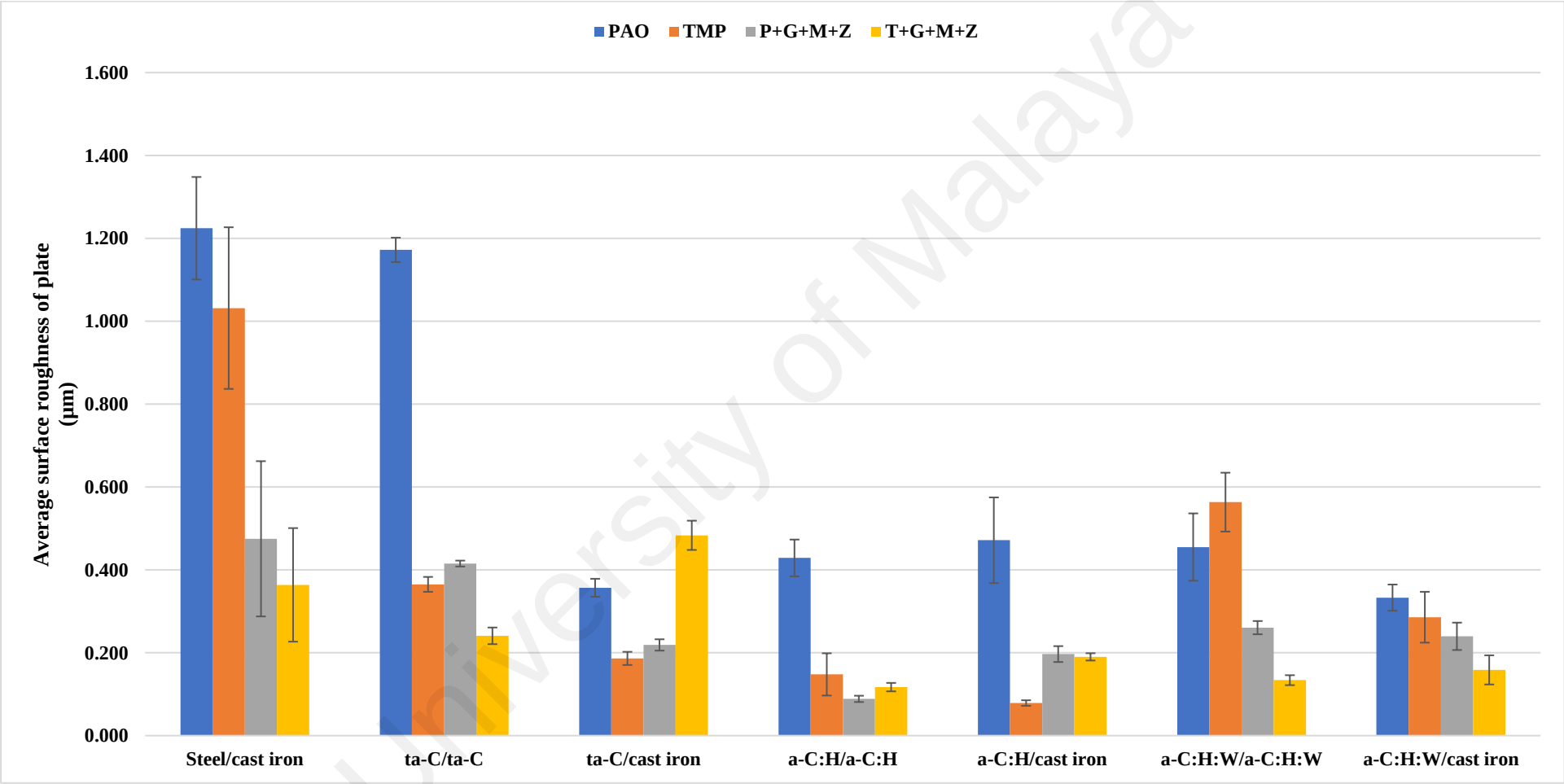

Figure 4.42: Average surface roughness values of uncoated and DLC-coated plates of steel/cast iron, DLC/DLC and DLC/cast iron contacts in the presence of PAO-based and TMP-based lubricants

4.5.6 Summary

Significant improvement in friction characteristics was observed when DLC-coated surfaces were used and friction coefficients were reduced up to 73%. Additive-free TMP proved to be more effective in reducing friction of contact compared to PAO irrespective of DLC coating type. An increase in coefficient of friction was observed when uncoated balls were used instead of DLC-coated ones as counterbodies against The only exception to this finding was seen with a-C:H:W coating. Lowest values of friction coefficients were observed with a-C:H/a-C:H contacts whereas a-C:H:W/a-C:H:W contacts resulted in highest values when multi-additive containing lubricants were used as lubricant. In terms of friction, P+G+M+Z was proved to be most effective lubricant whereas PAO appeared to be least effective in mitigating the friction between ball and plate surface.

Similar to friction results, an improvement in wear coefficient values of pins (up to 85%) were seen when DLC-coated surfaces were used instead of uncoated ones. Contrary to friction results, additive-free PAO appeared to be more effective in reducing wear of pins compared to PAO in most of the contacts. An increase in wear coefficient of pins was observed when uncoated pins were used instead of DLC-coated ones as counterbodies against DLC-coated plates irrespective of their type. Lowest values of wear coefficient of pins were observed with a-C:H/a-C:H contacts whereas ta-C/cast iron contacts resulted in highest values when multi-additive containing lubricants were used. In terms of wear of pins, P+G+M+Z was proved to be most effective lubricant whereas additive-free TMP appeared to be least effective in mitigating the wear.

Up to 89% reduction in wear coefficient of plates was observed when DLC-coatings were deposited on them. Lowest values of wear coefficient of plates were observed with a-C:H/a-C:H contacts whereas ta-C/ta-C contacts resulted in highest values when multi-additive containing lubricants were used. T+G+M+Z appeared to be most effective in

mitigating wear of uncoated and DLC-coated plates whereas PAO proved to be least lubricant.

Based on the above-mentioned observation, it can be concluded that conventional lubricant additives have tribological compatibility with TMP and various types of DLC coatings especially a-:C-H coating.

4.6 Cylinder head testing of Mercedes Benz OM646LA diesel engine using direct acting valve train test rig

On the basis of tribotesting results, a-C:H and a-C:H:W were selected for testing in cylinder head of Mercedes Benz OM646LA diesel engine by depositing them on tappets and camlobes in combination with base oils and multi-additive containing lubricants. Since, deterioration in tribological performance of DLC coatings was observed when ferrous counterbodies were used instead of DLC-coated ones, therefore, only DLC/DLC contacts (DLC-coated cams against DLC-coated tappets) are evaluated during cylinder head testing.

4.6.1 Friction analysis

4.6.1.1 Uncoated cam / uncoated tappet (U - U) interface

Instantaneous drive torque of exhaust camshaft under motored condition with uncoated tappets and uncoated camlobes at lubricant temperatures of 40ºC and 90ºC and camshaft speeds of 400 RPM, 800 RPM and 1200 RPM in the presence of PAO-based and TMP-based lubricants are shown in **Figure 4.43** and **Figure 4.44** whereas average friction torque is shown in **Figure 4.45**.

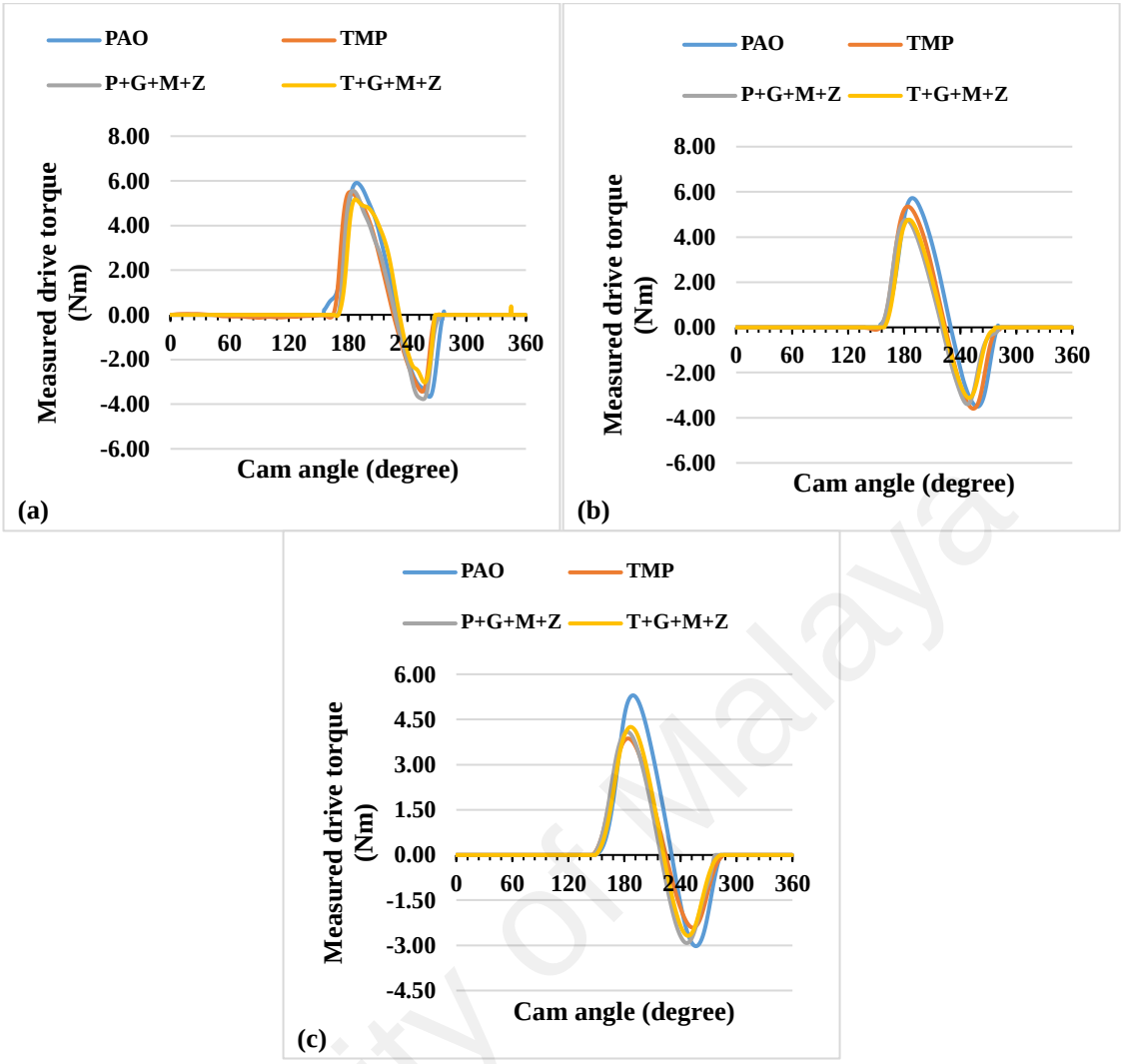

Figure 4.43: Instantaneous exhaust camshaft drive torque under motored condition with uncoated tappets and uncoated camlobes at lubricant temperature of 40ºC and camshaft speeds of (a) 400 RPM, (b) 800 RPM and (c) 1200 RPM

At 90ºC and camshaft speed of 400 RPM, additive-free TMP proved to be more effective in facilitating the sliding and resulted in lower value of friction torque compared to PAO due to presence of polar components in its structure (**Figure 4.45**). Although, a similar behavior was also seen during tribotesting of steel/cast iron contact but difference in friction performance was more pronounced in cylinder head testing (**Figure 4.25**). Additives were proved to be effective in further enhancing the friction behavior of U- U interface compared to base oils especially when mixed with PAO resulting in lowest friction torque among tested lubricants. This observation shows that conventional

additives are more compatible with PAO compared to TMP when used in in combination with uncoated valve train components. Effectiveness of additives in further augmenting the friction characteristics of base oils was also seen during tribotesting phase. With an increase in camshaft speed from 400 RPM to 800 RPM and 1200 RPM, instantaneous drive torque and friction torque of U – U interface was either decreased or remained at the same level irrespective of lubrication formulation (**Figure 4.45**). Only exception to this finding was when P+G+M+Z was used as lubricant at camshaft speed of 1200 RPM. Decreasing trend of friction with an increase in camshaft speed was also seen when cylinder head testing was carried out at lubricant temperature of 40ºC. This improved friction performance of cam/tappet interface at higher camshaft speeds can be attributed to increased lubricant entrainment and reduced cam load at the nose resulting in improved lubricant condition (Riaz A Mufti & Priest, 2003). It is mentioned in the literature that value of cam load is influenced by valve spring compression especially at low camshaft speed whereas at high speeds, inertia of tappet plays a key role. Due to inertia, deceleration of tappet around the cam nose increases with an increase in camshaft speed resulting in decrease in cam load (Baniasad & Emes, 1998).

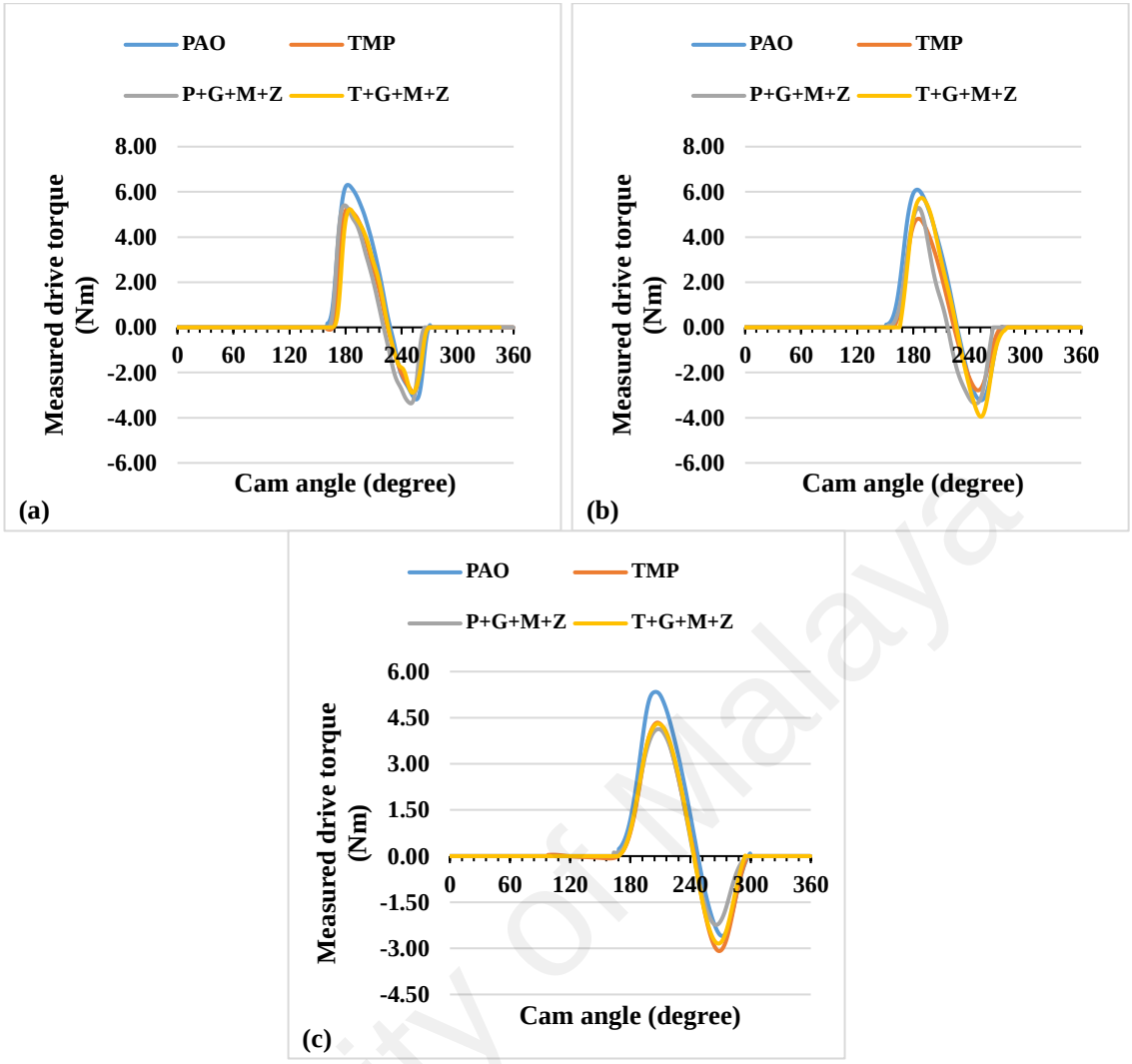

Figure 4.44: Instantaneous exhaust camshaft drive torque under motored condition with uncoated tappets and uncoated camlobes at lubricant temperature of 90ºC and camshaft speed of (a) 400 RPM, (b) 800 RPM and (c) 1200 RPM

When cylinder head tests were performed at lubricant temperature of 40°C, a decrease in instantaneous drive torque and friction torque were observed especially in the presence of PAO (**Figure 4.45**). At lower temperatures, lubricant has higher viscosity due to which hydrodynamic lubrication prevails in the contact area instead of mixed and boundary lubrication resulting in less metal-to-metal contact and asperity interlocking. Contrary to that, higher values of friction torque were witnessed at 40ºC in the presence of additive-containing lubricants especially at low camshaft speeds. It is widely accepted that additives are temperature sensitive and there is threshold temperature below which they

cannot play their role in enhancing tribological performance of a contact (Rizvi, 1999; Rowe, 1988).

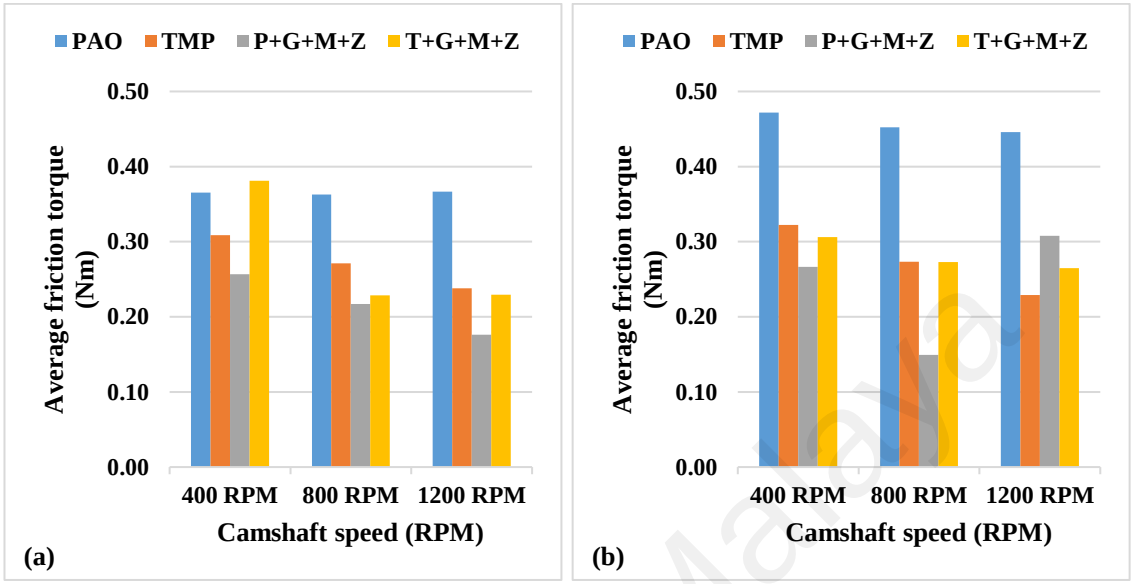

Figure 4.45: Average friction torque of exhaust camshaft under motored condition with uncoated tappets and uncoated camlobes at camshaft speeds of 400 RPM, 800 RPM and 1200 RPM and lubricant temperatures of (a) 40ºC and (b) 90ºC

4.6.1.2 a-C:H-coated cam / a-C:H-coated tappet (a-C:H - a-C:H) interface

Instantaneous drive torque and average friction torque of exhaust camshaft under motored condition with a-C:H-coated tappets and a-C:H-coated camlobes at lubricant temperature of 40 ºC and 90ºC and engine speeds of 400, RPM, 800 RPM and 1200 RPM in the presence of PAO-based and TMP-based lubricants are presented in **Figure 4.46** and **Figure 4.47** respectively whereas average friction torque is shown in **Figure 4.48**. Similar to U – U interface results, additive-free TMP also resulted in better friction performance of a-C:H – a-C:H interface compared to PAO at lubricant temperature of 90ºC and camshaft speed of 400 RPM **(Figure 4.48**). Although, formulated lubricants were able to reduce the friction torque when used in combination with U- U interface but no such behavior was seen when a-C:H-coated components were used. Rather, an increase in values average friction torque was witnessed when P+G+M+Z and T+G+M+Z

were used as lubricants instead of their additive-free versions. Inability of additives to tribochemically interact with a-C:H-coated components can be attributed to its chemically inert nature.

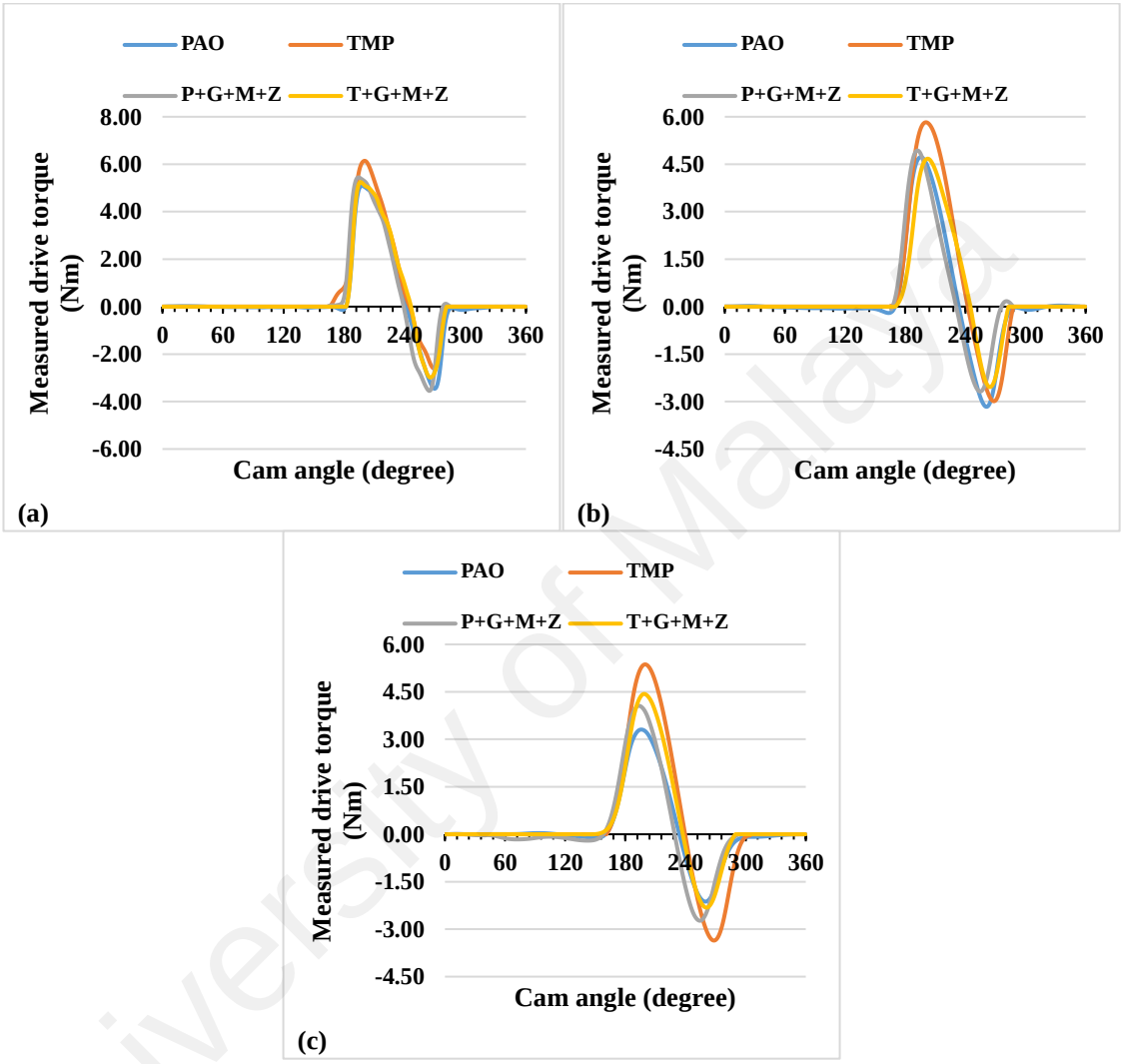

Figure 4.46: Instantaneous exhaust camshaft drive torque under motored condition with a-C:H-coated tappets and a-C:H-coated camlobes at lubricant temperature of 40ºC and camshaft speeds of (a) 400 RPM, (b) 800 RPM and (c) 1200 RPM

An indirect relation between camshaft speed and average friction torque of a-C:H - a-C:H interface was observed irrespective of lubricant formulation. Only exception to this finding was seen when TMP was used as lubricant and average friction torque was increased substantially at 800 RPM. On further increasing the speed to 1200 RPM, an

improvement in friction performance was seen and friction torque was reduced. This abnormality in friction behavior raised as a result of extremely low of average friction torque of a-C:H – a-C:H interface in the presence of TMP compared to other lubricants at 400 RPM. A possible justification for this behavior can be graphitization of a-C:H-coated components in the presence of TMP at low engine speeds which was also seen during tribotesting phase. At higher camshaft speeds, a decrease in average friction torque values of a-C:H-coated cam/tappet interface was seen when formulated lubricants were used instead of additive-free ones. This can be attributed to effective lubrication of contact at higher camshaft speeds due to which lubricant additives get more chances to tribochemically interact with interacting components resulting in the formation of tribofilms. Tribofilm formation mechanisms and their effect on tribological performance will be discussed in more detail in SEM/EDS analysis (**section 4.6.4**).

Significant decrease in average friction torque values was seen when cylinder head testing was carried out at lubricant temperature of 40°C instead of 90ºC with most of the lubricant formulations (**Figure 4.48**). As mentioned before, this improved friction performance can be attributed to high viscosity of lubricant at 40ºC compared to 90°C due to which thick lubricant film resides between the interacting components resulting in hydrodynamic/elastohydrodynamic lubrication regime and less chances of metal-to-metal contact. Exceptions to above finding was seen when TMP and T+G+M+Z were used as lubricants separately at camshaft speeds of 400 RPM and 1200 RPM respectively. As discussed above, low friction torque in the presence of TMP at 90ºC and 400 RPM can be attributed to graphitization. It is widely accepted that graphitization is a temperature-dependent phenomenon and chances of its occurrence decreases at lower contact temperature (Al Mahmud et al., 2014a).

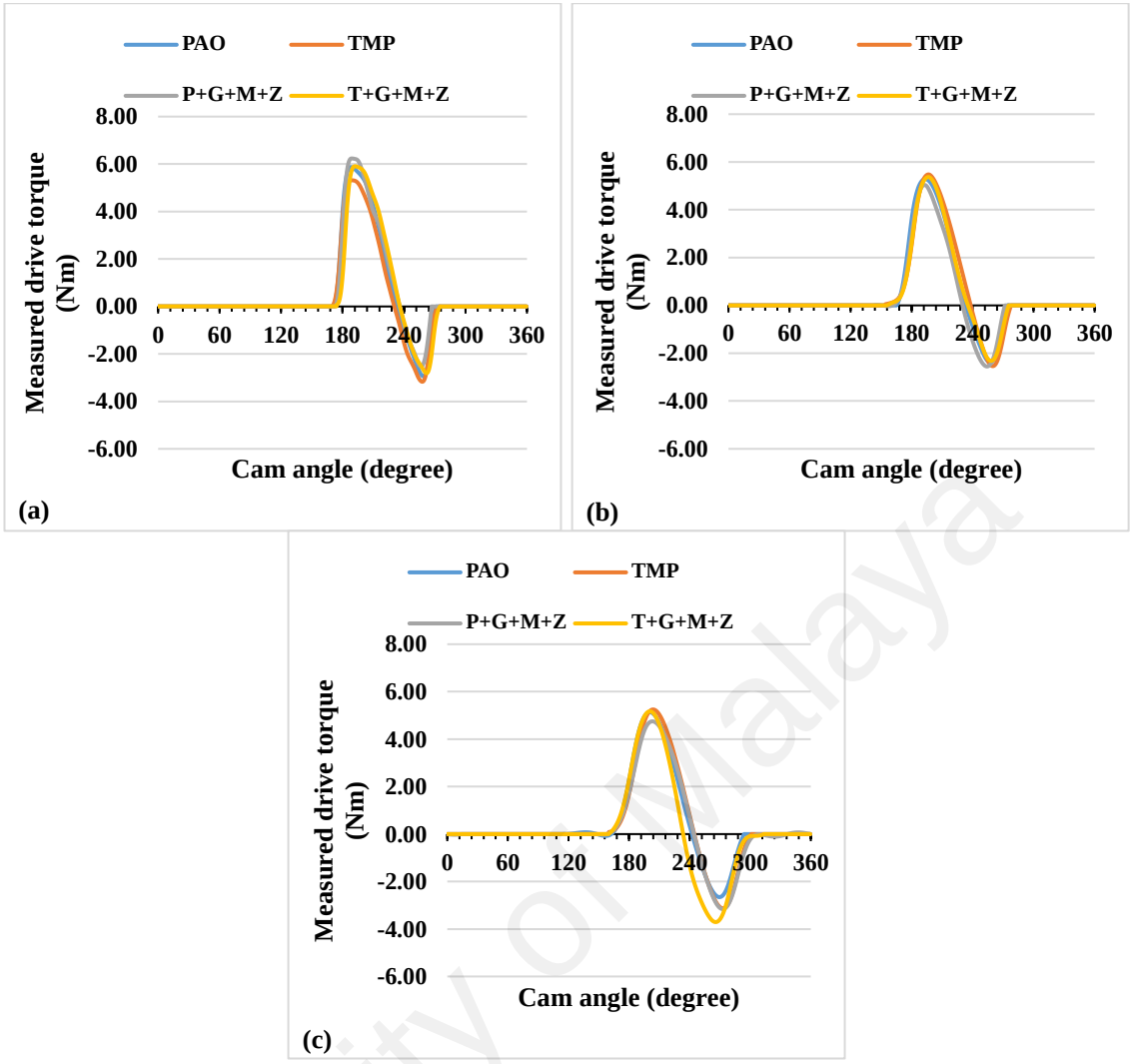

Figure 4.47: Instantaneous exhaust camshaft drive torque under motored condition with a-C:H-coated tappets and a-C:H-coated camlobes at lubricant temperature of 90ºC and camshaft speeds of (a) 400 RPM, (b) 800 RPM and (c) 1200 RPM

On comparing average friction torque of U- U interface with a-C:H – a-C:H interface, it can be clearly seen that latter was able to give better friction performance compared to former when additive-free PAO was used as lubricant irrespective of lubricant temperature and camshaft speed. However, a-C:H – a-C:H interface resulted in either in same or higher values of average friction torque compared to U - U interface when lubricants other than PAO were used. This behavior can be attributed to chemically inert nature of a-C:H coating due to which polar components of TMP-based lubricants were not able to adsorb on the contact surface resulting in lubricant slippage and high friction.

In the presence of P+G+M+Z, a-C:H – a-C:H interface performed better than U – U interface at camshaft speed of 1200 RPM irrespective of lubricant temperature. Similar behavior was also seen with T+G+M+Z when cylinder head testing was carried out at 90°C and camshaft speed of 1200 RPM.

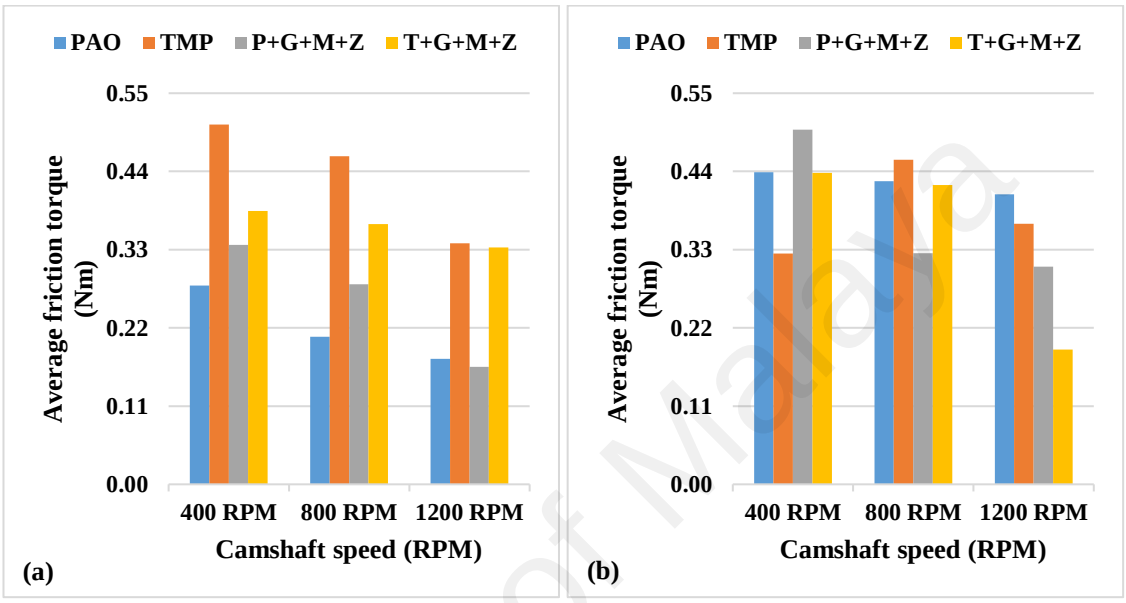

Figure 4.48: Average friction torque of exhaust camshaft under motored condition with a-C:H-coated tappets and a-C:H-coated camlobes at camshaft speeds of 400 RPM, 800 RPM and 1200 RPM and lubricant temperatures of (a) 40ºC and (b) 90ºC

4.6.1.3 a-C:H:W-coated cam / a-C:H:W-coated tappet (a-C:H:W - a-C:H:W) interface

Instantaneous drive torque of exhaust camshaft under motored condition with a-C:H:W-coated tappets and a-C:H:W-coated camlobes at lubricant temperature of 40ºC and 90ºC and camshaft speeds of 400 RPM, 800 RPM and 1200 RPM in the presence of PAO-based and TMP-based lubricants are shown in **Figure 4.49** and **Figure 4.50** whereas average friction torque are presented in **Figure 4.51**.

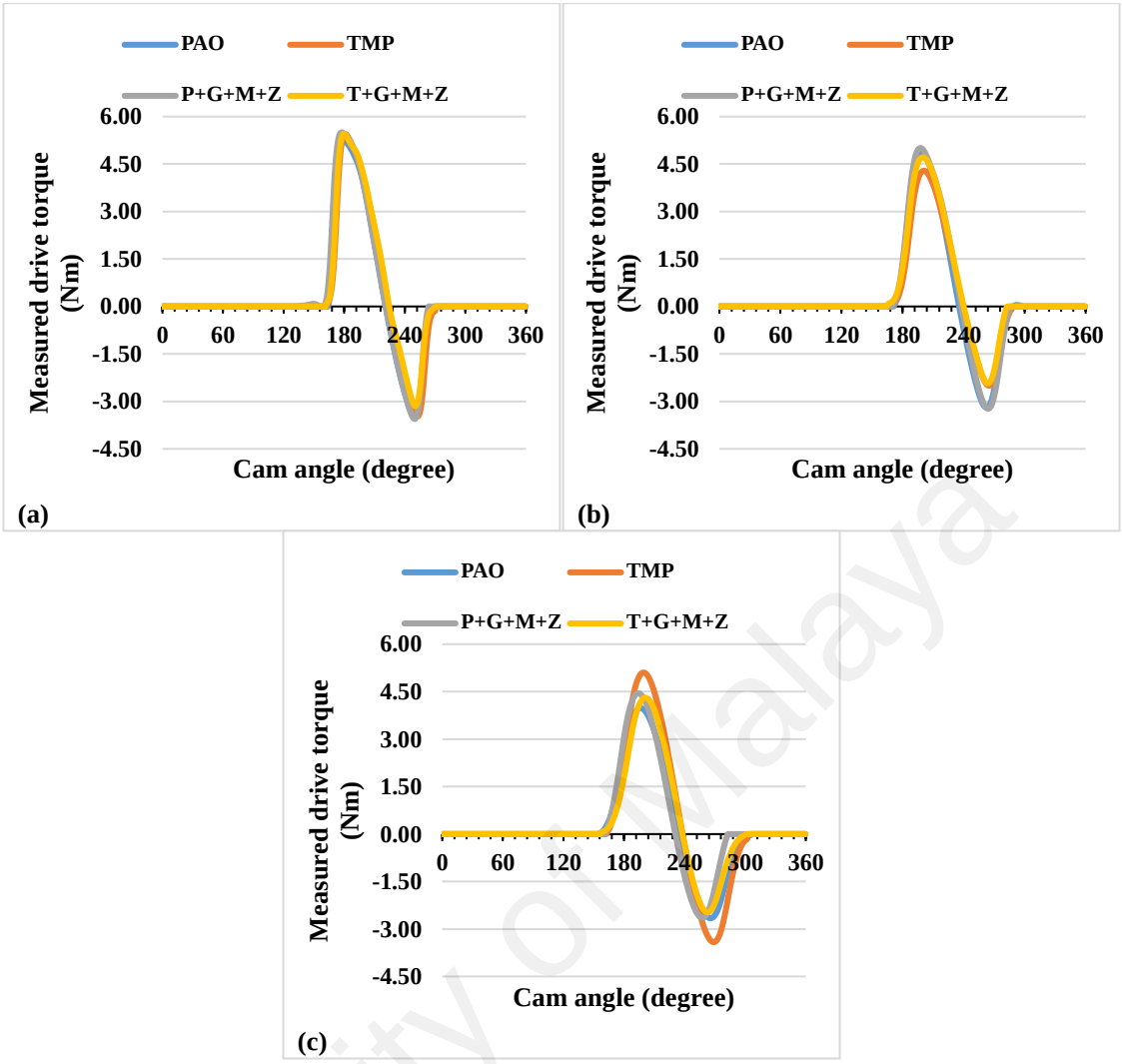

Figure 4.49: Instantaneous exhaust camshaft drive torque under motored condition with a-C:H:W-coated tappets and a-C:H:W-coated camlobes at lubricant temperature of 40ºC and camshaft speeds of (a) 400 RPM, (b) 800 RPM and (c) 1200 RPM

Although, additive-free TMP resulted in low friction torque compared to TMP at lubricant temperature of 90ºC and camshaft speed of 400 RPM but difference was trivial (3%)(**Figure 4.51**). Additives were proved to be effective when mixed with TMP and resulted in further enhancement in friction performance of a-C:H:W – a-C:H:W interface compared to additive-free TMP but no such behavior was seen with P+G+M+Z (**Figure 4.51**). Rather an increase in friction torque was witnessed when P+G+M+Z was used as lubricant instead of additive-free PAO. A similar deterioration in friction behavior in the presence of P+G+M+Z was also observed with a-C:H – a-C:H interface (**Figure 4.48**).

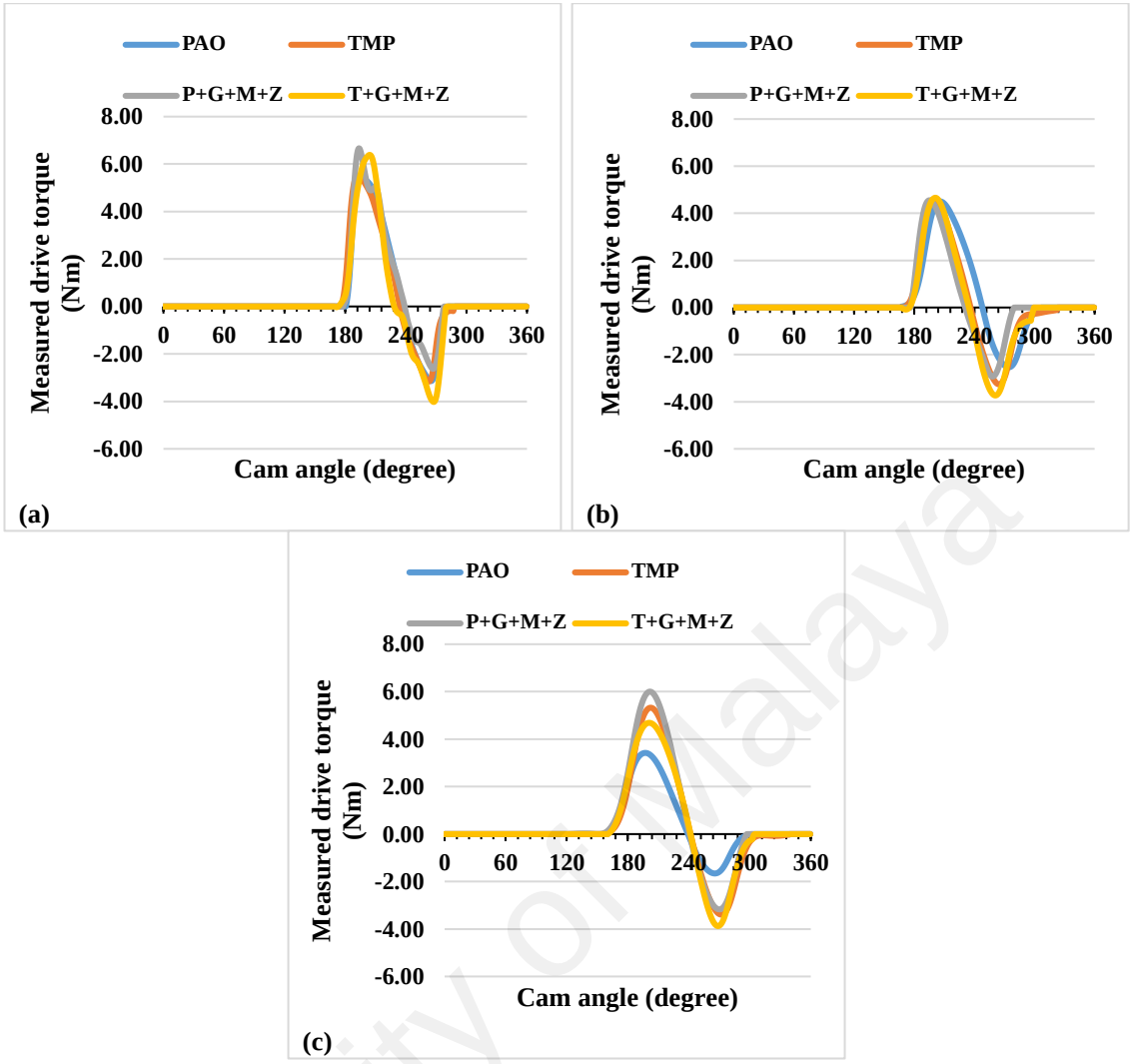

Figure 4.50: Instantaneous exhaust camshaft drive torque under motored condition with a-C:H:W-coated tappets and a-C:H:W-coated camlobes at lubricant temperature of 90ºC and camshaft speeds of (a) 400 RPM, (b) 800 RPM and (c) 1200 RPM

Reduction in average friction torque of a-C:H:W – a-C:H:W interface was seen when camshaft speed was increased from 400 RPM to 800 RPM irrespective of lubricant formulation. A similar behavior was also seen with U – U and a-C:H – a-C:H interfaces (**Figure 4.45** and **Figure 4.48**). When camshaft speed was further increased to 1200 RPM, friction torque was raised again almost to the same level of 400 RPM. This abnormality in friction behavior of a-C:H:W – a-C:H:W interface compared to U – U and a-C:H - a-C:H interface will be discussed in **section 4.6.4**.

When cylinder head testing was carried out at lubricant temperature of 40ºC, lower levels of friction between a-C:H:W-coated cam and tappet were witnessed compared to 90ºC, irrespective of camshaft speed and lubricant formulations. However, few exceptions to this finding were seen at camshaft speed of 800 RPM. Unlike friction results obtained at 90ºC, further decrease in friction torque values were observed when camshaft speed was increased from 800 RPM to 1200 RPM. An increase in friction torque of a-C:H:W – a-C:H:W interface was witnessed when formulated lubricants were used instead of additive-free ones. Like stated earlier, additives have a threshold temperature under which they cannot perform their intended role therefore, possible justification for this behavior can be ineffectiveness of additives at lower lubricant temperature.

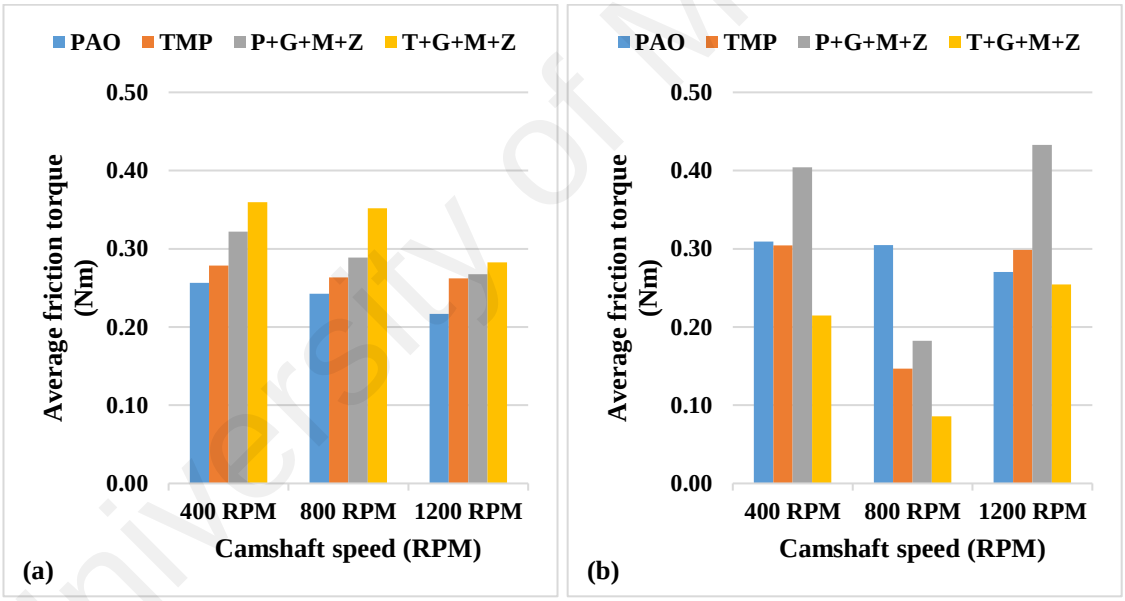

Figure 4.51: Average friction torque of exhaust camshaft under motored condition with a-C:H:W-coated tappets and a-C:H:W-coated camlobes at camshaft speeds of 400 RPM, 800 RPM and 1200 RPM and lubricant temperatures of (a) 40ºC and (b) 90ºC

4.6.2 Wear analysis

Wear volume of uncoated and DLC-coated tappets and nose wear of uncoated and DLC-coated camlobes after cylinder head testing at various conditions in the presence of

PAO-based and TMP-based lubricants are presented in **Figure 4.52** and **Figure 4.53** respectively.

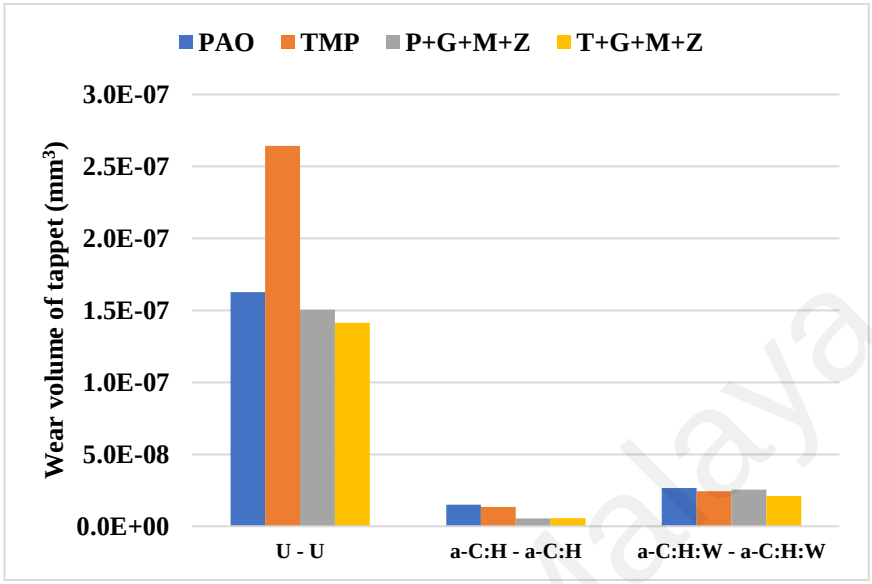

Figure 4.52: Wear volume of uncoated and DLC-coated tappets after cylinder head testing at various conditions in the presence of PAO-based and TMP-based lubricants

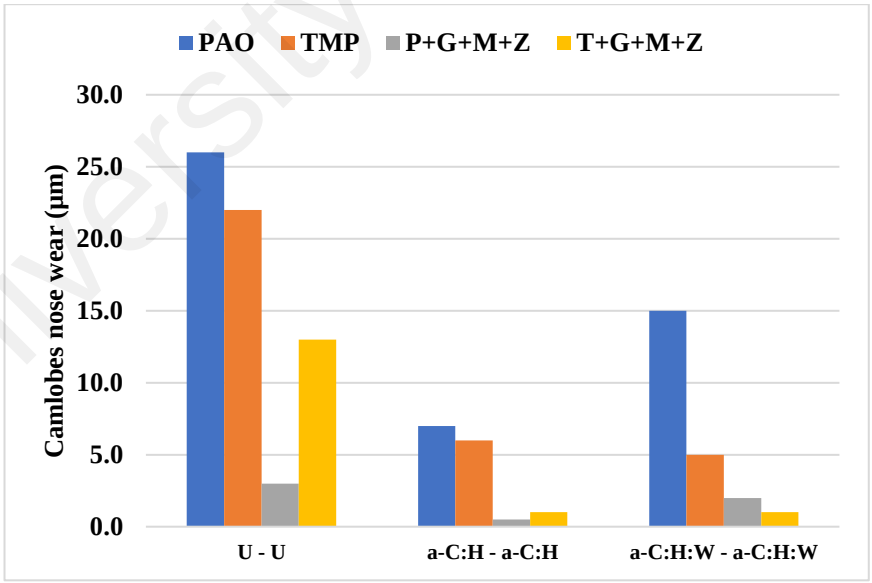

Figure 4.53: Nose wear of uncoated and DLC-coated camlobes after cylinder head testing at various conditions in the presence of PAO-based and TMP-based lubricants

4.6.2.1 Uncoated cam / uncoated tappet (U - U) interface

Optical images of uncoated tappets and uncoated camlobes are shown in **Figure 4.54** and **Figure 4.55** respectively. Among the base oils, additive-free PAO proved to be more effective in protecting the tappets from wearing-out compared to TMP whereas opposite trend was seen in the nose wear of camlobes (**Figure 4.52** and **Figure 4.53**). Different wear rates of interacting surfaces in the presence of same lubricant and test conditions was also noticed during tribotesting with pin-on-plate geometric configuration (**Figure 4.26** and **Figure 4.27**).

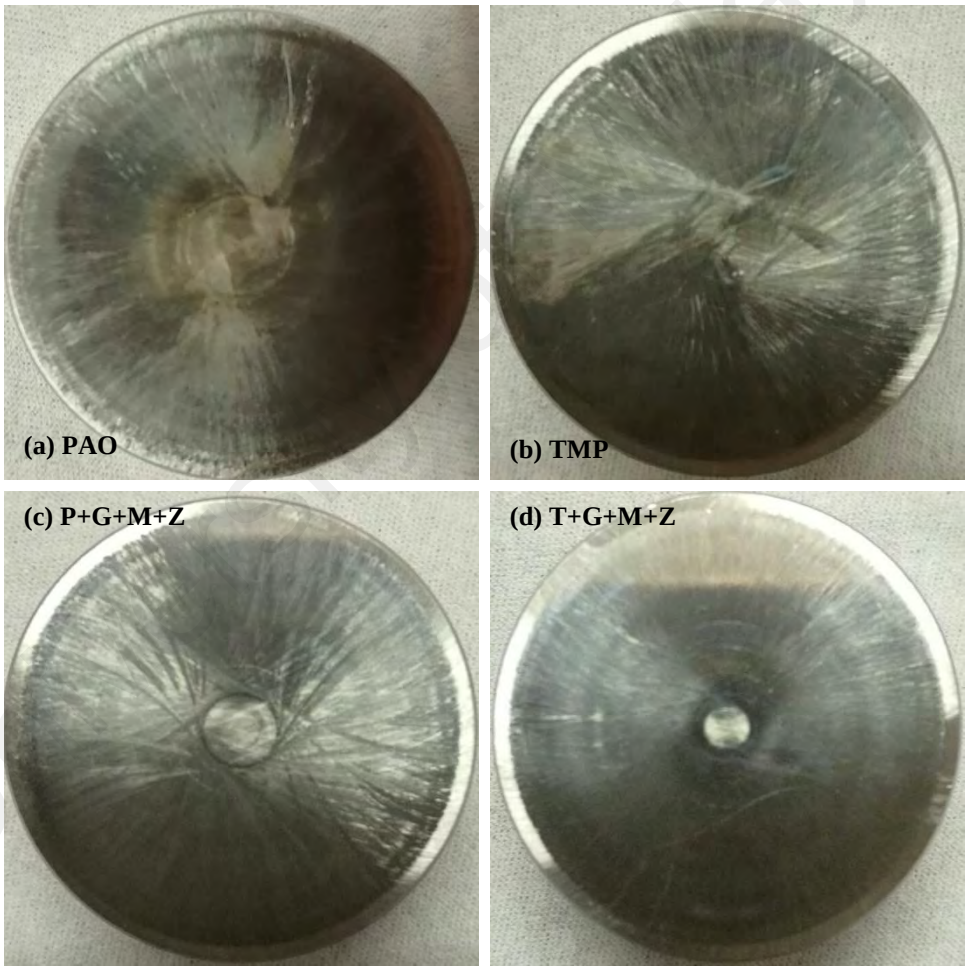

Figure 4.54: Optical images of uncoated tappets after cylinder head testing in combination with uncoated camlobes at various conditions in the presence of PAO-based and TMP-based lubricants

Additives were proved to be effective in further enhancing the wear characteristics of uncoated cam/tappet interface and resulted in significant decrease in wearing-out of both components. Lowest value of camlobe nose wear was seen when multi-additive containing PAO was used as lubricant whereas maximum wear protection to tappet was provided by T+G+M+Z. This improvement in wear behavior of uncoated cam/tappet interface in the presence of formulated lubricants can be attributed to formation of tribofilm as a result of tribochemical interaction between components and additives which will be discussed further in **section 4.6.4**..

Figure 4.55: Optical images of uncoated camlobes after cylinder head testing in combination with uncoated tappets at various conditions in the presence of PAO-based and TMP-based lubricants

4.6.2.2 a-C:H-coated cam / a-C:H-coated tappet (a-C:H - a-C:H) interface

Optical images of a-C:H-coated tappets and a-C:H-coated camlobes after cylinder head testing at various conditions are presented in **Figure 4.56** and **Figure 4.57**. Substantial improvement in wear behavior was observed when a-C:H-coated components were used instead of uncoated ones irrespective of lubricant formulation (**Figure 4.52** and **Figure 4.53**). Among the base oils, additive-free PAO proved to be more effective in protecting the tappet surface from wear compared to TMP. Further reduction in wear

volume of tappets were observed when formulated lubricants were used instead of additive-free ones. A similar trend was also seen in nose wear of a-C:H-coated camlobes. No signs of any peeling off or delamination of coating from the tappets was seen in the optical images irrespective of lubricant formulation. Although, most of the coating also remained intact on camlobe surface during cylinder head test, however, some delamination/wear was seen on one side of the cam nose especially when additive-free lubricants were used.

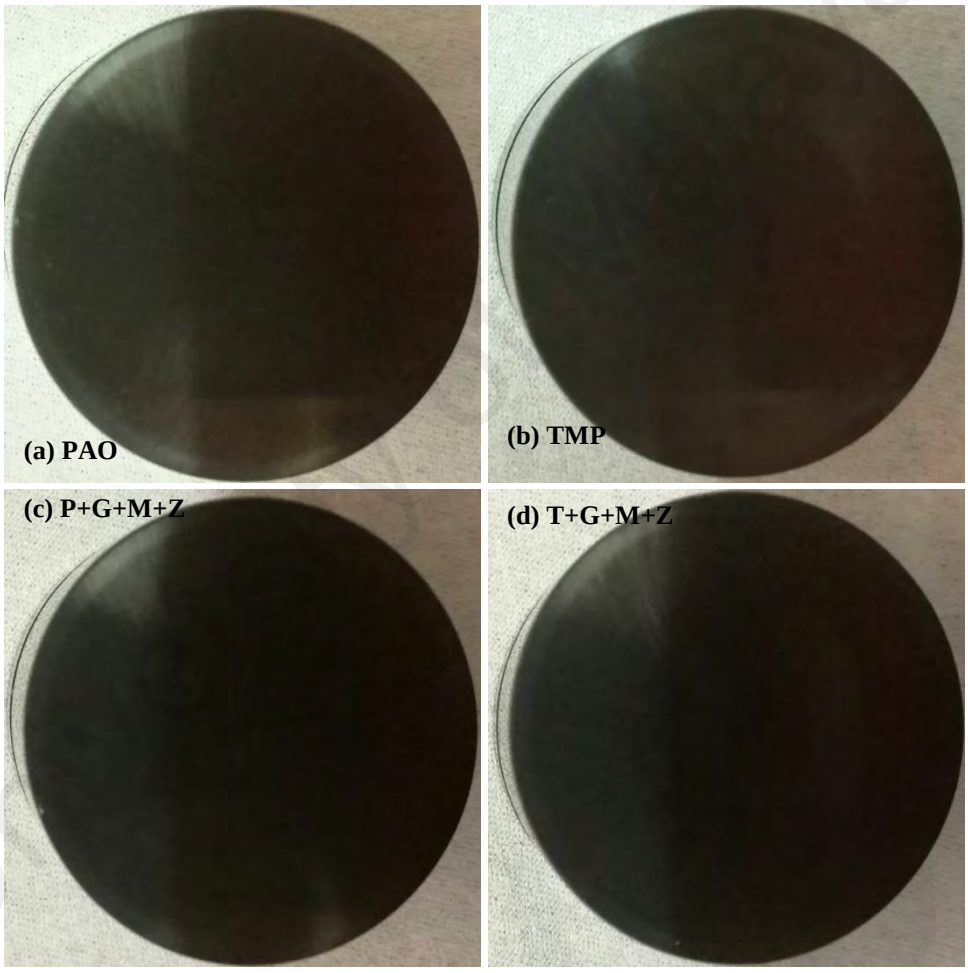

Figure 4.56: Optical images of a-C:H-coated tappets after cylinder head testing in combination with a-C:H-coated camlobes at various conditions in the presence of PAO-based and TMP-based lubricants

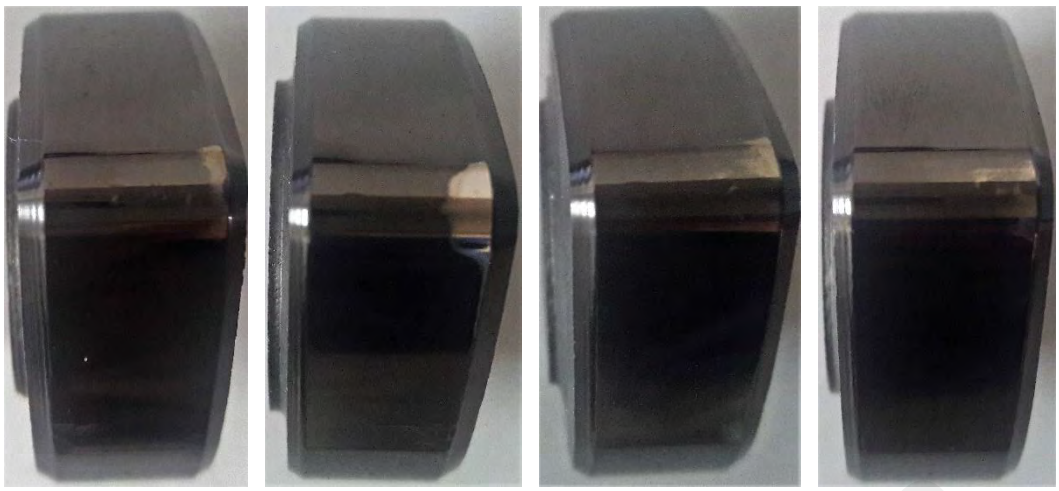

(a) PAO (b) TMP (c) P+G+M+Z (d) T+G+M+Z

Figure 4.57: Optical images of a-C:H-coated camlobes after cylinder head testing in combination with a-C:H-coated tappets at various conditions in the presence of PAO-based and TMP-based lubricants

4.6.2.3 a-C:H:W-coated cam / a-C:H:W-coated tappet (a-C:H:W - a-C:H:W) interface

Optical images of a-C:H:W-coated tappets and a-C:H:W-coated camlobes after cylinder head testing at various conditions are presented in **Figure 4.58** and **Figure 4.59**. On comparing wear volumes of uncoated and coated tappets, it can be seen that a-C:H:W-coated tappet lie in between the uncoated and a-C:H-coated one (**Figure 4.52**). A similar trend was also seen in the wear behavior of camlobes (**Figure 4.53**). Among the base oils, TMP proved to be more effective in providing wear protection to a-C:H:W – a-C:H:W interface compared to PAO. Coating was completely delaminated from the tappet surface when PAO-based lubricants were used. However, coating remained intact on outer periphery of tappet's top surface in the presence of TMP-based lubricants. Reduction in wearing-out of a-C:H:W-coated camlobes was observed when multi-additive containing lubricants, especially T+G+M+Z, were used,. A similar behavior was also seen when uncoated and a-C:H-coated cam/tappet interface as well. However, additives were not able to further enhance the wear characteristics of a-C:H-coated tappets. On comparing

the nose wear values of a-C:H:W-coated camlobes with the actual thickness of coating (3 μm), it can be easily apprehend that coating was completely delaminated or worn out after cylinder head testing in the presence of base oils but additives resulted in improved wear resistance of a-C:H:W-coated camlobes and delamination of coating was avoided. Since, LVDT measurements were only taken at one point of the camlobe nose due to design constraints, therefore, we cannot be sure whether delamination of coating was occurred at the whole width of camlobe nose or not when additive-free base oils were used.

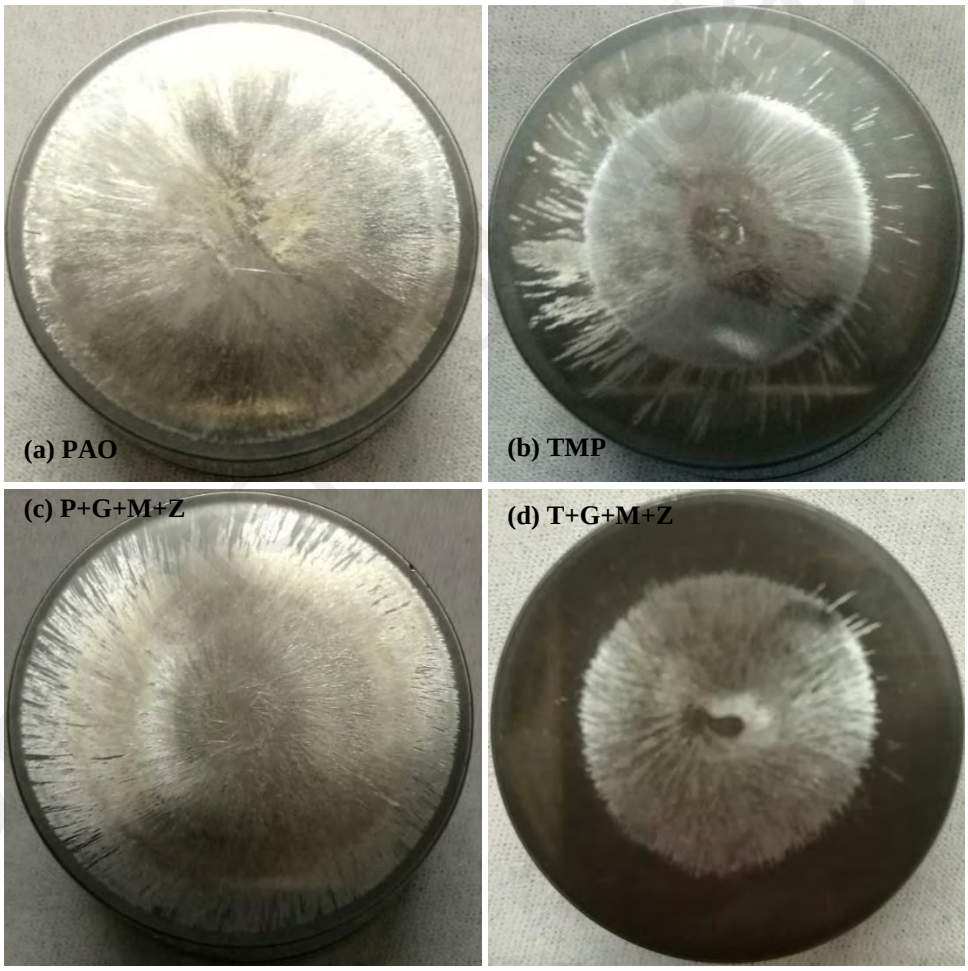

Figure 4.58: Optical images of a-C:H:W-coated tappets after cylinder head testing in combination with a-C:H:W-coated camlobes at various conditions in the presence of PAO-based and TMP-based lubricants

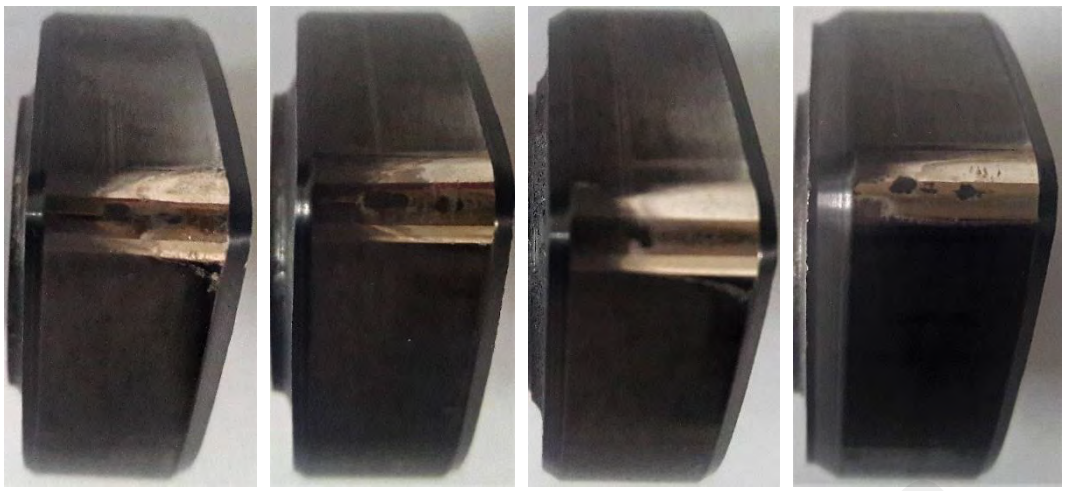

Figure 4.59: Optical images of a-C:H:W-coated camlobes after cylinder head testing in combination with a-C:H:W-coated tappets at various conditions in the presence of PAO-based and TMP-based lubricants

4.6.3 Tappet rotation analysis

Average rotational speed of uncoated and DLC-coated tappets during cylinder head testing at lubrication temperatures of 40ºC and 90ºC and camshaft speeds of 400 RPM, 800 RPM and 1200 RPM in the presence of PAO-based and TMP-based lubricants are shown in **Figure 4.60** and **Figure 4.61** respectively

4.6.3.1 Uncoated cam / uncoated tappet (U - U) interface

At lubricant temperature of 90ºC and camshaft speed of 400 RPM, PAO-based lubricants proved to be more effective in rotating the tappets in its bore compared to additive-free TMP and T+G+M+Z (**Figure 4.61**). Polar nature of TMP, due to which it adsorbs on the cam/tappet interface, results not only in friction reduction but also reduce cam traction to drive the tappet. Inability of tappets to rotate at high temperatures and low engine speed in the presence of certain lubricants was also reported by other researchers as well (Riaz A. Mufti & Jefferies, 2008; Riaz Ahmad Mufti, Zahid, Qureshi, & Aslam, 2015). An increase in rotational speed of tappet was seen when multi-additive containing PAO was used instead of additive-free PAO. It was also observed that rotational speed of

tappet was substantially lower than that of camshaft speed. This behavior shows significant amount of slippage between camlobe and tappet. Eloquent increase in rotational speed of tappet was observed when camshaft speed was increased from 400 RPM to 800 RPM and 1200 RPM irrespective of lubricant formulation (**Figure 4.61**). Increase in rotational speed of tappet at higher camshafts speeds can be attributed to increase in entraining velocity of lubricant and reduction in friction at tappet/bore interface (Riaz A. Mufti & Jefferies, 2008; Riaz Ahmad Mufti, Zahid, Qureshi, Aslam, et al., 2015). When camshaft speed increases, contribution of friction from tappet/bore interface decreases thus, it becomes easy for tappet to rotate. In the presence of T+G+M+Z, tappet started rotating at camshaft speed of 800 RPM and kept on rotating at 1200 RPM, however, rotational speeds were lower compared to rotational speeds obtained with P+G+M+Z. Similar to camshaft speed of 400 RPM, no rotational motion of tappet was seen in the presence of additive-free TMP even at 800 RPM and 1200 RPM.

When cylinder head tests were carried out at lubricant temperature of 40°C with U- U interface, a significant increase in rotational speed of tappet was observed irrespective of lubricant formulation (**Figure 4.60**). This ease of tappet rotation at 40°C can be attributed to hydrodynamic/elastohydrodynamic lubricant regime and low friction of tappet/bore interface compared to 90°C. Additive-free TMP, which was not able to rotate tappet at any of the tested camshaft speeds when lubricant temperature was kept at 90°C, demonstrated the similar behavior at 40°C. A significant increase in rotational speed of tappet was observed when P+G+M+Z was used as lubricant compared to additive-free PAO. A possible justification for this behavior can be increase in traction force between camlobes and tappet due to the presence of additives and reduction of circumferential friction at tappet/bore interface. A similar behavior was also seen by other researchers as well (Riaz A. Mufti & Jefferies, 2008; Riaz Ahmad Mufti, Zahid, Qureshi, & Aslam, 2015).

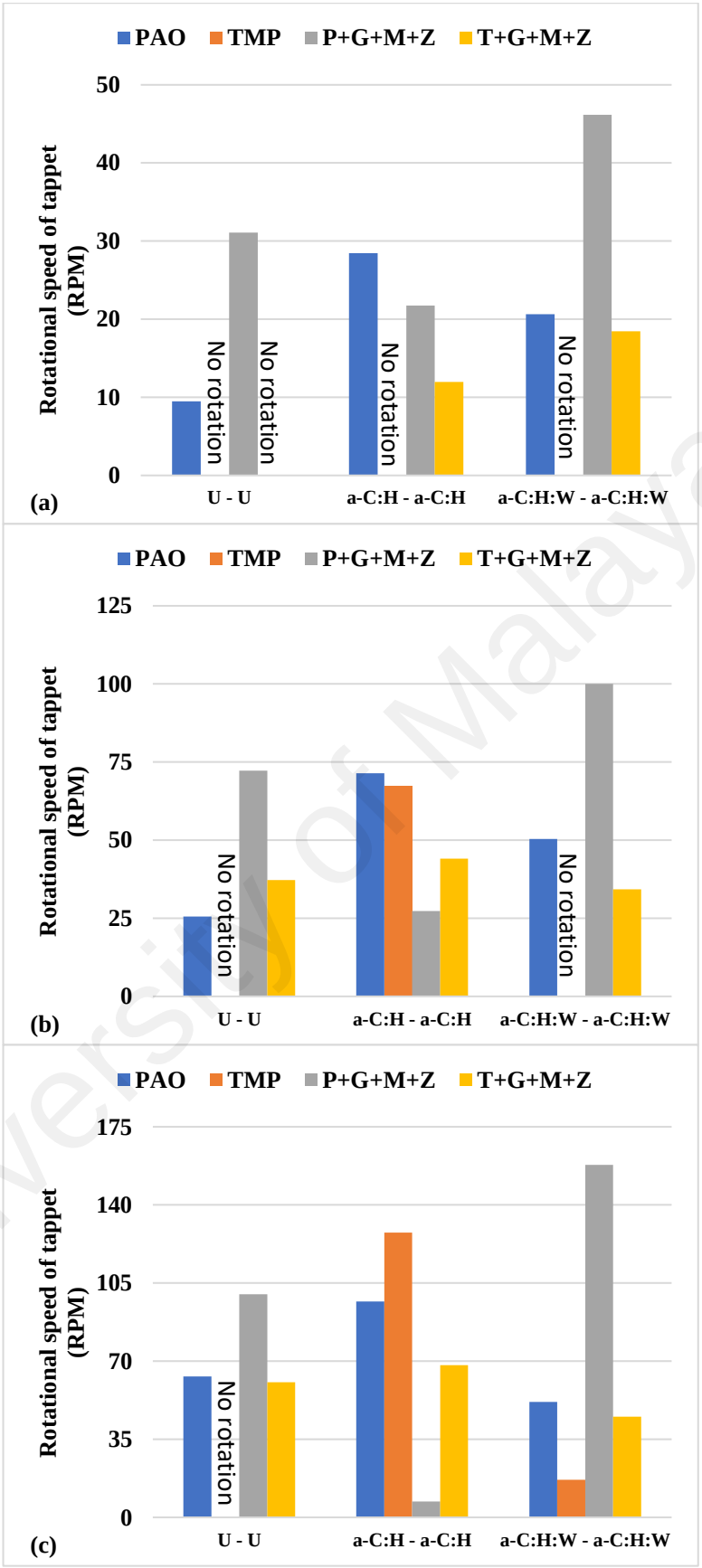

Figure 4.60: Average rotational speed of uncoated and DLC-coated tappets during cylinder head testing at lubrication temperature of 40ºC and camshaft speeds of (a) 400 RPM, (b) 800 RPM and (c) 1200 RPM in the presence of PAO-based and TMP-based lubricants

4.6.3.2 a-C:H-coated cam / a-C:H-coated tappet (a-C:H - a-C:H) interface

Similar to U -U interface, additive-free PAO proved to be more effective in uniformly rotating the a-C:H-coated tappet in its bore compared to TMP at lubricant temperature of 90ºC and camshaft speed of 400 RPM (**Figure 4.61**. Although, further increase in rotational speed of a-C:H-coated tappet was seen when P+G+M+Z was used as lubricant instead of additive-free PAO but opposite behavior was seen in TMP-based lubricants. A direct relation between rotational speed of tappet and wearing rates of a-C:H-coated tappets and camlobes was witnessed and lower values of wear volume of tappets and nose wear of camlobes were seen in the presence of P+G+M+Z compared to T+G+M+Z (**Figure 4.52** and **Figure 4.53**). An increase in rotational speed of a-C:H-coated tappets was seen when camshaft speed was increased from 400 RPM to 800 RPM. However, exceptions were seen when cylinder head tests were carried out in the presence of PAO-based lubricants at camshaft speed of 1200 RPM (**Figure 4.61**).

Similar to uncoated tappets, increase in rotational speeds of a-C:H-coated tappets were witnessed when engine tests were carried out at lubricant temperature of 40ºC irrespective of camshaft speed and lubricant formulation (**Figure 4.60**). Only exception to above finding was seen when P+G+M+Z was used as lubricant especially at 1200 RPM. Like stated before, increase in rotational speed of tappet at 40°C, compared to 90°C, can be related to hydrodynamic/elastohydrodynamic lubricant regime and low friction of tappet/bore interface. Among the tested lubricants, highest rotational speed of a-C:H-coated tappet of 127.66 RPM was observed when TMP was used as lubricant at 40°C and camshaft speed of 1200 RPM whereas no rotation of tappet was detected when camshaft speed was reduced to 400 RPM in the presence of same lubricant at the same temperature.

In comparison to uncoated tappets, a-C:H-coated ones rotated at higher rotational speeds irrespective of lubricant formulation, lubricant temperature and camshaft speed.

A possible justification for this behavior can be lower levels of tappet/bore friction due to presence of the coating at the outer periphery of the tappets. High rotational speed of a-C:H-coated tappets resulted in effective lubrication of the contact due to which wear resistance of sliding components were greatly improved (**Figure 4.52** and **Figure 4.53**). Another difference was seen in the rotational behavior of uncoated and a-C:H-coated tappet when additive-free TMP was used as lubricant. Although, TMP was not able to rotate uncoated tappet irrespective of cylinder head running conditions but very high rotational speeds of tappet were observed when a-C:H – a-C:H interface was used.

4.6.3.3 a-C:H:W-coated cam / a-C:H:W-coated tappet (a-C:H:W - a-C:H:W) interface

Inability of a-C:H:W-coated tappet to rotate inside its bore was witnessed when additive-free PAO was used as lubricant at lubricant temperature of 90ºC and camshaft speed of 400 RPM (**Figure 4.61**). Although, TMP was able to rotate tappet around its axis but at very low speeds. Similar rotational behavior was also seen when uncoated tappets were slid against uncoated camlobes in the presence of base oils but inability of tappet to rotate was seen with TMP instead of PAO. A significant increase in rotational speed of a-C:H:W-coated tappet was observed with formulated lubricants resulting in efficient lubrication of contact and eloquent decrease in wearing-out of valve train components (**Figure 4.52** and **Figure 4.53**). A possible justification for this behavior can be increase in traction force between camlobes and tappet due to the formation of additive-derived tribofilm and reduction of circumferential friction at tappet/bore interface. An increase in rotational speed of a-C:H:W-coated tappets was seen when camshaft speed was increased. Although, low rotational speed of tappet was observed in the presence of TMP at 400 RPM but when the speed was increased to 800 RPM, tappet stopped rotating. Inability of tappet to rotate in the presence of PAO continued at 800 RPM but when camshaft speed was further increased to 1200 RPM, tappet started to rotate

around its axis. On comparing rotational behavior of uncoated and coated tappets, it can be clearly seen that a-C:H:W-coated tappets rotated at much higher speeds compared to others when cylinder tests were carried out at lubricant temperature of 90°C and camshaft speeds of 800 RPM and 1200 RPM (**Figure 4.61**).

Eloquent increase in rotational speed of a-C:H:W-coated tappet was witnessed when cylinder head testing was conducted at lubricant temperature of 40ºC irrespective of camshaft speed and lubricant formulation (**Figure 4.60**). Among uncoated and DLC-coated tappets, highest rotational speed of 157 RPM was witnessed with a-C:H:W-coated tappet in the presence of P+G+M+Z, lubricant temperature of 40°C and camshaft speed of 1200 RPM. Exceptions to above-mentioned finding were witnessed at camshaft speed of 800 RPM and 1200 RPM in the presence of T+G+M+Z. Although, rotational motion of tappet was not seen when temperature of PAO was maintained at 90ºC but when it was reduced to 40ºC, tappet started to rotate. On the other hand, tappet stopped rotating when temperature of TMP was reduced to 40ºC at camshaft speed of 400 RPM. These observations show that cam/tappet and tappet/bore interactions are complex and interlinked with each other, and to encourage tappet rotation, a balance of forces is required between the two interactions.

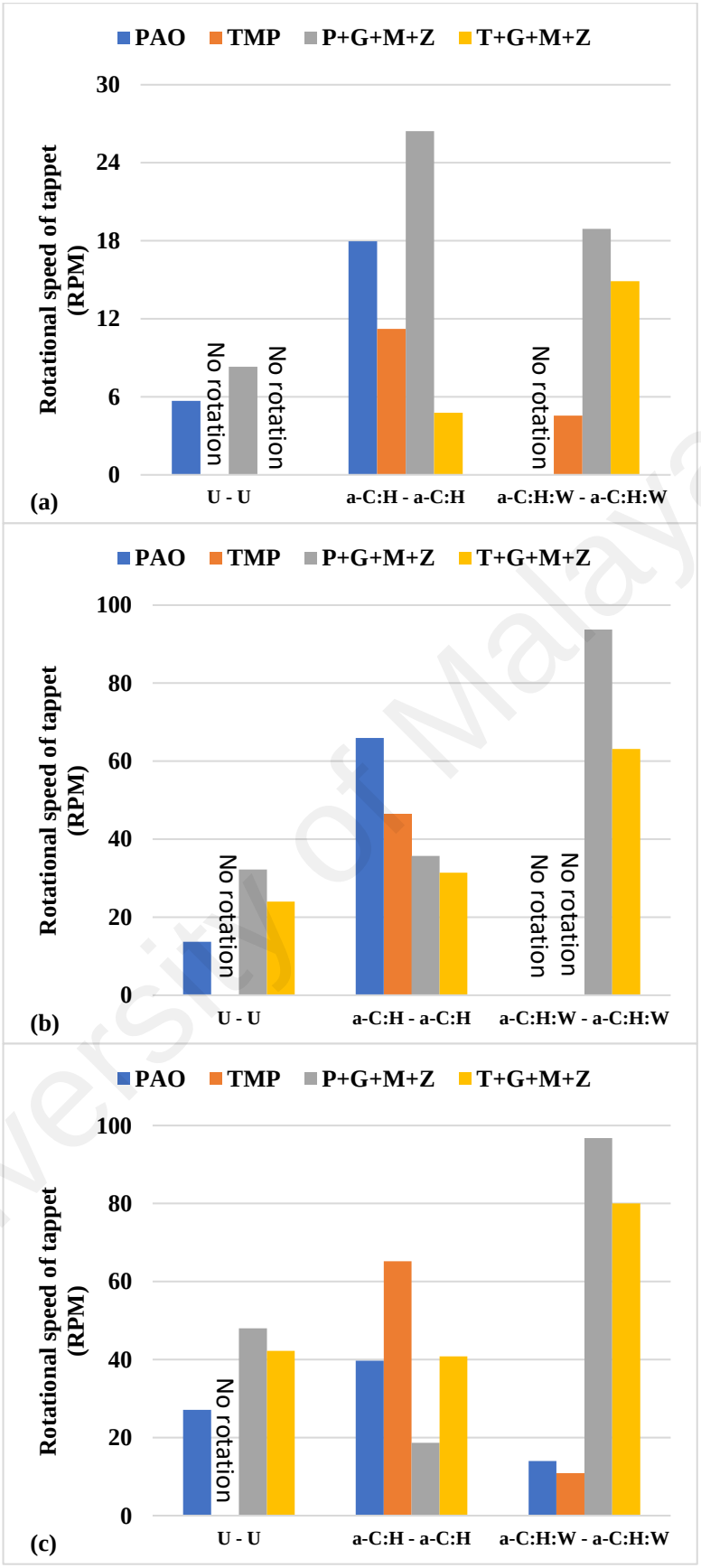

Figure 4.61: Average rotational speed of uncoated and DLC-coated tappets during cylinder head testing at lubrication temperature of 90ºC and camshaft speeds of (a) 400 RPM, (b) 800 RPM and (c) 1200 RPM in the presence of PAO-based and TMP-based lubricants

4.6.4 SEM/EDS analysis

4.6.4.1 Uncoated cam / uncoated tappet (U - U) interface

SEM micrographs of uncoated tappets after cylinder head testing at various conditions in combination with uncoated camlobes in the presence of PAO-based and TMP-based lubricants are shown in **Figure 4.62** whereas atomic percentage of elements found on uncoated tappets are presented in **Table 4.20**. In **Figure 4.62a**, horizontal lines shown at the left-hand side of the micrograph represents unaltered outer boundary of the tappet on its top surface whereas vertical lines show scratch marks due to sliding of camlobe. Severe deterioration on tappet surface can be seen in **Figure 4.62b** and **Figure 4.62c** in the presence of additive-free PAO due to formation of cracks and crevices as a result of adhesive wear. When TMP was used as lubricant instead of PAO, adhesive wear by replaced by abrasive and corrosive wear (**Figure 4.62e** and **Figure 4.62f**). Another significant difference which was seen in the micrographs of PAO and TMP was the direction of scratch lines. In case of PAO, scratch lines were found to be parallel to each other due to uniform rotation of tappet in one direction. On the other hand, crisscross pattern was formed when TMP was used as lubricant due to bidirectional jerky motion of tappet inside the bore due to which tappet was not able to complete rotation resulting in rotational speed of zero at all test conditions. Bidirectional jerky motion of tappet was confirmed after seeing it through the transparent cylinder head cover. As a result, accelerated wearing out of tappet was observed in the presence of TMP (**Figure 4.52**). Significant improvement in wear resistance of uncoated tappets was seen when formulated lubricants were used and adhesive/corrosive wear was replaced by abrasive wear. Although, crisscross pattern was also seen in the micrograph of T+G+M+Z but it was not as much concentrated as additive-free TMP (**Figure 4.62l)** because jerky bidirectional motion of tappet was only observed at camshaft speed of 400 RPM irrespective of lubricant temperature.

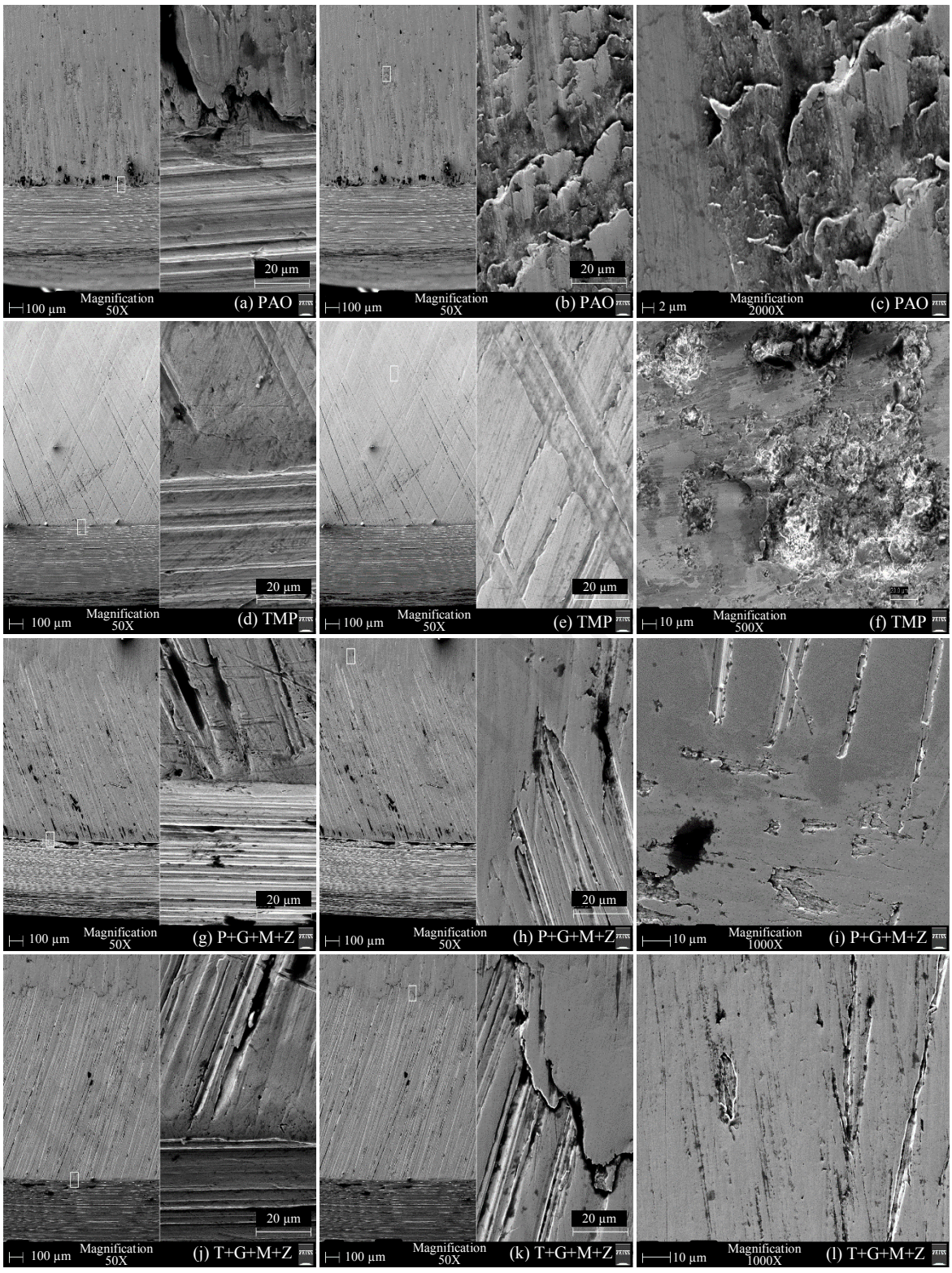

Figure 4.62: SEM micrographs of uncoated tappets after cylinder head testing at various conditions in combination with uncoated camlobes in the presence of PAO-based and TMP-based lubricants

EDS analysis shows that improvement in friction and wear behavior of U – U interface, observed when formulated lubricants were used instead of additive-free base oils, was due to the tribofilm formation composed of molybdenum, sulfur, phosphorus and zinc, on tappet surface as a result of tribochemical interaction between additives and sliding surfaces (**Table 4.20**).

Table 4.20: Atomic percentage of elements found on uncoated tappets after cylinder head testing at various conditions in combination with uncoated camlobes in the presence of PAO-based and TMP-based lubricants

Lubricants	Elements						
	C	P	S	Mo	Zn	Fe	O
PAO	13.18	-	-	-	-	68.09	18.73
TMP	14.33	-	-	-	-	70.56	15.11
P+G+M+Z	13.61	2.58	1.29	2.37	3.41	68.71	8.03
T+G+M+Z	20.69	1.29	0.71	1.49	2.11	65.84	7.87

4.6.4.2 a-C:H-coated cam / a-C:H-coated tappet (a-C:H - a-C:H) interface

SEM micrographs of a-C:H-coated tappets after cylinder head testing are presented in **Figure 4.63** whereas atomic percentage of elements found on a-C:H-coated tappets are shown in **Table 4.21**. In these micrographs, abrasive wear can be seen as predominant wear mechanisms resulting in scratch lines on the top tappet surface due to sliding of camlobes. Although, coating was slightly worn-out when TMP-based lubricants were used especially additive-free TMP, resulting in exposed CrN interlayer and ferrous substrate but no sign of severe coating delamination were seen in any of these micrographs. When additive-free PAO was used, a-C:H coating was able to maintain its structural integrity and sustained the testing conditions with few scratch marks and wear debris (**Figure 4.63c**). Contrary to that, top DLC layer was removed from the tappet surface resulting in exposed CrN interlayer and ferrous substrate in the presence of TMP

(**Figure 4.63e** and **Table 4.21**). White-colored dots which can be seen in **Figure 4.63e and Figure 4.63f** are actually due to the exposed CrN interlayer whereas white-colored patches in **Figure 4.63f** represents ferrous substrate. Low content of carbon and presence of chromium, nitrogen and ferrous in EDS results confirmed the removal of top DLC layer resulting in the exposed CrN inlayer and ferrous substrate. An increase in oxygen content was also seen when TMP was used as lubricant instead of PAO. This can be attributed to oxidation of exposed ferrous substrate resulting in the formation of FeO and Fe_2O_3. Significant improvement in wear resistance of a-C:H-coated tappets was seen when formulated version of TMP was used as lubricant instead of additive-free TMP. Although, exposed CrN interlayer was seen at few spots but ferrous substrate was neither seen in SEM micrographs nor in EDS analysis. Similar to SEM micrographs of PAO, scratch lines and fine wear debris can be seen in the micrographs of P+G+M+Z. Although, white-colored patch can be seen which actually represents exposed ferrous substrate due to the delamination of both top a-C:H and CrN interlayer in **Figure 4.63h** but overall coating was able to strongly adhered to be substrate till the end of cylinder head testing as can be seen in **Figure 4.63i**. Since, low concentrations of additive-derived elements were seen in EDS analysis, therefore, tribological improvement seen in a-C:H - a-C:H interface was mostly due to the hindrance in the occurrence of graphitization phenomenon in addition to tribofilm formation.

Table 4.21: Atomic percentage of elements found on a-C:H-coated tappets after cylinder head testing at various conditions in combination with a-C:H-coated camlobes in the presence of PAO-based and TMP-based lubricants

Lubricants	Elements									
	C	**Cr**	**N**	**P**	**S**	**Mo**	**Zn**	**Fe**	**O**	**Ar**
PAO	97.07	-	-	-	-	-	-	-	2.52	0.41
TMP	64.52	7.61	3.41	-	-	-	-	11.72	12.74	-
P+G+M+Z	94.41	0.67	-	0.12	0.32	1.66	1.33	-	1.49	-
T+G+M+Z	79.33	7.94	2.98	0.12	0.25	1.03	0.37	-	7.98	-

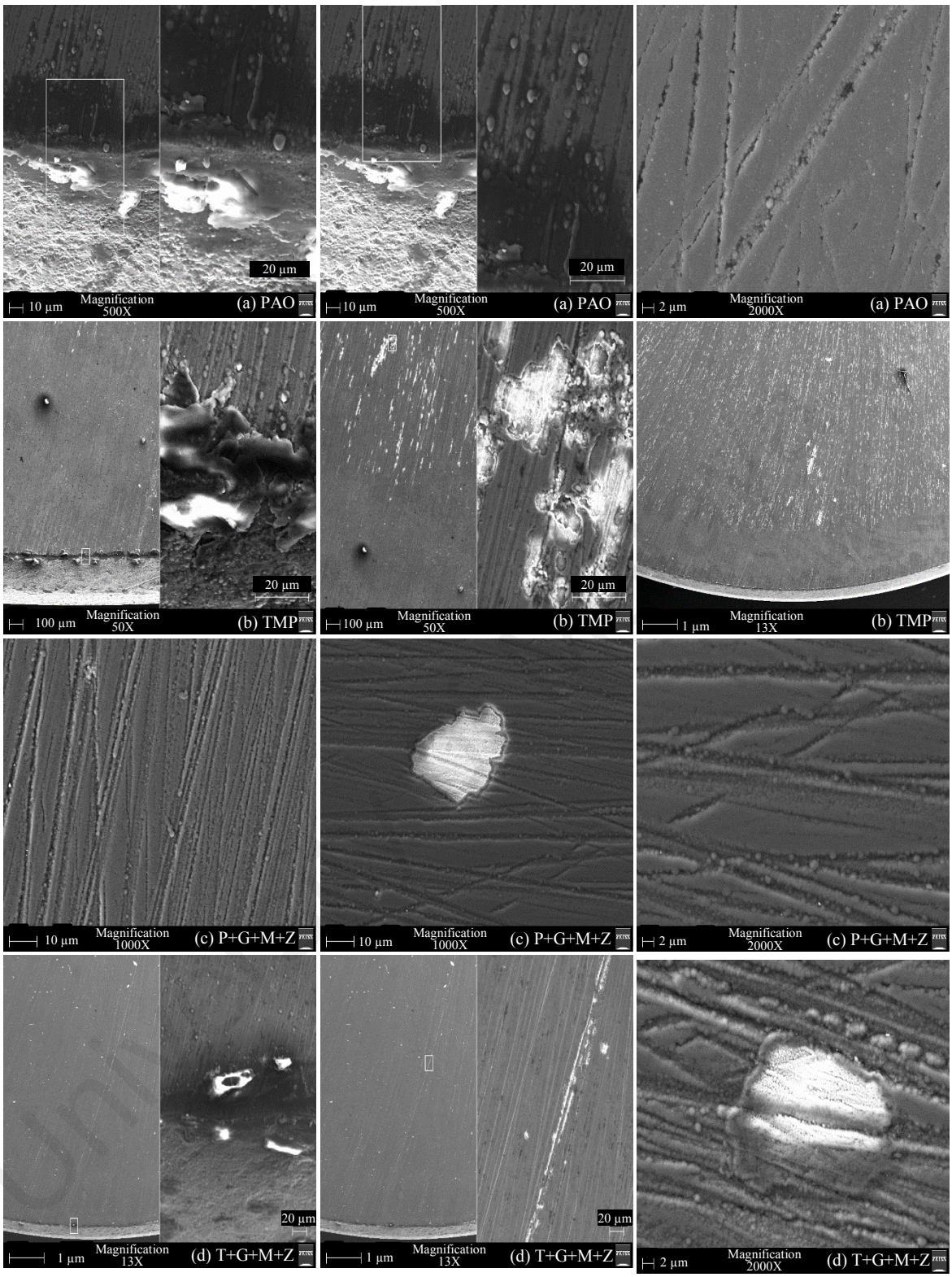

Figure 4.63: SEM micrographs of a-C:H-coated tappets after cylinder head testing at various conditions in combination with a-C:H-coated camlobes in the presence of PAO-based and TMP-based lubricants

4.6.4.3 a-C:H:W-coated cam / a-C:H:W-coated tappet (a-C:H:W - a-C:H:W) interface

SEM micrographs of a-C:H:W-coated tappets after cylinder head testing at various conditions in combination with a-C:H:W-coated camlobes in the presence of PAO-based and TMP-based lubricants are shown in **Figure 4.64** whereas atomic percentage of elements found on a-C:H:W-coated tappets are presented in **Table 4.22**. Severe delamination of top a-C:H:W coating was observed resulting in exposed CrN interlayer and ferrous substrate when additive-free PAO was used. In **Figure 4.64b**, three distinct layers of top a-C:H:W layer (dark grey layer at top left and top right corners), CrN interlayer (light grey layer at the top center) and ferrous substrate (white layer at the bottom) can be clearly seen. As a result, a-C:H:W - a-C:H:W interface was changed to CrN - CrN and/or U – U interface. Presence of chromium, nitrogen and ferrous in higher concentration and reduction in percentage of carbon and tungsten compared to as-deposited a-C:H:W coating in EDS analysis also confirmed severe deterioration. Significant improvement in wear resistance of a-C:H:W-coated tappet was observed when additive-free TMP was used as lubricant. Although, removal of top DLC layer was also seen in the presence of TMP resulting in exposed CrN interlayer and ferrous substrate but not to the extent of PAO. In the presence of base oils, pitting and abrasive wear was also seen as predominant wear mechanism in addition to delamination. Improvement in structural integrity of DLC coating was observed when formulated lubricants were used as a result of which its delamination was avoided especially at the outer boundary of the tappet. Not only this, significant reduction in nose wear was also seen when P+G+M+Z and T+G+M+Z were used as lubricant instead of their additive-free versions. Hindrance in the occurrence of graphitization phenomenon due to the presence of additives and formation of additive-derived tribofilm can be possible reasons for this enhanced wear

behavior. Formation of additive-derived tribofilm composed of molybdenum, sulfur, phosphorus and zinc was also confirmed by EDS analysis.

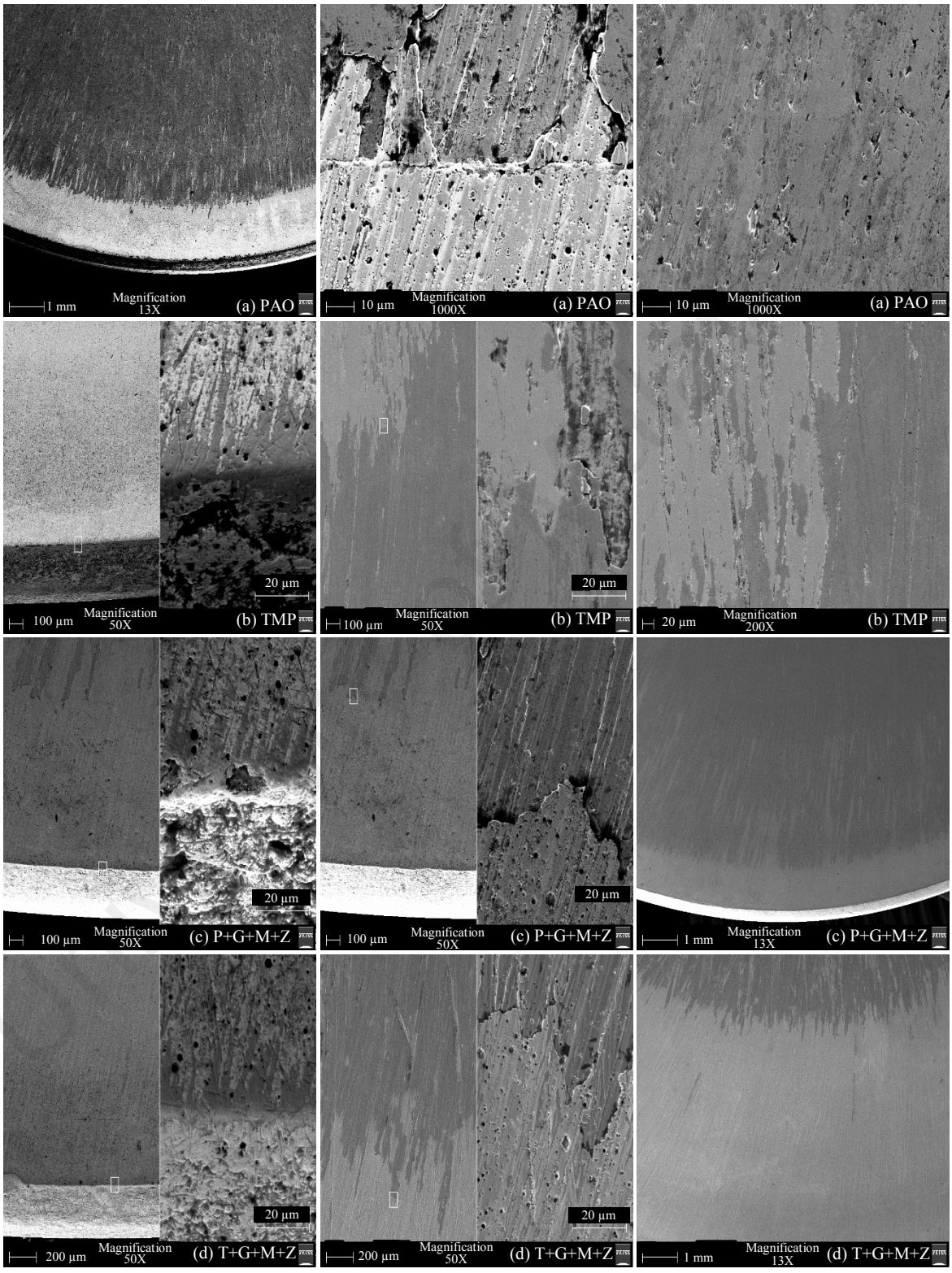

Figure 4.64: SEM micrographs of a-C:H:W-coated tappets after cylinder head testing at various conditions in combination with a-C:H:W-coated camlobes in the presence of PAO-based and TMP-based lubricants

Table 4.22: Atomic percentage of elements found on a-C:H:W-coated tappets after cylinder head testing at various conditions in combination with a-C:H:W-coated camlobes in the presence of PAO-based and TMP-based lubricants

Lubricants	Elements						
	C	**W**	**Cr**	**N**	**Fe**	**O**	**Ni**
PAO	35.3	7.3	4.8	6.0	32.5	10.7	3.4
TMP	60.1	14.9	6.2	2.4	2.7	9.0	4.6
P+G+M+Z	39.6	11.5	10.1	9.2	21.9	3.4	4.2
T+G+M+Z	11.9	0.4	11.0	10.7	57.3	8.7	-

4.6.5 Surface roughness analysis

R_a value of uncoated and DLC-coated tappets after cylinder head testing at various conditions in combination with uncoated and DLC-coated camlobes in the presence of PAO-based and TMP-based lubricants is shown in **Figure 4.65**.

4.6.5.1 Uncoated cam / uncoated tappet (U - U) interface

TMP-based lubricants resulted in severe deterioration of top tappet surface and high values of surface roughness compared to those containing PAO as base oil. This can be attributed to inability of tappet to rotate when TMP and T+G+M+Z were used as lubricants separately resulting in localized wear, pitting and fatigue. On the other hand, uniform rotational speed of tappet in the presence of PAO-based lubricants culminated in effective lubrication of cam/tappet interface, uniform wearing of interacting components and reduced sliding friction. Although, additives were proved to be effective in reducing friction and wear of U -U interface but they were not able to protect the tappet surface from severe roughening. As a result, an increase in surface roughness values was observed when formulated lubricants were used compared to their additive-free versions.

4.6.5.2 a-C:H-coated cam / a-C:H-coated tappet (a-C:H - a-C:H) interface

Among the base oils, additive-free TMP proved to be less effective, compared to PAO, in protecting the a-C:H-coated tappet from surface deterioration. Highest R_a value of a-C:H-coated tappet observed in the presence of TMP can be attributed to removal of top DLC coating and exposure of CrN interlayer and ferrous substrate. Another justification for this behavior can be chemically inert nature of a-C:H coating due to which polar components of TMP were not able to adsorb on the contact area resulting in lubricant slippage and metal-to-metal contact. As a result, TMP resulted in inferior tribological performance compared to PAO at most of the cylinder head running conditions. When formulated version of TMP was used instead of TMP, delamination and wearing-out of DLC coating was replaced by polishing wear as a result of which significant decrease in R_a value was seen. A similar behavior was also seen when PAO-based lubricants were used.

4.6.5.3 a-C:H:W-coated cam / a-C:H:W-coated tappet (a-C:H:W - a-C:H:W) interface

Contrary to uncoated and a-C:H-coated cam/tappet interface, more deterioration in the top surface of a-C:H:W-coated tappet was observed with additive-free PAO instead of TMP. A possible justification for this behavior can be complete delamination of DLC coating in the presence of PAO resulting in exposed ferrous substrate whereas delamination of coating was avoided especially at the outer boundary of the tappet when TMP was used as lubricant (**Figure 4.58**). Although, formulated version of PAO was able to protect the tappet surface from deterioration but still value of surface roughness was higher than that of additive-free TMP. No such behavior was seen when T+G+M+Z was used as lubricant instead of TMP. Rather, 50% increase in surface roughness value of tappet was observed in the presence of T+G+M+Z. This difference in surface protection capability of same additives when mixed in different base oils can be attributed to

variation in rotational speeds of tappets during cylinder head testing. High rotational speeds of tappets were observed in the P+G+M+Z compared to T+G+M+Z irrespective of lubricant temperature and camshaft speed.

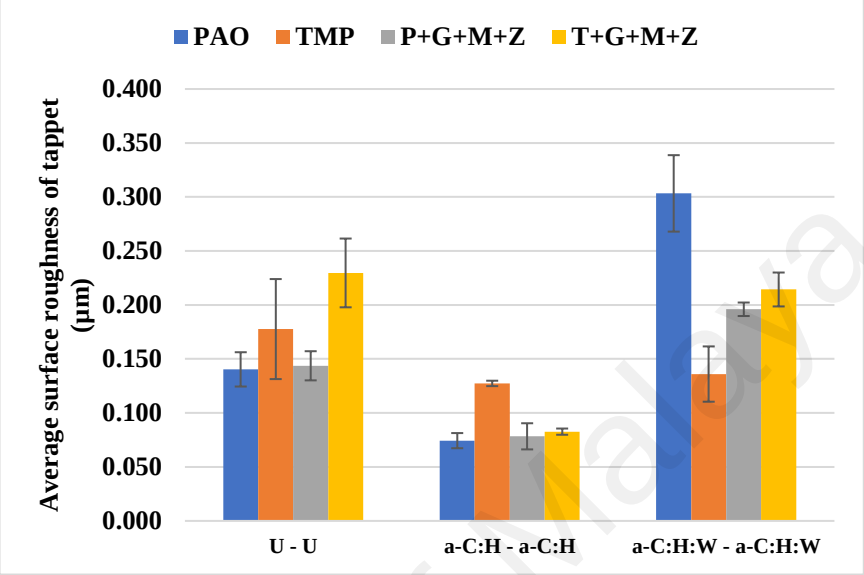

Figure 4.65: Average surface roughness of uncoated and DLC-coated tappets after cylinder head testing at various conditions in combination with uncoated and DLC-coated camlobes in the presence of PAO-based and TMP-based lubricants

4.6.6 Summary

Generally, reduction in friction torque between camlobe and tappet was observed with an increase in camshaft speed and decrease in lubrication temperature. During cylinder head testing, lowest values of friction torque were observed when a-C:H:W-coated components were used whereas maximum friction was seen with uncoated tappets and camlobes. Among the tested lubricants, P+G+M+Z proved to be most effective in reducing the friction between cam and tappet whereas PAO proved to be least effective.

Lowest values of wear volumes of tappets and nose wear of camlobes were observed when a-C:H-coated components were used followed by a-C:H:W-coated ones. T+G+M+Z was proved to be most effective in protecting the tappets from surface

deterioration and excessive wearing whereas TMP resulted in aggravated wear. Maximum camlobe nose wear was observed when PAO was used as lubricant whereas P+G+M+Z resulted in maximum wear protection.

In optical images of uncoated and DLC-coated tappets after cylinder head testing, a lot of surface deterioration was seen in the uncoated tappets especially when additive-free lubricants were used. On the other hand, a-C:H coating was able to maintain its structural integrity throughout the test and delamination was not observed irrespective of lubricant type. Contrary to that, most of the coating was delaminated from a-C:H:W-coated tappets especially when PAO-based lubricants were used. Similar delamination pattern and wear behavior was also seen in camlobes. However, some of the coating was also removed from right edge of the nose of a-C:H-coated camlobes as well. In case of camlobes, coating was only delaminated from the nose area and cam flanks whereas it remained intact on base circle.

Rotation of tappet in its bore is very necessary to proper lubrication of cam/tappet interface that's why rotational speed of tappets were measured. DLC coatings proved to be very helpful in achieving high rotational speeds of the tappets compared to uncoated ones. An increase in rotational speed of tappets was seen with an increase in camshaft speed and decrease in lubricant temperature. Highest rotational speed was observed when a-C:H:W-coated tappet was used in combination with P+G+M+Z at 40ºC and camshaft speed of 1200 RPM.

Based on the above-mentioned observations, it can be concluded that a-C:H coating is most suitable coating for cam/tappet interface of direct acting valve train assembly of commercial diesel engine. Moreover, conventional lubricant additives which are actually optimized for conventional base oils and materials are also tribologically compatible with TMP and a-C:H coating.

CHAPTER 5: CONCLUSIONS AND SUGGESTIONS FOR FUTURE WORK

5.1 Conclusions

In this study, tribological compatibility of conventional lubricant additives with various types of DLC coatings and TMP has been analyzed for cam/tappet interface of direct acting valve train assembly of passenger car diesel engine. Important conclusions which can be drawn from the experimental results and discussions are as follows:

1. Viscosity index of additive-free TMP is 1.5 times more compared to PAO which shows its viscosity is more stable over a wide range of temperature. Other physicochemical properties such as kinematic viscosity and density of both base oils are comparable. No significant change in physicochemical properties was observed when base oils were formulated with additives.

(a) Extreme pressure characteristics and load carrying capacity of additive-free and formulated versions of TMP proved to be superior compared to PAO-based lubricants. Although, LNSL and ISL were higher but TMP-based lubricants were able to carry 10-20 kg more load without welding of interacting surfaces.

(b) Formulated versions of TMP showed better extreme pressure characteristics at medium and high values of applied load whereas additives seemed to be ineffective at lower values of applied loads.

2. Additive-free TMP demonstrated better friction performance compared to PAO whereas latter proved to be more effective in mitigating the wear of interacting surfaces compared to former when tribotesting was carried out using universal wear testing machine with ball-on-plate geometric configuration.

(a) Deterioration in tribological performance was seen when uncoated steel ball was used as counterbody against DLC-coated plate resulting in higher friction coefficient and accelerated wearing-out of ball. However, a decrease in wear coefficient of DLC-

coated plate was seen when uncoated steel ball was used as counterbody instead of DLC-coated one.

(b) Conventional lubricant additives (GMO, MoDTC and ZDDP), which are actually optimized for conventional base oils and materials, also proved to be effective in TMP and resulted in improved tribological performance of symmetrical and asymmetrical DLC contacts.

(c) Optimum tribological performance was observed when a-C:H-coated plate and ball were used as sliding surfaces. On the other hand, highest friction and wear coefficient of plate were observed with ta-C/ta-C contact whereas a-C:H:W/steel contact resulted in highest wear coefficient of ball. TMP+GMO proved to be most effective lubricant in facilitating the sliding whereas ZDDP-based lubricants and PAO+GMO resulted in lowest wear coefficients irrespective of interacting surface material.

3. Due to its unsaturated and polar structure, additive-free TMP demonstrated better friction performance and wear behavior of plate when tribotesting was carried out using universal wear testing machine with pin-on-plate geometric configuration. Exceptions to this finding were observed when uncoated cast-iron pins were used in combination with DLC-coated plates

(a) Additive-free PAO outperformed TMP in mitigating the wear of pin. Additive-free TMP was not able to provide sufficient wear protection and resulted in high wear coefficients.

(b) Tribological improvements seen in symmetrical and asymmetrical DLC contacts in the presence of formulated lubricants were due to their inherent self-lubrication characteristics, tribochemical interactions with additives resulting in the formation of tribofilm and/or surface graphitization.

(c) Optimum tribological performance of pin-on-plate contact was observed when a-C:H-coated plate and pin were used as sliding surfaces. On the other hand, highest friction

was observed with a-C:H:W/a-C:H:W contact whereas ta-C/cast iron and ta-C/ta-C contacts resulted in highest wear coefficients of pins and plates respectively. P+G+M+Z proved to be most effective lubricant in facilitating the sliding and enhancing wear resistance of pins whereas T+G+M+Z exhibited lowest wear coefficient of plates.

4. During cylinder head testing, lowest values of friction torque were observed with a-C:H:W - a-C:H:W interface whereas maximum friction was seen when uncoated tappets and camlobes were used. However, lowest values of wear volumes of tappets and nose wear of camlobes were observed when a-C:H-coated components were used.

(a) Among the tested lubricants, P+G+M+Z proved to be most effective in reducing the friction between cam and tappet whereas PAO proved to be least effective. Lowest wear volumes and nose wear of uncoated and DLC-coated tappets and camlobes was seen when T+G+M+Z was used as lubricant.

(b) Highest rotational speed of tappet was observed when P+G+M+Z was used as lubricant in combination with a-C:H/a-C:H-coated components. An increase in rotational speed of tappets was seen with an increase in camshaft speed and decrease in lubricant temperature irrespective of lubricant formulation and type of DLC coating used.

Based on these conclusions, it can be summarized that a-C:H and TMP has the potential to be used as surface protective coating and lubricant base oil for cam/tappet interface of direct acting valve train assembly with existing lubricant additives. However, there is a need to evaluate other engine assemblies in combination with formulated TMP to further validate its potential.

5.2 Suggestions for future work

In order to make TMP technologically competitive and suitable for engine lubricant base oil, there is a need to further evaluate its compatibility with other types of environmentally friendly friction modifiers and antiwear additives which include ashless dithiophosphates, AP, amine sulfuric-phosphate diester, butylated triphenyl phosphorothionate etc. In the future studies, it is recommended to investigate the role of detergents, dispersants, viscosity modifiers, emulsifiers etc. on the rate of tribofilm formation of friction modifiers, antiwear additives and extreme pressure additives on various types of DLC coatings. Since, conventional additives used in this study proved to be more effective with PAO, it is required to synthesize specialized and more compatible additives for TMP. In order to completely eliminate sulfur, phosphorus and zinc-based environmentally hazardous additives and formulate a completely green engine lubricant, there is a need to analyze the compatibility of TMP with environment-friendly nanoparticles which include MoS_2, titanium dioxide (TiO_2), silicon dioxide (SiO_2), WS_2, copper(II) oxide (CuO), graphene, aluminum oxide (Al_2O_3), zirconium dioxide (ZrO_2) etc. Since, ionic liquids are also one of the potential candidates to replace conventional additives therefore, their compatibility with TMP and DLC coatings also needs to be analyzed.

There is also a need to examine the tribological behavior of interacting surfaces coated with different types of DLC coatings under boundary lubrication condition e.g. ta-C/ a-C:H:W contact, ta-C/a-C:H ccontact etc. Since, mechanisms of additive-derived tribofilm formation on various types of DLC coatings are still unclear, therefore, it would also be interesting to further explore them with the aid of advanced material characterization techniques. By doing so, it would be possible to dope DLC coatings and make surface modifications in such a way that tribochemical interactions between additives and interacting surfaces results in the formation of faster, stronger and strongly-adhered

tribofilms. Evaluating the effect of substrate hardness, roughness and surface-texturing on the adhesion strength of DLC coatings can also be an interesting topic for future studies. Moreover, other types of DLC coatings which include fluorine-doped DLC coating, titanium-doped DLC coating and hybrid DLC coatings also needs to be evaluated for cam/tappet interface of direct acting valve train assembly of commercial diesel engine.

REFERENCES

Aisenberg, S., & Chabot, R. W. (1973). Physics of ion plating and ion beam deposition. *Journal of Vacuum Science & Technology, 10*(1), 104–107.

Al Mahmud, K. A. H., Kalam, M., Masjuki, H., & Abdollah, M. (2015). Tribological Study of a Tetrahedral Diamond-Like Carbon Coating under Vegetable Oil–Based Lubricated Condition. *Tribology Transactions, 58*(5), 907-913.

Al Mahmud, K. A. H., Varman, M., Kalam, M., Masjuki, H., Mobarak, H., & Zulkifli, N. (2014a). Tribological characteristics of amorphous hydrogenated (aC: H) and tetrahedral (ta-C) diamond-like carbon coating at different test temperatures in the presence of commercial lubricating oil. *Surface and Coatings Technology, 245*, 133-147.

Al Mahmud, K. A. H., Varman, M., Kalam, M. A., Masjuki, H. H., Mobarak, H. M., & Zulkifli, N. W. M. (2014b). Tribological characteristics of amorphous hydrogenated (a-C:H) and tetrahedral (ta-C) diamond-like carbon coating at different test temperatures in the presence of commercial lubricating oil. *Surface and Coatings Technology, 245*, 133-147.

Andersson, L., Berg, S., Norström, H., Olaison, R., & Towta, S. (1979). Properties and coating rates of diamond-like carbon films produced by RF glow discharge of hydrocarbon gases. *Thin Solid Films, 63*(1), 155-160.

Annema, J. A., Van den Brink, R., & Walta, L. (2013). Transport technology to reduce transport's negative impacts. *The Transport System and Transport Policy: An Introduction*, 163.

Balakos, M. W., & Hernandez, E. E. (1997). Catalyst characteristics and performance in edible oil hydrogenation. *Catalysis Today, 35*(4), 415-425.

Baniasad, S. M., & Emes, M. R. (1998). Design and development of method of valve-train friction measurement (No. 980572). *SAE Technical Paper*.

Barriga, J., Kalin, M., Acker, K. V., Vercammen, K., Ortega, A., & Leiaristi, L. (2006). Tribological performance of titanium doped and pure DLC coatings combined with a synthetic bio-lubricant. *Wear, 261*(1), 9-14.

Bewilogua, K., & Hofmann, D. (2014). History of diamond-like carbon films — From first experiments to worldwide applications. *Surface and Coatings Technology, 242*, 214-225.

Bhushan, B. (2013). *Principles and applications of tribology*: John Wiley & Sons.

Bilgili, M., Ozbek, A., Sahin, B., & Kahraman, A. (2015). An overview of renewable electric power capacity and progress in new technologies in the world. *Renewable and Sustainable Energy Reviews, 49*, 323-334.

Bowden, F. P., & Tabor, D. (2001). *The friction and lubrication of solids* (Vol. 1): Oxford university press.

Campanella, A., Rustoy, E., Baldessari, A., & Baltanas, M. A. (2010). Lubricants from chemically modified vegetable oils. *Bioresour Technol, 101*(1), 245-254. doi:10.1016/j.biortech.2009.08.035

Cho, D.-H., Lee, S.-A., & Lee, Y.-Z. (2009). The Effects of Surface Roughness and Coatings on the Tribological Behavior of the Surfaces of a Piston Skirt. *Tribology Transactions, 53*(1), 137-144.

Choi, U., Ahn, B., Kwon, O., & Chun, Y. (1997). Tribological behavior of some antiwear additives in vegetable oils. *Tribology International, 30*(9), 677-683.

Cui, J., Qiang, L., Zhang, B., Ling, X., Yang, T., & Zhang, J. (2012). Mechanical and tribological properties of Ti-DLC films with different Ti content by magnetron sputtering technique. *Applied Surface Science, 258*(12), 5025-5030. doi:10.1016/j.apsusc.2012.01.072

Czichos, H., & Habig, K. (1992). Tribologie Handbuch: Systemanalyse, Prüftechnik, Werkstoffe und Konstruktionselemente: Wiesbaden, Vieweg Verlag.

de Barros'Bouchet, M. I., Martin, J. M., Le-Mogne, T., & Vacher, B. (2005). Boundary lubrication mechanisms of carbon coatings by MoDTC and ZDDP additives. *Tribology International, 38*(3), 257-264.

Dearnaley, G., & Arps, J. H. (2005). Biomedical applications of diamond-like carbon (DLC) coatings: A review. *Surface and Coatings Technology, 200*(7), 2518-2524.

del Castillo-Mussot, M., Ugalde-Véle, P., Montemayor-Aldrete, J. A., de la Lama-García, A., & Cruz, F. (2016). Impact of Global Energy Resources Based on Energy Return on their Investment (EROI) Parameters. *Perspectives on Global Development and Technology, 15*(1-2), 290-299.

Deng, X., Kousaka, H., Tokoroyama, T., & Umehara, N. (2014). Tribological behavior of tetrahedral amorphous carbon (ta-C) coatings at elevated temperatures. *Tribology International, 75*, 98-103.

Dobrenizki, L., Tremmel, S., Wartzack, S., Hoffmann, D., Brögelmann, T., Bobzin, K., . . . Hosenfeldt, T. (2016). Efficiency improvement in automobile bucket tappet/camshaft contacts by DLC coatings–Influence of engine oil, temperature and camshaft speed. *Surface and Coatings Technology, 308*, 360-373.

Doll, K. M., Sharma, B. K., & Erhan, S. Z. (2008). Friction reducing properties and stability of epoxidized oleochemicals. *CLEAN–Soil, Air, Water, 36*(8), 700-705.

Durham, J., & Kidson, A. (2014). The effects of low sulfated ash, phosphorus and sulfur oils on camshaft/tappet tribocouples with various diamond-like-carbon coated tappets in motored and fired engines. *Lubrication Science, 26*(6), 411-427.

Enomoto, Y., & Yamamoto, T. (1998). New materials in automotive tribology. *Tribology Letters, 5*(1), 13-24.

Equey, S., Roos, S., Mueller, U., Hauert, R., Spencer, N. D., & Crockett, R. (2008a). Reactions of zinc-free anti-wear additives in DLC/DLC and steel/steel contacts. *Tribology International, 41*(11), 1090-1096.

Equey, S., Roos, S., Mueller, U., Hauert, R., Spencer, N. D., & Crockett, R. (2008b). Tribofilm formation from ZnDTP on diamond-like carbon. *Wear, 264*(3-4), 316-321.

Erdemir, A. (2001). The role of hydrogen in tribological properties of diamond-like carbon films. *Surface and Coatings Technology, 146*, 292-297.

Erdemir, A., Bindal, C., Fenske, G., Zuiker, C., & Wilbur, P. (1996). Characterization of transfer layers forming on surfaces sliding against diamond-like carbon. *Surface and Coatings Technology, 86*, 692-697.

Erdemir, A., & Donnet, C. (2006). Tribology of diamond-like carbon films: recent progress and future prospects. *Journal of Physics D: Applied Physics, 39*(18), R311-R327.

Erdemir, A., Eryilmaz, O. L., & Kim, S. H. (2014). Effect of tribochemistry on lubricity of DLC films in hydrogen. *Surface and Coatings Technology, 257*, 241-246.

Erhan, S. Z., Sharma, B. K., & Perez, J. M. (2006). Oxidation and low temperature stability of vegetable oil-based lubricants. *Industrial Crops and Products, 24*(3), 292-299.

Etsion, I., Halperin, G., & Becker, E. (2006). The effect of various surface treatments on piston pin scuffing resistance. *Wear, 261*(7-8), 785-791.

Feng, X., & Xia, Y. (2012). Tribological properties of Ti-doped DLC coatings under ionic liquids lubricated conditions. *Applied Surface Science, 258*(7), 2433-2438.

Ferrari, A., & Robertson, J. (2000). Interpretation of Raman spectra of disordered and amorphous carbon. *Physical review B, 61*(20), 14095.

Forsberg, P., Gustavsson, F., Renman, V., Hieke, A., & Jacobson, S. (2013). Performance of DLC coatings in heated commercial engine oils. *Wear, 304*(1-2), 211-222.

Franklin, S. E., & Baranowska, J. (2007). Conditions affecting the sliding tribological performance of selected coatings for high vacuum bearing applications. *Wear, 263*(7-12), 1300-1305.

Gangopadhyay, A., McWatt, D. G., Zdrodowski, R. J., Simko, S. J., Matera, S., Sheffer, K., & Furby, R. S. (2012). Valvetrain Friction Reduction through Thin Film Coatings and Polishing. *Tribology Transactions, 55*(1), 99-108.

Gangopadhyay, A., Sinha, K., Uy, D., McWatt, D. G., Zdrodowski, R. J., & Simko, S. J. (2011). Friction, Wear, and Surface Film Formation Characteristics of Diamond-Like Carbon Thin Coating in Valvetrain Application. *Tribology Transactions, 54*(1), 104-114.

Gangopadhyay, A., Zdrodowski, R. J., & Simko, S. J. (2014). Interactions of Diamond-Like Carbon Coatings with Fully Formulated Engine Oils. *Tribology Transactions, 57*(3), 503-514.

García-Zapateiro, L., Delgado, M., Franco, J., Valencia, C., Ruiz-Méndez, M., Garcés, R., & Gallegos, C. (2010). Oleins as a source of estolides for biolubricant applications. *Grasas y Aceites, 61*(2), 171-174.

García-Zapateiro, L., Franco, J., Valencia, C., Delgado, M., Gallegos, C., & Ruiz-Méndez, M. (2013). Chemical, thermal and viscous characterization of high-oleic sunflower and olive pomace acid oils and derived estolides. *Grasas y Aceites, 64*(5), 497-508.

Gorla, G., Kour, S. M., Padmaja, K. V., Karuna, M. S., & Prasad, R. B. (2013). Preparation and properties of lubricant base stocks from epoxidized karanja oil and its alkyl esters. *Industrial & Engineering Chemistry Research, 52*(47), 16598-16605.

Grill, A. (1999a). Diamond-like carbon: state of the art. *Diamond and Related Materials, 8*(2), 428-434.

Grill, A. (1999b). Plasma-deposited diamondlike carbon and related materials. *IBM Journal of Research and Development, 43*(1.2), 147-162.

Hamid, H. A., Yunus, R., Rashid, U., Choong, T. S., & Ala'a, H. (2012). Synthesis of palm oil-based trimethylolpropane ester as potential biolubricant: Chemical kinetics modeling. *Chemical engineering journal, 200*, 532-540.

Haque, T., Morina, A., Neville, A., Kapadia, R., & Arrowsmith, S. (2007). Non-ferrous coating/lubricant interactions in tribological contacts: Assessment of tribofilms. *Tribology International, 40*(10-12), 1603-1612.

Haque, T., Morina, A., Neville, A., Kapadia, R., & Arrowsmith, S. (2008). Study of the ZDDP antiwear tribofilm formed on the DLC coating using AFM and XPS techniques. *Automotive Lubricant Testing and Advanced Additive Development, 4*(7), 92.

Haque, T., Morina, A., Neville, A., Kapadia, R., & Arrowsmith, S. (2009). Effect of oil additives on the durability of hydrogenated DLC coating under boundary lubrication conditions. *Wear, 266*(1), 147-157.

Hauert, R. (2004). An overview on the tribological behavior of diamond-like carbon in technical and medical applications. *Tribology International, 37*(11), 991-1003.

Henderson, K., & Maggi, C. (2008). Viscometric temperature sensitivity of engine lubricants at low temperature and moderately high shear conditions *Automotive Lubricant Testing and Advanced Additive Development*: ASTM International.

Holmberg, K., Andersson, P., & Erdemir, A. (2012). Global energy consumption due to friction in passenger cars. *Tribology International, 47*, 221-234.

Hwang, H.-S., & Erhan, S. Z. (2001). Modification of epoxidized soybean oil for lubricant formulations with improved oxidative stability and low pour point. *Journal of the American Oil Chemists' Society, 78*(12), 1179-1184.

International Energy Outlook. (2016). Retrieved from https://www.eia.gov/outlooks/ieo/

Jayadas, N., & Nair, K. P. (2006). Coconut oil as base oil for industrial lubricants—evaluation and modification of thermal, oxidative and low temperature properties. *Tribology International, 39*(9), 873-878.

Jayadas, N. H., Prabhakaran Nair, K., & G, A. (2007). Tribological evaluation of coconut oil as an environment-friendly lubricant. *Tribology International, 40*(2), 350-354. doi:10.1016/j.triboint.2005.09.021

Kalin, M., Kogovšek, J., Kovač, J., & Remškar, M. (2014). The Formation of Tribofilms of MoS2 Nanotubes on Steel and DLC-Coated Surfaces. *Tribology Letters, 55*(3), 381-391.

Kalin, M., Roman, E., Ožbolt, L., & Vižintin, J. (2010). Metal-doped (Ti, WC) diamond-like-carbon coatings: Reactions with extreme-pressure oil additives under tribological and static conditions. *Thin Solid Films, 518*(15), 4336-4344.

Kalin, M., Roman, E., & Vižintin, J. (2007). The effect of temperature on the tribological mechanisms and reactivity of hydrogenated, amorphous diamond-like carbon coatings under oil-lubricated conditions. *Thin Solid Films, 515*(7-8), 3644-3652.

Kalin, M., Velkavrh, I., Vižintin, J., & Ožbolt, L. (2008). Review of boundary lubrication mechanisms of DLC coatings used in mechanical applications. *Meccanica, 43*(6), 623-637.

Kalin, M., & Vižintin, J. (2005). The tribological performance of DLC-coated gears lubricated with biodegradable oil in various pinion/gear material combinations. *Wear, 259*(7-12), 1270-1280.

Kalin, M., & Vižintin, J. (2006a). A comparison of the tribological behaviour of steel/steel, steel/DLC and DLC/DLC contacts when lubricated with mineral and biodegradable oils. *Wear, 261*(1), 22-31.

Kalin, M., & Vižintin, J. (2006b). Differences in the tribological mechanisms when using non-doped, metal-doped (Ti, WC), and non-metal-doped (Si) diamond-like carbon against steel under boundary lubrication, with and without oil additives. *Thin Solid Films, 515*(4), 2734-2747.

Kalin, M., Vižintin, J., Barriga, J., Vercammen, K., Van Acker, K., & Arnšek, A. (2004). The effect of doping elements and oil additives on the tribological performance of boundary-lubricated DLC/DLC contacts. *Tribology Letters, 17*(4), 679-688.

Kalin, M., Vižintin, J., Vercammen, K., Barriga, J., & Arnšek, A. (2006). The lubrication of DLC coatings with mineral and biodegradable oils having different polar and saturation characteristics. *Surface and Coatings Technology, 200*(14-15), 4515-4522.

Kano, M. (2006). Super low friction of DLC applied to engine cam follower lubricated with ester-containing oil. *Tribology International, 39*(12), 1682-1685.

Kano, M., Yasuda, Y., Okamoto, Y., Mabuchi, Y., Hamada, T., Ueno, T., . . . Le Mognee, T. (2005). Ultralow friction of DLC in presence of glycerol mono-oleate (GNO). *Tribology Letters, 18*(2), 245-251.

Khaemba, D. N., Neville, A., & Morina, A. (2016). New insights on the decomposition mechanism of Molybdenum DialkyldiThioCarbamate (MoDTC): a Raman spectroscopic study. *RSC Adv., 6*(45), 38637-38646.

Khurram, M., Mufti, R. A., Zahid, R., Afzal, N., Bhutta, M. U., & Khan, M. (2014). Effect of lubricant chemistry on the performance of end pivoted roller follower valve train. *Tribology International, 93*, 717-722.

Kim, D.-W., & Kim, K.-W. (2013). Effects of sliding velocity and normal load on friction and wear characteristics of multi-layered diamond-like carbon (DLC) coating prepared by reactive sputtering. *Wear, 297*(1-2), 722-730.

Kim, D.-W., & Kim, K.-W. (2014). Effects of sliding velocity and ambient temperature on the friction and wear of a boundary-lubricated, multi-layered DLC coating. *Wear, 315*(1), 95-102. doi:10.1016/j.wear.2014.04.002

Kimock, F. M., & Knapp, B. J. (1993). Commercial applications of ion beam deposited diamond-like carbon (DLC) coatings. *Surface and Coatings Technology, 56*(3), 273-279.

Komanduri, R., & Shaw, M. (1975). Wear of synthetic diamond when grinding ferrous metals. 211-213.

Komori, K., & Umehara, N. (2015). Effect of surface morphology of diamond-like carbon coating on friction, wear behavior and tribo-chemical reactions under engine-oil lubricated condition. *Tribology International, 84*, 100-109. doi:10.1016/j.triboint.2014.11.010

Kong, X., Kong, X., Zhou, B., Zhou, B., Wang, J., Wang, J., . . . Li, W. (2016). Engineering research of DLC coating in piston pins and bucket tappets. *Industrial Lubrication and Tribology, 68*(5), 530-535.

Kosarieh, S., Morina, A., Lainé, E., Flemming, J., & Neville, A. (2013a). The effect of MoDTC-type friction modifier on the wear performance of a hydrogenated DLC coating. *Wear, 302*(1-2), 890-898.

Kosarieh, S., Morina, A., Lainé, E., Flemming, J., & Neville, A. (2013b). Tribological performance and tribochemical processes in a DLC/steel system when lubricated in a fully formulated oil and base oil. *Surface and Coatings Technology, 217*, 1-12.

Kržan, B., Novotny-Farkas, F., & Vižintin, J. (2009). Tribological behavior of tungsten-doped DLC coating under oil lubrication. *Tribology International, 42*(2), 229-235.

Kržan, B., & Vižintin, J. (2003). Tribological properties of an environmentally adopted universal tractor transmission oil based on vegetable oil. *Tribology International, 36*(11), 827-833. doi:10.1016/s0301-679x(03)00100-2

Lawes, S. D. A., Fitzpatrick, M. E., & Hainsworth, S. V. (2007). Evaluation of the tribological properties of DLC for engine applications. *Journal of Physics D: Applied Physics, 40*(18), 5427-5437.

Lawes, S. D. A., Hainsworth, S. V., & Fitzpatrick, M. E. (2010). Impact wear testing of diamond-like carbon films for engine valve-tappet surfaces. *Wear, 268*(11-12), 1303-1308.

Liu, Z., Sharma, B. K., Erhan, S. Z., Biswas, A., Wang, R., & Schuman, T. P. (2015). Oxidation and low temperature stability of polymerized soybean oil-based lubricants. *Thermochimica Acta, 601*, 9-16.

Love, C., Cook, R. B., Harvey, T., Dearnley, P., & Wood, R. (2013). Diamond like carbon coatings for potential application in biological implants—a review. *Tribology International, 63*, 141-150.

Mabuchi, Y., Hamada, T., Izumi, H., & Yasuda, Y. (2007). The Development of Hydrogen-Free DLC Coated Valve-Lifter (No. 2007-01-1752). *SAE Technical Paper*.

Mang, T., Bobzin, K., & Bartels, T. (2011). *Industrial tribology: tribosystems, friction, wear and surface engineering, lubrication*: John Wiley & Sons.

Mathiesen, B. V., Lund, H., Connolly, D., Wenzel, H., Østergaard, P. A., Möller, B., . . . Hvelplund, F. K. (2015). Smart Energy Systems for coherent 100% renewable energy and transport solutions. *Applied Energy, 145*, 139-154.

McArdle, S., Curtin, T., & Leahy, J. (2010). Hydrogenation of sunflower oil over platinum supported on silica catalysts: Preparation, characterisation and catalytic activity. *Applied Catalysis A: General, 382*(2), 332-338.

McNutt, J., & He, Q. (2016). Development of biolubricants from vegetable oils via chemical modification. *Journal of Industrial and Engineering Chemistry, 36*, 1-12.

Mistry, K., Morina, A., & Neville, A. (2012). Single cam tribometer for evaluating tribological parameters and tribochemistry of DLC coated valve train follower. *Tribology-Materials, Surfaces & Interfaces, 6*(1), 31-37.

Mobarak, H. M., Masjuki, H. H., Mohamad, E. N., Kalam, M. A., Rashedul, H. K., Rashed, M. M., & Habibullah, M. (2014). Tribological properties of amorphous hydrogenated (a-C:H) and hydrogen-free tetrahedral (ta-C) diamond-like carbon coatings under jatropha biodegradable lubricating oil at different temperatures. *Applied Surface Science, 317*, 581-592.

Mobarak, H. M., Niza Mohamad, E., Masjuki, H. H., Kalam, M. A., Al Mahmud, K. A. H., Habibullah, M., & Ashraful, A. M. (2014). The prospects of biolubricants as

alternatives in automotive applications. *Renewable and Sustainable Energy Reviews, 33*, 34-43.

Morrison, N., Muhl, S., Rodil, S., Milne, W., Robertson, J., Weiler, M., . . . Brown, L. (1997). High rate deposition of ta-C: H using an electron cyclotron wave resonance plasma source. *Thin Solid Films, 337*(1), 71-73.

Morrison, N., Rodil, S., Ferrari, A., Robertson, J., & Milne, W. (1999). High rate deposition of ta-C: H using an electron cyclotron wave resonance plasma source. *Thin Solid Films, 337*(1), 71-73.

Mufti, R. A., & Jefferies, A. (2008). Novel method of measuring tappet rotation and the effect of lubricant rheology. *Tribology International, 41*(11), 1039-1048.

Mufti, R. A., & Priest, M. (2003). Experimental and theoretical study of instantaneous engine valve train friction. *Journal of tribology, 125*(3), 628-637.

Mufti, R. A., Zahid, R., Qureshi, F., & Aslam, J. (2015). Innovative technique of measuring follower rotation in real production engine using Gradiometer sensor and the effect of friction modifier. *Industrial Lubrication and Tribology, 67*(4), 285-291.

Mufti, R. A., Zahid, R., Qureshi, F., Aslam, J., Afzal, N., & Bhutta, M. U. (2015). Measuring the tribological performance of all the tappets in a production engine using magnetometer sensors and the effect of lubricant rheology. *Lubrication Science, 27*(4), 251-263.

Mutafov, P., Lanigan, J., Neville, A., Cavaleiro, A., & Polcar, T. (2014). DLC-W coatings tested in combustion engine — Frictional and wear analysis. *Surface and Coatings Technology, 260*, 284-289.

Nagendramma, P., & Kaul, S. (2012). Development of ecofriendly/biodegradable lubricants: An overview. *Renewable and Sustainable Energy Reviews, 16*(1), 764-774. doi:10.1016/j.rser.2011.09.002

Neale, M. J. (1995). *The tribology handbook*: Butterworth-Heinemann.

Neuville, S., & Matthews, A. (2007). A perspective on the optimisation of hard carbon and related coatings for engineering applications. *Thin Solid Films, 515*(17), 6619-6653.

Neville, A., Morina, A., Haque, T., & Voong, M. (2007). Compatibility between tribological surfaces and lubricant additives—How friction and wear reduction can be controlled by surface/lube synergies. *Tribology International, 40*(10-12), 1680-1695. doi:10.1016/j.triboint.2007.01.019

Oksanen, J., Hakala, T. J., Tervakangas, S., Laakso, P., Kilpi, L., Ronkainen, H., & Koskinen, J. (2014). Tribological properties of laser-textured and ta-C coated surfaces with burnished WS2 at elevated temperatures. *Tribology International, 70*, 94-103.

Okubo, H., Tadokoro, C., & Sasaki, S. (2015). Tribological properties of a tetrahedral amorphous carbon (ta-C) film under boundary lubrication in the presence of organic friction modifiers and zinc dialkyldithiophosphate (ZDDP). *Wear, 332-333*, 1293-1302.

Ong, H. C., Mahlia, T. M. I., & Masjuki, H. H. (2012). A review on energy pattern and policy for transportation sector in Malaysia. *Renewable and Sustainable Energy Reviews, 16*(1), 532-542.

Ouyang, J. H., & Sasaki, S. (2005). Friction and wear characteristics of a Ti-containing diamond-like carbon coating with an SRV tester at high contact load and elevated temperature. *Surface and Coatings Technology, 195*(2-3), 234-244.

Ouyang, J. H., Sasaki, S., Murakami, T., Zhou, Y., & Zhang, J. (2009). Mechanical and unlubricated tribological properties of titanium-containing diamond-like carbon coatings. *Wear, 266*(1-2), 96-102.

Park, C.-S., Choi, S. G., Park, H.-H., Jang, J.-N., Hong, M., & Kwon, K.-H. (2012). Compensation effect of boron and nitrogen codoping on the hardness and electrical resistivity of diamond-like carbon films prepared by magnetron sputtering deposition. *Journal of Materials Research, 27*(23), 3027-3032.

Podgornik, B., Hren, D., & Vižintin, J. (2005). Low-friction behaviour of boundary-lubricated diamond-like carbon coatings containing tungsten. *Thin Solid Films, 476*(1), 92-100.

Podgornik, B., Hren, D., Vižintin, J., Jacobson, S., Stavlid, N., & Hogmark, S. (2006). Combination of DLC coatings and EP additives for improved tribological behaviour of boundary lubricated surfaces. *Wear, 261*(1), 32-40. doi:10.1016/j.wear.2005.09.007

Pop, L., Puşcaş, C., Bandur, G., Vlase, G., & Nuţiu, R. (2007). Basestock Oils for Lubricants from Mixtures of Corn Oil and Synthetic Diesters. *Journal of the American Oil Chemists' Society, 85*(1), 71-76.

Quinchia, L., Delgado, M., Franco, J., Spikes, H., & Gallegos, C. (2012). Low-temperature flow behaviour of vegetable oil-based lubricants. *Industrial Crops and Products, 37*(1), 383-388.

Quinn, T., Sullivan, J., & Rowson, D. (1984). Origins and development of oxidational wear at low ambient temperatures. *Wear, 94*(2), 175-191.

Rizvi, S. Q. (1999). Additives for automotive fuels and lubricants. *Tribology & Lubrication Technology, 55*(4), 33.

Roberts, A., Brooks, R., & Shipway, P. (2014). Internal combustion engine cold-start efficiency: A review of the problem, causes and potential solutions. *Energy Conversion and Management, 82*, 327-350.

Robertson, J. (2002). Diamond-like amorphous carbon. *Materials Science and Engineering: R: Reports, 37*(4), 129-281.

Rodil, S., & Muhl, S. (2004). Deposition of ta-C: N: H as Function of Experimental Parameters. *Surface Engineering, 20*(1), 17-24.

Rosenberg, R. C. (1982). *General friction considerations for engine design* (0148-7191). Retrieved from

Rowe, C. N. (1988). Lubricated wear *CRC Handbook of Lubrication: Theory and Practice of Tribology, Volume II: Theory and Design* (pp. 209-225): CRC Press.

Rudnick, L. R. (2006). Synthetic, mineral oils and bio-based lubricants. *Chemistry and Technology, CRC Taylor and Francis, Boca Raton New York London*.

Salimon, J., Salih, N., & Yousif, E. (2011). Synthesis, characterization and physicochemical properties of oleic acid ether derivatives as biolubricant basestocks. *Journal of oleo science, 60*(12), 613-618.

Saurabh, T., Patnaik, M., Bhagt, S., & Renge, V. (2011). Epoxidation of vegetable oils: a review. *Int. J. Adv. Eng. Technol, 2*, 491-501.

Schamel, A., Grischke, M., & Bethke, R. (1997). Amorphous carbon coatings for low friction and wear in bucket tappet valvetrains. *Stroke, 2015*, 06-22.

Schwan, J., Ulrich, S., Jung, K., Ehrhardt, H., Samlenski, R., & Brenn, R. (1995). Deposition of ta-C: H films by rf plasma discharges. *Diamond and Related Materials, 4*(4), 304-308.

Senge, P. M. (2014). Creating the schools of the future: Education for a sustainable society. *Creating a Sustainable and Desirable Future: Insights from 45 Global Thought Leaders*, 321.

Sharma, B. K., Adhvaryu, A., & Erhan, S. Z. (2009). Friction and wear behavior of thioether hydroxy vegetable oil. *Tribology International, 42*(2), 353-358.

Shimada, S., Tanaka, H., Higuchi, M., Yamaguchi, T., Honda, S., & Obata, K. (2004). Thermo-chemical wear mechanism of diamond tool in machining of ferrous metals. *CIRP Annals-Manufacturing Technology, 53*(1), 57-60.

Shinyoshi, T., Fuwa, Y., & Ozaki, Y. (2007). Wear analysis of DLC coating in oil containing Mo-DTC (No. 2007-01-1969). *SAE Technical Paper*.

Snidle, R., & Evans, H. (2009). Some aspects of gear tribology. *Proceedings of the Institution of Mechanical Engineers, Part C: Journal of Mechanical Engineering Science, 223*(1), 103-141.

Somidi, A. K., Sharma, R. V., & Dalai, A. K. (2014). Synthesis of Epoxidized Canola Oil Using a Sulfated-SnO2 Catalyst. *Industrial & Engineering Chemistry Research, 53*(49), 18668-18677.

Soni, S., & Agarwal, M. (2014). Lubricants from renewable energy sources–a review. *Green Chemistry Letters and Reviews, 7*(4), 359-382.

Spencer, N. D., & Tysoe, W. T. (2015). *The Cutting Edge of Tribology: A Decade of Progress in Friction, Lubrication and Wear*: World Scientific.

Spikes, H. (2004). The history and mechanisms of ZDDP. *Tribology Letters, 17*(3), 469-489.

Stachowiak, G., & Batchelor, A. (2014). Chapter 8 - Boundary and Extreme Pressure Lubrication *Engineering Tribology (Fourth Edition)* (pp. 371-428). Boston: Butterworth-Heinemann.

Suda, S., Yokota, H., Inasaki, I., & Wakabayashi, T. (2002). A synthetic ester as an optimal cutting fluid for minimal quantity lubrication machining. *CIRP Annals-Manufacturing Technology, 51*(1), 95-98.

Tan, Z. (2014). Air Emissions *Air Pollution and Greenhouse Gases* (pp. 1-24): Springer.

Tasdemir, A., Tokoroyama, T., Kousaka, H., Umehara, N., & Mabuchi, Y. (2013). Friction and Wear Performance of Boundary-lubricated DLC/DLC Contacts in Synthetic base Oil. *Procedia Engineering, 68*, 518-524.

Tasdemir, A., Tokoroyama, T., Kousaka, H., Umehara, N., & Mabuchi, Y. (2014). Influence of zinc dialkyldithiophosphate tribofilm formation on the tribological performance of self-mated diamond-like carbon contacts under boundary lubrication. *Thin Solid Films, 562*, 389-397.

Tasdemir, A., Wakayama, M., Tokoroyama, T., Kousaka, H., Umehara, N., Mabuchi, Y., & Higuchi, T. (2013a). Ultra-low friction of tetrahedral amorphous diamond-like carbon (ta-C DLC) under boundary lubrication in poly alpha-olefin (PAO) with additives. *Tribology International, 65*, 286-294.

Tasdemir, A., Wakayama, M., Tokoroyama, T., Kousaka, H., Umehara, N., Mabuchi, Y., & Higuchi, T. (2013b). Wear behaviour of tetrahedral amorphous diamond-like carbon (ta-C DLC) in additive containing lubricants. *Wear, 307*(1-2), 1-9.

Tasdemir, A., Wakayama, M., Tokoroyama, T., Kousaka, H., Umehara, N., Mabuchi, Y., & Higuchi, T. (2014). The effect of oil temperature and additive concentration on the wear of non-hydrogenated DLC coating. *Tribology International, 77*, 65-71.

Topolovec-Miklozic, K., Lockwood, F., & Spikes, H. (2008). Behaviour of boundary lubricating additives on DLC coatings. *Wear, 265*(11-12), 1893-1901.

Tung, S. C., & Gao, H. (2003). Tribological characteristics and surface interaction between piston ring coatings and a blend of energy-conserving oils and ethanol fuels. *Wear, 255*(7-12), 1276-1285.

Uosukainen, E., Linko, Y.-Y., Lämsä, M., Tervakangas, T., & Linko, P. (1998). Transesterification of trimethylolpropane and rapeseed oil methyl ester to environmentally acceptable lubricants. *Journal of the American Oil Chemists' Society, 75*(11), 1557-1563.

Vandevelde, T., Vandierendonck, K., Van Stappen, M., Du Mong, W., & Perremans, P. (1999). Cutting applications of DLC, hard carbon and diamond films. *Surface and Coatings Technology, 113*(1), 80-85.

Vanhulsel, A., Velasco, F., Jacobs, R., Eersels, L., Havermans, D., Roberts, E. W., . . . Gaillard, L. (2007). DLC solid lubricant coatings on ball bearings for space applications. *Tribology International, 40*(7), 1186-1194.

Velkavrh, I., Kalin, M., & Vizintin, J. (2008). The performance and mechanisms of DLC-coated surfaces in contact with steel in boundary-lubrication conditions: a review. *Strojniški vestnik, 54*(3), 189-206.

Vengudusamy, B., Grafl, A., & Preinfalk, K. (2014a). Influence of Silicon on the Wear Properties of Amorphous Carbon Under Dry and Lubricated Conditions. *Tribology Letters, 53*(3), 569-583.

Vengudusamy, B., Grafl, A., & Preinfalk, K. (2014b). Tribological properties of hydrogenated amorphous carbon under dry and lubricated conditions. *Diamond and Related Materials, 41*, 53-64.

Vengudusamy, B., Green, J. H., Lamb, G. D., & Spikes, H. A. (2011). Tribological properties of tribofilms formed from ZDDP in DLC/DLC and DLC/steel contacts. *Tribology International, 44*(2), 165-174.

Vengudusamy, B., Green, J. H., Lamb, G. D., & Spikes, H. A. (2012). Behaviour of MoDTC in DLC/DLC and DLC/steel contacts. *Tribology International, 54*, 68-76.

Vengudusamy, B., Green, J. H., Lamb, G. D., & Spikes, H. A. (2013a). Durability of ZDDP Tribofilms Formed in DLC/DLC Contacts. *Tribology Letters, 51*(3), 469-478.

Vengudusamy, B., Green, J. H., Lamb, G. D., & Spikes, H. A. (2013b). Influence of hydrogen and tungsten concentration on the tribological properties of DLC/DLC contacts with ZDDP. *Wear, 298-299*, 109-119.

Vengudusamy, B., Mufti, R. A., Lamb, G. D., Green, J. H., & Spikes, H. A. (2011). Friction properties of DLC/DLC contacts in base oil. *Tribology International, 44*(7-8), 922-932.

Vercammen, K., Van Acker, K., Vanhulsel, A., Barriga, J., Arnsek, A., Kalin, M., & Meneve, J. (2004). Tribological behaviour of DLC coatings in combination with biodegradable lubricants. *Tribology International, 37*(11-12), 983-989.

Waara, P., Hannu, J., Norrby, T., & Byheden, Å. (2001). Additive influence on wear and friction performance of environmentally adapted lubricants. *Tribology International, 34*(8), 547-556.

Wagner, H., Luther, R., & Mang, T. (2001). Lubricant base fluids based on renewable raw materials: their catalytic manufacture and modification. *Applied Catalysis A: General, 221*(1), 429-442.

Wang, L., Bai, L., Lu, Z., Zhang, G., & Wu, Z. (2013). Influence of Load on the Tribological Behavior of a-C Films: Experiment and Calculation Coupling. *Tribology Letters, 52*(3), 469-475.

Windom, B. C., Sawyer, W. G., & Hahn, D. W. (2011). A Raman Spectroscopic Study of MoS2 and MoO3: Applications to Tribological Systems. *Tribology Letters, 42*(3), 301-310.

World lubricant. (2015). Retrieved from www.freedoniagroup.com

Wu, L., Zhang, Y., Yang, G., Zhang, S., Yu, L., & Zhang, P. (2016). Tribological properties of oleic acid-modified zinc oxide nanoparticles as the lubricant additive in poly-alpha olefin and diisooctyl sebacate base oils. *RSC Adv., 6*(74), 69836-69844.

Yang, L., Neville, A., Brown, A., Ransom, P., & Morina, A. (2014). Friction reduction mechanisms in boundary lubricated W-doped DLC coatings. *Tribology International, 70*, 26-33.

Yasuada, Y. (2003). Research on Diamond-Like Carbon Coatings for Low-Friction Valve Lifters. *Stroke, 2014*, 10-05.

Yunus, R., Fakhru'l-Razi, A., Ooi, T. L., Iyuke, S. E., & Perez, J. M. (2004). Lubrication properties of trimethylolpropane esters based on palm oil and palm kernel oils. *European journal of lipid science and technology, 106*(1), 52-60.

Zahid, R., Masjuki, H. H., Varman, M., Mufti, R., Kalam, M. A., & Gulzar, M. (2015). Effect of Lubricant Formulations on the Tribological Performance of Self-Mated Doped DLC Contacts: a review. *Tribology Letters, 58*(2), 1-28.

Zulkifli, N. W. M., Azman, S. S. N., Kalam, M. A., Masjuki, H. H., Yunus, R., & Gulzar, M. (2016). Lubricity of bio-based lubricant derived from different chemically modified fatty acid methyl ester. *Tribology International, 93*, 555-562.

Zulkifli, N. W. M., Kalam, M. A., Masjuki, H. H., Al Mahmud, K. A. H., & Yunus, R. (2014). The Effect of Temperature on Tribological Properties of Chemically Modified Bio-Based Lubricant. *Tribology Transactions, 57*(3), 408-415. doi:10.1080/10402004.2013.878777

Zulkifli, N. W. M., Kalam, M. A., Masjuki, H. H., Shahabuddin, M., & Yunus, R. (2013). Wear prevention characteristics of a palm oil-based TMP (trimethylolpropane) ester as an engine lubricant. *Energy, 54*, 167-173.

LIST OF PUBLICATIONS AND PAPERS PRESENTED

Journal papers

1. **Zahid, R.**, Masjuki, H. H., Varman, M., Mufti, R. A., Kalam, M. A., Gulzar, M. (2015). Effect of Lubricant Formulations on the Tribological Performance of Self-Mated Doped DLC Contacts: a review. Tribology Letters, 58(2), 1-28

2. **Zahid, R.**, Masjuki, H. H., Varman, M., Kalam, M. A., Mufti, R. A., Zulkifli, N. W. M., Gulzar, M., Azman, S. S. B. N. (2016). Influence of intrinsic and xtrinsic conditions on the tribological characteristics of diamond-like carbon coatings: A review. Journal of Materials Research, 31(13), 1814-1836

3. **Zahid, R.**, Masjuki, H. H., Varman, M., Kalam, M. A., Mufti, R. A., Zulkifli, N. W. M., Gulzar, M. (2016). A review on effects of lubricant formulations on tribological performance and boundary lubrication mechanisms of non-doped DLC/DLC contacts. Critical Reviews in Solid State and Materials Sciences. doi 10.1080/10408436.2016.1186599

4. **Zahid, R.**, Masjuki, H. H., Alabdulkarem A., Varman, M., Mufti, R. A., Kalam, M. A., Zulkifli, N. W. M., Gulzar, M., Lee, T. (2017). Investigation on tribochemical interactions of tungsten-doped diamond-like carbon coating (W-DLC) with formulated palm trimethylolpropane ester (TMP) and polyalphaolefin (PAO). RSC Advances, 7(43), 26513-26531

5. **Zahid, R.**, Masjuki, H. H., Alabdulkarem A., Varman, M., Kalam, M. A., Mufti, R. A., Zulkifli, N. W. M., Gulzar, M., Bhutta, M. U., Ali, M. A., Abdullah, U., Yunus, R. (2017) Tribological characteristics comparison of palm trimethylolpropane ester (TMP) and polyalphaolefin (PAO) formulated with GMO, MoDTC and ZDDP. Industrial and Lubrication Tribology (Accepted)

6. **Zahid, R.**, Masjuki, H. H., Alabdulkarem A., Varman, M., Kalam, M. A., Mufti, R. A., Zulkifli, N. W. M., Gulzar, M., Yunus, R. (2017) Tribological compatibility analysis of conventional lubricant additives with palm trimethylolpropane ester (TMP) and tetrahedral amorphous diamond-like carbon coating (ta-C). Proceedings of the iMeche, Part J: Journal of Engineering Tribology (minor revision submitted)

Conference Proceedings

1. **Zahid, R.**, Masjuki, H. H., Varman, M., Kalam, M. A., Mufti, R. A., Zulkifli, N. W. M. (2015). Tribological Evaluation of Palm Oil-based Trimethylopropane (TMP) Ester with Glycerol Mono Oleate (GMO) using Four-ball Machine. International Sustainable Technology Energy and Civilization Conference (ISTECC 2015), Kuala Lumpur, Malaysia

2. **Zahid, R.**, Masjuki, H. H., Varman, M., Kalam, M. A., Mufti, R. A., Gulzar, M., Yunus, R. (2016). Tribological performance comparison of zinc dialkyldithiophosphate (ZDDP) in poly-alpha-olefin (PAO) and palm oil-based

trimethylopropane (TMP) ester, Malaysian International Tribology Conference (MITC 2015), Penang, Malaysia

3. **Zahid, R.**, Masjuki, H. H., Varman, M., Mufti, R. A., Kalam, M. A., Zulkifli, N. W. M., Gulzar, M. (2016). Tribological performance evaluation of palm trimethylolpropane (TMP) ester as a substitute for conventional lubricant base oil, 4th Malaysia-Japan Tribology Symposium (MJTS 2016), Kuala Lumpur, Malaysia

4. **Zahid, R.**, Masjuki, H. H., Mufti, R. A., Kalam, M. A., Abdullah, U., Afzal N., Varman, M., Gulzar, M., Yunus, R. (2017). Effect of Lubricant Formulations on the Friction Performance of Diamond-Like Carbon (DLC) Coated Direct-Acting Valve Train Components, 4th International Congress on Technology – Engineering and Science (ICONTES), Kuala Lumpur, Malaysia

Poster

1. **Zahid, R.**, Masjuki, H. H., Varman, M., Mufti, R. A., Kalam, M. A., Zulkifli, N. W. M., Gulzar, M. (2016). A step towards development of tribologically-advanced and environment-friendly automotive engine, MYTRIBOS Tribology Poster Competition, Kuala Lumpur, Malaysia